PHYTOALEXINS FROM CRUCIFERS: STRUCTURES, SYNTHESES AND BIOSYNTHESES

A thesis submitted to the
College of Graduate Studies and Research
in partial fulfillment of the requirements
for the degree of
Doctor of Philosophy
in the
Department of Chemistry
University of Saskatchewan
Saskatoon

By

Denis Paskal Okinyo Owiti

Permission to use

In presenting this thesis in partial fulfillment of the requirements for a Postgraduate degree from the University of Saskatchewan, I agree that the Libraries of this University may make it freely available for inspection. I further agree that permission for copying of this thesis in any manner, in whole or in part, for scholarly purposes may be granted by the professor who supervised this thesis work, or in her absence, by the Head of the Department of Chemistry, or the Dean of the College of Graduate Studies and Research. It is understood that any copying, publication, or use of this thesis or parts thereof for financial gain shall not be allowed without my written permission. It is also understood that due recognition shall be given to me and to the University of Saskatchewan in any scholarly use which may be made of any material in my thesis.

Requests for permission to copy or to make other use of material in this thesis in whole or part should be addressed to:

The Head
Department of Chemistry
University of Saskatchewan
Saskatoon, Saskatchewan,
S7N 5C9. CANADA.

Abstract

The search for antifungal secondary metabolites from cruciferous plants exhibiting resistance to pathogenic fungi led to the investigation of *Eruca sativa* (rocket). Chemical analysis of extracts showed arvelexin (**51**) as the only inducible component. Bioassay guided isolation (FCC, PTLC) and characterization (NMR, MS) led to the identification of two phytoanticipins, 4-methylthiobutyl isothiocyanate (**166**) and bis(4-isothiocyanatobutyl)disulfide (**167**). Compounds **166** and **167** inhibited the germination of spores of *Cladosporium cucumerinum* in TLC biodetection assays.

Next, isotopically labeled compounds containing ^{2}H and ^{34}S at specific sites were synthesized for use in studying of the biosynthetic pathway of crucifer phytoalexins and indolyl glucosinolates. Among the synthesized precursors, [4',5',6',7'-$^{2}H_4$]indolyl-3-[^{34}S]acetothiohydroxamic acid (**174a**), the first sulfur-34 containing indolyl derivative was synthesized. In addition, non-isotopically labeled compounds (containing 1-methyl, 1-boc and 1-acetyl groups), that is, substrates used for precursor-directed biosynthesis, were also prepared.

With the precursors in hand, the biosynthetic pathway(s) and biogenetic relationship between phytoalexins was investigated using the tuberous crucifers, *Brassica napus* L. ssp *rapifera* (rutabaga) and *B. rapa* (turnip), and detached leaves of *Erucastrum gallicum* (dog mustard). The biosynthetic relationship between indolyl glucosinolates and phytoalexins was investigated in rutabaga and turnip. The indolyl moiety of the phytoalexins cyclobrassinin (**28**), rutalexin (**33**), spirobrassinin (**34**), brassicanate A (**43**), and rapalexin A (**53**), as well as indolyl glucosinolates glucobrassicin (**70**), 4-methoxyglucobrassicin (**156**), and neoglucobrassicin (**199**) was confirmed to derive from *L*-tryptophan (**78**). The 1-methoxy-containing phytoalexins, erucalexin (**38**) and 1-methoxyspirobrassinin (**35**) were shown to derive from indolyl-3-acetaldoxime (**112**) through 1-methoxyindolyl-3-acetaldoxime (**116**). The 1-methoxy substituent of neoglucobrassicin was also shown to derive from 1-methoxyindolyl-3-acetaldoxime (**116**).

The incorporation of indolyl-3-acetothiohydroxamic acid (**174**) into the phytoalexins cyclobrassinin, rutalexin, brassicanate A, rapalexin A, and spirobrassinin, and into the glucosinolate glucobrassicin is reported for the first time. On the other hand,

incorporation of **174** into 4-methoxyglucobrassicin and neoglucobrassicin was not detected under current experimental conditions. Cyclobrassinin was incorporated into spirobrassinin among the NH-containing phytoalexins, whereas sinalbin B (**31**) [biosynthesized from 1-methoxybrassinin (**18**)] was incorporated into erucalexin and 1-methoxyspirobrassinin. The efficient metabolism of [SC^2H_3]brassicanal A into [SC^2H_3]brassicanate A suggested a biogenetic relationship between these two phytoalexins, whereas absence of incorporation of indolyl-3-acetonitrile (**49**) into rutabaga phytoalexins or indolyl glucosinolates indicated that **49** is not a precursor of these secondary metabolites under the current experimental conditions.

The rutabaga and turnip tubers separately metabolized 1-methylindolyl-3-acetaldoxime (**170**) and 1-methylindolyl-3-acetothiohydroxamic acid (**178**) into 1-methylglucobrassicin (**201**); however, no 1-methyl-containing phytoalexins were detected in the extracts. Rutabaga tissues metabolized 1-(*tert*-butoxycarbonyl)indolyl-3-methylisothiocyanate (**180**) into 1-(*tert*-butoxycarbonyl)brassinin (**181**) and 1-(*tert*-butoxycarbonyl)spirobrassinin (**196**), whereas 1-acetylbrassinin (**184**) was the only detectable metabolic product of 1-acetylindolyl-3-methylisothiocyanate (**183**) in both rutabaga and turnip root tissues.

In conclusion, indolyl-3-acetothiohydroxamic acid (**174**) seems to be the branching point between brassinin and glucobrassicin. The biosynthetic pathway of NH-containing crucifer phytoalexins was mapped and follows the sequence *L*-tryptophan, indolyl-3-acetaldoxime, indolyl-3-acetothiohydroxamic acid, brassinin (possibly through indolyl-3-methylisothiocyanate), and other phytoalexins. The biosynthetic pathway of 1-methoxy-containing phytoalexins follows a similar sequence through 1-methoxyindolyl-3-acetaldoxime (biosynthesized from indolyl-3-acetaldoxime).

Acknowledgements

I would like to express my sincere appreciation to my supervisor, Prof M. Soledade C. Pedras, Thorvaldson Professor, Department of Chemistry, University of Saskatchewan, for giving me a chance to work in her laboratory and for her excellent supervision of this thesis work. Her persistent guidance, encouragement, support and vast knowledge in the biosynthesis of natural products has significantly contributed to the successful completion of the present thesis work.

I am also grateful to the members of my Advisory Committee: Prof. D. E. Ward and Prof. J. Müller, Department of Chemistry, University of Saskatchewan; and Prof. H. Wang, Department of Biochemistry, University of Saskatchewan. Their valuable advice and help during my PhD. work is greatly acknowledged. I also thank my external examiner, Prof. R. L. White, Department of Chemistry, Dalhousie University, for his review of my thesis, suggestions and advice.

I would like to acknowledge the support and encouragement from all past and present members of Prof. Pedras group: Dr. A. Adio, Dr. P. W. K. Ahiahonu, Dr. P. B. Chumala, Dr. R. Gadagi, Dr. M. Hossain, Dr. A. Jha, Dr. M. Jha, Dr. O. Oladapo, Dr. Z. Minic, Dr. S. Montaut, Dr. M. Suchy, Dr. Q-A. Zheng, S. Hossain, S. Islam, W. Jin, I. Khalaff, J. Liu, V. K. Sarma-Mamillapalle, Md. G. Sarwar, R. B. Snitynsky, and Y. Yu. I also greatly acknowledge the support and encouragement from my friends Dr. E. Bagu, J. M. Chitanda, D. Covelli, J. O. Maina, and H. Mohammed, with special thanks to C. M. Bulogosi.

I also wish to extend my warmest thanks to K. Thoms, Dr. K. Brown, and Dr. G. Schatte for their technical assistance. I wish to acknowledge the Department of Chemistry and the College of Graduate Studies and Research, University of Saskatchewan for financial support.

Dedication

To my parents,

Mr. Jacob Joseph Owiti and Mrs. Elizabeth Atieno Owiti

And to my siblings,

Emmanuel Odhiambo, Fredrick Obondi, and Maurine Awuor

Table of contents

List of figures

List of tables

List of abbreviations

Ac	Acetyl
Ac_2O	Acetic anhydride
AcOH	Acetic acid
APCI	Atmospheric pressure chemical ionization
BCAT4	BRANCHED-CHAIN AMINOTRANSFERASE4
Boc	*tert*-Butoxycarbonyl
Boc_2O	Di-*tert*-butyl dicarbonate
B.	*Brassica*
br	Broad
^{13}C NMR	Carbon-13 nuclear magnetic resonance
calcd.	Calculated
DBU	1,8-Diazabicyclo[5.4.0]undec-7-ene
DIBAH	Diisobutylaluminium hydride
DMAP	4-(Dimethylamino)pyridine
DMF	Dimethylformamide
DMSO	Dimethylsulfoxide
LC-MS-ESI	Liquid chromatography-mass spectrometry-electrospray ionization
Et_2O	Diethyl ether
EtOAc	Ethyl acetate
EtOH	Ethanol
FCC	Flash column chromatography
FTIR	Fourier transformed infrared
GC	Gas chromatography
GC-MS	Gas chromatography-mass spectrometry
β-D-Glc	β-D-Glucose
GST	Glutathione-*S*-transferase
h	Hour(s)
^{1}H NMR	Proton nuclear magnetic resonance

HPLC	High performance liquid chromatography
HR-EIMS	High-resolution-electron ionization mass spectrometry
Hz	Hertz
i-PrOH	Isopropanol
J	Coupling constant
L-DOPA	(*S*)-3,4-Dihydroxyphenylalanine
MAM1	Methylthioalkylmalate synthase 1
MAM3	Methylthioalkylmalate synthase 3
MAMS	2-(ω-Methylthioalkyl)malate synthases
MHz	Megahertz
min	Minute(s)
m/z	Mass/charge ratio
NBS	N-Bromosuccinimide
PAD3	Phytoalexin deficient 3
PCC	Pyridinium chlorochromate
PDA	Potato dextrose broth
ppm	Parts per million
PTLC	Preparative thin layer chromatography
quant.	Quantitative
RP-FCC	Reversed phase flash column chromatography
rpm	Revolutions per minute
r.t.	Room temperature
STD	Standard deviation
SUR1	SUPERROOT1
THF	Tetrahydrofuran
TLC	Thin layer chromatography
t_R	Retention time
v	volume
UV	ultraviolet

CHAPTER 1

1. Introduction

1.1 General objectives

Plants belonging to the family Brassicaceae biosynthesize *de novo*, indolyl phytoalexins of diverse chemical structures in response to various forms of stress (Pedras et al., 2007b). This family is also known to produce phytoanticipins including indolyl glucosinolates (Fahey et al., 2001), a class of secondary metabolites that is a part of the complex chemical defense system that these plants use to protect themselves against various forms of stress including microbial attack (Halkier and Gershenzon, 2006). Many crucifers are susceptible to pathogenic fungal diseases such as blackspot, blackleg, clubroot, stem rot, and root rot among others, leading to massive yield losses and low food production for the growing world population. Some crucifers (wild and cultivated) that are resistant to devastation by some of the fungal diseases have been identified (Conn et al., 1988; Gugel et al., 1990; Lefol et al., 1997; Pedras and Zaharia, 2000). Some of the resistant crucifers produce phytoalexins with unique structural characteristics, and possessing remarkable antifungal activity against a variety of pathogens (Pedras et al., 2007b; 2007c). Such resistant species may provide a good genetic source for controlling the devastating effect of the various fungal pathogens. The identification and structural characterization of the various phytoalexins provides an opportunity for the synthesis of precursors to study their biosynthetic pathway(s). An understanding of the biosynthetic pathway(s) of secondary metabolites produced by resistant crucifers may facilitate the transfer of such pathway(s) to the susceptible species, allowing them to produce similar secondary metabolites that may confer resistance to pathogens (Dixon, 2005). Due to environmental impact of synthetic

chemical compounds, such genetic manipulations provide an alternative to protecting crop plants against various pathogens, in addition to design and synthesis of safe crop protecting agents (Pedras et al., 2007f; Pedras and Hossain, 2006).

Objectives of my research were:

(1) Investigation of the antifungal secondary metabolites of *Eruca sativa* (rocket).

(2) Investigation of the biosynthetic pathways of phytoalexins produced in *Erucastrum gallicum* (dog mustard).

(3) Investigation of the biosynthetic pathway(s) of phytoalexins and indolyl glucosinolates produced in *Brassica napus* L. ssp *rapifera* (rutabaga), and *B. rapa* (turnip).

The research above included:

(1) Syntheses of isotopically labeled (^{2}H and ^{34}S) precursors for the study of biosynthetic pathway(s) and biogenetic relationship of crucifer phytoalexins and indolyl glucosinolates.

(2) Syntheses of non-natural indolyl-based precursors as probes for the biosynthetic pathway(s) of crucifer phytoalexins and indolyl glucosinolates.

1.2 Plant secondary metabolites

Plants, like all other living organisms, possess primary metabolic pathways by which they synthesize and utilize essential compounds such as sugars, amino acids, common fatty acids, and nucleotides for their normal growth, development and reproduction. These chemical compounds are generally referred to as primary metabolites. Plants also have secondary metabolic pathways by which they produce compounds (secondary metabolites) that are not essential for their basic metabolic processes, but are necessary for their survival ability. Secondary metabolite production may be activated during particular stages of growth and development, their importance is of an ecological nature as they can mediate interactions such as plant-plant, plant-insect,

plant-microbial and plant-animal. There are three principal building blocks for secondary metabolites: (i) shikimic acid, the precursor of many aromatic compounds including aromatic amino acids and various polyphenols, (ii) amino acids giving rise to alkaloids and peptide antibiotics, (iii) acetate, precursor of polyacetylenes, polyphenols, and isoprenoids (Mann, 1994). Some of these precursors are also utilized in the biosynthesis of certain primary metabolites such as proteins and fatty acids. Secondary metabolic pathways are products of the genetic make-up of the producing organisms (Mann, 1994). Their production and distribution is limited within a group of closely related species, thus making them important chemotaxonomic markers. For example, the plant genus *Potentilla* with more than 300 species in the family Rosaceae was characterized by the occurrence of certain polyphenolic and triterpenoid compounds. The common occurrence of ellagic acid and its derivatives in *Potentilla* is thought to be of taxonomic importance in this genus (Tomczyk, 2006; Xue et al., 2005). The plant genus *Ligularia* in the family Compositae comprises of about 100 species. The species within *Ligularia* were chemotaxonomically characterized by the presence of typical pyrrolizidine alkaloids and sesquiterpenoids. Moreover, many genera within Compositae are known to contain bisaboline sesquiterpenoids (Tan et al., 2007). Classification of the genera *Stemona* and *Croomia* within the plant family Stemonaceae was not complete because some specialists thought that they should be separated (Jiang et al., 2006). Chemotaxonomic investigation of the two genera, *Stemona* and *Croomia* revealed that they both produce stemona alkaloids that are only found in the family Stemonaceae in the plant kingdom. It was therefore proposed that the two genera belong to the same family as they had been placed and should not be separated (Jiang et al., 2006). These examples reveal the importance of secondary metabolites in the chemotaxonomy of plant kingdom.

1.2.1 Plant chemical defenses

Plants are continuously challenged by biotic and abiotic factors in their environment, both above and below the ground. Plants must therefore adapt to their environment for their survival. Part of this adaptation involves the evolutionary production of a diverse array of secondary metabolites to counter the various forms of

challenges. The term allelopathy has been used to refer to chemical interaction between plants and their environment. This term is derived from the Latin words *allelon* 'of each other' and *pathos* 'to suffer' (Weir et al. 2004). Use of the term allelopathy has been extended from plant-plant interaction to microbe-microbe, plant-microbe, and plant-insect or plant-herbivore chemical communication (Weir et al. 2004). Allelochemicals occur in aerial and sub aerial parts of the plant; they are delivered into the rhizosphere through volatile emissions, root exudation, foliar leaching and decomposing residue. These compounds can affect the growth and development of other neighboring plants, they act as feeding deterrents against herbivores, and they have antimicrobial activities. Due to the environment impact and human health concerns about synthetic pesticides and fungicides, the naturally occuring allelochemicals are receiving special attention for their applicability in agronomy (Dayan et al., 2000).

One of the strongest known allelochemicals is (*S*)-3,4-dihydroxyphenylalanine (L-DOPA, **1**) (Nishihara et al., 2004), a non-protein amino acid and a precursor of alkaloids, phenylpropanoids, flavonoids, lignin, and melanin (Mann, 1994). L-DOPA is exuded by the roots of *Mucuna pruriens* (velvet beans), a tropical leguminous plant that has found among other uses, control of weeds (Nishihara et al, 2005). Velvet beans were found to be allelopathic to *Lactuta sativa* (lettuce). Chemical analysis showed that L-DOPA exuding from velvet bean roots inhibited lettuce radicle growth (Hachinohe and Matsumoto, 2005; Nishihara et al, 2005), and soybean root growth (Soares et al., 2007). L-DOPA was also shown to suppress carrot cell growth by 60% (Hachinohe and Matsumoto, 2005). Studies on the absorption, translocation, and metabolism of L-DOPA using susceptible (lettuce) and tolerant (*Echinochloa crus-galli*, barnyardgrass) plants suggested that L-DOPA is itself the active species-selective toxin and not its metabolic products (Hachinohe et al., 2004).

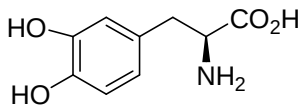

1

Some invasive weeds use allelochemicals to displace other competing plant species. *Acroptilon repens* (Russian knapweed) and *Centaurea maculosa* (spotted knapweed) are two examples of successful exotic plants in North America that replace native plant species (Bais et al., 2003; Stermitz et al., 2003). Chemical analysis of the root exudates of Russian knapweed yielded 7,8-benzoflavone (**2**) as the allelopathic compound (Stermitz et al., 2003). 7,8-Benzoflavone was isolated from soil samples collected from areas infested with Russian knapweed; the concentration of **2** from the soil samples supported the previous claims that it is the active allelopathic compound that these plants use to invade the native plant species (Alford et al., 2007). In bioassays, 7,8-benzoflavone caused mortality in plant species such as *Gaillardia aristata*, *Linaria dalmatica*, and *Arobidopsis thaliana* (Stermitz et al., 2003). The spotted knapweed, another successful invasive weed of North American plant species exudes from its roots a mixture of (-)-catechin (**3**) and (+)-catechin (**4**) (Bais et al., 2002; 2003; Perry et al., 2005). (-)-Catechin exhibited allelopathic activity by inhibiting growth and germination of other native plant species, whereas (+)-catechin was inactive (Bais et al., 2002). The allelopathic activity of (-)-catechin was confirmed by its isolation together with (+)-catechin from soil collected from spotted knapweed-invaded fields (Bais et al., 2002; 2003; Perry et al., 2005). Interestingly, (+)-catechin (**4**) exhibited antibacterial activity against root-infesting pathogens, a property that (-)-catechin did not have. These observations suggested the biological significance of root exudation of the racemic mixture of catechins (Bais et al., 2002). One other example of successful invasive weed is *Mikania micrantha* (bittervine), a native to South and Central America that has become a serious problem in Southeast Asia and Pacific regions (Shao et al., 2005). Bittervine suppresses the growth of crops and trees in its neighborhood leading to their eventual death. Chemical analysis of aerial extracts of bittervine led to the isolation and identification of three compounds, dihydromikanolide (**5**), deoxymikanolide (**6**), and 2,3-epoxy-1-hydroxy-4,9-germcradiene-12,8:15,6-diolide (**7**). All the three compounds were found to inhibit seed germination and radicle elongation of other plant species. The three compounds were therefore thought to be responsible for the allelopathic activity of bittervine (Shao et al., 2005).

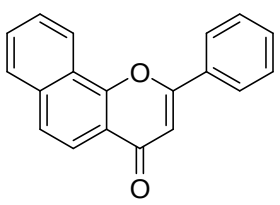

2

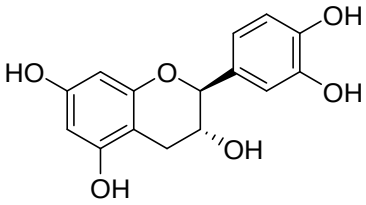

3

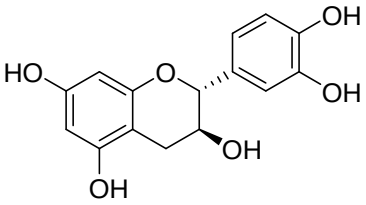

4

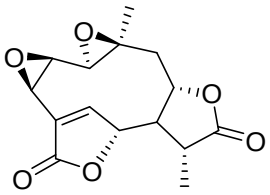

5

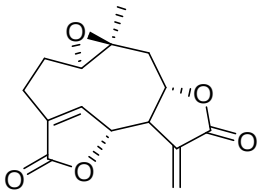

6

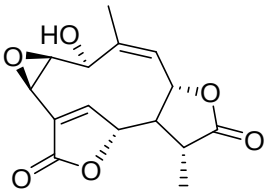

7

Many *Oryza sativa* (rice) varieties inhibited growth of several plant species including weeds when they were grown together under field and/or laboratory conditions. These observations have suggested that probably rice produces and releases allelochemicals into the neighboring environment causing the inhibitory effect on other plant species (Kato-Noguchi, 2004; Kato-Noguchi and Ino, 2004; Kong et al., 2006). Chemical investigation of rice root exudates led to the isolation of momilactone B (**8**) as the possible allelopathic candidate. Momilactone B was previously isolated from rice leaves, husks and straw as growth inhibitor, Kato-Noguchi and co-workers (2002) later isolated momilactone B from rice root exudates for the first time. Bioassays revealed that momilactone B was an active allelopathic compound that inhibited the growth of lettuce, *Lepidium sativum* (cress), and *Medicago sativa* (alfalfa) (Kato-Noguchi et al., 2002; 2004; Kato-Noguchi and Ino, 2004).

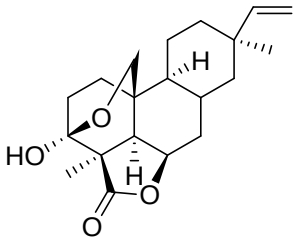

8

Plant secondary metabolites may also act as feeding and oviposition deterrents against specialized or generalized herbivores (Anaya et al., 2003; Harvey et al., 2005). One such plant species is the *Callicarpa accuminata* (alahualte), a shrub or small tree that was suspected to have allelopathic activity. Chemical investigation of alahualte leaf extracts led to the isolation and characterization of a number of secondary metabolites (Anaya et al., 2003). Laboratory testing of some of the secondary metabolites showed that methyl isopimaric acid (**9**), akhdarenol (**10**), and α-amyrin (**11**) had strong insect anti-feedant activity against *Leptinotarsa decemlineata* (Colorado potato beetle). These tests suggested that these compounds protect alahualte against herbivory by these beetles (Anaya et al., 2003). The fresh water plant *Micranthemum umbrosum* (baby tears) exhibited feeding deterrence to crayfish, a property that was thought to be due to allelopathic compounds produced by this plant species. Chemical analysis of whole plant extract led to the isolation of two compounds, elemicin (**12**), and β-apopicropodophyllin (**13**). In anti-feedant bioassays, the two compounds, **12** and **13**, exhibited remarkable activity against crayfish, suggesting that they are the allelopathic components of baby tears (Lane and Kubanek, 2006).

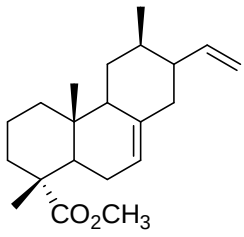

9

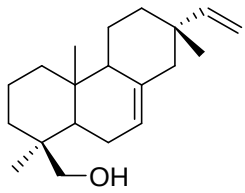

10

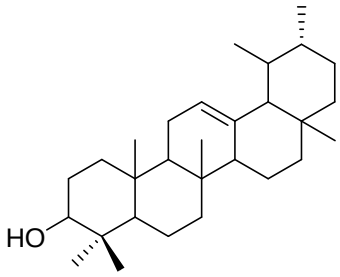

11

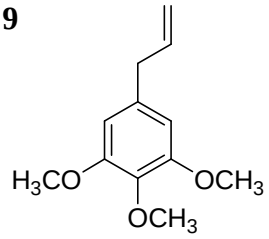

12

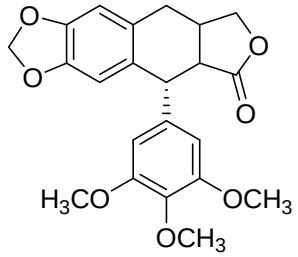

13

A number of plants also respond to various forms of stress including microbial attack by producing *de novo* secondary metabolites that are generally referred to as

phytoalexins. The term phytoalexin was proposed to refer to defensive substances that plants produce during infection (Bailey and Mansfield, 1982). The term was coined from Greek words meaning, “warding-off agents in plants” (Bailey and Mansfield, 1982). Müller and co-workers established that infecting potato (*Solanum tuberosum*) tuber tissues with an incompatible race of *Phytophthora infestans* induces resistance to subsequent infection by inoculation with a compatible race of *P. infestans* or a tuber-infecting *Fusarium* (Hammerschmidt, 1999). Based on these observations, it was hypothesized that the tuber tissues responded to the incompatible interaction by producing compounds (phytoalexins) that inhibited further growth of the pathogen as well as protecting the tissues against later infection (Hammerschmidt, 1999). Following the proposal of phytoalexin concept in 1940, the first antifungal compound that fit the definition of a phytoalexin, (+)-pisatin (**14**) was isolated a few years later from *Pisum sativum* (pea) pods inoculated with fungal spores of *Moniliania fructiocola*. Soon after, a closely related compound, (-)-phaseollin (**15**) was isolated from fungus-inoculated pods of *Phaseolus vulgaris* (beans) (Bailey and Mansfield, 1982). It was further established that phytoalexin production was not only elicited by biotic factors, but also abiotic factors such as mercuric or copper chloride spray (Bailey and Mansfield, 1982).

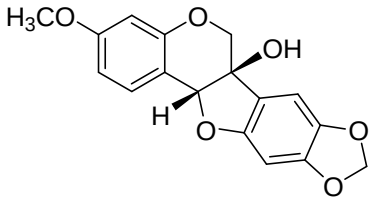

14

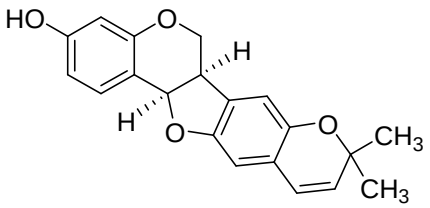

15

Figure 1.1 Chemical structures of (+)-pisatin (**14**) and (-)-phaseollin (**15**).

Since isolation of the first two phytoalexins, many others have been isolated and identified from different plant families (Bailey and Mansfield, 1982). With the progresses in isolation, characterization and understanding of phytoalexins, a working definition for the term phytoalexin has been changed to “low molecular weight antimicrobial compounds produced by plants in response to infection or stress” (Kuć,

1995). Besides microbial attack, phytoalexin accumulation may result from response to stress by elicitors such as inorganic salts, oligoglucans, ethylene, fatty acids, chitosan oligomers, and polypeptides (Kuć, 1995). The localization of phytoalexin production at the site of infection suggests the significant role played by these compounds in response to pathogen invasion (Dixon et al., 1994).

1.3 Cruciferous chemical defenses

Brassicaceae (syn. Cruciferae) is a plant family containing a large number of economically important crops generally referred to as crucifers. The cruciferous crops comprise cabbages (*Brassica oleraceae* var. *capitata*), a variety of vegetables such as broccoli (*B. oleraceae* var. *botrytis*), and kales (*B. oleraceae* var. *acephala*) among others. The crucifer family also comprises a number of economically important oilseeds canola and rapeseed (*B. napus* and *B. rapa*), and condiments such as mustards (*B. juncea*, *B. carinata*, *Sinapis alba*) and wasabi (*Wasabiae japonica*) that are cultivated and consumed worldwide (Pedras et al., 1998; 2000). Most of the cultivated crucifers are susceptible to a number of fungal diseases leading to massive yield losses. The disease resistance of cruciferous plants (like in many other plant species) can be attributed to complex metabolic processes involving both induced (phytoalexins) and constitutive (phytoanticipins) chemical defenses (Pedras and Sorensen, 1998; Pedras et al., 2000).

A number of wild crucifers have been reported to exhibit resistance to a variety of crucifer pathogens. For example, *Camelina sativa* (false flax), *Capsella bursa-pastoris* (Shepherd's purse) and *Eruca sativa* (rocket) were reported to exhibit resistance against *Alternaria brassicae* (Conn et al., 1988). *Erucastrum gallicum* (dog mustard) was reported to exhibit resistance against *Sclerotinia sclerotiorum*, a fungal pathogen that causes stem rot disease of crucifers and many other plant families (Lefol et al., 1997). Resistance of *Thlaspi arvense* (stinkweed/pennycress) against blackleg disease has also been reported (Gugel et al., 1990). The blackleg disease of crucifers is caused by the fungus *Leptosphaeria maculans* (Desm.) Ces et de Not. [asexual stage *Phoma lingam* (Tode ex Fr.) Desm.]. Some cultivated crucifers have been reported to exhibit resistance to the devastating effect of fungal pathogens. For example, *Sinapis alba* (white mustard) exhibited resistance to economically important diseases of crucifers such as Alternaria

blackspot and Phoma blackleg that are caused by the fungal pathogens *A. brassicae* and *L. maculans*/*P. lingam*, respectively (Pedras and Zaharia, 2000).

1.3.1 Phytoalexins

Crucifer phytoalexins were the first sulfur-containing phytoalexins reported (Takasugi et al., 1986). Brassinin (**16**), 1-methoxybrassinin (**18**), and cyclobrassinin (**28**) were isolated from Chinese cabbage (*B. campestris* L. ssp. *pekinensis*) following inoculation with the bacterium *Pseudomonas cichorri* (Takasugi et al., 1986) (**Figure 1.2**). Since this first isolation, close to 40 crucifer phytoalexins have been reported (**Figures 1.2**). Several of these phytoalexins have been isolated and characterized from more than one plant species, and their elicitation by diverse pathogens and/or abiotic factors has been demonstrated (Pedras et al., 2007b). Considering the early development and wide use of dithiocarbamate fungicides and pesticides, it is interesting to note that crucifers are the only plants reported to produce compounds containing as toxophore a dithiocarbamate or thiocarbamate group (**16**, **17**, **18**, **19**, **20**) (Pedras et al., 2007b). A general structural characteristic among the crucifer phytoalexins includes the presence of an indole ring or derivative with substitution at C-3 and additional nitrogen or sulfur atoms (**Figure 1.2**). The only non-sulfur containing crucifer phytoalexins are methyl 1-methoxyindole-3-carboxylate (**47**), caulexin B (**48**), indolyl-3-acetonitrile (**49**), caulexin C (**50**), arvelexin (**51**), and isalexin (**52**) (**Figure 1.2**). The synthesis and biosynthesis of crucifer phytoalexins was recently reviewed (Pedras et al., 2007b). Of the 40 crucifer phytoalexins isolated, erucalexin (**38**, isolated from dog mustard) is the first phytoalexin to have a carbon substituent at C-2, whereas all other phytoalexins have carbon substituents at C-3 (Pedras et al., 2006a; 2007b). In mycelial growth inhibition assays, erucalexin displayed remarkable potency against *Rhizoctonia solani* whereas its regioisomer 1-methoxyspirobrassinin (**35**) displayed higher inhibitory effect on *S. sclerotiorum* (Pedras et al., 2006a; Pedras et al., 2007b). Caulilexins A (**42**), B (**48**) and C (**50**) were isolated from cauliflower florets and displayed antifungal activity against *Leptosphaeria maculans*, *R. solani* and *S. sclerotiorum* in mycelial growth inhibition assays (Pedras et al., 2006b; 2007b). Caulilexin A (**42**) is the first known phytoalexin to possess a disulfide bridge and to date it is the most potent phytoalexin against *S.*

sclerotiorum (Pedras et al., 2006b; 2007b). Rapalexins A (**53**) and B (**54**) isolated from *B. rapa* (canola) represent the first known naturally occurring aromatic isothiocyanates (Pedras et al., 2007a; 2007b). Both **53** and **54** inhibited the germination of *Albugo candida* zoospores on impregnated cellulose membranes, rapalexin A was more potent than B (Pedras et al., 2007a). Wasalexins A (**23**) and B (**24**) were first isolated from wasabi (Pedras et al., 1999; 2007b), they were recently isolated from *Thellungiella halophila* (Pedras and Adio, 2007), whereas wasalexin A was also isolated from stinkweed (Pedras et al., 2003a). Wasalexin A displayed antifungal activity against isolates of *L. maculans* in mycelial growth inhibition assays (Pedras et al., 2003a; 2007b), as well as inhibition of *L. maculans* spore germination (Pedras et al., 1999; 2007b). Arvelexin (**51**), first isolated from stinkweed, displayed higher antifungal activity against *R. solani* than against *L. maculans* and *S. sclerotiorum* in mycelial growth inhibition assays (Pedras et al., 2003a; 2006b; 2007b). Sinalbins A (**30**) and B (**31**) were first isolated from white mustard (Pedras and Zaharia, 2000; 2007b). Sinalbin A displayed higher activity than sinalbin B in *L maculans* spore germination inhibition assays (Pedras and Zaharia, 2000; 2007b). The phytoalexins rutalexin (**33**), brassicanate A (**43**) and isalexin (**52**) were isolated from rutabaga tubers for the first time (Pedras et al., 2004; 2007b). At the same concentration, brassicanate A completely inhibited mycelial growth of *L. maculans*, *R. solani* and *S. sclerotiorum*, whereas isalexin only displayed moderate antifungal activity against *L. maculans* (Pedras et al., 2004; 2007b). Brassicanals A (**39**) and C (**41**) displayed high antifungal activity against *L. maculans*, but moderate activity against *R. solani* and *S. sclerotiorum* in mycelial growth inhibition assays (Pedras et al., 2006b; 2007b). The two compounds also inhibited conidial germination of *Bipolaris leersiae* (Monde et al., 1991a; Pedras et al., 2007b). Other phytoalexins that inhibited *B. leersiae* conidial germination include, brassicanal B (**40**) (Monde et al., 1990a; Pedras et al., 2007b), brassitin (**17**), 1-methoxyspirobrassinol (**36**), 1-methoxyspirobrassinol methyl ether (**37**) (Monde et al., 1995b; Pedras et al., 2007b), dehydro-4-methoxycylobrassinin (**32**) (Monde et al., 1994b; Pedras et al., 2007b), dioxybrassinin (**25**) (Monde et al., 1991a; Pedras et al., 2007b), 1-methoxybrassenins A (**21**) and B (**22**) (Monde et al., 1991b; Pedras et al., 2007b), 1-methoxybrassinin (**18**), 1-methoxybrassitin (**20**) (Takasugi et al., 1988; Pedras et al., 2007b), and 4-

methoxybrassinin (**19**) (Monde et al., 1990b; Pedras et al., 2007b). The antifungal and antibacterial properties of camalexin (**44**) against many fungi and bacteria have been investigated (Pedras et al., 2007b). For example, camalexin displayed mycelial growth and spore germination inhibition of fungi *L. maculans*, and *A. brassicae*, as well as mycelial growth inhibition of phytopathogenic bacteria *Pseudomona syringae*, *P. cichorii*, *Erwinia carotovora*, and *Xanthomonas campestris* (Pedras et al., 1998b). The antifungal and antibacterial activity of 6-methoxycamalexin (**45**) was investigated with a similar range of phytopathogens as that of camalexin (**44**) (Pedras et al., 2007b), whereas 1-methxylcamalexin (**46**) was found to inhibit germination of *C. cucumerinum* spores (Jimenez et al., 1997; Pedras et al., 2007b). Methyl 1-methoxyindole-3-carboxylate (**47**) inhibited *L. maculans* and *Phoma wasabiae* mycelial growth; it also inhibited spore germination of *C. cucumerinum* on TLC plates (Pedras et al., 2007b; Pedras and Sorensen, 1998). Cyclobrassinin (**28**) and spirobrassinin (**34**) displayed strong inhibitory effects on mycelial growth of *A. brassicae* and spore germination of *C. cucumerinum*, but the two phytoalexins exhibited moderate antifungal activity against *L. maculans*, *R. solani*, *S. sclerotiorum*, *Botrytis cinerea*, *Fusarium nivale*, and *Pithium ultimum* (Dahyia and Rimmer, 1988). The antifungal activity of cyclobrassinin (**28**) and spirobrassinin (**34**) against other fungal species has also been investigated (Pedras et al., 2007b). The structural difference between brassilexin (**26**) and sinalexin (**27**) is the presence of 1-methoxy group in **27**. The two phytoalexins displayed complete inhibition of mycelial growth in *R. solani* and *S. sclerotiorum*, but moderate antifungal activity against *A. brassicae* and *L. maculans* at same concentrations (Pedras and Zaharia, 2001). Sinalexin (**27**) also inhibited *C. cucumerinum* spore germination in TLC biodetection assays (Pedras and Smith, 1997). Production of 1-methoxy-containing phytoalexins in elicited stinkweed and white mustard indicates the role played by these phytoalexins as a part of defense response to pathogen invasion. Since the last review (Pedras et al., 2007b) one new phytoalexin, brussalexin A (**55**) was isolated from *B. oleracea* var. *gemmifera* (Brussels sprouts) (Pedras et al., 2007c). Brussalexin A is the first phytoalexin known to contain an allyl thiolcarbamate group, a skeletal structure that does not seem to fit with the presently known biosynthetic pathway of crucifer phytoalexins isolated to date (**Figure 1.2**) (Pedras et al., 2007b). In mycelial growth inhibition assays, brussalexin A

displayed higher inhibitory effect against *S. sclerotiorum* than against other pathogens *Alternaria brassicicola*, *L. maculans*, and *R. solani* (Pedras et al., 2007c).

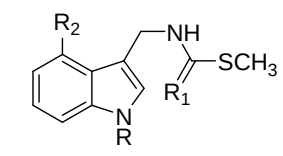

16 R = H; R_1 = S; R_2 = H
17 R = H; R_1 = O; R_2 = H
18 R = OCH_3; R_1 = S; R_2 = H
19 R = H; R_1 = S; R_2 = OCH_3
20 R = OCH_3; R_1 = O; R_2 = H

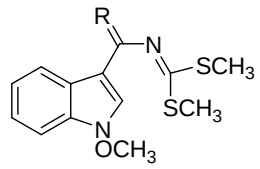

21 R = H_2
22 R = O

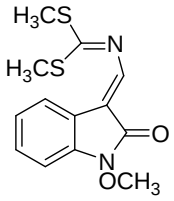

23

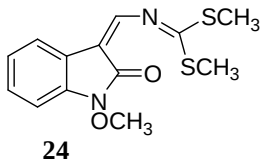

24

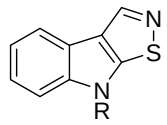

26 R = H
27 R = OCH_3

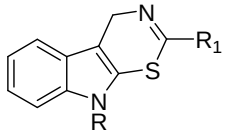

28 R = H; R_1 = SCH_3
29 R = H; R_1 = $S(O)CH_3$
30 R = OCH_3; R_1 = $S(O)CH_3$
31 R = OCH_3; R_1 = SCH_3

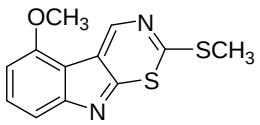

32

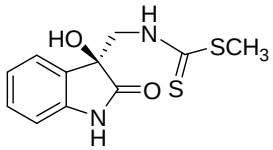

25

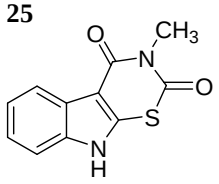

33

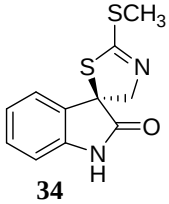

34

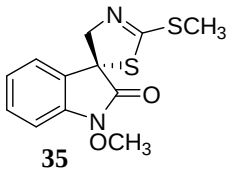

35

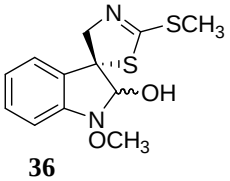

36

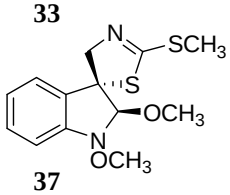

37

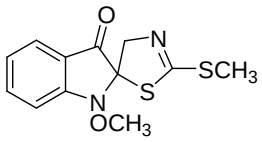

38

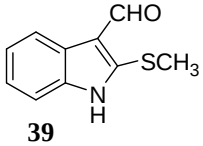

39

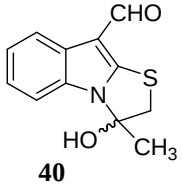

40

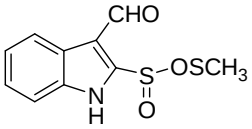

41

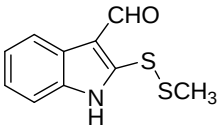

42

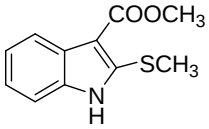

43

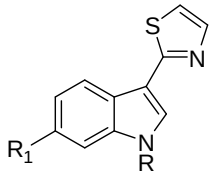

44 R = R_1 = H_2
45 R = H; R_1 = OCH_3
46 R = CH_3; R_1 = H

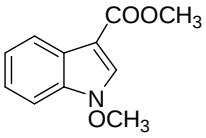

47

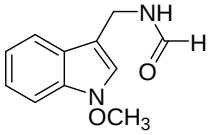

48

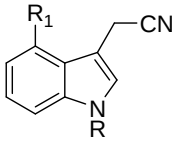

49 R = R_1 = H_2
50 R = OCH_3; R_1 = H
51 R = H; R_1 = OCH_3

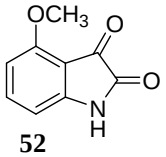

52

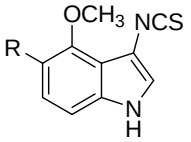

53 R = H
54 R = OH

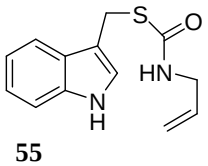

55

Figure 1.2 Structure of cruciferous phytoalexins: brassinin (**16**), brassitin (**17**), 1-methoxybrassinin (**18**), 4-methoxybrassinin (**19**), 1-methoxybrassitin (**20**), 1-methoxybrassenin A (**21**), 1-methoxybrassenin B (**22**), wasalexin A (**23**), wasalexin B (**24**), dioxibrassinin (**25**), brassilexin (**26**), sinalexin (**27**), cyclobrassinin (**28**), cyclobrassinin sulfoxide (**29**), sinalbin A (**30**), sinalbin B (**31**), dehydro-4-methoxycyclobrassinin (**32**), rutalexin (**33**), (*S*)-spirobrassinin (**34**), (*R*)-1-methoxyspirobrassinin (**35**), 1-methoxyspirobrassinol (**36**), (2*R*,3*R*)-1-methoxyspirobrassinol methyl ether (**37**), erucalexin (**38**), brassicanal A (**39**), brassicanal B (**40**), brassicanal C (**41**), caulilexin A (**42**), brassicanate A (**43**), camalexin (**44**), 6-methoxycamalexin (**45**), 1-methylcamalexin (**46**), methyl 1-methoxyindole-3-carboxylate (**47**), caulilexin B (**48**), indolyl-3-acetonitrile (**49**), caulilexin C (**50**), arvelexin (**51**), isalexin (**52**), rapalexin A (**53**), rapalexin B (**54**), brussalexin A (**55**) (Pedras et al., 2007b; 2007c).

1.3.2 Phytoanticipins

Constitutive chemical defenses exist in healthy plants in their biologically active form, or as inactive precursors that are activated in response to tissue damage or pathogen attack. The activation of these chemical defenses involves plant enzymes that breakdown the preformed compounds to release biologically active products (Osbourne, 1996). The preformed compounds have been referred to as phytoanticipins in order to distinguish them from phytoalexins (biosynthesized *de novo*), the name phytoanticipins was coined by Mansfield (VanEtten et al., 1994). Phytoanticipins were thus defined as "low molecular weight antimicrobial compounds that are present in plants before challenge by microorganism or are produced after infection solely from preexisting constituents" (VanEtten et al., 1994). A large number of phytoanticipins exhibit antifungal activity and these include phenols and phenolic glycosides, unsaturated lactones, sulfur compounds, saponins, cyanogenic glycosides, and glucosinolates (Osbourne, 1996).

Since the isolation of the first two glucosinolates sinigrin (**56**) and sinalbin (**57**) (**Figure 1.3**) from black (*B. nigra*) and white (*S. alba*) mustard seeds, respectively, in the 1980s, about 120 glucosinolates have been isolated and characterized (Fahey et al., 2001; Halkier and Gershenzon, 2006). The importance of these nitrogen- and sulfur-containing compounds has increased following their discovery as potential cancer-

preventing agents, crop-protection compounds, and biofumigants in agriculture (Halkier and Gershenzon, 2006; Sarwar et al., 1998). Although glucosinolates have been reported almost exclusively from the order Capparales, which contain 15 families including Brassicaceae, some glucosinolates have been isolated from the genus *Drypetes* from the family Euphorbiaceae that is completely unrelated to other glucosinolate containing families (Halkier and Gershenzon, 2006). Structurally glucosinolates are β-D-thioglucoside *N*-hydroxysulfates also know as (*Z*)-*N*-hydroximinosulfate esters or *S*-glucopyranosyl thiohydroximates with a side chain R (**58**) (**Figure 1.3**, Fahey et al., 2001; Halkier and Gershenzon, 2006).

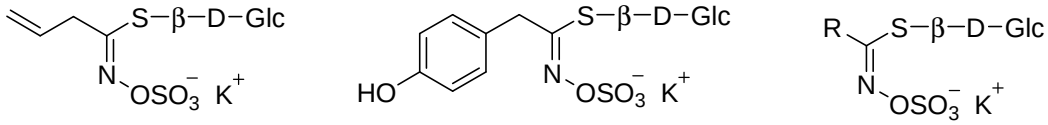

56 **57** **58**

Figure 1.3 Chemical structures of sinigrin **(56),** sinalbin **(57),** and glucosinolates **(58)**.

Glucosinolates are derived from one of the eight amino acids and are classified by their precursor amino acids and types of modification to the side chain (Halkier and Gershenzon, 2006). Those derived from alanine, leucine, isoleucine, methionine, or valine are called aliphatic glucosinolates, those derived from phenylalanine and tyrosine are called aromatic glucosinolates, and those derived from tryptophan are called indolyl glucosinolates (Halkier and Gershenzon, 2006). All the three classes of glucosinolates, i.e. aliphatic, aromatic and indolyl glucosinolates have been isolated from Brassicaceae family (Fahey et al., 2001). Glucosinolates have been used as taxonomic markers to support evolution based classification schemes (Fahey et al., 2001; Mithen et al., 1987). Methyl glucosinolate, for example, does not occur in Brassicaceae, but is found in the closely related Capparaceae. Glucosinolates having glycosylated R-groups appear to be majorly produced by the families Resedaceae and Moringaceae (Fahey et al., 2001).

Glucosinolate producing plants also possess thioglucosidases known as myrosinases that occur in a cell compartment (myrosin cells) different from the

glucosinolates (vacuole) (Bones and Rossiter, 2006; Grubb and Abel, 2006; Rask et al., 2000). Upon tissue damage, myrosinases are released and they hydrolyze the glucose moiety of the respective glucosinolates located in the vacuoles to yield glucose and an unstable aglycone (**59**) that can rearrange to form isothiocyanates (**60**), thiocyanates (**61**), nitriles (**62**), oxazolidine-2-thione (**63**), and other products that possess biological (including antifungal) activity (**Figure 1.4**, Bones and Rossiter, 2006; Halkier and Gershenzon, 2006; Rask et al., 2000). Some of these degradation products are also responsible for distinctive flavor of the members of Brassicaceae family (Rask et al., 2000).

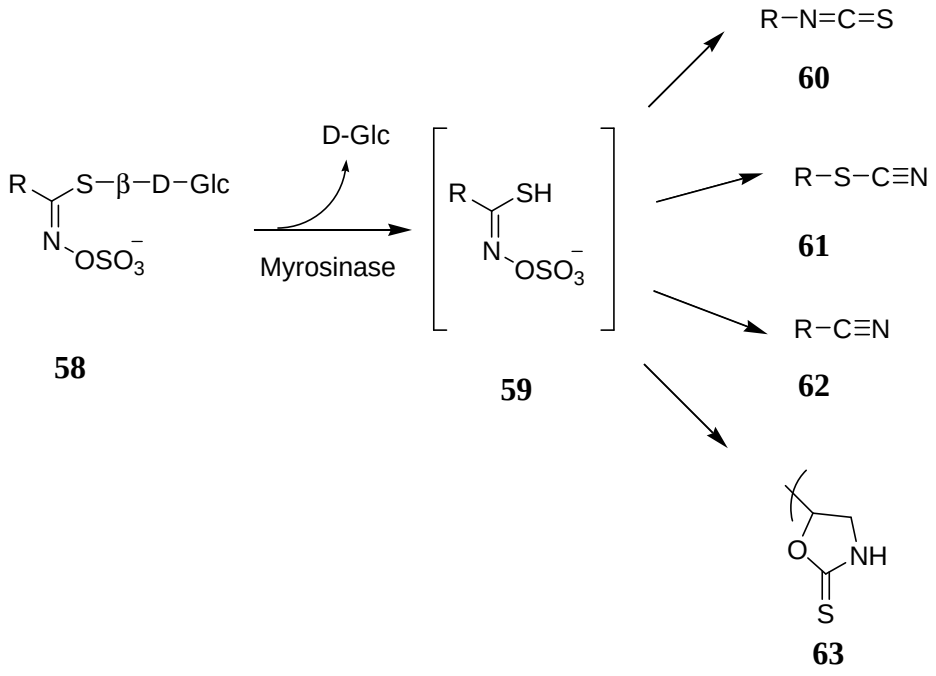

Figure 1.4 Products of degradation and rearrangement of glucosinolates (**58**) (Bones and Rossiter, 2006; Halkier and Gershenzon, 2006; Grubb and Abel, 2006).

A number of studies have been carried out to determine whether glucosinolates and/or their degradation products play a significant role in plant defense. Studies correlating glucosinolate contents of different plant genotypes to their disease resistance levels have been performed. It was reported that the pathogen resistance of various *Brassica* species does not correlate with the glucosinolate levels (Doughty et al., 1991;

Giamoustaris and Mithen, 1992; Mithen and Magrath, 1992). On the other hand, Li and co-workers (1999) noted a correlation between pathogen-induced production of indole glucosinolates on oilseed rape and its resistance to *S. sclerotiorum*. These observations suggested that glucosinolates have a role in microbial disease resistance (Li et al., 1999). Similarly, the level of indolyl glucosinolates increased in the model plant *A. thaliana* upon inoculation with the plant pathogen *Erwinia carotovora*; the increase was attributed to the induction of indolyl glucosinolate biosynthetic pathway by this pathogen (Brader et al., 2001). Since the concentration of the phytoalexin camalexin (**44**) from *A. thaliana* did not increase significantly when compared to the accumulation of indolyl glucosinolates, these results suggested the importance of glucosinolates in defense against the plant bacterium *E. carotovora* (Brader et al., 2001). The antimicrobial activities of some glucosinolate degradation products against various plant pathogens (inhibition of pathogen growth or production of spores) have been investigated and compared with those of parent glucosinolates (Brader et al., 2001; Manici et al., 1997; 2000; Mayton et al., 1996; Olivier et al., 1999; Mithen et al., 1986). From a comparative study of the antifungal activity of several isothiocyanate breakdown products, it was shown that aromatic isothiocyanates are more potent than aliphatic isothiocyanates against various fungal pathogens. A general trend was noted in which the fungal toxicity of aliphatic isothiocyanates decreased with increasing side chain length (Manici et al., 1997; Mithen et al., 1986; Sarwar et al., 1998). Although these studies showed that the various breakdown products of glucosinolates had antimicrobial activity, additional evidence for their significant role in protecting plants against various pathogens was shown in the model plant *A. thaliana* (Tierens et al., 2001). In their investigation, Tierens and co-workers found that 4-methylsulphinylbutyl isothiocyanate (**64**), a degradation product of 4-methylsulphinylbutyl glucosinolate (**65**), accumulated in *A. thaliana* wild type leaves but was absent in glucosinolate-deficient *gsm1-1* mutant. 4-Methylsulphinylbutyl isothiocyanate displayed antimicrobial activity against a number of fungi and bacteria in growth inhibition bioassays (Tierens et al., 2001). Manici and co-workers established that 3-methylsulfinylpropyl isothiocyanate (**66**) could completely inhibit the growth of the plant pathogens *Fusarium culmorum*, *R. solani*, *S. sclerotiorum*, *Diaporthe phaseolorum*, and *Phythium irregulare*, whereas the parent compound

glucoiberin (3-methylsulfinylpropyl glucosinolate, **67**) was inactive towards these fungi (Manici et al., 1997; 2000).

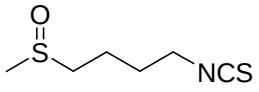

64

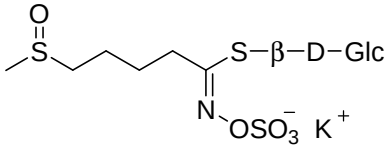

65

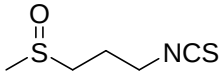

66

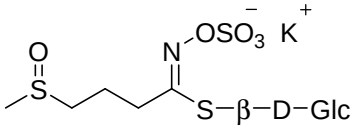

67

Volatiles from macerated leaves of genotypes of the crucifers, black mustard (*Brasssica nigra*) and Indian mustard (*B. juncea*), were shown to inhibit fungal growth and sporulation in two plant pathogens, *Helminthosporium solani* and *Verticillium dahliae* (Mayton et al., 1996; Olivier et al., 1999). Whereas cultivars of black and Indian mustard predominantly produce allyl glucosinolate, sinigrin (**56**) (Daxenbichler et al., 1991, Olivier et al., 1999), GC analyses of their macerated leaf volatiles showed that allyl isothiocyanate (**68**) (enzymatic hydrolysis product of **56**) was the major volatile component and that its production significantly varied in different genotypes (Olivier et al., 1999). The fungicidal activity of the genotypes investigated was reported to correlate with the production of allyl isothiocyanate (**68**); for example, genotypes producing higher amounts of allyl isothiocyanate also exhibited higher fungitoxicity (Olivier et al., 1999). Allyl isothiocyanate obtained from commercial sources or derived from *B. juncea* was shown to exhibit fungitoxicity against *Pennicilium expansum* strains that were resistant to the synthetic fungicide thiabendazole (**69**) (Mari et al, 2002). It was shown that allyl isothiocyanate could reduce the incidence of blue mould caused by *P. expansum* by as much as 90% (Mari et al, 2002), thus making it a potential biofungicide that can be used to control the devastating effects of this pathogen. Allyl isothiocyanate also showed remarkable fungitoxity towards *L. maculans*, an economically important pathogen of crucifers (Mithen et al., 1986).

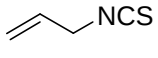

68

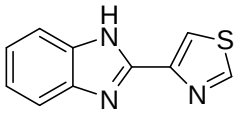

69

Mithen and co-workers (1986) investigated the antifungal activity of glucobrassicin (**70**) and its degradation products against *L. maculans*. From these investigations, it was reported that a mixture of glucobrassicin and myrosinase significantly inhibited fungal growth in the cultures compared to glucobrassicin alone (Mithen et al., 1986). Antifungal bioassays were also conducted with indole-3-methanol (**71**), indolyl-3-acetonitrile (**49**) and 3,3'-diindolylmethane (**72**) (Mithen et al., 1986), the degradation products of glucobrassinin (**70**) (Hanley et al., 1990). The three compounds **49**, **71** and **72** reportedly showed stronger antifungal activity against *L. maculans* than the parent glucobrassicin (**70**), and indole-3-methanol (**71**) had the greatest activity (Mithen et al., 1986). 2-Phenylethyl glucosinolate (**73**) is the dominant glucosinolate of canola roots (Gardiner et al. 1999). In antimicrobial bioassays using phenylethyl isothiocyanate (**74**), a degradation product of phenylethyl glucosinolate (**73**), **74** inhibited the growth of a range of fungi, oomycetes and bacteria (Smith and Kirkegaard, 2002). The results obtained supported the possible application of these compounds in biofumigation to control soil pathogens.

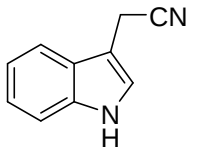

49

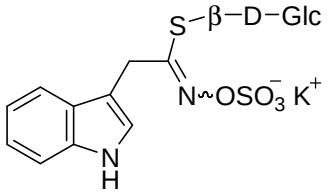

70

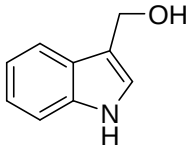

71

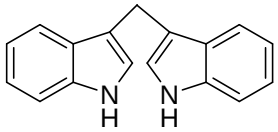

72

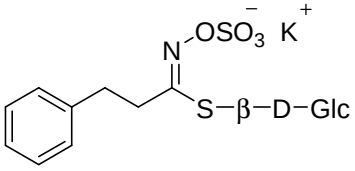

73

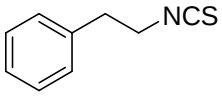

74

Besides antimicrobial activity, several studies have shown that glucosinolates and their degradation products play a significant role in plant-insect interaction. These activities include stimulation of insect feeding and oviposition, direct plant defense by acting as feeding deterrents (including mammals, birds), and indirect defense by providing cues to natural enemies of the herbivores (Baker et al., 2006; Halkier and Gershenzon, 2006; Rask et al., 2000). Glucosinolates and their volatile degradation products that protect plants against some herbivores may also attract specialized herbivores or serve as oviposition stimulants (Gabrys and Tjallingii, 2002; Mewis et al., 2002). Sinigrin **(56)** for example acted as a feeding detterent to *Acyrthosiphon pisum* (pea aphid), but attracted *Brevicoryne brassicae* (cabbage aphids) to a non-host plant (Gabrys and Tjallingii, 2002). Non-host plants treated with extracts from host plants stimulated oviposition behavior of cabbage webworm, *Hellula hundalis* (Mewis et al., 2002). Chemical analysis of the host plant (white mustard) extracts revealed that it predominantly contained aromatic glucosinolates, sinalbin (**57**) and benzyl glucosinolate (**75**), unlike the less preferred plants that contained higher amounts of aliphatic and indolyl glucosinolates (Mewis et al., 2002). Stimulation of oviposition in cabbage root fly (*Delia radicum*) was attributed to indolyl glucosinolate, glucobrassicin (**70**) (Roessingh et al., 1992), whereas both aliphatic alkenyl glucosinolates 3-butenyl- (**76**) and 4-pentenyl glucosinolates (**77**) and glucobrassicin (**70**) stimulated oviposition behavior in turnip root fly (*D. floralis*) (Simmonds et al., 1994). Both flies possessed chemoreceptors that responded to different glucosinolates, the response was correlated to the number of eggs laid (Roessing et al., 1992; Simmonds et al., 1994). Sinigrin (**56**), **s**inalbin (**57**), and allyl isothiocyanate (**68**) triggered oviposition-probing behavior of turnip sawfly (*Athalia rosae*), these findings indicated that both glucosinolates and their degradation products play a significant role in host-finding and oviposition among insects (Baker et al., 2006). The volatile isothiocyanates derived from short chain aliphatic glucosinolates may serve to attract insects from a distance and help them to locate the host plant, whereas glucosinolates within leaf surface waxes (e.g. indolyl glucosinolates) may serve as stimulants for egg laying (Giamoustaris and Mithen, 1995; Renwick, 2002).

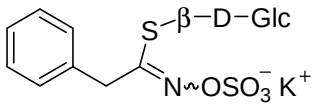

75

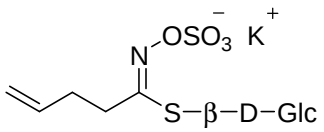

76

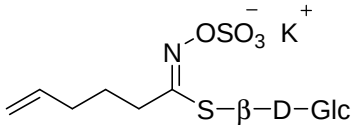

77

Various studies have demonstrated that plants respond to insect herbivory by accumulating higher levels of glucosinolates presumably to increase the plants resistance to subsequent attacks (Agrawal et al., 2002; Mewis et al., 2005; Traw, 2002; van Dam et al., 2005). The levels of sinigrin (**56**) and glucobrassicin (**70**) were found to increase by 19 and 16%, respectively, in black mustard when fed on by white butterfly (Traw, 2002). Some plants use glucosinolate degradation products to protect themselves against specialist herbivores. For example, allyl isothiocyanate (**68**), but not allyl glucosinolate sinigrin (**56**) reduced the growth and survival of the crucifer specialist, *Pieris rapae* (white butterfly) (Agrawal and Kurashige, 2003). Although glucosinolates and their degradation products may be advantageous to specialist herbivores (e.g. host-recognition and feeding stimulation), they are deleterious to generalists. Sinigrin and its allyl isothiocyanate degradation product were found to be lethally toxic to the crucifer generalist *Spodoptera eridania* (southern armyworm), whereas the specialist *Plutella xylostella* (cabbage moth) was only affected by allyl isothiocyanate (Li et al., 2000). Developing plant lines with increased levels of glucosinolates resulted in greater damage by the specialists, while reducing grazing levels by the generalists (Giamoustaris and Mithen, 1995). The Brassicaceae specialists seemed to respond to particular glucosinolates, suggesting that the plant glucosinolate profile is more important for plant-insect interaction rather than the total glucosinolate concentration (Giamoustaris and Mithen, 1995). The specialists adapted to particular crucifers have developed mechanisms for overcoming the toxic effect of glucosinolates, including rapid excretion, inhibition of hydrolysis, or sequestering the glucosinolates (Barker et al., 2006; Halkier

and Gershenzon, 2006; Renwick, 2002). The insects that sequester glucosinolates use them for their own protection by dettering predators such as birds, lizards and ants (Halkier and Gershenzon, 2006).

1.4 Biosynthetic studies in crucifers

Cruciferous plants produce phytoalexins and phytoanticipins of diverse chemical structures. These secondary metabolites play a role in protecting plants against various pathogens and have other biological activities, including cytotoxicity and oviposition stimulation, as described in previous sections (Halkier and Gershenzon, 2006; Pedras et al., 2007b). Understanding of the biosynthetic pathways of these secondary metabolites is of vital importance, as this will facilitate the transfer of genes from a resistant to a susceptible species (Dixon, 2005). Such genetic manipulations will allow the susceptible species to produce secondary metabolites that may confer resistance to pathogens (Dixon, 2005).

1.4.1 Syntheses of precursors

Biosynthetic investigations can involve administration of precursors (labeled or non-labeled) to enzyme preparations or *in vivo* feeding experiments employing cell cultures or plant stems, roots, or leaves. Labeling experiments using stable isotopes, radioisotopes, or non-natural substrates allows for the quantification of incorporation and mapping of biosynthetic pathways.

1.4.1.1 L-Tryptophan and tryptamine

This section covers the synthesis of *L*-[4'-^{2}H]tryptophan (**78a**) and [2',4',5',6',7'-$^{2}H_5$]tryptamine (**79a**).

[4'-^{2}H]Tryptophan (79a)

The *L*-[4'-^{2}H]tryptophan (**78a**) was synthesized from *L*-tryptophan (**78**) by photochemical hydrogen-deuterium exchange reaction (**Scheme 1.1**, Monde et al., 1994; Saito et al, 1984; Shizuka et al., 1988). Thus, irradiation of a solution of *L*-tryptophan in

^2H_2O resulted in incorporation of ^2H into the indole nucleus to give *L*-[4'-^{2}H]tryptophan (Saito et al, 1984; Shizuka et al., 1988).

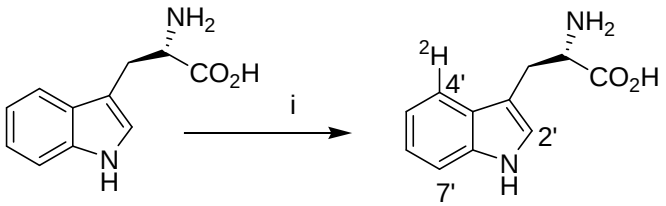

78 **78a**

Scheme 1.1 Reagents and conditions: i) hν, ^2H_2O, p^{2}H 5.5 (Saito et al., 1984; Shizuka et al., 1988).

[2',4',5',6',7'-$^2H_4$]Tryptamine (79a)

[2',4',5',6',7'-$^2H_4$]Tryptamine (**79a**) was prepared from [2',4',5',6',7'-$^2H_5$]tryptophan (**78b**) in one step using catalytic amount of 2-cyclohexene-1-one in cyclohexanol (**Scheme 1.2**, Pedras et al., 2004).

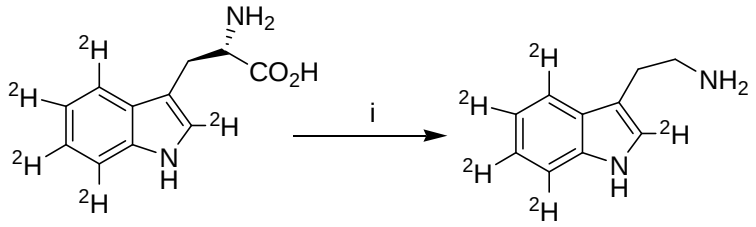

78b **79a**

Scheme 1.2 Reagents and conditions: i) $C_6H_{12}O$, C_6H_8O (Pedras et al., 2004).

1.4.1.2 Thiohydroxamic acids and [4',5',6',7'-$^2H_4$]glucobrassicin (70a)

Thiohydroximic acids are proposed intermediates in the biosynthesis of glucosinolates (Halkier and Gershenzon, 2006; Grubb and Abel, 2006). Thiohydroxamic acids (**80**) contain different atoms: C, S, N, and O and can coordinate with metal ions to form colored complexes that have been utilized in detection and quantification of

different metals (Chimiak et al., 2002). Thiohydroxamic acids also play a significant role in bacterial ion-transport systems (Hwu and Tsay, 1990; Mizukami and Nagata, 1966). Thiohydroxamic acids (**80**) exist in equilibrium with thiohydroximic acids (**81**) (**Figure 1.5**). Whereas the thione (**80**) exist predominantly in the solid state, both thione (**80**) and thiol (**81**) tautomers exist in solution, although the thiol isomer does not occur in significant concentrations (Chimiak et al., 2002; Mizukami and Nagata, 1966).

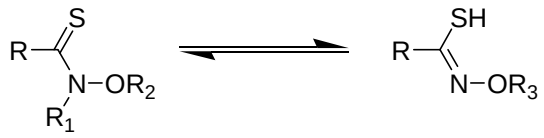

80 **81**

Figure 1.5 Thiohydroxamic acids (**80**) and thiohydroximic acids (**81**): R = alkyl, aryl; $R_1 = R_2 = R_3 = H$ (Chimiak et al., 2002).

Unsubstituted thiohydroxamic acids ($R_1 = R_2 = H$) decompose by extrusion of sulfur to yield nitriles and water (Walter and Schaumann, 1971) whereas N-substituted derivatives (R = aryl; R_1 = aryl; $R_2 = H$) are reportedly stable (Brydan and Ryan, 1966). A number of methods have been developed for synthesis of thiohydroxamic acids based on thioacylation of hydroxylamine and its N- or O-alkyl derivatives, for example, thioacylation of hydroxylamines with dithiocarboxylic acids, dithiocarboxylic acid esters, thionocarboxylic acid esters, or thioacyl chlorides, and also by reaction of hydroximic acid chlorides or nitrile oxides with hydrogen sulfide (Chimiak et al., 2002; Walter and Schaumann, 1971).

Dithiocarboxylates (**83**) obtained by reaction of Grignard reagents (**82**) with carbon disulfide are treated with hydroxylamine to give the respective thiohydroxamic acids (**80**) (**Scheme 1.3**). This method was used to prepare benzohydroxamic acid (Walter and Schaumann, 1971). Reaction of hydroxylamine with dithiocarboxylates (**83**) gives low yields of thiohydroxamic acids, but N- and O-derivatives have been prepared in fairly good yields (Chimiak et al., 2002). This reaction has been used in preparation of alkyl and aromatic thiohydroxamic acids (Walter and Schaumann, 1971). Thiohydroxamic acids can be prepared in good yields from *S*-thioacylthioglycolic acids (**86**) (Walter and Schaumann, 1971) (**Scheme 1.3**). The *S*-thioacylthioglycolic acids (**86**) can be prepared

by reaction of the dithiocarboxylates (**83**) with chloroacetic acid (Jensen and Pedersen, 1961; Ramadas et al., 1983) (**Scheme 1.3**). *S*-Thioacylthioglycolic acids (**86**) have been prepared from dithioacids (**85**) which are obtained from reaction of aldehydes (**84**) with ammonium polysulfide (Jensen and Pedersen, 1961; Ramadas et al., 1983). Treatment of dithioacids (**85**) with chloroacetic acid yields *S*-thioacylthioglycolic acids (**86**) (**Scheme 1.3**). Reaction of the *S*-thioacylthioglycolic acids (**86**) with hydroxylamines or their N- and O-derivatives gives the respective thiohydroxamic acids in good yields of 70-80% (Chimiak et al., 2002; Jensen and Pedersen, 1961; Ramada et al., 1983; Walter and Schaumann, 1971).

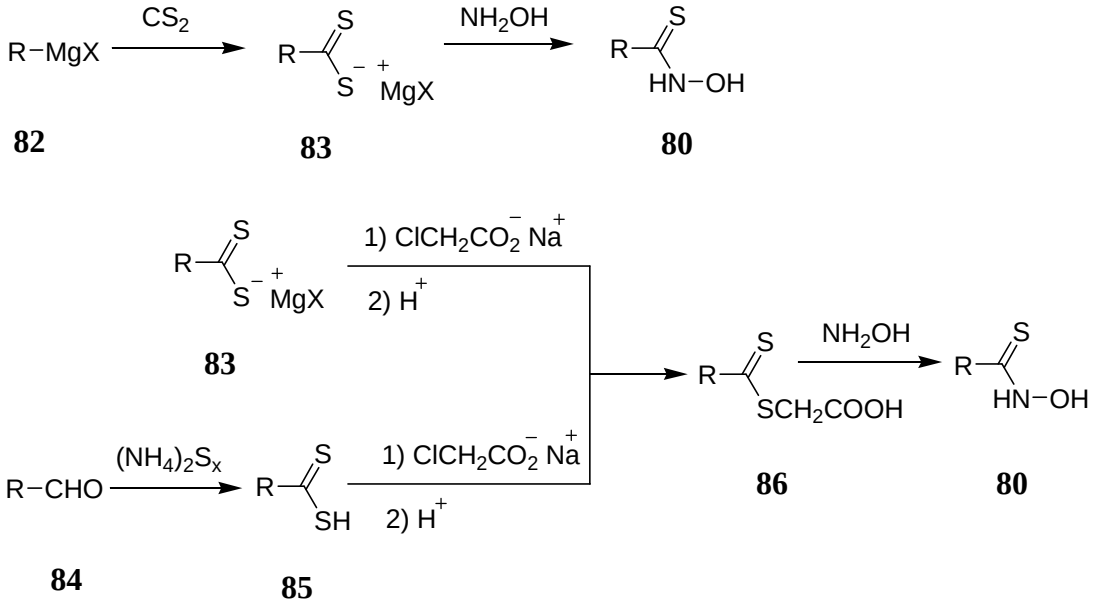

Scheme 1.3 Thioacylation of hydroxylamine with dithiocarboxylate (**83**) and *S*-thioacylthioglycolic acid (**86**); R = alkyl or aryl (Chimiak et al., 2002; Jensen and Pedersen, 1961; Ramada et al., 1983).

Thioacylation of hydroxylamine with thionocarboxylic acid esters (**87**) give thiohydroxamic acids (**80**) in low yields compared to dithiocarboxylic acid esters (**88**) (Chimiak et al., 2002) (**Scheme 1.4**). Thiocarboxylic acid chlorides (**89**) have not found wide application in preparation of thiohydroxamic acids because they are labile compounds and are not easily accessible (Chimiak et al., 2002) (**Scheme 1.4**).

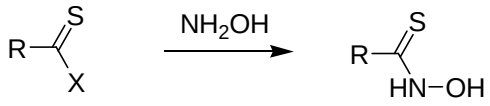

87 X = OMe, OEt
88 X = *S*-alkyl or *S*-aryl
89 X = Cl

80

Scheme 1.4 Thioacylation of hydroxylamine with thiocarboxylic acid esters (**87**), dithiocarboxylic acid esters (**88**), and thiocarboxylic acid chlorides (**89**): R = alkyl or aryl (Chimiak et al., 2002; Walter and Schaumann, 1971).

Nucleophilic attack of hydroximic acid chlorides (**90**) by hydrosulfide ion yields thiohydroxamic acids in low yields. Elimination of hydrogen chloride by hydroximic acid chlorides gives nitrile oxides (**91**) that can react with sodium hydrogen sulfide to yield the respective thiohydroxamic acids in good yields (Chimiak et al., 2002; Walter and Schaumann, 1971) (**Scheme 1.5**).

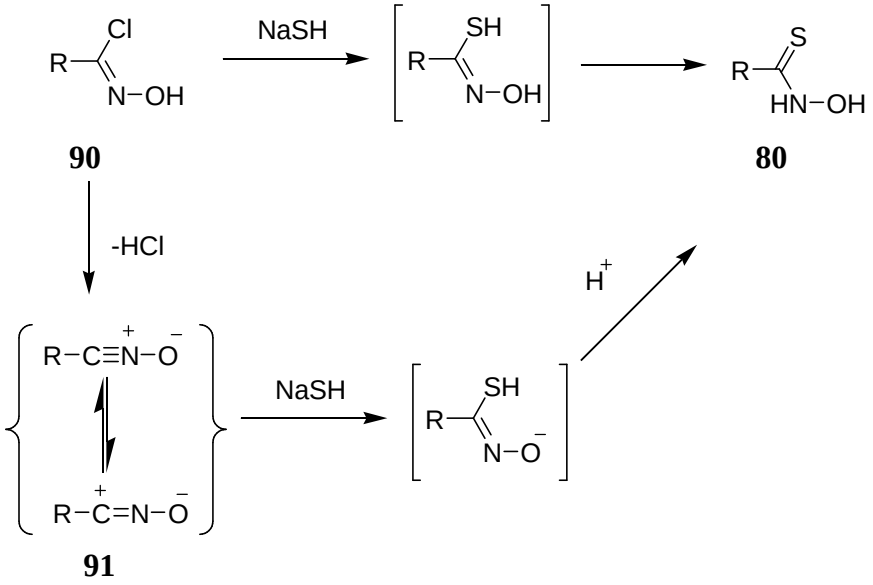

90

80

91

Scheme 1.5 Preparation of thiohydroxamic acids (**80**) from hydroximic acid chlorides (**90**) and nitrile oxides (**91**); R = alkyl or aryl (Chimiak et al., 2002; Walter and Schaumann, 1971).

Direct thionation of hydroxamic acids with Lawesson's reagent have been carried out on N-alkyl derivatives (**92** R^2 = alkyl) to yield N-alkylthiohydroxamic acids (**94**)

(Przychodzen, 2006; Przychodzen et al., 2005) (**Scheme 1.6**). Lawesson's reagent thionation of unsubstituted hydroxamic acids (**93** R^2 = H) does not appear in literature reports, perhaps due to instability of the resulting thiohydroxamic acids (**80**) under these conditions. The most recently developed synthesis of thiohydroxamic acids uses the concept of counterattack reagent. In these preparations, primary nitro compounds (**95**) are treated with potassium hydride, followed by hexamethyldisilathiane [$(CH_3)_3SiSSi(CH_3)_3$] to give thiohydroxamic acids (**80**) in 56-92% (**Scheme 1.6**). This synthesis is a "one-flask" reaction and can be performed in the presence of additional functional groups such as esters, acetals, arenes, and sulfides that are stable under the reaction conditions (Hwu et al., 2005; Hwu and Tsay, 1990; Chimiak et al., 2002).

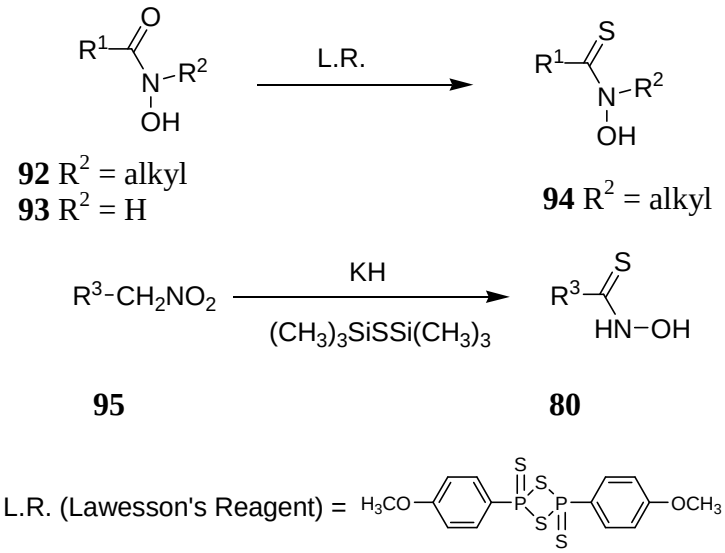

Scheme 1.6 Preparation of thiohydroxamic acids (**80**) and N-alkyl thiohydroxamic acids (**94**); R^1 = alkyl, phenyl, benzyl, R^2 = alkyl, R^3 = alkyl, benzyl, $CH_2CH_2CO_2Et$, (Chimiak et al., 2002; Hwu and Tsay, 1990).

The sodium salts of 2-(3-indolyl)acetothiohydroximate (**99**) and 3-phenylpropanothiohydroximate (**100**) have been prepared from their respective nitriles (**96**) in unreported yields (**Scheme 1.7**, Reed et al., 1993). The nitriles (**96**) are converted to imidate hydrochlorides (**97**) using methanolic hydrochloric acid. Reaction of **97** with hydrogen sulfide gives the thioates (**98**) (Marvel et al., 1955), which are treated with

hydroxylamine hydrochloride in the presence of sodium methoxide to yield the desired thiohydroximate salts (Mizukami and Nagata, 1966; Reed et al., 1993).

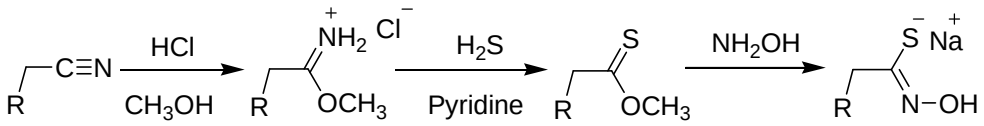

96 R = Indole or R = Benzyl **97** **98** **99** R = Indole **100** R = Benzyl

Scheme 1.7 Synthesis of sodium 2-(3-indolyl)acetothiohydroximate (**99**) and sodium 3-phenylpropanothiohydroximate (**100**) from their respective nitriles (Mizukami and Nagata, 1966; Reed et al., 1993).

[4',5',6',7'-$^{2}H_4$]Glucobrassicin (**70a**) was prepared from [4,5,6,7-$^{2}H_4$]indole (**105a**) as shown in **Scheme 1.8** (Pedras et al., 2002). Firstly, [4,5,6,7-$^{2}H_4$]indole was synthesized starting from [$^{2}H_8$]toluene (**101a**) (Pedras et al., 1998). Treatment of nitric acid with [$^{2}H_8$]toluene in acetic anhydride gave [3,4,5,6-$^{2}H_4$]2-nitrotoluene (**102a**) which was converted to nitrobenzylbromide **103a** with N-bromosuccinimide. The nitrobenzylbromide **103a** was allowed to react with potassium cyanide to give [3,4,5,6-$^{2}H_4$]2-nitrophenylacetonitrile (**104a**). Catalytic reduction of [3,4,5,6-$^{2}H_4$]2-nitrophenylacetonitrile yielded [4,5,6,7-$^{2}H_4$]indole (**105a**). Next, [4,5,6,7-$^{2}H_4$]indole was transformed to [4,5,6,7-$^{2}H_4$]indole-3-carboxaldehyde (**106a**) which was allowed to react with nitromethane to give [4,5,6,7-$^{2}H_4$]-3-(2'-nitrovinyl)indole (**107a**). The [4,5,6,7-$^{2}H_4$]-3-(2'-nitrovinyl)indole was transformed to 1-acetyl-[4,5,6,7-$^{2}H_4$]-3-(2'-nitrovinyl)indole (**108a**) which was reacted with titanium (IV) chloride and triethylsilane, the resulting hyroxymoyl intermediate was then treated with 1-thio-β-D-glucose tetraacetate to give glycosyl thiohydroximate **109a**. The *O*-sulfation of **109a** followed by removal of acetate groups from **110a** gave [4',5',6',7'-$^{2}H_4$]glucobrassicin (**70a**) (**Scheme 1.8**, Pedras et al., 2002).

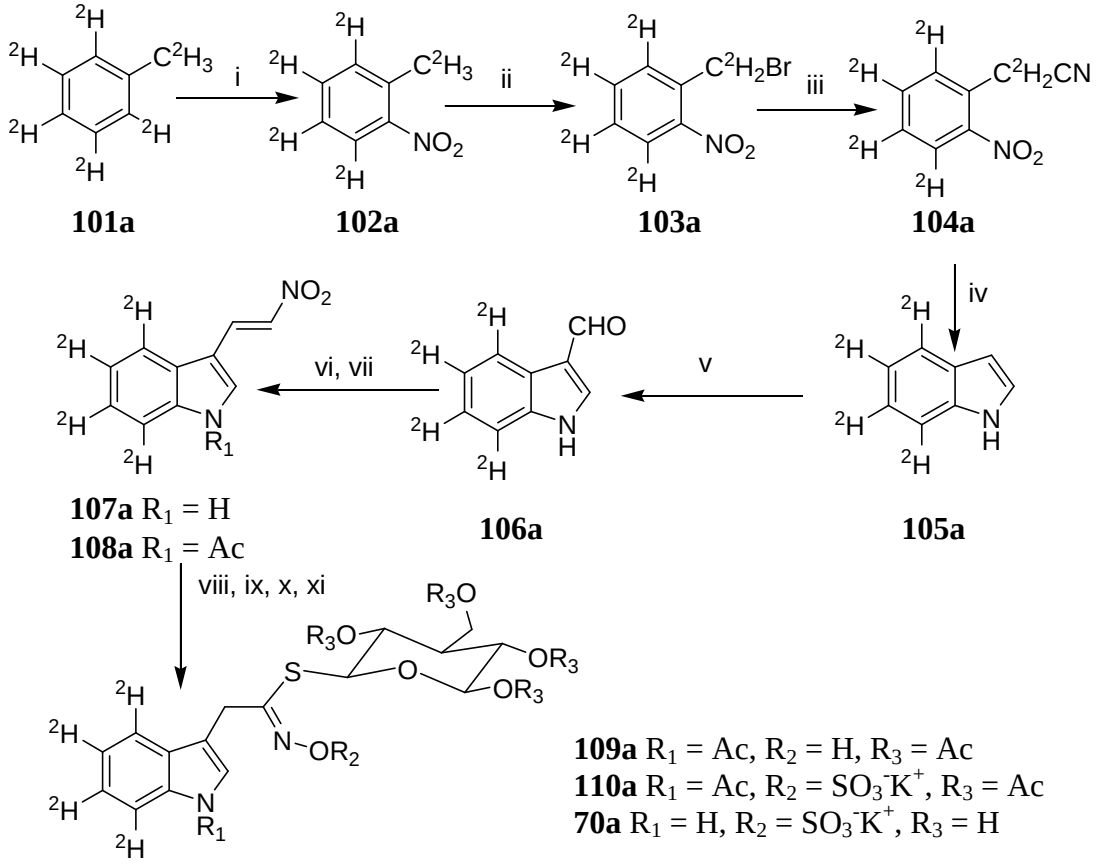

Scheme 1.8 Reagents and conditions: i) HNO_3, Ac_2O; ii) NBS; iii) KCN; iv) H_2, 10% Pd/C; v) DMF/$POCl_3$; vi) CH_3NO_2, NH_4OAc; vii) Ac_2O, DMAP; viii) $TiCl_4$, Et_3SiH; ix) 1-thio-β-D-glucose tetraacetate, Et_3N; x) HSO_3Cl, pyridine, $KHCO_3$; xi) CH_3OK, CH_3OH (Pedras et al., 2002).

1.4.1.3 Synthesis of indolyl-3-acetaldoximes

This section covers the synthesis of [4',5',6',7'-$^2H_4$]indolyl-3-acetaldoxime (**112a**) and [1",1",1"-$^2H_3$]1-methoxyindolyl-3-acetaldoxime (**116a**).

[4',5',6',7'-$^2H_4$]Indolyl-3-acetaldoxime (112a)

[4',5',6',7'-$^2H_4$]Indolyl-3-acetaldoxime (**112a**) was prepared from [4,5,6,7-$^2H_4$]indole-3-carboxaldehyde (**106a**) as shown in **Scheme 1.9** (Pedras et al., 2002). Firstly [4,5,6,7-$^2H_4$]indole-3-carboxaldehyde was transformed to [4',5',6',7'-$^2H_4$]indolyl-3-methoxyethylene (**111a**) which was hydrolyzed to give [4',5',6',7'-$^2H_4$]indolyl-3-acetaldehyde. Treatment of [4',5',6',7'-$^2H_4$]indolyl-3-acetaldehyde with hydroxylamine

hydrochloride and sodium acetate yielded [4',5',6',7'-$^{2}H_4$]indolyl-3-acetaldoxime (**112a**, **Scheme 1.9**) (Pedras et al., 2002).

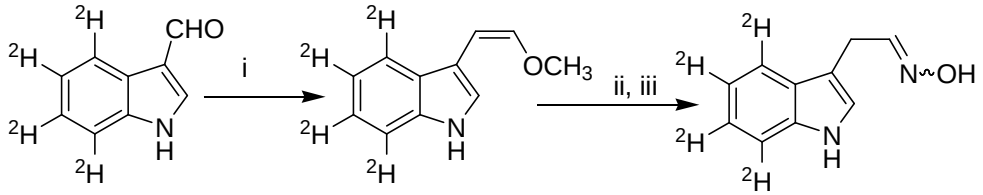

106a **111a** **112a**

Scheme 1.9 Reagents and conditions: i) BuLi, $Ph_3P(Cl)CH_2OCH_3$; ii) HCl, $(CH_3)_2CO$; iii) $HONH_2 \cdot HCl$, NaOAc (Pedras et al., 2002).

[1",1",1"-$^{2}H_3$]1-Methoxyindolyl-3-acetaldoxime (116a)

[1",1",1"-$^{2}H_3$]1-Methoxyindolyl-3-acetaldoxime (**116a**) was synthesized in 6 steps beginning from tryptamine (**Scheme 1.10**) (Pedras and Montaut, 2004). The N_b amino group of tryptamine was acetylated with acetic anhydride in pyridine to provide N_b-acetyltryptamine (**113**) that was reduced with sodium cyanoborohydride in glacial acetic acid to yield N_b-acetyl-2,3-dihyroindolyl-3-ethylamine (**114**). Sodium tungstate catalyzed oxidation of **114** with hydrogen peroxide followed by methylation of the 1-hydroxyindolyl intermediate with hexadeuterated dimethylsulphate (Somei and Kawasaki, 1989) yielded [1",1",1"-$^{2}H_3$]N_b-acetyl-1-methoxytryptamine (**115a**). The N_b-acetyl group was hydrolyzed with sodium hydroxide to provide [1",1",1"-$^{2}H_3$]1-methoxytryptamine which was oxidized with hydrogen peroxide (Burckard et al., 1965) to yield [1",1",1"-$^{2}H_3$]1-methoxyindolyl-3-acetaldoxime (**116a**) (**Scheme 1.10**).

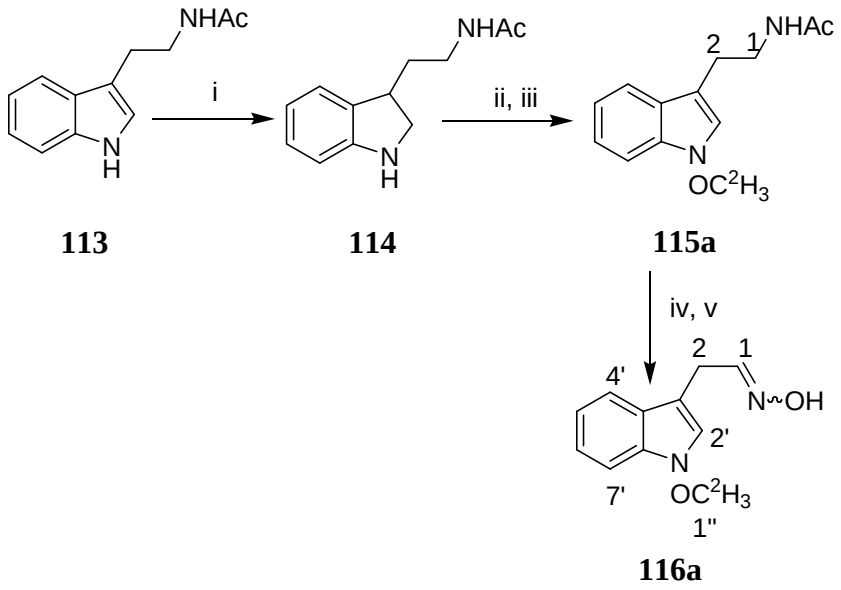

Scheme 1.1.10 Reagents and conditions: i) $NaBH_3CN$, AcOH; ii) $Na_2WO_4 \cdot 2H_2O$, H_2O_2, CH_3OH; iii) $(C^2H_3O)_2SO_2$, K_2CO_3, CH_3OH; iv) NaOH, CH_3OH, reflux; vii) $Na_2WO_4 \cdot 2H_2O$, H_2O_2, CH_3OH, (Pedras and Montaut, 2004).

1.4.1.4 Synthesis of labeled brassinins, cyclobrassinins, and (±)-[3,3,3-$^2H_3$]dioxibrassinin (25b)

This section covers the synthesis of [4',5',6',7'-$^2H_4$]brassinin (**16a**), [3,3,3-$^2H_3$]brassinin (**16b**), [2-^{14}C]brassinin (**16c**), [4',5',6',7'-$^2H_4$]cyclobrassinin (**28a**), [3,3,3-$^2H_3$]cyclobrassinin (**28b**), and (±)-[3,3,3-$^2H_3$]dioxybrassinin (**25b**).

[4',5',6',7'-$^2H_4$]Brassinin (16a), [4',5',6',7'-$^2H_4$]cyclobrassinin (28a)

[4',5',6',7'-$^2H_4$]Cyclobrassinin (**28a**) was synthesized from [4',5',6',7'-$^2H_4$]brassinin (**16a**) as shown in **Scheme 1.11** (Pedras et al., 1998). [4,5,6,7-$^2H_4$]Indole-3-carboxaldehyde (**106a**) was allowed to react with hydroxylamine hydrochloride to yield a mixture of (*E*)- and (*Z*)-oximes that were reduced with Devarda's alloy to yield [4',5',6',7'-$^2H_4$]indole-3-methanamine (**117a**). Reaction of **117a** with carbon disulfide in the presence of pyridine and triethylamine followed by methylation with methyl iodide gave [4',5',6',7'-$^2H_4$]brassinin (**16a**) in 80% (Pedras et al., 1998). Treatment of [4',5',6',7'-

$^{2}H_4$]brassinin with pyridinium bromide perbromide followed by triethylamine gave [4',5',6',7'-$^{2}H_4$]cyclobrassinin in 40% (**Scheme 1.11**).

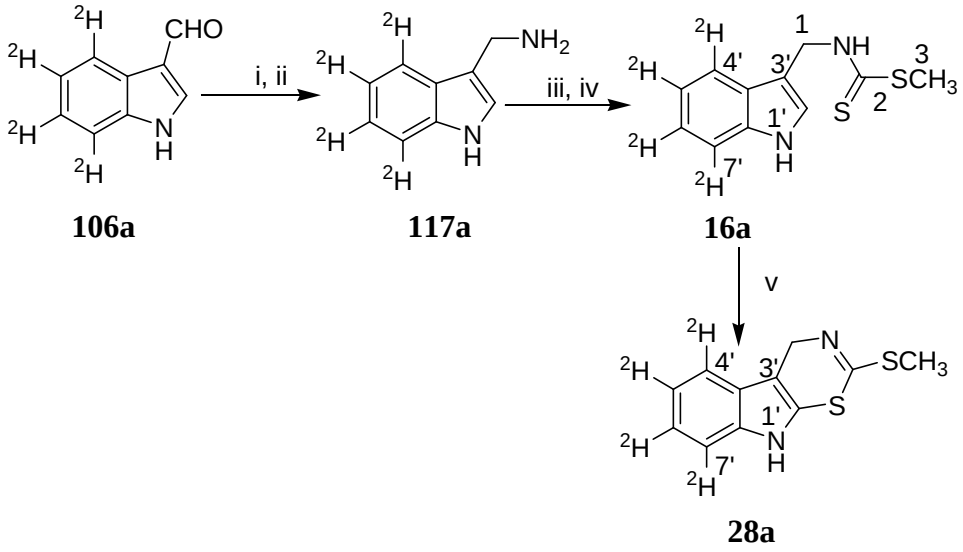

Scheme 1.11 Reagents and conditions: i) $HONH_2 \cdot HCl$, EtOH; ii) NaOH, Devarda's alloy, CH_3OH, 70%; iii) Et_3N, CS_2; iv) ICH_3, 80%; v) pyridine/HBr/Br_2 40% (Pedras et al., 1998).

[3,3,3-$^{2}H_3$]Brassinin (16b) and [3,3,3-$^{2}H_3$]cyclobrassinin (28b)

[3,3,3-$^{2}H_3$]Brassinin (**16b**) and [3,3,3-$^{2}H_3$]cyclobrassinin (**28b**) were synthesized as shown on **Scheme 1.12** (Monde et al., 1994). [3,3,3-$^{2}H_3$]Brassinin (**16b**) was synthesized as described for [4',5',6',7'-$^{2}H_4$]brassinin (**16a**), but starting from indole-3-carboxaldehyde (**106**) (**Scheme 1.12**). [3,3,3-$^{2}H_3$]Cyclobrassinin (**28b**) was prepared in 25% yield from [3,3,3-$^{2}H_3$]brassinin (**Scheme 1.12**) (Monde et al., 1994).

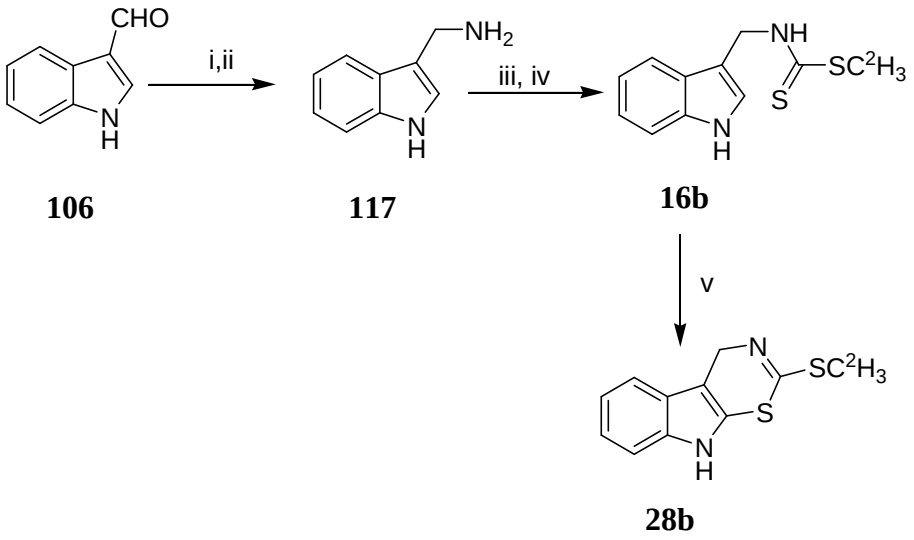

Scheme 1.12 Reagents and conditions: i) $HONH_2 \cdot HCl$, EtOH; ii) NaOH, Devarda's alloy, CH_3OH; iii) Py, Et_3N, CS_2; iv) IC^2H_3, rt, 18 h 34%; v) pyridine/HBr/Br_2, 25% (Monde et al., 1994).

[2-^{14}C]Brassinin (16c)

[2-^{14}C]Brassinin (**16c**) was synthesized from [2-^{14}C]indole (**105b**) as shown in **Scheme 1.13** (Pedras et al., 2002). Formylation of [2-^{14}C]indole gave [2-^{14}C]indole-3-carboxaldehyde (**106b**) which was used to prepare [2-^{14}C]brassinin (**16c**) as described for **16a** (Pedras et al., 2002).

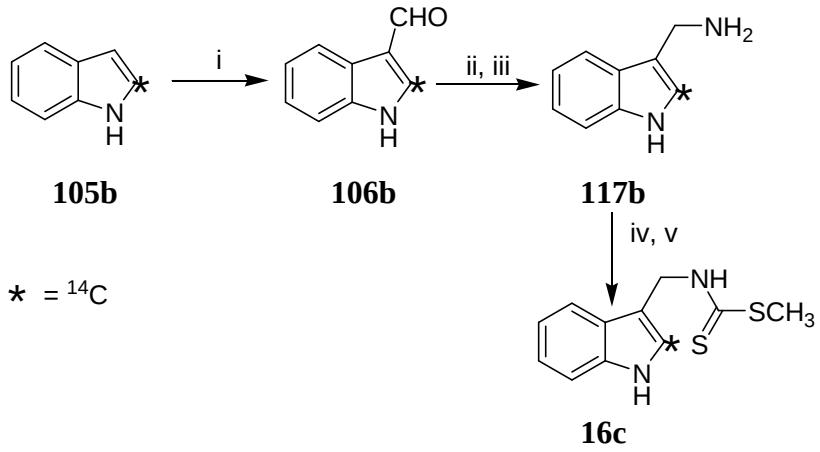

Scheme 1.13 Reagents and conditions: i) $POCl_3$, DMF; ii) $HONH_2 \cdot HCl$, NaOAc; iii) $NaBH_3CN$, $TiCl_3$, NH_4OAc; iii) Pyridine, Et_3N, CS_2; iv) ICH_3 (Pedras et al., 2002).

(±)-[3,3,3-$^2H_3$]Dioxibrassinin (25a)

(±)-[3,3,3-$^2H_3$]Dioxibrassin (**25a**) was synthesized starting from isatin (**118**) (**Scheme 1.14**). Addition of nitromethane to isatin followed by hydrogenation yielded 3-hydroxyindolyl-3-methanamine (**119**). Reaction of amine **119** with carbon disulfide in the presence of pyridine and triethylamine, followed by deuterated methyl iodide (IC^2H_3) yielded [3,3,3-$^2H_3$]dioxybrassinin (**25a**) in 78% (Monde et al., 1994).

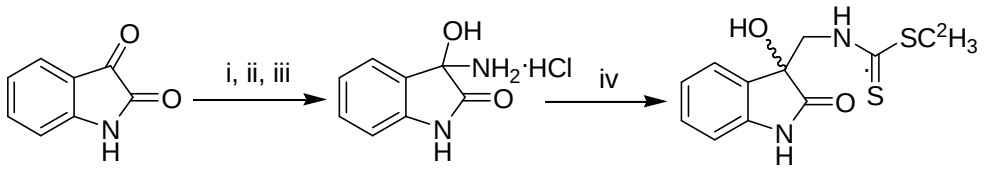

118 **119** **25a**

Scheme 1.14 Reagents and conditions; i) CH_3NO_2; ii) H_2, Pd/AcOH; iii) HCl; iv) Pyridine, Et_3N, CS_2, IC^2H_3, 78% (Monde et al., 1994; Pedras et al., 2003b).

1.4.2 Biosynthesis

The biosynthetic pathways of crucifer phytoalexins and glucosinolates have been mapped via feeding experiments employing synthetic precursors labeled with stable and radio-isotopes, as well as non-natural compounds (Halkier and Gershenzon, 2006; Pedras et al., 2007b).

1.4.2.1 Phytoalexins

The biosynthesis of phytoalexins was previously reviewed by Pedras and co-workers (2003b and 2007b, **Figure 1.6**).

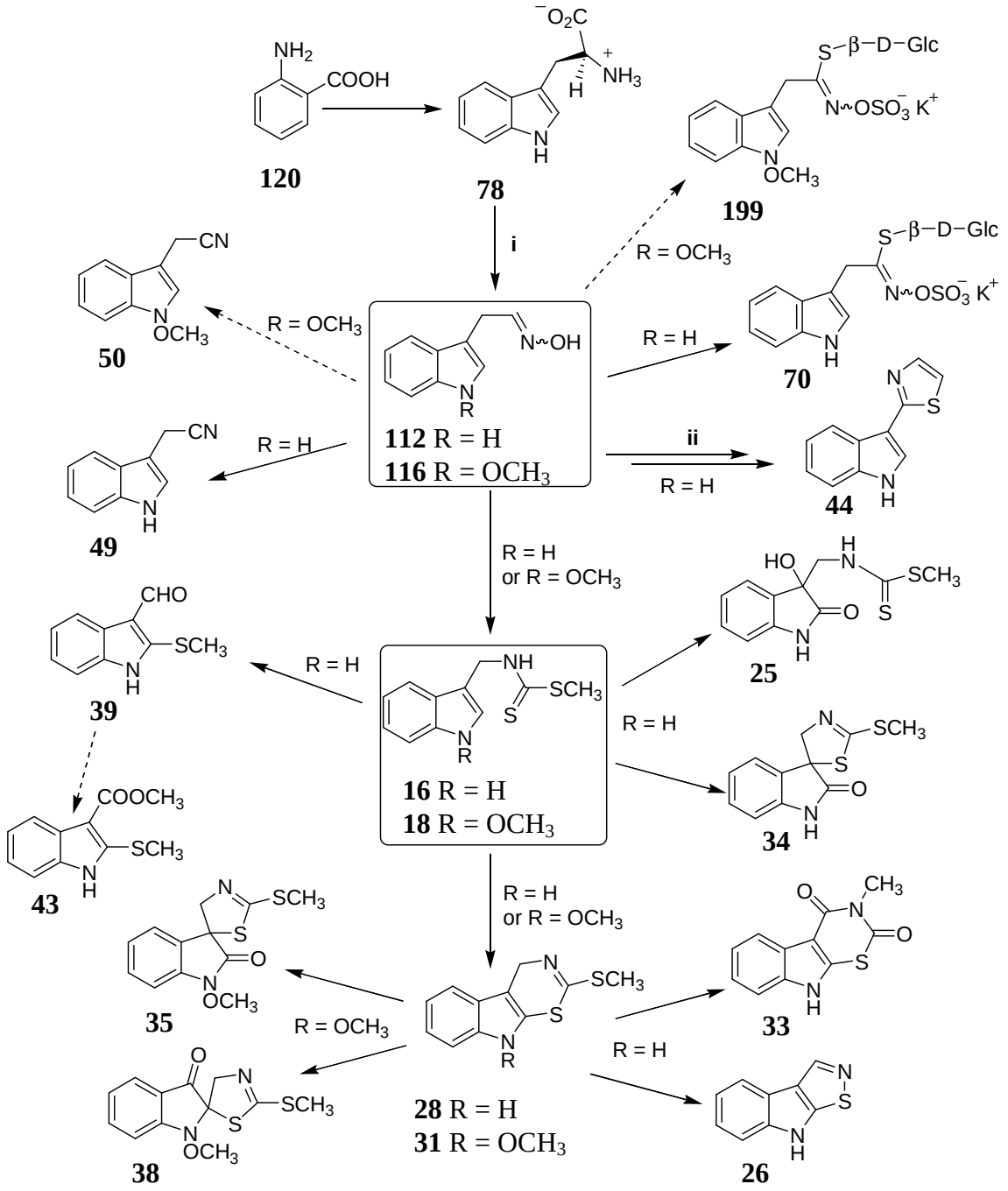

Figure 1.6 Map of biosynthetic pathways of crucifer phytoalexins and indolyl glucosinolates **70** and **199**. Dashed arrows represent proposed steps. Enzymes involved in the biosynthetic pathway: i) CYP79B2 and CYP79B3; ii) CYP71A13, and CYP79B15 (Pedras et al., 2007b).

L-Tryptophan (**78**), a precursor of majority of crucifer phytoalexins is biosynthesized from anthranilic acid (**120**) via the shikimate pathway (Dewick, 1998). In plants, anthranilic acid (**120**) is transformed to indole (**105**) which is conjugated with *L*-serine (**122**) to produce *L*-tryptophan (Dewick, 1998; Shraudolf, 1966). Biosynthesis of phytoalexins from *L*-tryptophan proceeds through indolyl-3-acetaldoxime (**112**) that appears to be the metabolic branching point in a few secondary pathways such as indole phytoalexins and indole glucosinolates (Pedras et al, 2007b) (**Figures 1.6** and **1.7**).

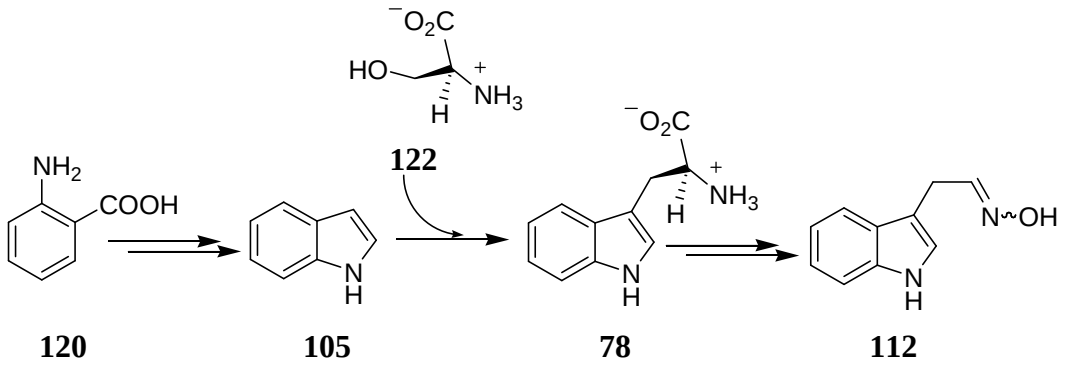

Figure 1.7 Biosynthetic pathway of *L*-tryptophan (**78**) and indolyl-3-acetaldoxime (**112**) from anthranilic acid (**120**).

Cytochrome P450 enzymes from the CYP79 family that catalyze conversion of *L*-tryptophan to indolyl-3-acetaldoxime have been isolated from different plant sources such as white mustard and the model plant *A. thaliana* (Hansen and Halkier, 2005; Hull et al., 2000; Mikkelsen et al., 2000; Naur et al., 2003b). The enzymes CYP79B1 (isolated from white mustard), CYP79B2, and CYP79B3 (isolated from *A. thaliana*) have been proposed to catalyze *N*-hydroxylation of *L*-tryptophan to *N*-hydroxy-*L*-tryptophan that decarboxylates to give indolyl-3-acetaldoxime (Hansen and Halkier, 2005; Hull et al., 2000; Mikkelsen et al., 2000; Naur et al., 2003b). These transformations have been extensively studied in the biosynthetic pathways of glucosinolates and are described in the next section (Hansen and Halkier, 2005; Hull et al., 2000; Mikkelsen et al., 2000; Naur et al., 2003b).

The biosynthesis of the crucifer phytoalexins, brassinin (**16**), cyclobrassinin (**28**) and spirobrassinin (**34**) was investigated in turnip roots using isotopically labeled (^{13}C and ^{2}H) precursors. The origin of indole group was confirmed through deuterium

labeling experiments using *L*-[4'-^{2}H]tryptophan (Monde et al., 1994) (**Figure 1.8**). The occurrence of a molecular rearrangement in the biosynthetic pathway from *L*-tryptophan (**78**) to brassinin (**16**) was investigated by administration of *DL*-[^{13}C-2]tryptophan to turnip root tissues. The ^{13}C NMR of isolated spirobrassinin revealed a 4-fold enhancement of the imino carbon NMR signal. These results suggested that a molecular rearrangement of *L*-tryptophan leads to indolyl-3-methylisothiocyanate (**123**) which is an intermediate in the biosynthetic pathway of brassinin (**16**), and that the thiocarbonyl carbon of brassinin originates from C-2 of *L*-tryptophan (**Figure 1.8**) (Monde et al., 1994). Administration of *L*-[3,3,3-$^{2}H_3$]methionine indicated that the methyl groups of brassinin, cyclobrassinin and spirobrassinin derived from *L*-methionine. Additional experiments employing a mixture of *L*-[3,3,3-$^{2}H_3$]methionine and *L*-[^{35}S]methionine revealed intact incorporation of *L*-methionine into brassinin. The origin of the thiocarbonyl sulfur from *L*-cysteine was confirmed after incubation of turnip tissues with *L*-[^{35}S]cysteine; high radioactivities of the isolated brassinin and spirobrassinin supported the conclusion that the thiocarbonyl sulfur atom originates from *L*-cysteine (Monde et al., 1994) (**Figure 1.8**). The biogenetic relationship between the phytoalexins brassinin (**16**), dioxibrassinin (**25**), cyclobrassinin (**28**), and spirobrassinin (**34**) in turnip root tissues was investigated with [3,3,3-$^{2}H_3$]brassinin (**16b**), [3,3,3-$^{2}H_3$]dioxibrassinin (**25a**), and [3,3,3-$^{2}H_3$]cyclobrassinin (**28b**) (**Figure 1.8**). Labeled brassinin was effectively incorporated into cyclobrassinin and spirobrassinin, but neither cyclobrassinin nor dioxibrassinin were incorporated in spirobrassinin. Incubation of Japanese radish roots (*Raphanus sativus* var. *hortensis*) with [3,3,3-$^{2}H_3$]brassinin further confirmed the intermediacy of brassinin in the biosynthetic pathway of cyclobrassinin (Monde et al., 1995). These experiments therefore revealed that brassinin (**16**) is an advanced precursor in the biosynthetic pathway of many other crucifer phytoalexins (Monde et al., 1994; 1995; Pedras et al., 2004).

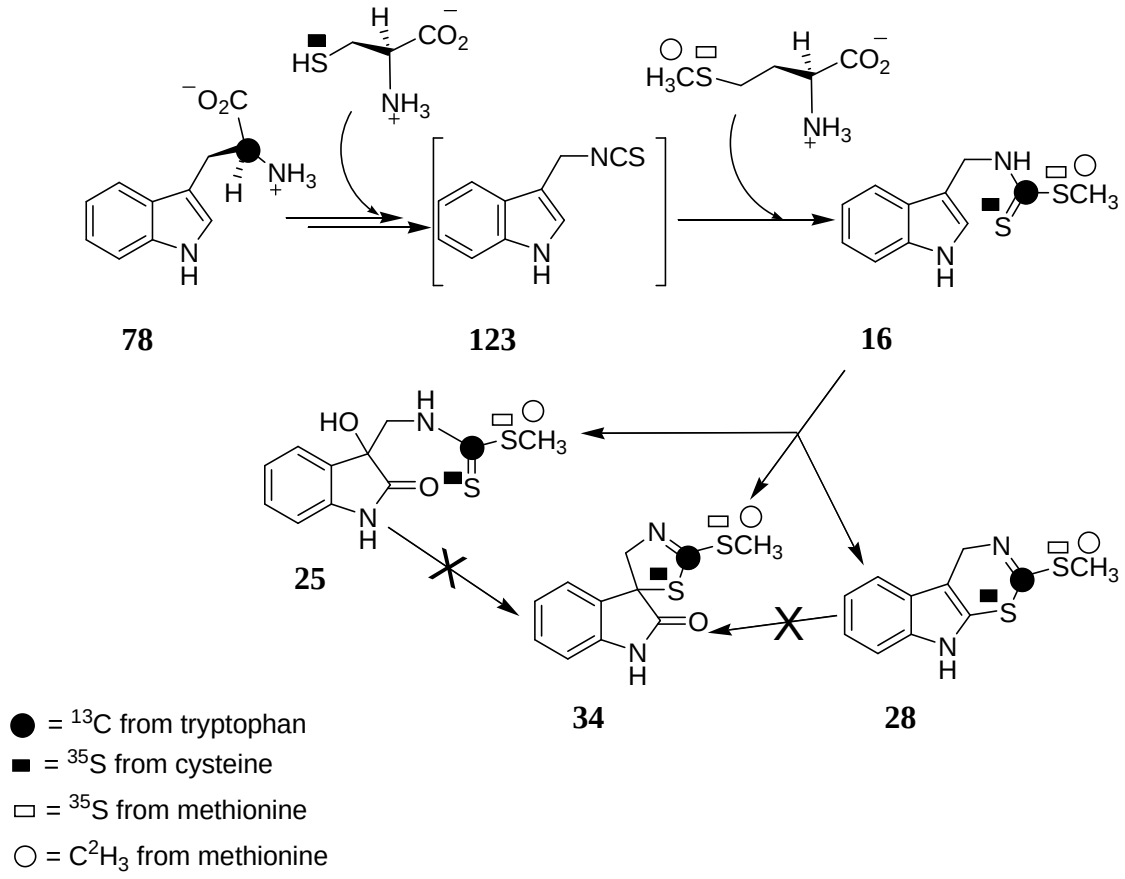

Figure 1.8 Biosynthesis of cruciferous phytoalexins: the occurrence of molecular rearrangement, and biogenetic relationship between brassinin (**16**) and other phytoalexins.

The biogenetic relationship between the phytoalexin brassinin (**16**) and the indole glucosinolate glucobrassicin (**70**) was subject of discussion. Glucobrassicin (**70**) appeared to be biogenetically related to brassinin (**16**) (**Figure 1.9**) since both are biosynthesized from *L*-tryptophan (Goetz and Schraudolf, 1983; Kutáček et al., 1962; Kutáček and Králová, 1972). Glucobrassicin (**70**) is also known to undergo enzymatic hydrolysis by myrosinases, Lossen-type rearrangement of the resulting intermediate yields indolyl-3-methylisothiocyanate (**123**, Agerbik et al., 1998; Hanley et al., 1990; Hanley and Parsley, 1990; Latxague et al., 1991), a proposed intermediate between tryptophan and brassinin (Monde et al., 1994).

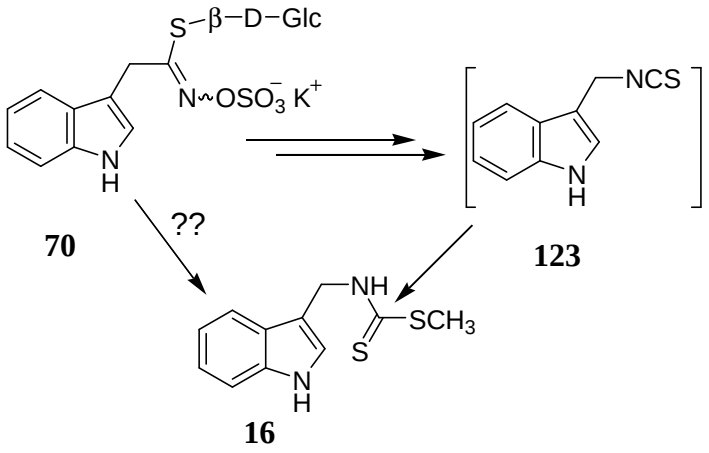

Figure 1.9 Plausible biogenetic relationship between brassinin (**16**) and glucobrassicin (**70**).

The preparation of indolyl-3-methylisothiocyanate (**123**) was unsuccessful (Kutschy et al., 1998) due to its instability (Hanley et al., 1990; Hanley and Parsley, 1990). Monde and co-workers (1994), however, attempted to trap the putative isothiocyanate **123** in the biosynthesis of brassinin. Monde and co-workers (1994) reported that homogenizing turnip roots in the presence of sodium methanethiolate yielded brassinin (**16**) and a compound that was identified as $PhCH_2$-CH_2-NH-CS-SCH_3, which was named phenylethylbrassinin (**124**). These metabolites were not isolated in the absence of sodium mathanethiolate (Monde et al., 1994). The putative role of isothiocyanate in the biosynthesis of brassinin was further demonstrated with benzyl isothiocyanate (**125**) (**Figure 1.10**). Administration of **125** to turnip tubers in the absence of sodium methanethiolate yielded a new metabolite that was named benzylbrassinin (**126**) (Monde et al., 1994).

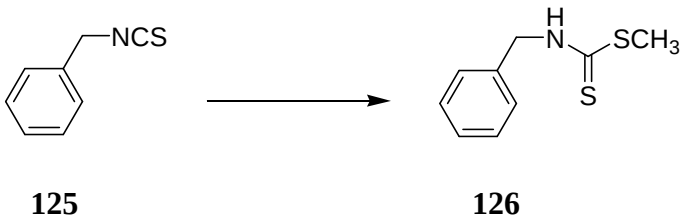

Figure 1.10 Biosynthesis of benzylbrassinin (**126**) (Monde et al., 1994).

The potential intermediacy of glucobrassicin (**70**) in the biosynthesis of brassinin (**16**) was investigated with [4',5',6',7'-$^2H_4$]glucobrassicin (**70a**) using brown mustard (*B. juncea*) leaves elicited with *L. maculans*, and with UV-irradiated turnip root slices. [4',5',6',7'-$^2H_4$]Glucobrassicin (**70a**) was not incorporated into any of the phytoalexins produced by either plant tissue, but was rather metabolized to indole-3-carboxaldehyde (**106a**) and methyl indole-3-carboxylate (**121a**) by turnip root slices (Pedras et al., 2001; 2003b) (**Figure 1.11**). On the other hand, [4',5',6',7'-$^2H_4$]indolyl-3-acetaldoxime (**112a**) was efficiently incorporated into brasslexin (**26a**), cyclobrassinin (**28a**) and spirobrassinin (**34b**) in turnip root slices (**Figure 1.11**). These results suggested that the biosynthetic pathway of brassinin possibly branches before formation of glucobrassicin, and that indolyl-3-acetaldoxime or other related intermediate is the common biosynthetic precursor between phytoalexins and glucosinolates (Pedras et al., 2003b).

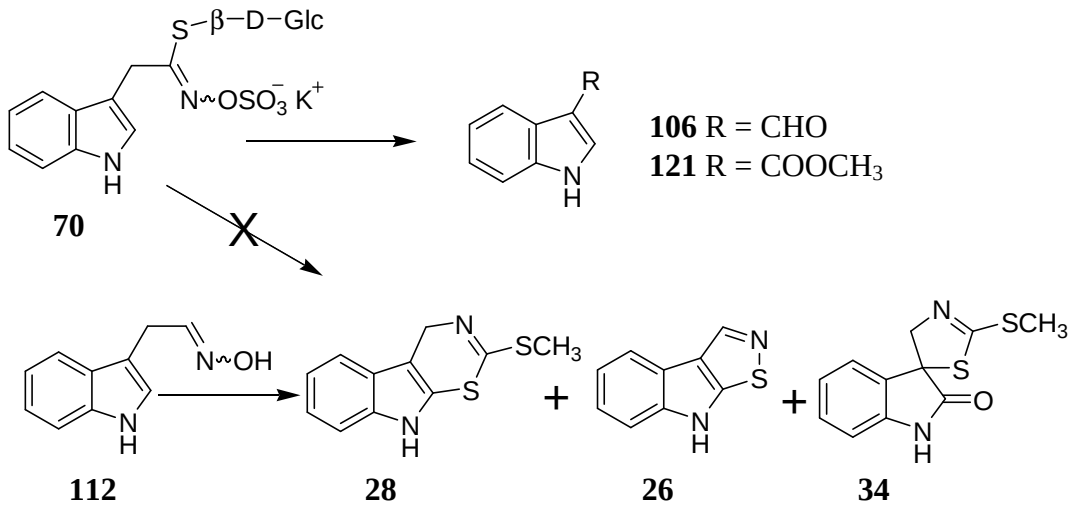

Figure 1.11 Biosynthesis of cruciferous phytoalexins: lack of incorporation of [4',5',6',7'-$^2H_4$]glucobrassicin (**70a**), and incorporation of [4',5',6',7'-$^2H_4$]indolyl-3-acetaldoxime (**112a**) (Pedras et al., 2003b).

[3,3,3-$^2H_3$]Dioxibrassinin (**25a**) and [3,3,3-$^2H_3$]cyclobrassinin (**28b**) were not incorporated into [3,3,3-$^2H_3$]spirobrassinin (**34a**) suggesting that cyclobrassinin and spirobrassinin derive from brassinin (**16**) via a common intermediate (Monde et al., 1994). The contribution of such an intermediate was probed with a non-natural precursor, 2-methylbrassinin (**127**, **Figure 1.12**). In feeding experiments, turnip tissues

metabolized 2-methylbrassinin (**127**) to two metabolites, **129** and **130**, that were suggested to form through a pinacol-type rearrangement of the diol intermediate **128**. These results suggested that a similar diol intermediate could be involved in the biosynthesis of cyclobrassinin (**28**) and spirobrassinin (**34**) from brassinin (**16**) (Monde et al., 1994).

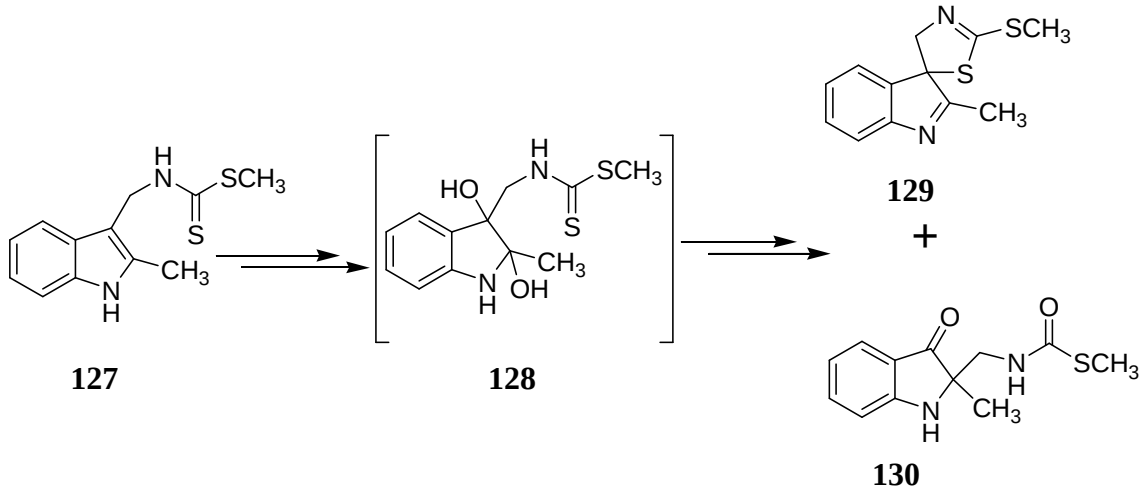

Figure 1.12 Probing for the common intermediate in the biosynthesis of cyclobrassinin (**28**) and spirobrassinin (**34**) from brassinin (**16**) (Monde et al., 1994).

In other biosynthetic investigations [4',5',6',7'-$^{2}H_4$]brassinin (**16a**) was incorporated into rutalexin (**33a**), brassicanal A (**39a**), and brassicanate A (**43a**) in rutabaga root slices (Pedras et al. 2004, **Figure 1.13**). The occurrence of brassicanal A and brassicanate A in rutabaga root tubers suggested a possible biogenetic relationship between these two metabolites. Interestingly, the percent incorporation of brassinin (**16a**) into brassicanate A (**43a**) was much higher than that for brassicanal A (**39a**) (Pedras et al., 2004). Additional deuterium incorporation experiments revealed cyclobrassinin (**28a**) to be an advanced biogenetic precursor of brassilexin (**26a**) (Pedras et al., 1998; 2007b) and rutalexin (**33a**) (Pedras et al., 2004; 2007b). Rutalexin (**33**) was isolated from rutabaga for the first time and its characterization was a revision of the structure of a compound that was previously misassigned as cyclobrassinone (**131**) (Pedras et al., 2004).

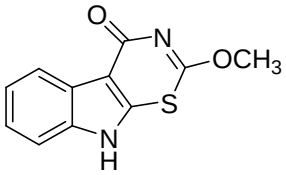

131

The biosynthesis of brassilexin (**26a**) from indolyl-3-acetaldoxime (**112a**), brassinin (**16a**), and cyclobrassinin (**28a**) was also established in feeding experiments with turnip root slices and in leaves of *B. carinata* and *B. juncea* (Pedras et al., 1998; 2001, 2007b) (**Figure 1.13**). The sequence of the biosynthetic pathway of brassilexin (**26**), rutalexin (**33**), brassicanal A (**39**), and brassicanate A (**43**) was therefore established (Pedras et al., 1998; 2001; 2007b) (**Figure 1.13**).

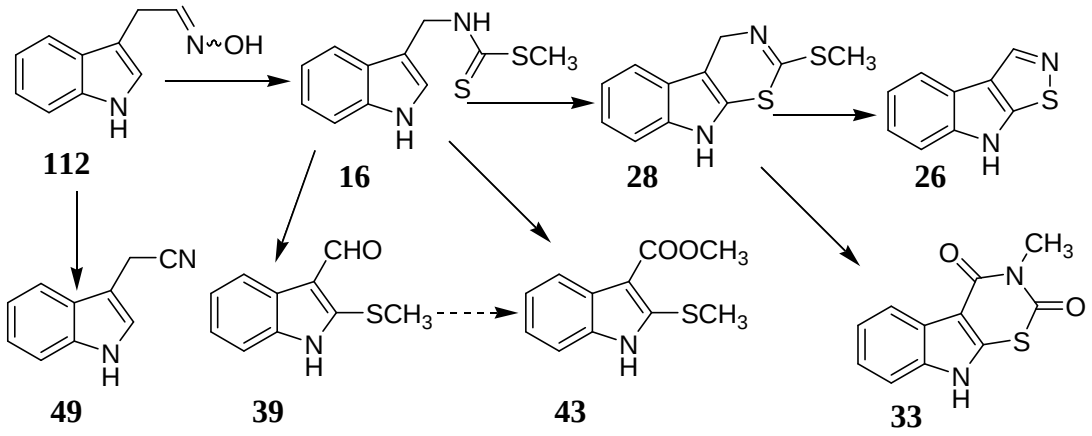

Figure 1.13 Biosynthetic sequence of brassilexin (**26a**), rutalexin (**33a**), brassicanal A (**39a**), and brassicanate A (**43a**) from indolyl-3-acetaldoxime (**112a**) (Pedras et al., 2002; 2004).

Efficient metabolism of [4',5',6',7'-$^{2}H_4$]indolyl-3-acetaldoxime (**112a**) to indolyl-3-acetonitrile (**49a**) (**Figure 1.13**) by *B. juncea* leaves suggested that under these experimental conditions **112**, but not glucobrassicin (**70**), is the key intermediate in the biosynthesis of **49** (Pedras et al., 2002).

The biosynthesis of camalexin (**44**), the principle phytoalexin of the model plant *A. thaliana* is shown in **Figure 1.14**. Camalexin was first proposed to be biosynthesized

through condensation of indole-3-carboxaldehyde (**106**) with cysteine followed by cyclization and decarboxylation (Browne et al., 1991). The thiazole ring of camalexin was established to originate from cysteine based on a more efficient incorporation of [^{35}S]cysteine than [^{35}S]methionine, thus supporting the initial hypothesis by Browne and co-workers (1991). Additional experiments showing incorporation of cysteine labeled with ^{2}H, ^{14}C, or ^{13}C and ^{15}N into camalexin supported the previous conclusions (Zook and Hammerschmidt, 1997). The efficient incorporation of radioactivity from [^{14}C]anthranilate than [^{3}H]tryptophan showed that anthranilic acid (**120**) but not *L*-tryptophan (**78**) was the precursor of camalexin (Tsuji et al., 1993; Zook and Hammerschmidt, 1997). Further biosynthetic experiments using *A. thaliana* cell cultures showed that the biosynthetic pathway of camalexin possibly diverges from that of tryptophan at the indole step. The efficiency of incorporation of [^{14}C]indole into camalexin was twice that of [^{14}C]anthranilate, suggesting that indole is a closer precursor to camalexin than anthranilic acid, whereas tryptophan is not a precursor (Zook, 1998). Contrary to these reports, *in vivo* labeling experiments showed that [^{14}C-2]indolyl-3-acetaldoxime was incorporated into camalexin in *A. thaliana* (Glawischnig et al., 2004; Pedras et al., 2007b, **Figure 1.14**). Additional experiments using *A. thaliana* leaves showed incorporation of 6-fluoroindolyl-3-acetaldoxime, 6-fluorotryptophan and ^{14}C-labeled tryptophan into camalexin and derivatives (Glawischnig et al., 2004). The fluorinated or ^{14}C-labeled tryptophan was incorporated albeit with low efficiency (Glawischnig et al., 2004), hence the previous assumption that tryptophan is not a precursor of camalexin (Tsuji et al., 1993; Zook and Hammerschmidt, 1997) did not hold. It was also established that the enzymes CYP79B2 and CYP79B3 catalyze the conversion of *L*-tryptophan (**78**) to indolyl-3-acetaldoxime (**112**) in the biosynthetic pathway of camalexin in *A. thaliana* (Glawischnig et al., 2004). Dihydrocamalexic acid (**132**) was shown to accumulate in infected root cultures of phytoalexin deficient *A. thaliana* mutant *pad3* (Bednarek et al., 2005). In other biosynthetic studies, (*S*)-dihydrocamalexic acid (**132**) was converted to camalexin (**44**) on incubation with CYP71B15 (PAD3) (Schuhegger et al., 2006). These results suggested that CYP71B15 catalyzes the oxidative decarboxylation of dihydrocamalexic acid (**132**), the last step in the biosynthetic pathway of camalexin (Pedras et al., 2007b; Schuhegger et al., 2006). In

the most recent report, involvement of CYP71A13 enzyme in camalexin biosynthesis was demonstrated. It was established that CYP71A13 is required for camalexin (**44**) production. Incubation of CYP71A13 with indolyl-3-acetaldoxime (**112**) indicated that CYP71A13 catalyzes the dehydration of **112** to indolyl-3-acetonitrile (**49**) in the biosynthesis of camalexin (Nafisi et al., 2007). These results rather suggested that indolyl-3-acetonitrile (**49**) is an intermediate in the biosynthesis of camalexin (**44**) (Nafisi et al., 2007). The conversion of indolyl-3-acetonitrile (**49**) to dihydrocamalexic acid (**132**) is neither understood nor established.

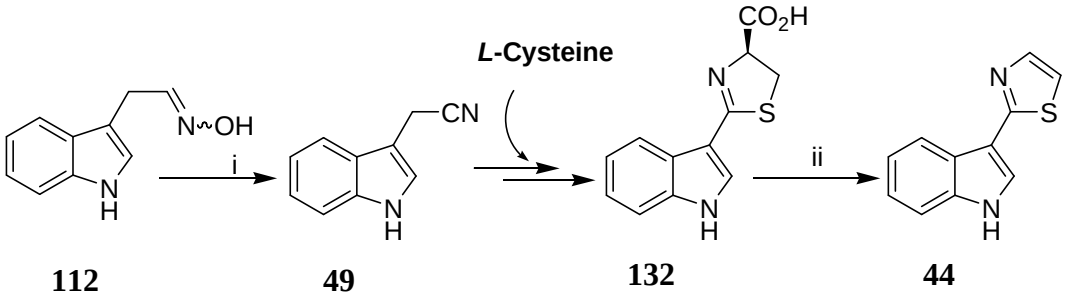

Figure 1.14 Biosynthetic intermediates of camalexin (**44**). Enzymes involved in the biosynthetic pathway: i) CYP71A13; ii) CYP71B15 (PAD3) (Pedras et al., 2007b; Schuhegger et al., 2006).

The phytoalexins brassicanal A (**39**) and brassicanate A (**43**) are examples of phytoalexins that have only one sulfur atom. Previously, a trapping experiment was performed to establish the potential intermediates in the biosynthetic pathway of brassicanal A (**39**) (**Figure 1.15**). Addition of aniline to UV-irradiated turnip root slices resulted in production of a new compound **136** (**Figure 1.15**). Compound **136** was suggested to be the aniline trapped biosynthetic intermediate 2-mercaptoindole-3-carboxaldehyde (**135**) since its biological methylation leads to brassicanal A (Monde et al., 1996). The proposed intermediate **135** was suggested to derive from hydrolysis of dehydrocyclobrassinin (**133**), which in turn would be formed from enzymatic dehydrogenation of cyclobrassinin (**28**). Dehydrocyclobrassinin (**133**) has not been isolated, although the 4-methoxy-dervative (**32**) is known (Monde et al., 1996). Biosynthetic investigations employing rutabaga root slices revealed [4',5',6',7'-$^{2}H_4$]brassinin incorporation into brassicanal A (**39a**) and brassicanate A (**43a**), whereas

incorporation of [4',5',6',7'-$^{2}H_4$]cyclobrassinin was not detected into either brassicanal A or brassicanate A (Pedras et al., 2004). Brassicanal A (**39**) is a putative precursor of brassicanate A (**43**) (Pedras et al., 2004), and luck of incorporation of cyclobrassinin under the experimental conditions suggested that possibly the trapped intermediate (Monde et al., 1996) was derived from brassinin (**16**) and not cyclobrassinin (**28**). Origin of the thiomethyl group at C-2 of indole therefore remains to be established, but could perhaps be deriving from methionine.

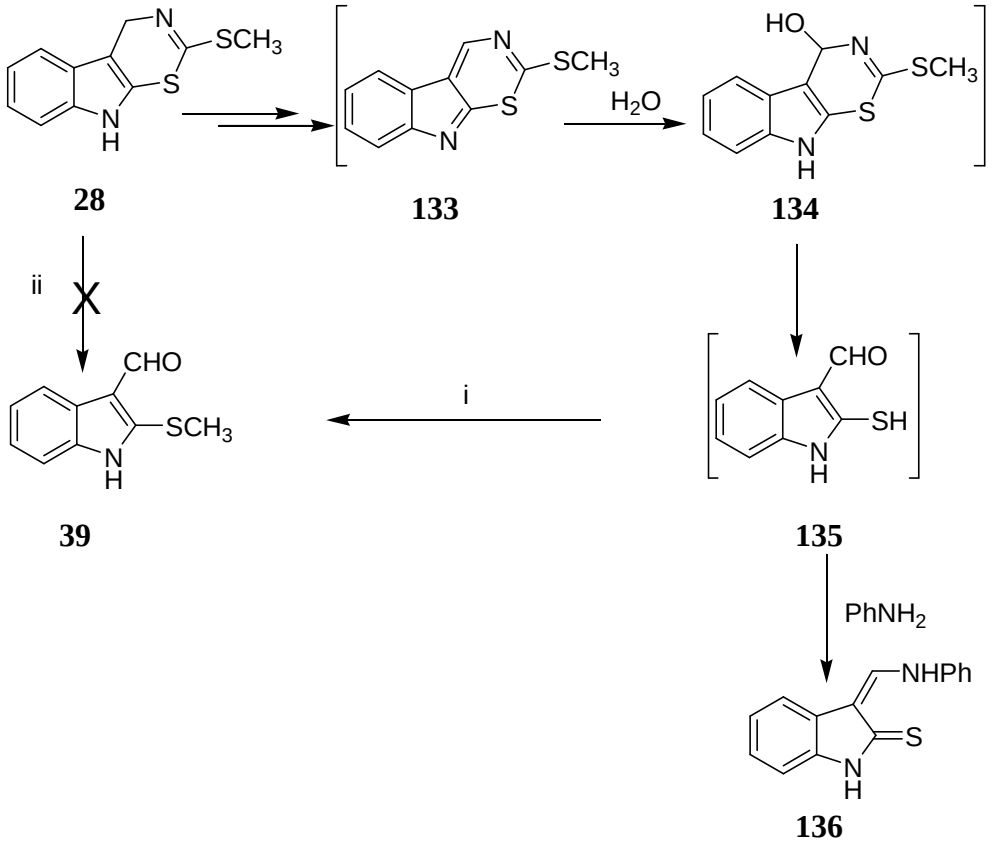

Figure 1.15 Putative biosynthetic pathway of brassicanal A (**39**). i) Biological methylation of 2-mercaptoindole-3-carboxaldehyde (**135**) yields brassicanal A; ii) Incorporation of cyclobrassinin (**28**) into brassicanal A (**39**) was not detected in rutabaga root slices. Compounds in bracket are proposed intermediates (Monde et al., 1996; Pedras et al., 2003b).

The occurrence of brassinin (**16**), 1-methoxybrassinin (**18**) and cyclobrassinin (**28**) in *Pseudomonas cichorii*-inoculated Chinese cabbage and Japanese radish roots

suggested a possible *N*-hydroxylation and subsequent methylation of brassinin to give 1-methoxybrassinin, and that oxidative cyclization of 1-methoxybrassinin would lead to cyclobrassinin (Monde et al., 1995; Pedras et al., 2003b). [3,3,3-$^{2}H_{3}$]Brassinin (**16b**) however, was efficiently incorporated into cyclobrassinin (**28b**) and not into 1-methoxybrassinin (**18a**) (Monde et al., 1995b) (**Figure 1.16**). These findings suggested that **28** is biosynthesized directly from brassinin (**16**) and not through 1-methoxybrassinin (**18**). These conclusions were further supported by absence of incorporation of [3,3,3-$^{2}H_{3}$]1-methoxybrassinin (**18a**) into cyclobrassinin (Monde et al., 1995b). These metabolic studies indicated that perhaps the biosynthetic pathway of 1-methoxy-containing phytoalexins diverges from the NH-containing phytoalexins before formation of brassinin (**16**), and that 1-methoxybrassinin (**18**) is the biosynthetic precursor of 1-methoxy-containing phytoalexins. Additional investigation employing rutabaga root slices showed equal incorporation of [4',5',6',7'-$^{2}H_{4}$]indolyl-3-acetaldoxime (**112a**) into [4',5',6',7'-$^{2}H_{4}$]brassinin (**16a**) and [4',5',6',7'-$^{2}H_{4}$]1-methoxybrassinin (**18b**) (Pedras et al., 2004), suggesting two parallel biosynthetic pathways leading to **16** and **18** (**Figure 1.16**) (Pedras et al., 2003b). To establish the plausible intermediate between indolyl-3-acetaldoxime (**112**) and 1-methoxybrassinin (**18**), [1",1",1"-$^{2}H_{3}$]1-methoxyindolyl-3-acetaldoxime (**116a**) was synthesized for the first time and was incubated with rutabaga and kohlrabi root slices. Mass spectrometry analysis of the isolated 1-methoxybrassinin (**18a**) revealed deuterium incorporation from [1",1",1"-$^{2}H_{3}$]1-methoxyindolyl-3-acetaldoxime (**116a**) in both rutabaga and kohlrabi root slices. Additional feeding experiments revealed incorporation of [4',5',6',7'-$^{2}H_{4}$]indolyl-3-acetaldoxime into brassinin (**16a**), 1-methoxybrassinin (**18b**), and spirobrassinin (**34b**) (Pedras et al., 2004). These metabolic studies were the first to demonstrate that biosynthetic pathway of NH-containing and 1-methoxy-containing phytoalexins divert at the aldoxime step. It was therefore surmised that indolyl-3-acetaldoxime (**112**) is transformed into brassinin and then to other NH-containing phytoalexins, whereas *N*-oxydation and methylation of **112** yields 1-methoxyindolyl-3-acetaldoxime (**116**), the precursor of 1-methoxybrassinin (**18**) which is the plausible precursor of other 1-methoxy-containing phytoalexins (Pedras and Montaut, 2004). Biosynthetic pathways of erucalexin (**38**) and 1-methoxyspirobrassinin (**35**) have been studied (Pedras et al.,

2007b; Pedras and Okinyo, 2006b) and are part of this thesis, as reported in the Results and Discussion sections.

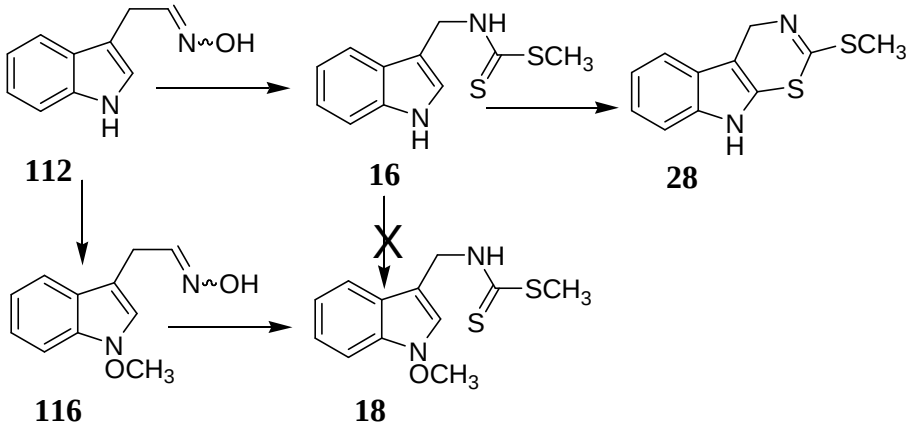

Figure 1.16 Biosynthesis of brassinin (**16a**) and cyclobrassinin (**28a**) from indolyl-3-acetaldoxime (**112a**), and 1-methoxybrassinin (**18b**) from 1-methoxyindolyl-3-acetaldoxime (**116a**) (Pedras and Montaut, 2004; Pedras et al., 2004).

The biosynthesis of many other 1-methoxy-containing phytoalexins such as 1-methoxybrassenins A (**21**) and B (**22**), wasalexins A (**23**) and B (**24**), and sinalbins A (**30**) and B (**31**), among others remain to be investigated. It is therefore necessary to carry out biosynthetic studies to unravel the pathways leading to such phytoalexins as this may facilitate transfer of these pathways to other cruciferous crops.

The three most recently reported phytoalexins, rapalexins A (**53**) and B (**54**), and brussalexin A (**55**) have introduced yet new structures among the crucifer phytoalexins (Pedras et al., 2007b; 2007c). The rapalexins A and B were proposed to derive from putative indolyl glucosinolates or from thiohydroximic acids such **137** and **138** (**Figure 1.17**). Lossen-type rearrangement to intermediate **139** would then yield **53** and **54** (**Figure 1.17**). Brussalexin A (**55**) represents a unique chemical structure that does not seem to fit with the presently known biosynthetic pathway of crucifer phytoalexins isolated to date (Pedras et al., 2007b). It was therefore proposed that brussalexin A could biosynthetically derive from addition of indolyl-3-methane thiol (**142**) to allyl isothiocyanate **68** (produced from myrosinase hydrolysis of sinigrin, **56**, **Figure 1.18**) (Pedras et al., 2007c).

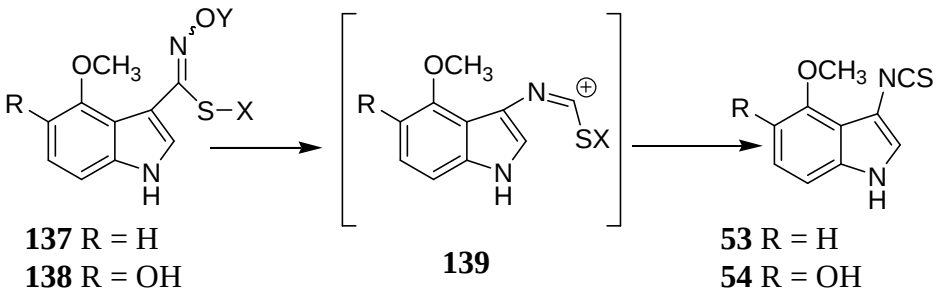

137 R = H
138 R = OH

139

53 R = H
54 R = OH

Figure 1.17 Proposed biosynthetic precursors of rapalexin A (**53**) and B (**54**) (Pedras et al., 2007b).

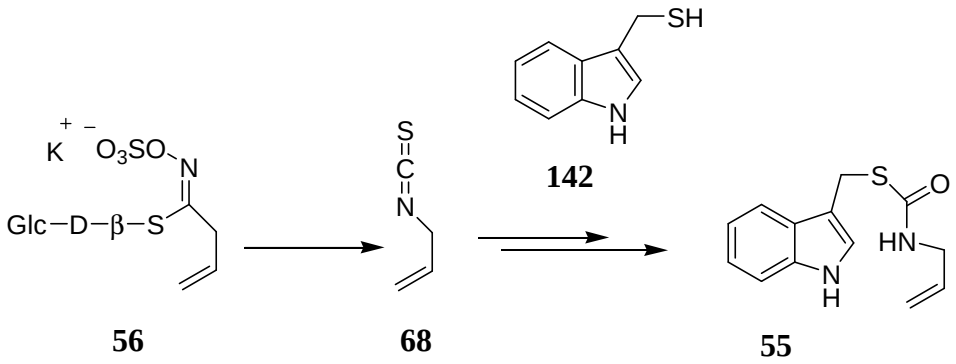

56 **68** **142** **55**

Figure 1.18 Proposed biosynthetic precursors **56** and **68** of brussalexin A (**55**) (Pedras et al., 2007c).

1.4.4.2 Glucosinolates

The biosynthesis of glucosinolates can be divided into three different stages: (i) chain elongation of certain aliphatic and aromatic amino acids via sequential addition of methylene groups, (ii) construction of the core structure of glucosinolates, and (iii) secondary modification of the side chain (Grubb and Abel, 2006; Halkier and Gershenzon, 2006).

Side chain elongation

Chain elongated aliphatic glucosinolates are the most abundant glucosinolates found in crucifers including the model plant *A. thaliana* and many other Brassicaceae species (Halkier and Gershenzon, 2006). The extent of side chain elongation and type of

modifications are important for the biological activity of the glucosinolate breakdown product (Manici et al., 1997; Mithen et al., 1986; Sarwar et al., 1998). The side chain-elongation reactions have been investigated using *in vivo* labeling studies, isolation of the participating intermediates, and characterization of the enzymes catalyzing various reactions of the biosynthetic pathway. Side chain elongation reactions are shown in **Figure 1.19**.

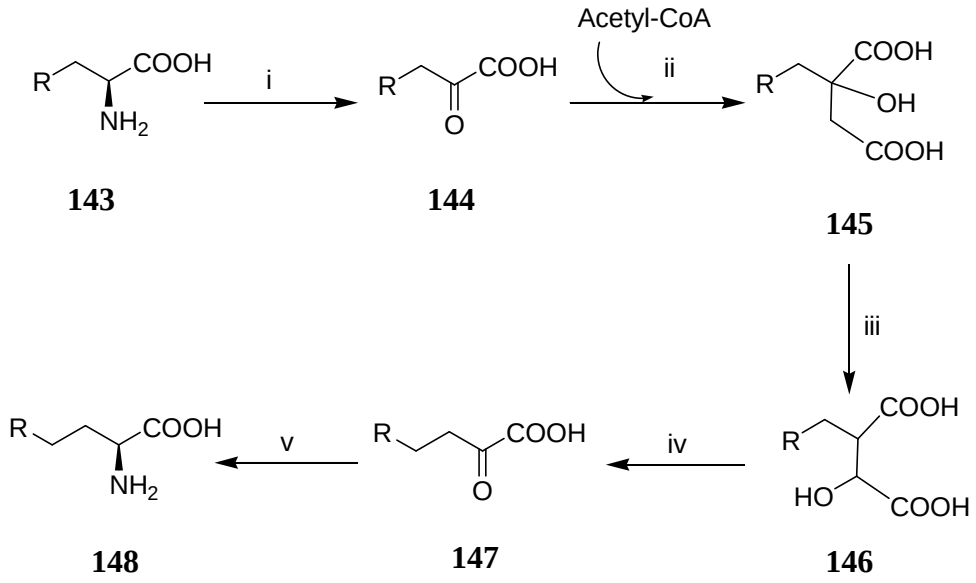

Figure 1.19 Side chain elongation: i) BRANCHED-CHAIN AMINOTRANSFERASE4 (BCAT4); ii) 2-(ω-Methylthioalkyl)malate synthase (MAMS) or Methylthioalkylmalate synthase 1 (MAM1) or Methylthioalkylmalate synthase 3 (MAM3); iii) Isomerization; iv) Oxidative decarboxylation; v) Transamination (Graser et al., 2000; Halkier and Gershenzon, 2006).

Side chain-elongation begins with oxidative deamination of the parent amino acid (**143**) to yield the corresponding 2-oxo acid (**144**). One of the enzymes catalyzing oxidative deamination of amino acids, BRANCHED-CHAIN AMINOTRANSFERASE4 (BCAT4) in the biosynthetic pathway of methionine-derived glucosinolates was characterized from *A. thaliana* (Schuster et al., 2006). The 2-oxo acid (**144**) enters a three step-cycle in which it (i) condenses with acetyl CoA to form a substituted 2-malate derivative (**145**) which (ii) isomerizes by a 1,2-shift of the hydroxyl group to form a 3-malate derivative (**146**) that is (iii) oxidatively decarboxylated to yield a new 2-oxo acid

with one additional methylene group (**147**) (Graser et al., 2000; Halkier and Gershenzon, 2006; Falk et al., 2004; Textor et al., 2004; 2007). The 2-oxo acid **147** can undergo transamination to regenerate the amino acid (**148**) which enters the biosynthetic pathway of short chain aliphatic or aromatic glucosinolates, or it may undergo further cycles of chain-elongation to form longer homologs (Textor et al., 2004; 2007). Chain elongation products of up to nine cycles are known to occur in plants (Fahey et al, 2001), but only six cycles are known in the model plant *A. thaliana* (Textor et al., 2004; 2007). All chain-elongated 2-oxo acids are converted back to the corresponding amino acids that participate in the biosynthetic pathway of glucosinolates of varying side-chain lengths (Graser et al., 2000).

An extensive study on the sequence of chain-elongation reactions was conducted by carrying out *in vivo* feeding experiments using stable and radiolabeled isotopes (Graser et al., 2000). These experiments revealed that only the acetate methyl group is incorporated to form the methylene group in chain-elongated products, thus suggesting that the carboxyl group of the first acetate residue is lost as carbon dioxide during the second round of chain-elongation, and during aldoxime formation (Graser et al., 2000).

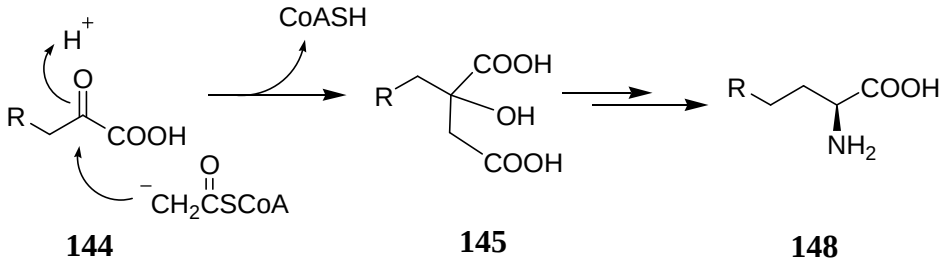

Figure 1.20 Condensation of acetyl CoA with a 2-oxo acid (**144**).

It was established that the nitrogen atom of the parent amino acid is incorporated into the core glucosinolate structure arising from the chain-elongated amino acid. It was therefore concluded that the transfer of amino group in the first step initiates the formation of 2-oxo acid, and re-incorporation into the biosynthetic pathway terminates the chain elongation reaction to regenerate the amino acid that is required to take part in the biosynthetic pathway of chain-elongated glucosinolates (Graser et al., 2000).

Detection of intermediates and isolation of chain-elongated homologs have further supported the chain elongation reactions (Halkier and Gershenzon, 2006). The enzyme catalyzing the first step of chain-elongation reaction, 2-(ω-methylthioalkyl)malate synthases (MAMS), was partially purified from rocket (Falk et al., 2004). MAMS however could not catalyze the second cycle of chain-elongation indicating that it was specific for the first round only (Falk et al., 2004). Another methylthioalkylmalate synthase, methylthioalkylmalate synthase 1 (MAM1) from *A. thaliana* was capable of catalyzing both first and second rounds of chain-elongation cycles (Kryomann et al., 2001; Textor et al., 2004). MAM1 was reported to exist together with MAM3 (formerly known as MAM-L for MAM-like) in *A. thaliana* (Textor et al., 2007). Unlike MAM1, MAM3 is capable of catalyzing all six condensation reactions of methionine chain-elongation that occur in *Arabidopsis*, it also exhibits a broad substrate range of other non-methionine derived 2-oxo acids (Textor et al., 2007).

Biosynthesis of the glucosinolate core structure

The biosynthesis of aliphatic, aromatic, and indolyl core glucosinolate structure involves common intermediates (*N*-hydroxy amino acid, aldoximes, *aci*-nitro or nitrile oxides, S-alkyl thiohydroximates, thiohydroxamic acids, and desulfoglucosinolates) (**Figure 1.21**).

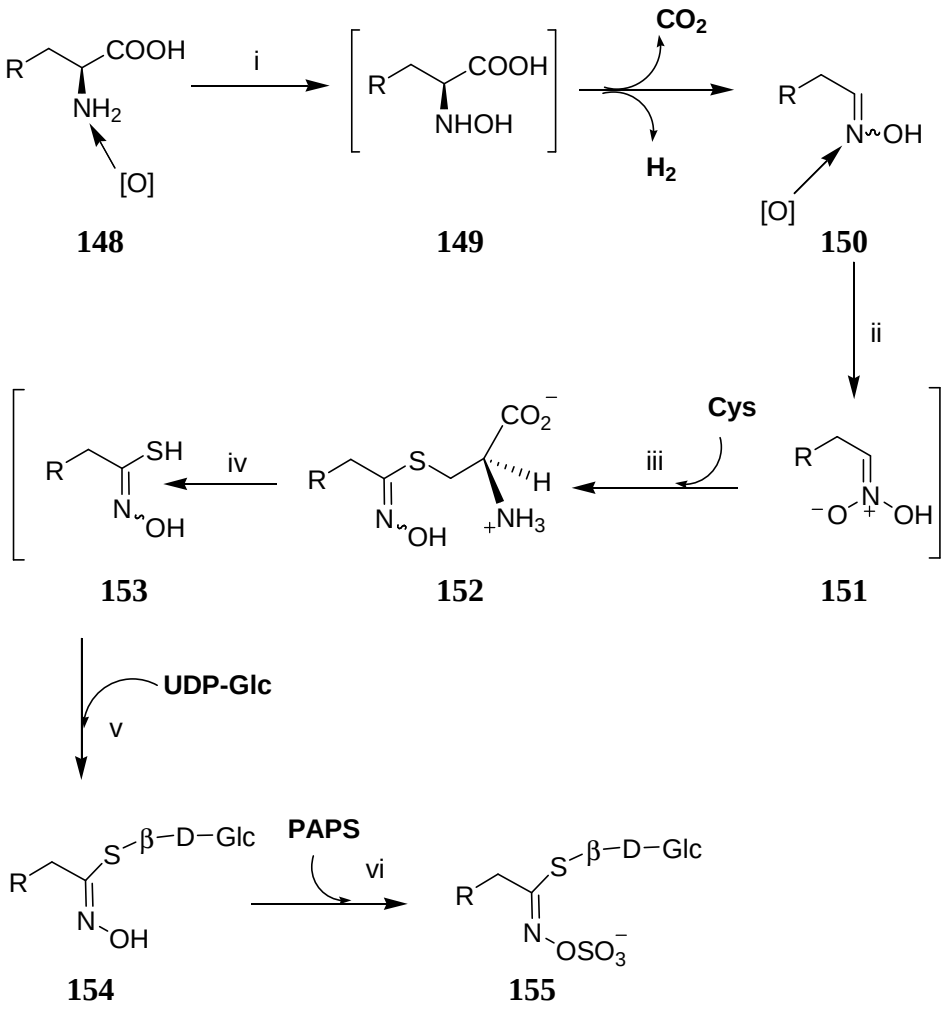

Figure 1.21 Proposed biosynthetic pathway of glucosinolates: i) CYP79F1, CYP79F2 (methionine), CYP79A2 (phenylalanine), CYP79B1, CYP79B3, CYP79B3 (tryptophan); ii) CYP83A1 (methionine), CYP83B1 (phenylalanine, tryptophan); iii) GST?; iv) *C-S* lyase; v) UGT74B1 v) AtST5a (phenylalanine, tryptophan), AtST5b, AtST5c (methionine). Structures in brackets are proposed intermediates (Halkier and Gershenzon, 2006).

The first common step in glucosinolate and cyanogenic glucoside biosynthesis is the conversion of amino acids (**148**) to their respective aldoximes (**150**) (Bennet et al., 1993; 1997; Dawson et al. 1993; Dewick, 1984; Du et al., 1995; Wittstock and Halkier, 2000). The aldoxime forming enzyme was proposed to catalyze *N*-hydroxylation of amino acids to the corresponding *N*-hydroxyamino acids (**149**) that decarboxylate to produce the aldoxime (**150**). Cytochrome P450 family type of enzymes were shown to catalyze such transformations (Halkier and Møller, 1991; Koch et al., 1992). The

enzymes CYP79F1 and CYP79F2 metabolize chain elongated derivatives of methionine to their respective aldoximes in the biosynthesis of aliphatic glucosinolates, but not tyrosine, tryptophan, or their derivatives (Chen et al., 2003; Hansen et al., 2001a; Reintanz et al., 2001). CYP79A2 on the other hand catalyzes the metabolism phenylalanine to phenylacetaldoxime in the biosynthetic pathway of aromatic glucosinolates (Wittstock and Halkier, 2000). The enzymes CYP79B1, CYP79B2 and CYP79B3 catalyze the conversion of *L*-tryptophan (**78**) to indolyl-3-acetaldoxime (**112**) in the biosynthesis of indolyl glucosinolates (Hansen and Halkier, 2005; Hull et al., 2000; Mikkelsen et al., 2000; Naur et al., 2003b). Overexpression of CYP79B2 in *Arabidopsis* resulted in significant increase in levels of indolyl glucosinolates glucobrassicin (**70**) and 4-methoxyglucobrassicin (**156**), but not of aliphatic or aromatic glucosinolates (Mikkelsen et al., 2000).

Following its formation, the aldoxime (**150**) is conjugated with a suitable thiol donor to yield an *S*-alkyl-thiohydroximate (**152**). Both cysteine and methionine are known thiol donors in the biosynthetic pathway of many secondary metabolites, the former is however a more efficient donor than the latter (Mikkelsen et al., 2002). The aldoxime metabolizing enzymes in the biosynthesis of glucosinolates (in *A. thaliana*) have been characterized. The enzyme CYP83A1 metabolizes aliphatic aldoximes much more efficiently than CYP83B1 (Bak and Feyereisen, 2001; Hemm et al., 2003; Naur et al., 2003a). The enzyme CYP83B1 catalyzes the metabolism of aromatic aldoximes derived from tyrosine and phenylalanine (Hansen et al., 2001b), as well as indolyl-3-acetaldoxime (Bak and Feyereisen, 2001). CYP83A1 enzyme is capable of metabolizing indolyl-3-acetaldoxime albeit with low efficiency (Bak and Feyereisen, 2001). Conjugation of the aldoxime (**150**) with the thiol donor (e.g. *L*-cysteine) requires conversion of **150** into a reactive intermediate that can be attacked by the nucleophilic thiol donor. The CYP83 enzymes have been proposed to catalyze the oxidation of respective aldoximes to highly reactive 1-*aci*-nitro compounds (**151**) or nitrile oxides (Bak et al., 2001; Bak and Feyereisen, 2001; Hansen et al., 2001b). Proper conjugation of the sulfur donor (*L*-cysteine) with the reactive intermediate (*aci*-nitro compound or nitrile oxide) is thought to be catalyzed by a glutathione-*S*-transferase type enzyme (Mikkelsen et al., 2004). The *C*-*S* bond of *S*-(thiohydroximoyl)-*L*-cysteine (**152**) is

hydrolyzed by *C-S* lyase to form thiohydroximic acid (**153**) which is the next intermediate in the biosynthetic pathway of glucosinolates. The *L*-cysteine conjugate (**152**) does not accumulate in plant tissues and has therefore not been isolated. *In vitro*, **152** rapidly cyclizes to 2-substituted thiazoline-4-carboxylic acid (**157**) (**Figure 1.22**), leading to a suggestion that the *C-S* lyases form tightly coupled complexes with CYP83 enzymes to prevent cylization of the *C-S* lyase substrates (Hansen et al., 2001b; Halkier and Gershenzon, 2006). SUPERROOT1 (SUR1) was characterized as a *C-S* lyase enzyme in the biosynthetic pathway of *A. thaliana* glucosinolates (**Figures 1.21** and **1.22**) (Mikkelsen et al., 2004).

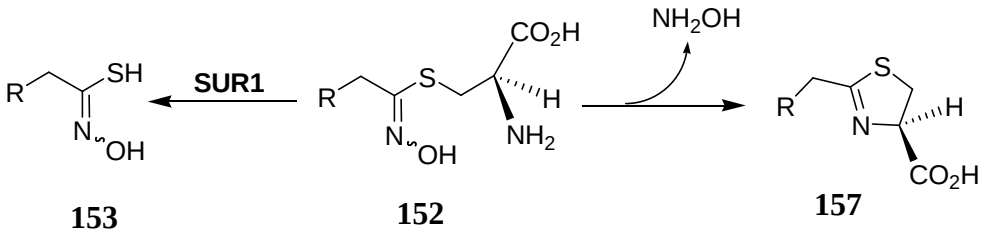

Figure 1.22 Cyclization of cysteine conjugate (**152**) to thiazoline-4-carboxylic acid (**157**), and SUPERROOT1 (SUR1) cleavage of *C-S* bond (Hansen et al., 2001b).

The thiohydroximic acid (**153**, **Figure 1.22**) formed is highly reactive and has not been isolated, but is subsequently glycosylated by a sugar nucleotide to produce desulfoglucosinolate (**154**, **Figure 1.21**). Uridine diphosphate glucose (UDPG) was found to be the most efficient glucose donor (Mitsuo and Underhill, 1971). A putative UDPG:thiohydroximate glucosyltransferase in the biosynthetic pathway of benzyl glucosinolate was isolated from *Arabidopsis* and was characterized as UGT74B1 (Grubb et al., 2004). Loss of UGT74B1 gene function only caused partial reduction of glucosinolate accumulation, suggesting that additional enzymes catalyzing glucosylation of thiohydroximates are present (Grubb et al., 2004). Enzyme preparations of UDPG:thiohydroximate glucosyltransferase purified from *Brassica napus* seedlings were reported to glycosylate sodium 3-phenylpropanothiohydroximate (**100**) to phenylethyl desulfoglucosinolate (**158**) (**Figure 1.23**, Reed et al., 1993). The use of similar enzyme preparations with sodium 2-(3-indolyl)acetothiohydroximate (**99**) were

reported to give only detectable amounts of desulfoglucobrassicin (**159**) since **99** was not stable in the buffer used (pH 6) (**Figure 1.23**, Reed et al., 1993).

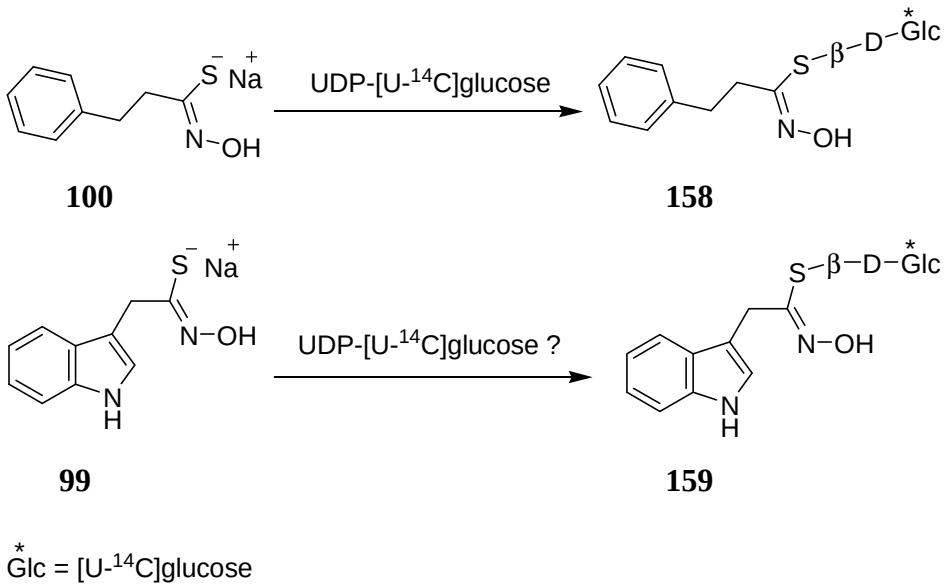

Figure 1.23 UDPG:thiohydroximate glucosyltransferase glycosylation of sodium 3-phenylpropanothiohydroximate (**100**) to phenylethyl desulfoglucosinolate (**158**) (Reed et al., 1993).

The last common step in building glucosinolate core structure (**155**) (for aliphatic, aromatic and indolyl glucosinolates) is the introduction of an active sulfate group from 3'-phosphoadenosine-5'-phosphosulfate (PAPS) to desulfoglucosinolate (**154**). Sulfation of desulfoglucosinolates is catalyzed by sulfotransferases (Glending and Poulton, 1988; 1990; Jain et al., 1989;1990; Klein et al., 2006; Piotrowski et al., 2004). Three sulfotransferases AtST5a, AtST5b, and AtST5c exhibiting broad substrate range have been characterized from *A. thaliana* (Piotrowski et al., 2004). Whereas AtST5b and AtST5c had higher affinity for aliphatic glucosinolates, AtST5a preferred tryptophan- and phenylalanine-derived desulfoglucosinolates (Piotrowski et al., 2004).

Side chain modification

Glucosinolate side chain modifications play a significant role in determining the biological activity of the hydrolysis product (Halkier and Gershenzon, 2006). The side chain modifications have been noted to occur in glucosinolates derived from methionine

and its homologs (**160**), the transformations may involve sequential oxidations, eliminations, alkylations, and esterifications (**Figure 1.24**) (Halkier and Gershenzon, 2006; Grubb and Abel, 2006). The sulfur can be successively oxidized to methylsulfinylalkyl (**161**) and methylsulfonylalkyl (**162**) moieties (Halkier and Gershenzon, 2006). Further modifications may involve oxidative cleavage of the methylsulfinylalkyl moiety to yield alkenyl (**163**) or hyroxyalkyl (**164**) side chains for which controlling genetic loci are known in *Arabidopsis* and *Brassica* species (Halkier and Gershenzon, 2006).

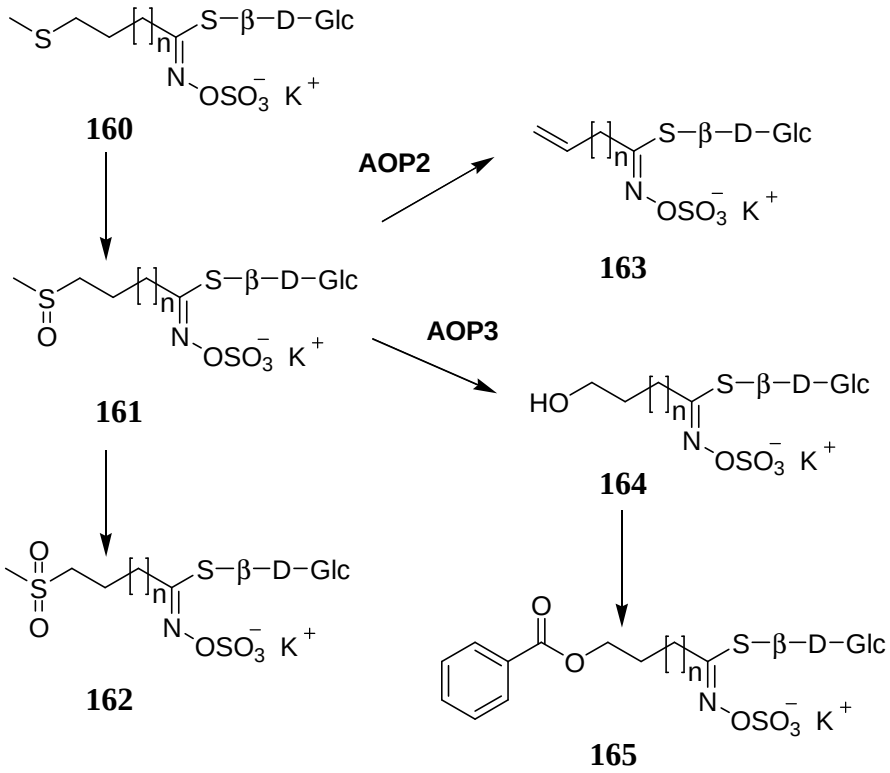

Figure 1.24 Side chain modifications of methionine-derived glucosinolates with varying side chain lengths. **APO2** and **APO3** are putative enzymes catalyzing the reactions in *Arabidopsis* (Halkier and Gershenzon, 2006; Kliebenstein et al., 2001).

The *AOP2* gene product catalyzes the conversion of methylsulfinylalkyl glucosinolates (**161**) to alkenyl glucosinolates (**163**), whereas the *AOP3* gene product controls the formation of hydroxyalkyl glucosinolates (**164**) from **161** (Kliebenstein et al., 2001). Although biosynthesis of glucosinolate esters (**165**) have been investigated

through administration of isotopically labeled precursors and intermediates, no studies have been carried out to determine the enzymes involved in their biosynthetic pathways (Graser et al., 2001).

1.5 Conclusion

Phytoalexins and glucosinolates are only two components of the complex mechanism by which plants respond to various forms of stress including overcoming microbial attack. The increased rate of accumulation of glucosinolates in infected or stressed plants is an indication of the role that they play in protecting plants against subsequent attacks (Agrawal et al., 2002; Mewis et al., 2005; Traw, 2002; van Dam et al., 2005). On the other hand, the timing, rate of accumulation and relative amounts of phytoalexins have shown their significant role in plant defense against pathogen invasion (Dixon, 1986; Dixon and Harrison, 1994; Kuć, 1995; Smith, 1996). Phytoalexins are often isolated in insufficient quantities that limit investigating their antimicrobial activity. In order to get sufficient amounts, synthetic strategies have been developed and the antimicrobial activities of the various phytoalexins have been established against a range of plant pathogens (Pedras et al., 2003b; 2007b; 2007c). Although there has been tremendous effort to unravel the biosynthetic pathway of glucosinolates, especially with the sequencing of *Arabidopsis* genome (Grubb and Abel, 2006; Halkier and Gershenzon, 2006), very little has been done in phytoalexin biosynthetic pathway in terms of genetic analysis. An increasing number of wild and cultivated plants exhibiting resistance to a variety of pathogens are being found and identified (Conn et al., 1988; Gugel et al., 1990; Lefol et al., 1997; Pedras and Zaharia, 2000). Such resistant species may provide good genetic sources to control the devastating effect of various pathogens, and yet most remain uninvestigated. By isolation and characterization of phytoalexins, their synthesis allows for further investigation of their interaction with various plant pathogens (Pedras et al., 2007b). For example, erucalexin (**38**) isolated as a phytoalexin of *Erucastrum gallicum* (dog mustard), a wild crucifer known to be resistant to *Sclerotinia sclerotiorum*, exhibited remarkable antifungal activity against this pathogen (Pedras et al., 2006a). To date, the phytoalexin caulilexin A (**42**) has exhibited the strongest antifungal activity against *S. sclerotiorum* (Pedras et al., 2006b), plants producing caulilexin A such as cauliflower are therefore good genetic sources for controlling *S. sclerotiorum*. Many more phytoalexins with unique skeletal structures such as rapalexins A (**53**) and B (**54**) (Pedras et al., 2007a), and brussalexin (**55**) (Pedras et al., 2007c) have

been isolated, synthesized and their antifungal activities against a range of pathogens established. Identification of phytoalexins from the resistant species also provides an opportunity for the synthesis of various biosynthetic intermediates that can be used to investigate their biosynthetic pathways (Pedras et al., 2003b; 2007b). An understanding of the biosynthetic pathways will allow for genetic manipulation of the susceptible species, to make them produce metabolites similar to those of resistant plants, thus enhancing their disease resistance with a result in improved crop production.

CHAPTER 2

2. Results

2.1 Analysis of antifungal secondary metabolites from *Eruca sativa* (rocket)

The search for phytoalexins from cruciferous plants resistant to economically important fungal diseases led to the investigation of rocket (*Eruca sativa*), a wild crucifer reported to exhibit resistance against *Alternaria brassicae* (Conn et al., 1988). Although a number of glucosinolates and their degradation products (isothiocyanates) have been isolated from rocket (Bennett et al., 2002; Cataldy et al., 2007; Cerny et al., 1996; Kim and Ishii, 2006), no phytoalexins have been reported to date. Previous investigations involving administration of destruxin B (a host-selective toxin produced by the pathogen *A. brassicae*) to petiolated leaves of rocket did not induce detectable amounts of phytoalexins (Pedras et al., 2003c). Since cruciferous plants produce different secondary metabolites depending on the type of stress (Pedras et al., 2007b; 2007e), the current investigation has undertaken abiotic elicitation of rocket with copper(II) chloride, followed by HPLC-DAD analyses and TLC biodetection of bioactive compounds employing spores of *Cladosporium cucumerinum*.

2.1.1 Time-course analysis

In preliminary experiments, time course analyses were conducted by spraying 14- and 21-day-old plants with copper(II) chloride to the point of run-off. After incubation for 24 hours, leaves were excised, extracted and subjected to HPLC-DAD analyses. Additional leaves were harvested every 24 hours up to 168 hours; control leaves were sprayed with water, were extracted and analyzed similarly. Comparison of the

metabolite profiles of elicited and control leaf extracts indicated that a peak in the chromatograms of elicited extracts was absent in those of control extracts. This peak with t_R =14.2 min was identified as arvelexin (**51**) by comparison of its retention time and UV spectra with those of an authentic sample. The amount of arvelexin in leaf extracts was determined by HPLC-DAD using calibration curves (**Table 2.1**). Amounts of arvelexin were generally higher in 21-day-old plants than in 14-day-old plants. The highest amount of arvelexin was detected in 21-day-old leaf extracts obtained after a 24-hour incubation period. Gradual decrease of arvelexin amounts was noted from 48 to 168-hour incubation periods (**Table 2.1**).

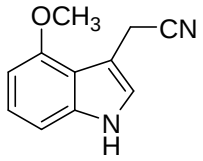

51

Table 2.1 Time-course HPLC analyses of production of arvelexin in rocket (*Eruca sativa*)

Phytoalexin	**Incubation time (h)**	**Total amount of phytoalexin (µmole/100 g of fresh tissue ± STD)[a]**
Arvelexin (**51**)	**24**	**6.7 ± 1.2**
	48	6.7 ± 2.3
	72	2.6 ± 0.8
	96	1.9 ± 1.0
	120	1.4 ± 0.3
	144	1.0 ± 0.6
	168	0.9 ± 0.8

[a]Amounts of arvelexin (**51**) determined by HPLC-DAD using calibration curves. Total amount ± standard deviation (STD); average of three independent experiments conducted in triplicate.

Since arvelexin (**51**) was the only induced metabolite of rocket detected by HPLC-DAD, an alternative method for detection of antifungal compounds (TLC biodetection) was used to supplement HPLC-DAD analyses. TLC biodetection was conducted using spores of *Cladosporium cucumerinum* to detect additional antifungal compounds present in the extracts (Pedras and Sorensen, 1998). Extracts from elicited and control leaves were spotted on TLC plates strips (developed with EtOAc-hexane, 60:40, followed by air drying). The dried plates were sprayed with a suspension of *C. cucumerinum* spores in double strength PDB and incubated for 36 hours in darkness; control plates were similarly developed and sprayed with a spore suspension. The TLC plates containing elicited or control extracts indicated three spots that appeared white on a gray background indicating the presence of antifungal compounds. The white spots were due to inhibition of spore germination on a gray background of fungal mycelia. Since HPLC-DAD analyses of these extracts indicated that arvelexin (**51**) was the only induced compound, the antifungal spots observed were likely due to constitutive secondary metabolites.

2.1.2 Isolation and identification of antifungal metabolites

In order to carry out isolation and identification of antifungal metabolites, 21-day-old plants were elicited and were extracted following experimental procedures similar to those of time course analyses. Extraction was carried out sequentially with *n*-hexane, ethyl acetate and methanol. The extracts were analyzed by HPLC-DAD and antifungal metabolites were detected by spore germination inhibition assays employing *Cladosporium cucumerinum* spores. Multiple chromatographic separations using FCC and PTLC were conducted; fractions obtained were subjected to HPLC-DAD analysis and TLC-biodetection. Two compounds with t_R = 22.5 (**166**) and 34.7 (**167**) min (HPLC-DAD) were purified from elicited and control leaf extracts. These two compounds inhibited spore germination in TLC-biodetection assays, suggesting that they are constitutive antifungal components of rocket. The third bioactive spot did not yield sufficient amount of compound for bioassays or for characterization. The two metabolites (**166** and **167**) were characterized by ^{1}H NMR, ^{13}C NMR, and HRMS-EI, as follows.

The HRMS-EI of compound **166** with t_R = 22.5 min indicated a molecular ion at *m/z* 161.0333 that was consistent with the molecular formula $C_6H_{11}NS_2$. The ^{1}H NMR spectrum showed 11 protons (four methylene protons at δ_H 1.77, 1.84, 2.56, 3.58, and a singlet at δ_H 2.12 indicating presence of a SCH_3 group) as suggested by HRMS. The ^{13}C NMR spectroscopic data corroborated the structural assignment based on ^{1}H NMR. From these data, the structure of compound **166** was assigned as 4-methylthiobutyl isothiocyanate. Compound **166** was previously isolated and identified from rocket extracts (Bennett et al., 2002); the spectroscopic data obtained were consistent with that reported (Vermeulen et al., 2003).

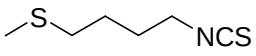

166

The HRMS-EI of compound **167** with t_R = 34.7 min (HPLC-DAD) indicated a molecular ion at *m/z* 292.0196 which was consistent with the molecular formula $C_{10}H_{16}N_2S_4$, and a fragment ion at *m/z* 146.0095 which was consistent with the molecular formula $C_5H_8NS_2$. ^{1}H NMR spectrum showed 8 protons (four methylene groups at δ_H 1.85, 2.74, and 3.59) whereas the ^{13}C NMR spectrum indicated the presence of 5 carbons (four methylene carbons at δ_C 45.1, 38.3, 29.0, 26.4, and a broad singlet at 130.9) thus suggesting a symmetrical structure. The structure of compound **167** was therefore assigned as bis(4-isothiocyanatobutyl)disulfide. Compound **167** was previously isolated and identified from rocket extracts; the spectroscopic data obtained were consistent with that reported (Cerny et al., 1996).

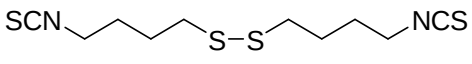

167

2.2 Biosynthesis of phytoalexins and glucosinolates

Phytoalexins and glucosinolates play a vital role in plant defense systems. Cultivated crucifers are susceptible to various fungal diseases such as blackleg, blackspot, and Sclerotinia stem rot among others. A few wild species have been reported to be resistant to some of these fungal diseases. Production of crops with enhanced disease resistance can be achieved through genetic manipulation by, for example, making them capable of producing metabolites involved in defense mechanisms (Dixon, 2005). The transfer of such positive traits will require an understanding of the biosynthetic pathways of these metabolites. The study of biosynthetic pathways requires synthesis of potential biosynthetic precursors containing isotopes that allow measurements of their incorporation.

2.2.1 Syntheses of compounds

The use of perdeuterated compounds in biosynthetic studies is invaluable as extremely small amounts of deuterated metabolites can be detected unambiguously by mass spectrometry, e.g. ESI-HRMS or APCI-HRMS (Pedras and Okinyo, 2006a). The indole derivatives of immediate interest needed to contain at least three deuterium atoms, as this number can allow the unambiguous detection and assignment of labeled phytoalexins using HRMS analysis of *m/z* $[M + 3]^{+/-}$ and corresponding fragment ions *m/z* $[M - X + 3]^{+/-}$. Potential precursors containing different amounts of deuterium were synthesized: [4',5',6',7'-$^{2}H_4$]indolyl-3-acetaldoxime (**112a**), [4',5',6',7'-$^{2}H_4$]1-methoxyindolyl-3-acetaldoxime (**116b**), [1",1",1",4',5',6',7'-$^{2}H_7$]1-methoxyindolyl-3-acetaldoxime (**116c**), [4',5',6',7'-$^{2}H_4$]indolyl-3-[^{34}S]acetothiohydroxamic acid (**174a**), [4',5',6',7'-$^{2}H_4$]1-methoxybrassinin (**18b**), [3,3,3,4',5',6',7'-$^{2}H_7$]1-methoxybrassinin (**18c**), [4',5',6',7'-$^{2}H_4$]sinalbin B (**31a**), [4',5',6',7'-$^{2}H_4$]cyclobrassinin (**28a**), and [S$C^{2}H_3$]brassicanal A (**39b**).

In addition compounds (non-isotopically labeled) that would lead to non-natural products if incorporated, i.e. substrates used for precursor-directed biosynthesis (Glaswischnig et al., 2004; Xu et al., 2007), were prepared: 1-methylindolyl-3-acetaldoxime (**170**), 1-methylindolyl-3-acetothiohydroxamic acid (**178**), 1-(*t*-butoxycarbonyl)indol-3-ylmethyl-isothiocyanate (**180**) and 1-acetylindol-3-

ylmethylisothiocyanate (**183**). Incorporation of such precursors can be determined by comparison of HPLC-DAD chromatograms of fed and control extracts. Synthesis of non-natural phytoalexin derivatives followed by HPLC-DAD and HPLC-MS-ESI analyses can be employed to unambiguously identify the phytoalexins incorporating the non-natural precursors.

2.2.1.1 Synthesis of [4',5',6',7'-$^2H_4$]indolyl-3-acetaldoxime (112a) and derivatives

This section covers the synthesis of [4',5',6',7'-$^2H_4$]indolyl-3-acetaldoxime (**112a**), [4',5',6',7'-$^2H_4$]1-methoxyindolyl-3-acetaldoxime (**116b**), [1",1",1",4',5',6',7'-$^2H_7$]1-methoxyindolyl-3-acetaldoxime (**116c**), and 1-methylindolyl-3-acetaldoxime (**170**)

[4',5',6',7'-$^2H_4$]Indolyl-3-acetaldoxime (112a)

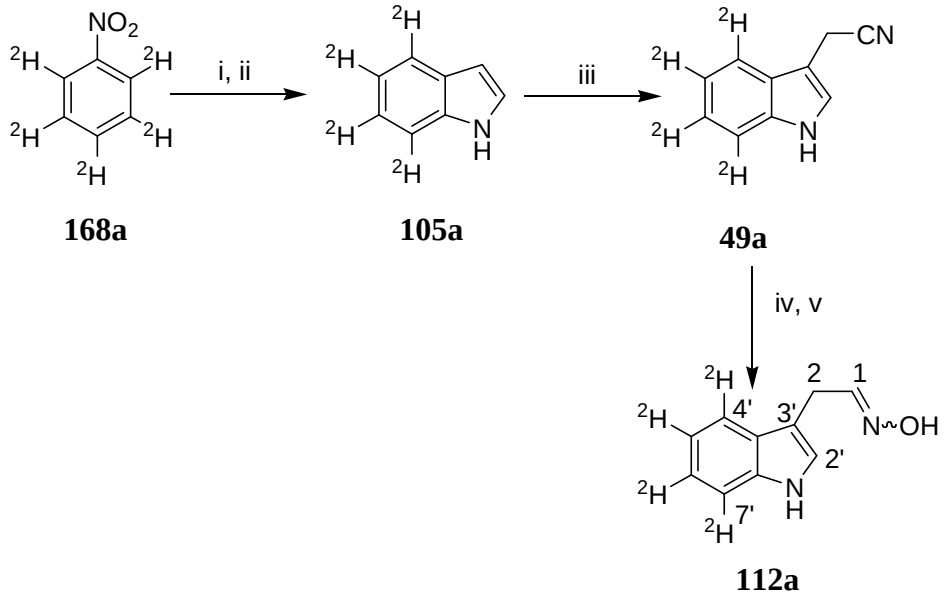

Scheme 2.1 Reagents and conditions: i) $ClCH_2CN$, NaOH, DMSO, 40%; ii) 10% Pd/C, H_2, EtOAc, 61%; iii) Mg, ICH_3, $BrCH_2CN$, Et_2O, 57%; iv) DIBAH; v) $HONH_2 \cdot HCl$, NaOAc, EtOH, 33% from **49a** (Pedras and Okinyo, 2006a).

[3,4,5,6-$^2H_4$]2-Nitrophenylacetonitrile was prepared from [2,3,4,5,6-$^2H_5$]nitrobenzene (**168a**) through vicarious nucleophilic substitution of hydrogen with

chloroacetonitrile (Makosza and Winiarski, 1984). This procedure provided a mixture of [3,4,5,6-$^{2}H_4$]2-nitrophenylacetonitrile and [2,3,5,6-$^{2}H_4$]4-nitrophenylacetonitrile in a 10:1 ratio at 40% yield in one step (Pedras and Okinyo, 2006a). Hydrogenation of the mixture under balloon pressure at room temperature yielded [4,5,6,7-$^{2}H_4$]indole (**105a**) and [2,3,5,6-$^{2}H_4$]4-aminophenylacetonitrile; [2,3,5,6-$^{2}H_4$]4-aminophenylacetonitrile was separated from the reaction mixture as a hydrochloride salt upon treatment of the reaction mixture with HCl (1 M), yielding [4,5,6,7-$^{2}H_4$]indole in 61% (Pedras and Okinyo, 2006a). [4',5',6',7'-$^{2}H_4$]Indolyl-3-acetonitrile (**49a**) was prepared by reacting indolylmagnesium iodide (prepared from [4,5,6,7-$^{2}H_4$]indole, and Mg/methyl iodide) with bromoacetonitrile (Pedras et al., 2003a). Reduction of [4',5',6',7'-$^{2}H_4$]indolyl-3-acetonitrile to the unstable [4',5',6',7'-$^{2}H_4$]indolyl-3-acetaldehyde with diisobutylaluminium hydride (DIBAH), followed by hydrolysis with HCl (2 M, Miyashita et al., 1997) and immediate treatment with hydroxylamine hydrochloride and sodium acetate yielded [4',5',6',7'-$^{2}H_4$]indolyl-3-acetaldoxime (**112a**, **Scheme 2.1**) in 33% over two steps (Pedras and Okinyo, 2006a).

[4',5',6',7'-$^2H_4$]1-Methoxyindolyl-3-acetaldoxime (116b) and [1",1",1",4',5',6',7'-$^2H_7$]1-methoxyindolyl-3-acetaldoxime (116c)

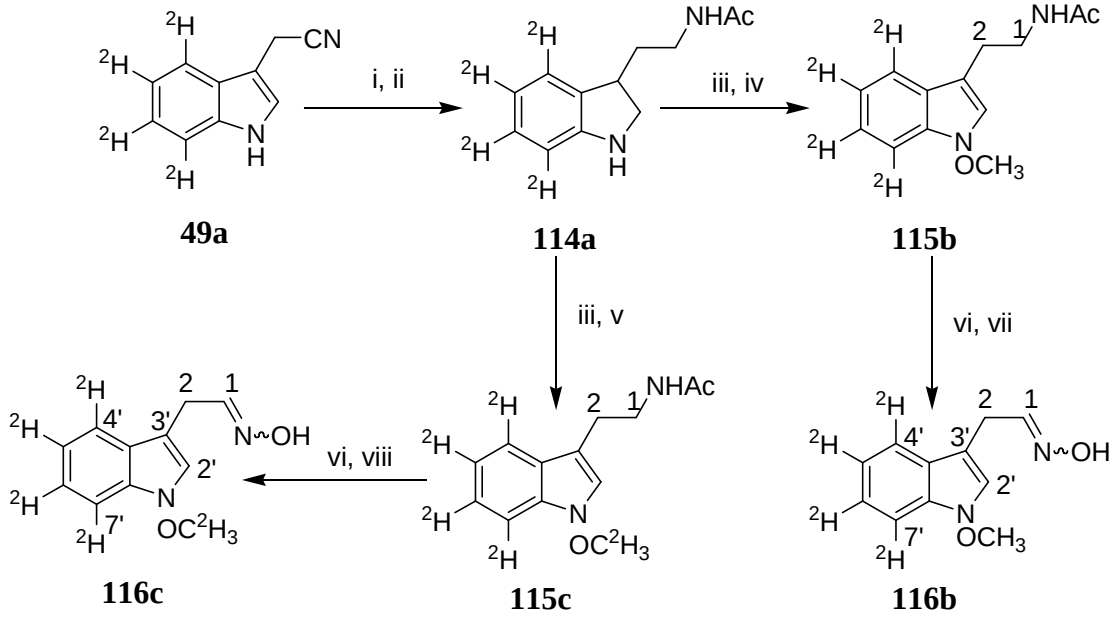

Scheme 2.2 Reagents and conditions: i) 10% Pd/C, H_2, Ac_2O; ii) $NaBH_3CN$, AcOH; iii) $Na_2WO_4{\cdot}2H_2O$, H_2O_2, CH_3OH; iv) $(CH_3O)_2SO_2$, K_2CO_3; v) $(C^2H_3O)_2SO_2$, K_2CO_3, CH_3OH; vi) NaOH, CH_3OH, reflux; vii) $Na_2WO_4{\cdot}2H_2O$, H_2O_2, CH_3OH, 5% from **49a** (Pedras and Okinyo, 2006a); viii) $Na_2WO_4{\cdot}2H_2O$, H_2O_2, CH_3OH, 4% from **49a** (Pedras and Okinyo, 2006a).

[4',5',6',7'-$^2H_4$]1-Methoxyindolyl-3-acetaldoxime and [1",1",1",4',5',6',7'-$^2H_7$]1-methoxyindolyl-3-acetaldoxime were synthesized as shown in **Scheme 2.2**. [4',5',6',7'-$^2H_4$]N_b-Acetyltryptamine was prepared in one step by hydrogenation of [4',5',6',7'-$^2H_4$]indolyl-3-acetonitrile in acetic anhydride at room temperature. Reduction of [4',5',6',7'-$^2H_4$]N_b-acetyltryptamine with sodium cyanoborohydride in glacial acetic acid yielded [4',5',6',7'-$^2H_4$]N_b-acetyl-2,3-dihyroindolyl-3-ethylamine (**114a**). Oxidation of **114a** with hydrogen peroxide followed by methylation of the 1-hydroxyindolyl intermediate with dimethylsulphate or hexadeuterated dimethylsulphate (Somei and Kawasaki, 1989) yielded [4',5',6',7'-$^2H_4$]N_b-acetyl-1-methoxytryptamine (**115b**) or [1",1",1",4',5',6',7'-$^2H_7$]N_b-acetyl-1-methoxytryptamine (**115c**), respectively. Sodium hydroxide hydrolysis of the N_b-acetyl groups of **115b** and **115c** yielded [4',5',6',7'-$^2H_4$]1-

methoxytryptamine and [1",1",1",4',5',6',7'-$^2H_7$]1-methoxytryptamine, respectively. Hydrogen peroxide oxidation of [4',5',6',7'-$^2H_4$]1-methoxytryptamine in the presence of sodium tungstate (Burckard et al., 1965) yielded [4',5',6',7'-$^2H_4$]1-methoxyindolyl-3-acetaldoxime (**116b**) in 5% over five steps. [1",1",1",4',5',6',7'-$^2H_7$]1-Methoxytryptamine was similarly oxidized to yield [1",1",1",4',5',6',7'-$^2H_7$]1-methoxyindolyl-3-acetaldoxime (**116c**) in 4% over five steps (**Scheme 2.2**, Pedras and Okinyo, 2006a). [1",1",1"-$^2H_3$]1-Methoxyindolyl-3-acetaldoxime (**116a**) and 1-methoxyindolyl-3-acetaldoxime (**116**) were similarly prepared.

1-Methylindolyl-3-acetaldoxime (170)

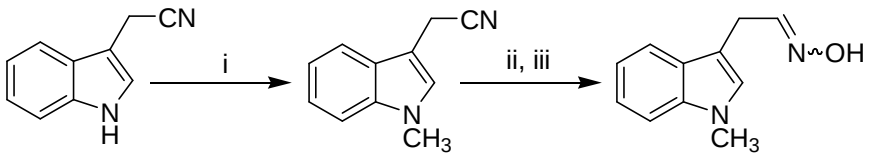

49 **169** **170**

Scheme 2.3 Reagents and conditions: i) NaH, ICH_3, 96%; ii) DIBAH; iii) $HONH_2 \cdot HCl$, NaOAc, EtOH, 66%.

1-Methylindolyl-3-acetonitrile (**169**) was obtained in 96% yield via methylation of indolyl-3-acetonitrile (**49**) with methyl iodide in the presence of sodium hydride. Reduction of 1-methylindolyl-3-acetonitrile with diisobutylaluminium hydride followed by hydrolysis with 5 % HCl (Pedras and Okinyo 2006a) provided 1-methylindolyl-3-acetaldehyde. Reacting 1-methylindole-3-acetaldehyde with hydroxylamine hydrochloride and sodium acetate yielded 1-methylindolyl-3-acetaldoxime (**170**) in 66% (**Scheme 2.3**).

2.2.1.2 Synthesis of [4',5',6',7'-$^{2}H_4$]indolyl-3-[^{34}S]acetothiohydroxamic acid (174a) and 1-methyl derivative

This section covers the synthesis of ^{34}S-hexamethyldisilathiane (**171a**), [4',5',6',7'-$^{2}H_4$]indolyl-3-[^{34}S]acetothiohydroxamic acid (**174a**), and 1-methylindolyl-3-acetothiohydroxamic acid (**178**).

[4',5',6',7'-$^{2}H_4$]indolyl-3-[^{34}S]acetothiohydroxamic acid (174a)

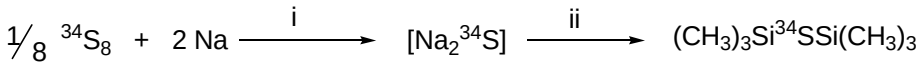

171a

Scheme 2.4 Reagents and conditions: i) Naphthalene, THF, reflux; ii) $(CH_3)_3SiCl$, r.t., 60% based on ^{34}S.

Preparation of [4',5',6',7'-$^{2}H_4$]indolyl-3-[^{34}S]acetothiohydroxamic acid (**174a**, **Scheme 2.5**) required an ^{34}S-labeled reagent to introduce the labeled sulfur atom. ^{34}S-Hexamethyldisilathiane (**171a**) was therefore synthesized by a modification of the procedure by So and Boudjouk (1989; 1992) as shown in **Scheme 2.4**. Thus, sodium was cut into small pieces under *n*-hexane and was introduced into a flask charged with sulfur and naphthalene in dry tetrahydrofuran under atmosphere of argon. After 2 hours of sonication and 2 hours of refluxing, the reaction flask was cooled in an ice-bath followed by drop wise addition of chlorotrimethylsilane. The reaction mixture was stirred for 10 minutes in ice-bath and 3 hours at room temperature after which excess tetrahydrofuran and chlorotrimethylsilane were distilled off at atmospheric pressure, followed by vacuum distillation to yield ^{34}S-hexamethyldisilathiane (**171a**, b.p. 68-71 ºC at 510 torr) as a vile smelling colorless liquid in 60% yield based on ^{34}S. The ^{34}S-hexamethyldisilathiane (**171a**) was analyzed by GC and GC-MS-EI. Non-labeled hexamethyldisilathiane (**171**) was similarly prepared and analyzed by GC-MS-EI which was consistent with that reported by So and Boudjouk (1989; 1992).

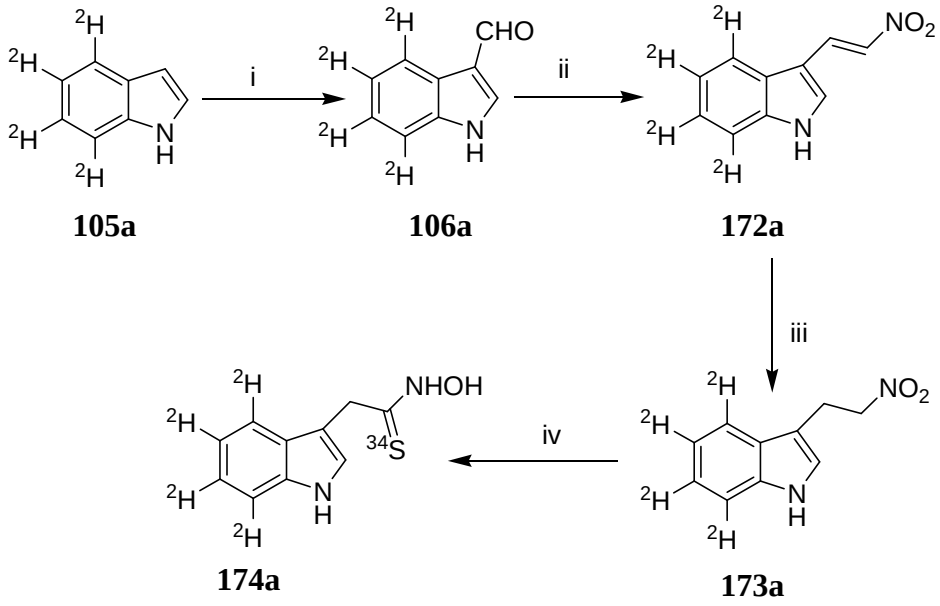

Scheme 2.5 Reagents and conditions: i) $POCl_3$, DMF, 87%; ii) NH_4OAc, CH_3NO_2, reflux 128-130 ºC, 99%; iii) $NaBH_4$, *i*-PrOH, SiO_2, $CHCl_3$, 42%; iv) KH, $(Me_3Si)_2{}^{34}S$ (**171a**), THF, 76%.

Vilsmeier-Haack formylation of [4,5,6,7-$^2H_4$]indole (**105a**) provided [4,5,6,7-$^2H_4$]indole-3-carboxaldehyde (**106a**) in good purity to be used in the next step without further purification (Pedras et al., 1998). Knöevenagel type condensation between [4,5,6,7-$^2H_4$]indole-3-carboxaldehyde with excess nitromethane in presence of catalytic amount of ammonium acetate under reflux conditions (Canoira et al., 1989) yielded [4,5,6,7-$^2H_4$]-3-(2'-nitrovinyl)indole (**172a**) in near quantitative yield. [4,5,6,7-$^2H_4$]-3-(2'-Nitroethyl)indole (**173a**) was prepared in 42% yield via sodium borohydride reduction of **172a** in the presence of silica gel and using chloroform and isopropanol as solvent (Sinhababu and Borchardt, 1983). In order to prepare thiohydroxamic acid **174a**, a solution of [4,5,6,7-$^2H_4$]-3-(2'-nitroethyl)indole in dry tetrahydrofuran was added drop wise to potassium hydride powder at 0 ºC under argon atmosphere, the reaction mixture was allowed to warm up to room temperature. Addition of ^{34}S-hexamethyldisilathiane (**171a**) to the resulting nitronate (Hwu and Tsay, 1990) yielded [4,5,6,7-$^2H_4$]indolyl-3-[^{34}S]acetothiohydroxamic acid (**174a**) in 76% (**Scheme 2.5**).

1-Methylindolyl-3-acetothiohyrodroxamic acid (178)

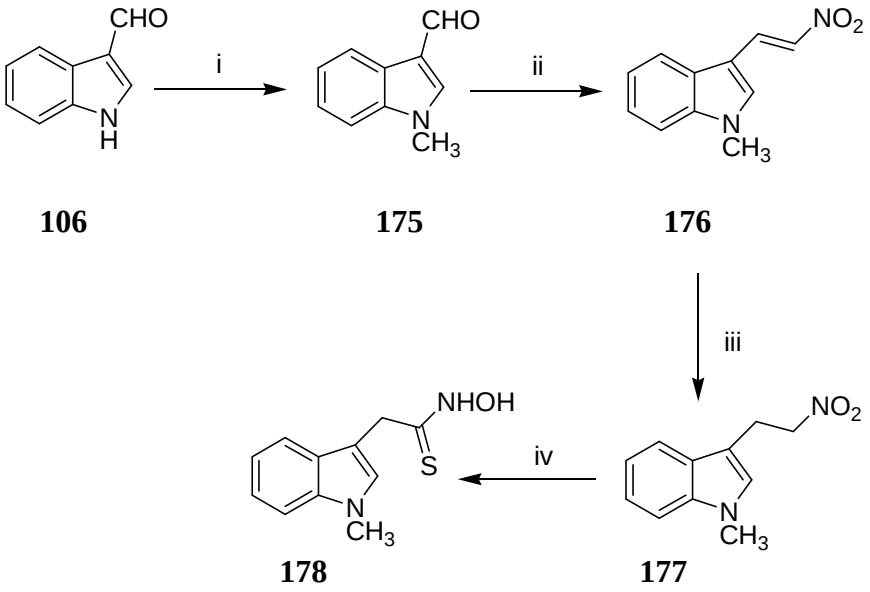

Scheme 2.6 Reagents and conditions: i) NaH, ICH_3, 98%; (ii) NH_4OAc, CH_3NO_2, reflux 128-130 ºC, 98%; (iii) $NaBH_4$, i-PrOH, SiO_2, $CHCl_3$, 63%; (iv) KH, $(Me_3Si)_2S$ (**171**), THF, 67%.

Preparation of 1-methylindolyl-3-acetothiohydroxamic acid (**178**, **Scheme 2.6**) began with methylation of indole-3-carboxaldehyde (**106**) using methyl iodide in the presence of sodium hydride. Knoevangel type condensation of the resulting 1-methylindole-3-carboxaldehyde (**175**) with excess nitromethane in the presence of catalytic amount of ammonium acetate (Canoira et al., 1989) provided 1-methyl-3-(2-nitrovinyl)indole (**176**) in 98% yield. Sodium borohydride reduction of **176** in the presence of silica gel (Sinhababu and Borchardt, 1983) gave 1-methyl-3-(2-nitroethyl)indole (**177**) in 63% yield. Reaction of **177** with potassium hydride followed by treatment of the resulting nitronate with hexamethyldisilathiane (**171**, Hwu and Tsay, 1990) afforded 1-methylindolyl-3-acetothiohydroxamic acid (**178**) in 67 % yield.

2.2.1.3 Synthesis of N-protected-indolyl derivatives of indolyl-3-methylisothiocyanate

This section covers the synthesis of (*tert*-butoxycarbonyl)indolyl-3-methyl-isothiocyanate (**180**), and 1-acetylindolyl-3-methylisothiocyanate (**183**) as probes for the role of indolyl-3-methylisothiocyanate (**123**) in the biosynthetic pathway of crucifer phytoalexins.

1-(tert-Butoxycarbonyl)indolyl-3-methyl isothiocyanate (180)

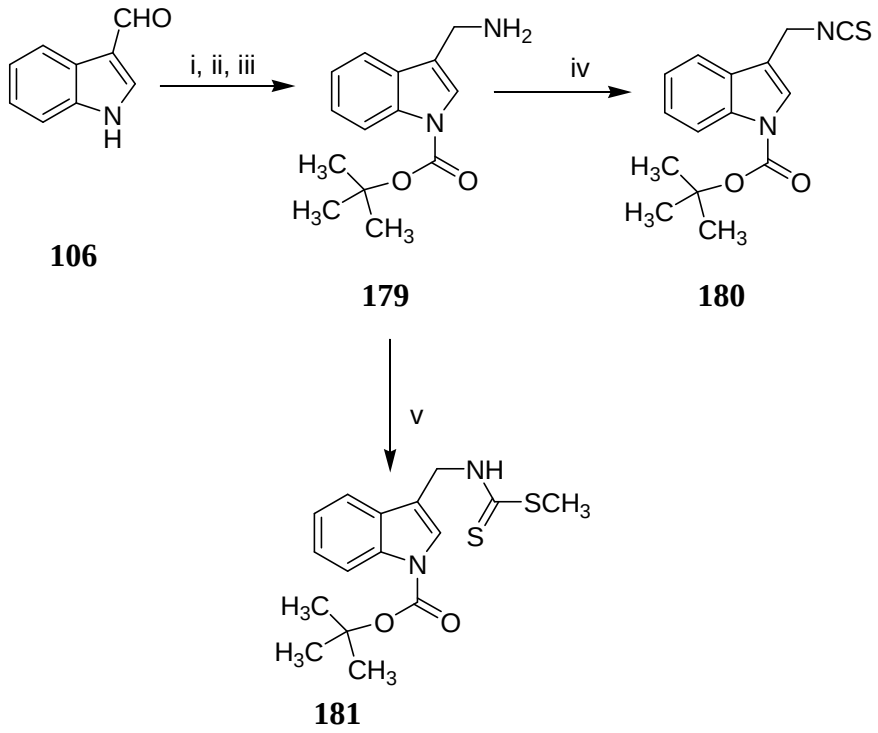

106 **179** **180** **181**

Scheme 2.7 Reagents and conditions: i) Boc_2O, DMAP, THF, quant.; ii) $HONH_2 \cdot HCl$, Na_2CO_3, EtOH, 48-50 ºC, quant.; iii) $NiCl_2 \cdot 6H_2O$, $NaBH_4$, CH_3OH; iv) Cl_2CS, $CaCO_3$, CH_2Cl_2-H_2O, 56 % from oxime (Kutschy et al., 1997; 1998); v) Pyridine, Et_3N, CS_2, ICH_3, 72% from oxime.

Indole-3-carboxaldehyde (**106**) was treated with di-*tert*-butyl dicarbonate (Boc_2O) and 4-(dimethylamino)pyridine (DMAP) in tetrahydrofuran to yield 1-(*tert*-butoxycarbonyl)indole-3-carboxaldehyde in quantitative yield. Standard oximation procedure employing hydroxylamine hydrochloride and sodium carbonate afforded 1-

(*tert*-butoxycarbonyl)indolyl-3-carboxaldehyde oxime that after sodium borohydride and nickel(II) chloride reduction yielded amine **179**. Reaction of amine **179** with thiophosgene in the presence of calcium carbonate yielded 1-(*tert*-butoxycarbonyl)indolyl-3-methyl isothiocyanate (**180**) in 56% (**Scheme 2.7**, Kutschy et al., 1997; 1998).

1-Acetylindolyl-3-methyl isothiocyanate (183)

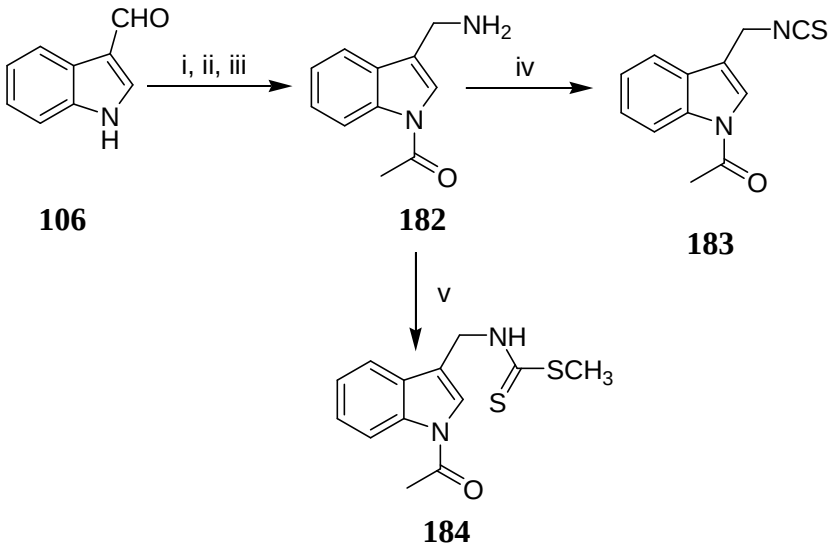

Scheme 2.8 Reagents and conditions: i) Ac_2O, pyridine, 96%; ii) $HONH_2 \cdot HCl$, NaOAc, EtOH, 45-50 ºC, 88%; iii) $NiCl_2 \cdot 6H_2O$, $NaBH_4$, CH_3OH; iv) Cl_2CS, $CaCO_3$, CH_2Cl_2-H_2O, 31% from oxime; v) Et_3N, CS_2, then ICH_3, pyridine, 41 % from oxime.

1-Acetylindole-3-carboxaldehyde was obtained in 96% yield from indole-3-carboxaldehyde (**106**) and acetic anhydride in pyridine. Heating 1-acetylindole-3-carboxaldehyde with sodium carbonate and hydroxylamine hydrochloride at temperatures above 50 ºC resulted in loss of acetyl group with formation of indolyl-3-carboxaldehyde oxime. Thus, 1-acetylindolyl-3-carboxaldehyde oxime was prepared in 84% yield by heating 1-acetylindole-3-carboxaldehyde with hydroxylamine hydrochloride and sodium acetate at 50 ºC for 10 minutes. Sodium borohydride and nickel(II) chloride reduction (Kutschy et al., 1997; 1998) of 1-acetylindolyl-3-carboxaldehyde oxime at 0 °C provided amine **182**, which was reacted with

thiophosgene in the presence of calcium carbonate (Kutschy et al., 1997; 1998) to give 1-acetylindolyl-3-methyl isothiocyanate (**183**) in 31% yield (**Scheme 2.8**).

2.2.1.4 Synthesis of [4',5',6',7'-$^2H_4$]brassinin (16a), [4',5',6',7'-$^2H_4$]cyclobrassinin (28a), [4',5',6',7'-$^2H_4$]1-methoxyspirobrassinin (35a) and derivatives

This section covers the synthesis of [4',5',6',7'-$^2H_4$]brassinin (**16a**), [4',5',6',7'-$^2H_4$]1-methoxybrassinin (**18b**), [3,3,3,4',5',6',7'-$^2H_7$]1-methoxybrassinin (**18c**), 1-methylbrassinin (**192**), 1-(*t*-butoxycarbonyl)brassinin (**181**), 1-acetylbrassinin (**184**), [4',5',6',7'-$^2H_4$]cyclobrassinin (**28a**), 1-methylcyclobrassinin (**193**), [4',5',6',7'-$^2H_4$]sinalbin B (**31a**), [4',5',6',7'-$^2H_4$]1-methoxyspirobrassinin (**35a**), 1-methylspirobrassinin (**194**), 1-acetylspirobrassinin (**195**), and 1-(*t*-butoxycarbonyl)spirobrassinin (**196**).

[4',5',6',7'-$^2H_4$]Brassinin (16a) and [4',5',6',7'-$^2H_4$]cyclobrassinin (28a)

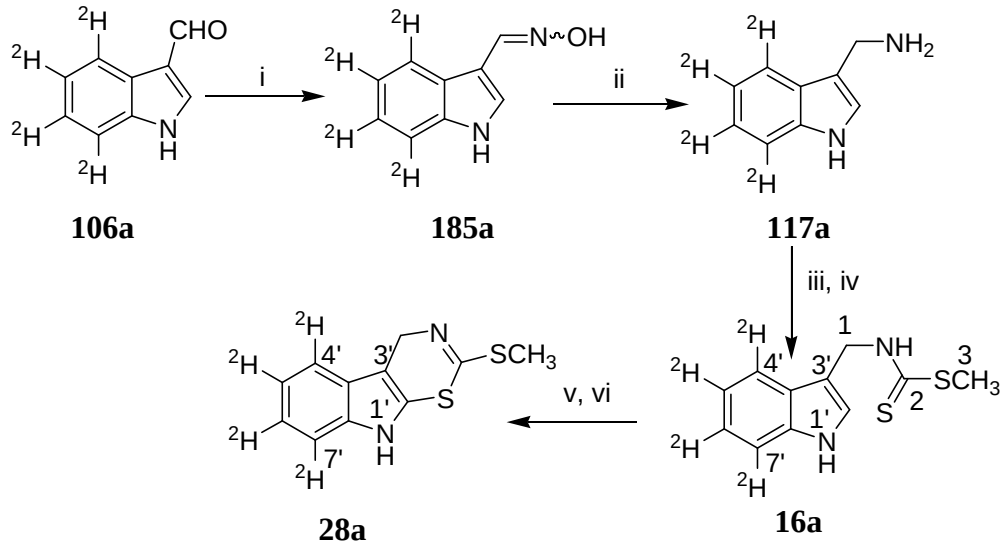

Scheme 2.9 Reagents and conditions: i) $HONH_2 \cdot HCl$, Na_2CO_3, EtOH, reflux, 87%; ii) NaOH, Devarda's alloy, CH_3OH; iii) Pyridine, Et_3N, CS_2, 60 min, 0 ºC; iv) ICH_3, 50%; v) pyridine/HBr/Br_2, THF; vi) DBU, 58% (Pedras et al., 1998).

[4',5',6',7'-$^{2}H_4$]Cyclobrassinin (**28a**) was synthesized following previously established procedure (Pedras et al., 1998). [4,5,6,7-$^{2}H_4$]Indole-3-carboxaldehyde (**106a**) was transformed to the corresponding oximes **185a** upon treatment with hydroxylamine hydrochloride and sodium carbonate. Reduction of **185a** yielded [4',5',6',7'-$^{2}H_4$]indole-3-methanamine (**117a**), which was treated with triethylamine and carbon disulfide in pyridine, followed by addition of methyl iodide to yield [4',5',6',7'-$^{2}H_4$]brassinin (**16a**) in 50%. [4',5',6',7'-$^{2}H_4$]Cyclobrassinin (**28a**), was prepared by treating **16a** with pyridinium bromide perbromide, followed by alkalynation with 1,8-diazabicyclo[5.4.0]undec-7-ene (DBU) to yield [4',5',6',7'-$^{2}H_4$]cyclobrassinin in 58% (**Scheme 2.9**).

[4',5',6',7'-$^2H_4$]1-Methoxybrassinin (18b) and [4',5',6',7'-$^2H_4$]sinalbin B (31a)

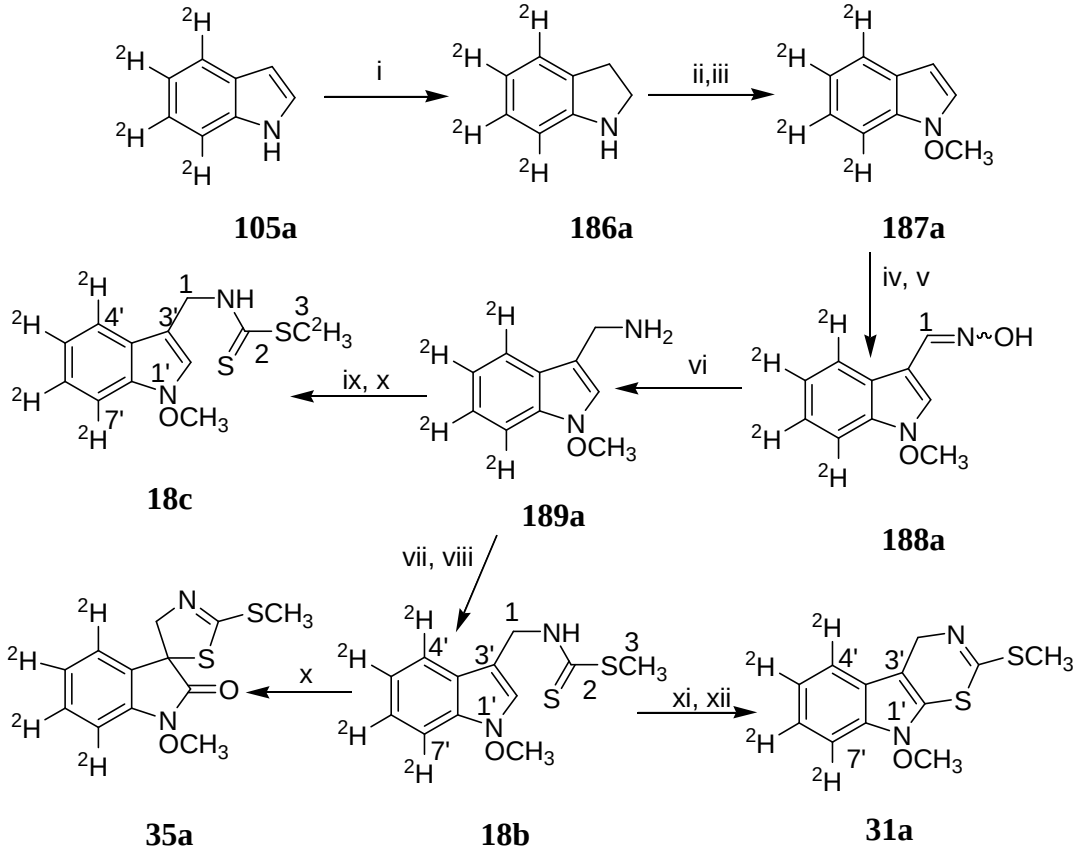

Scheme 2.10 Reagents and conditions: i) $NaBH_3CN$, AcOH, 82%; ii) $Na_2WO_4 \cdot H_2O$, H_2O_2; iii) $(CH_3O)_2SO_2$, K_2CO_3, CH_3OH, 52%; iv) $POCl_3$, DMF, 93%; v) $HONH_2 \cdot HCl$, Na_2CO_3, EtOH, reflux, 99%; vi) $NaBH_3CN$, $TiCl_3$, NH_4OAc, CH_3OH; vii) Pyridine, Et_3N, CS_2, 60 min, 0 ºC; viii) ICH_3, 67%; ix) Pyridine, Et_3N, CS_2, 60 min, 0 ºC; x) IC^2H_3, 68% (Pedras and Okinyo, 2006a); xi) NBS, CH_2Cl_2; xii) Et_3N, 47% (adapted from Pedras and Zaharia, 2000); xiii) PCC, CH_2Cl_2, 41% (adapted from Pedras et al., 2006a).

[4',5',6',7'-$^2H_4$]1-Methoxybrassinin (**18b**) was obtained from [4,5,6,7-$^2H_4$]indole (**Scheme 2.10**). First [4,5,6,7-$^2H_4$]indole was reduced with sodium cyanoborohydride in acetic acid to provide [4,5,6,7-$^2H_4$]indoline (**186a**) which was obtained in 82%. Hydrogen peroxide oxidation of [4,5,6,7-$^2H_4$]indoline to 1-hydroxyindole intermediate followed by dimethylsulphate methylation (Somei and Kawasaki, 1989) yielded [4,5,6,7-

$^{2}H_4$]1-methoxyindole (**187a**) in 52%. Standard Vilsmeier-Haack formylation of **187a** yielded [4,5,6,7-$^{2}H_4$]1-methoxyindole-3-carboxaldehyde, which was transformed to [4',5',6',7'-$^{2}H_4$]1-methoxyindolyl-3-carboxaldehyde oxime (**188a**) on treatment with hydroxylamine hydrochloride and sodium carbonate. Reduction of the oxime **188a** employing sodium cyanoborohydride and titanium (III) chloride in presence of ammonium acetate (Pedras and Zaharia, 2000) yielded [4',5',6',7'-$^{2}H_4$]1-methoxyindolyl-3-methanamine (**189a**) which was used in the next step without further purification. Triethylamine and carbon disulfide treatment of a solution of amine **189a** in pyridine yielded dithiocarbamate intermediate *in situ*, which was reacted with methyl iodide to afford [4',5',6',7'-$^{2}H_4$]1-methoxybrassinin in 67% yield over two steps from the oxime **188a** (Pedras and Okinyo, 2006a). By adapting experimental procedure for preparation of sinalbin B (**31**, Pedras and Zaharia, 2000), [4',5',6',7'-$^{2}H_4$]1-methoxybrassinin was reacted with *N*-bromosuccinimide (NBS) followed by triethylamine to yield [4',5',6',7'-$^{2}H_4$]sinalbin B (**31a**, **Scheme 2.10**) in 47%.

[3,3,3,4',5',6',7'-$^{2}H_7$]1-Methoxybrassinin (18c)

[3,3,3,4',5',6',7'-$^{2}H_7$]1-Methoxybrassinin (**18c**) was prepared following similar experimental procedure as that for [4',5',6',7'-$^{2}H_4$]1-methoxybrassinin (**Scheme 2.10**). Methylation of the dithiocarbamate intermediate was conducted with deuterated methyl iodide to provide [3,3,3,4',5',6',7'-$^{2}H_7$]1-methoxybrassinin in 68% yield over two steps from oxime **188a** (Pedras and Okinyo, 2006a).

1-Methylbrassinin (192)

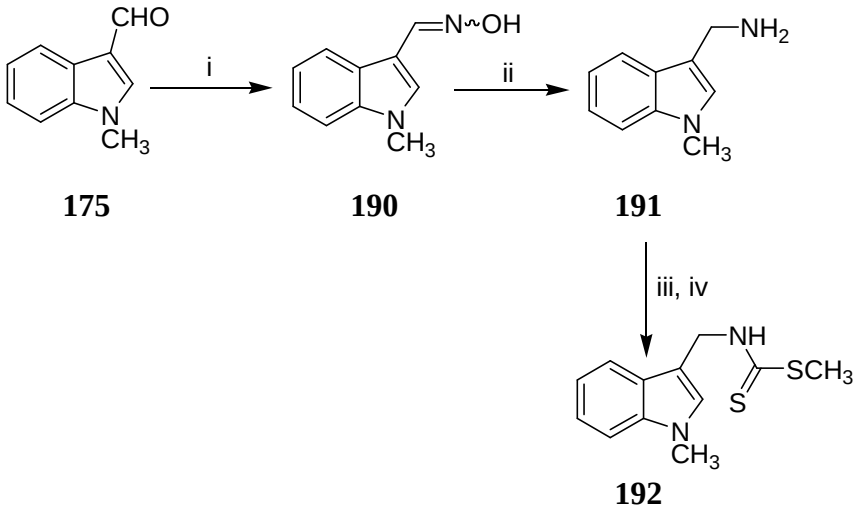

Scheme 2.11 Reagents and conditions: i) $HONH_2 \cdot HCl$, Na_2CO_3, EtOH, reflux, 93%; ii) NaOH, Devarda's alloy, CH_3OH; iii) Pyridine, Et_3N, CS_2, 60 min, 0 ºC; iv) ICH_3, 52%.

Reaction of 1-methylindole-3-carboxaldehyde (**175**) with hydroxylamine hydrochloride in the presence of sodium carbonate provided 1-methylindolyl-3-carboxaldehyde oxime (**190**) in 93% yield. Devarda's alloy reduction of oxime **190** provided 1-methylindolyl-3-methanamine (**191**) which was transformed to 1-methylbrassinin (**192**) in 52% yield following established experimental procedure for synthesis of brassinin (Pedras et al., 2000; 2003b).

1-(tert-Butoxycarbonyl)brassinin (181)

1-(*tert*-Butoxycarbonyl)brassinin (**181**) was previously prepared in 97% yield from 1-(*tert*-butoxycarbonyl)indolyl-3-methylisothiocyanate and sodium methane thiolate (Kutschy et al., 1997; 1998); however, in my work, this route provided **181** in only 40% yield. Thus, the traditional route for brassinin synthesis was used (Pedras et al., 2003b). Freshly prepared amine **179** was treated with triethylamine and carbon disulfide to afford a dithiocarbamate intermediate *in situ*, methylation of this intermediate with methyl iodide yielded 1-(*tert*-butoxycarbonyl)brassinin in 72% (**Scheme 2.7**).

1-Acetylbrassinin (184)

1-Acetylbrassinin (**184**) was synthesized from the freshly prepared amine **182** (**Scheme 2.8**) by slight modification of procedure used for preparation of brassinin. Addition of triethylamine and carbon disulfide to a solution of freshly prepared amine **182** at room temperature with stirring for 90 minutes provided intermediate 1-acetylindolyl-3-methyl dithiocarbamate *in situ*, which was reacted with methyl iodide to give 1-acetylbrassinin (**184**, **Scheme 2.8**) in 41% yield.

1-Methylcyclobrassinin (193)

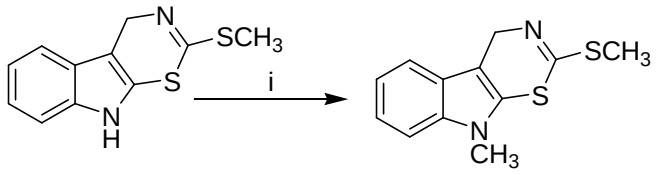

28 **193**

Scheme 2.12 Reagents and conditions: i) NaH, ICH_3, THF, 0 ºC, 82%.

1-Methylcyclobrassinin (**193**) was obtained from a reaction of cyclobrassinin (**28**) with methyl iodide at 0 ºC (**Scheme 2.12**). 1-Methylcyclobrassinin (**193**) was previously prepared from 1-methylbrassinin (**192**) (Kutschy et al., 1998).

[4',5',6',7'-$^2H_4$]1-Methoxyspirobrassinin (35a)

[4',5',6',7'-$^2H_4$]1-Methoxyspirobrassinin (**35a**) was prepared from [4',5',6',7'-$^2H_4$]1-methoxybrassinin ((**18b**, **Scheme 2.10**) following previously set route (Pedras et al., 2006a). Thus, a solution of [4',5',6',7'-$^2H_4$]1-methoxybrassinin in dichloromethane was treated with pyridinium chlorochromate to provide [4',5',6',7'-$^2H_4$]1-methoxyspirobrassinin in 41% yield.

1-Methylspirobrassinin (194)

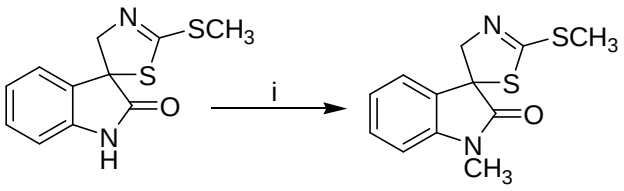

34 **194**

Scheme 2.13 Reagents and conditions: i) NaH, ICH_3, THF, 0 ºC, 91% (Pedras and Hossain, 2006).

1-Methylspirobrassinin (**194**) was obtained in 91% yield via methylation of spirobrassinin (**34**) with methyl iodide and sodium hydride at 0 °C (Pedras and Hossain, 2006, **Scheme 2.13**).

1-Acetylspirobrassinin (195)

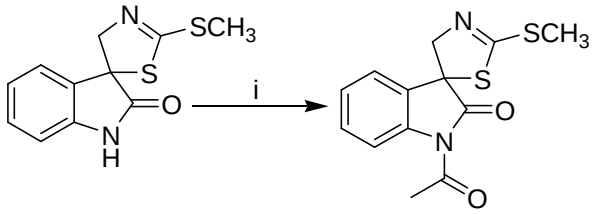

34 **195**

Scheme 2.14 Reagents and conditions: i) Pyridine, Ac_2O, 80%.

1-Acetylspirobrassinin (**195**) was obtained in 80% yield from reaction of spirobrassinin (**34**) with acetic anhydride in pyridine.

1-(tert-Butoxycarbonyl)spirobrassinin (196)

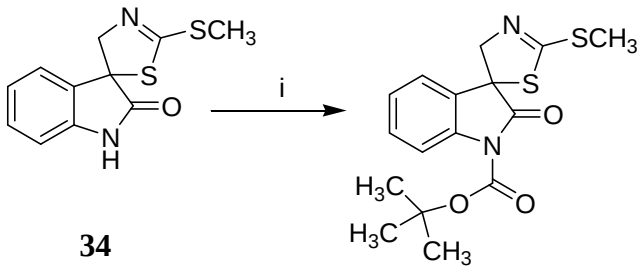

34 **196**

Scheme 2.15 Reagents and conditions: i) Boc_2O, DMAP, THF, Quant.

1-(*tert*-Butoxycarbonyl)spirobrassinin (**196**) was prepared in 99% yield from spirobrassinin (**34**) and Boc_2O in the presence of DMAP (**Scheme 2.15**).

2.2.1.5 Synthesis of [SC^2H_3]brassicanal A (39b)

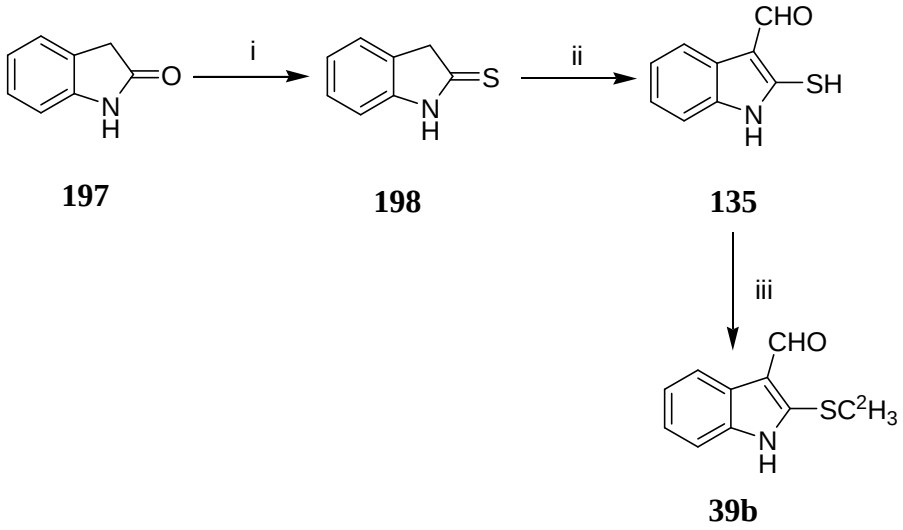

197 **198** **135** **39b**

Scheme 2.16 Reagents and conditions: i) $NaHCO_3$, P_4S_{10}, THF, 72%; ii) NaH, HCO_2Et (Pedras and Okanga, 1999); iii) Et_3N, IC^2H_3, Et_2O, 56%.

2-Mercaptoindole-3-carboxaldehyde (**135**) was synthesized following previously established procedure (Pedras and Okanga, 1999). Reaction of **135** with deuterated

methyl iodide in the presence of triethylamine afforded [SC^2H_3]brassicanal A (**39b**) in 56 % isolated yield.

2.2.2 Incorporation experiments using synthetic compounds

The present biosynthetic studies involved administration of perdeuterated precursors and ^{34}S containing indolyl-3-acetothiohydroxamic acid to different plant tissues that were known to produce a variety of phytoalexins and glucosinolates. Non-natural compounds containing methyl, acetyl and Boc groups at the indole nitrogen were also administered to these plant tissues. The *N*-substituents served as non-isotopic labels to probe biosynthetic pathway(s) of phytoalexins and glucosinolates. The main plant tissues used were *Brassica napus* (rutabaga), *B. rapa* (turnip), and *Erucastrum gallicum* (dog mustard).

2.2.2.1 Brassica napus L. ssp. rapifera (rutabaga) and B. rapa (turnip)

Rutabaga and turnip are two examples of tuberous brassicas that produce a variety of indole phytoalexins and indole glucosinolates (Monde et al., 1994; Pedras et al., 2004; Pedras and Montaut, 2004). The incorporation of phytoalexin precursors was established to be more efficient in tubers than in leaves or stems of brassicas (Pedras and Montaut, 2004). For this reason, these plant tissues were used to investigate biosynthetic pathway(s) of crucifer phytoalexins and glucosinolates.

In feeding experiments, rutabaga and turnip tubers were sliced horizontally after which cylindrical holes were made on one surface. Following overnight incubation at 20 °C in darkness, the slices were irradiated with UV on the surface with holes for 20 minutes, and further incubated for 24 hours. The slices were then incubated separately with (i) labeled precursors (5×10^{-4} M), (ii) non-labeled precursors (5×10^{-4} M), and (iii) carrier solution. The aqueous phase was collected (24, 48, 72 or 96 hours after administration), was extracted and was subjected to preliminary clean up to yield fractions containing phytoalexins (established by HPLC-DAD and HPLC-MS-ESI). The percentage of isotope (^2H, and/or ^{34}S) incorporation was established from analysis of

data obtained by HPLC-HRMS-ESI (positive or negative ion modes) according to the equation:

% of (^{2}H, and/or ^{34}S) incorporation = $\{[M + n]^{+/-}/([M]^{+/-} + [M + n]^{+/-})\} \times 100$ (n = 3, 4, 5), n is the number of deuterium atoms, and M is the peak area or relative intensity of the molecular ion peak.

The HPLC-HRMS-ESI data indicated that the ions $[M + n]^{+/-}$ were not present in natural abundance samples.

Extracts containing indolyl glucosinolates were obtained by cutting tissue around the holes, soaking in methanol, and grinding (mortar and pestle), followed by overnight extraction with aqueous methanol solution. The tissue extracts were subjected to RP-FCC to yield a fraction that contained indolyl glucosinolates (established by HPLC-DAD and HPLC-MS-ESI). The percentage of isotope (^{2}H, and ^{34}S) incorporation was established from HPLC-HRMS-ESI (negative ion mode) data similar to phytoalexins.

Incorporation of L-[2',4',5',6',7'-$^2H_5$]tryptophan (78b)

Rutabaga slices were prepared as previously described. Commercially available *L*-[2',4',5',6',7'-$^2H_5$]tryptophan (**78b**) was administered to UV-elicited slices followed by 72-hour incubation. The aqueous solution was collected, was extracted, and was subjected to preliminary clean up to yield fraction A that contained the phytoalexins cyclobrassinin (**28**), rutalexin (**33**), brassicanate A (**43**), rapalexin A (**53**), and fraction B that contained spirobrassinin (**34**) (established by HPLC-DAD and HPLC-MS-ESI) (**Figure 2.1**). Control slices were incubated with *L*-tryptophan (**78**) or with carrier solution and were treated similarly. HPLC-HRMS-ESI analyses (positive ion mode) of the phytoalexin fraction resulting from feeding *L*-[2',4',5',6',7'-$^2H_5$]tryptophan displayed the cyclobrassinin peak at t_R = 30.5 min containing two ions at *m/z* 235.0358 and 239.0609, that were consistent with the molecular formulae $C_{11}H_{11}N_2S_2$ and $C_{11}H_7{}^2H_4N_2S_2$, respectively. The ion at *m/z* 239.0609 was not detected in control samples incubated with non-labeled *L*-tryptophan. Based on the peak area of each ion,

the percentage of deuterium incorporation was found to be 7% {[1/(14 + 1)] × 100} (**Table 2.2**).

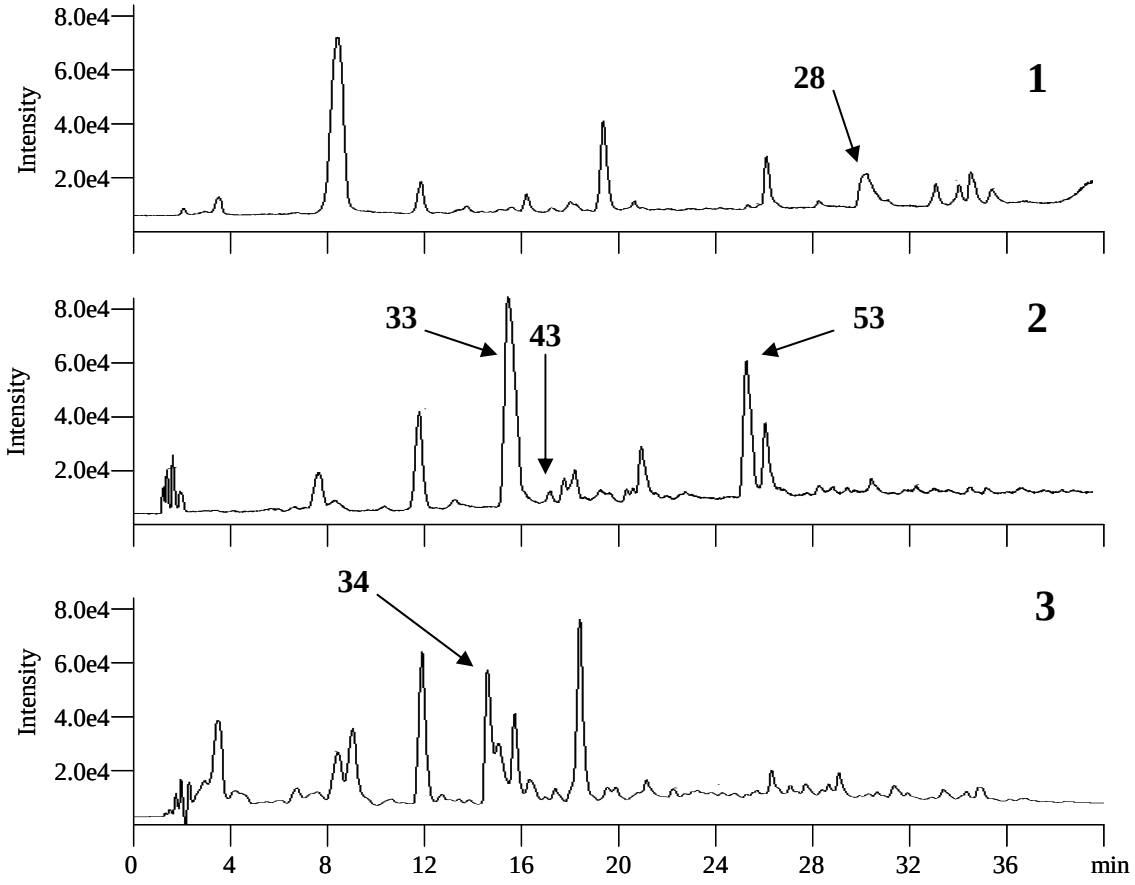

Figure 2.1 HPLC-HRMS-ESI chromatograms of rutabaga phytoalexins: cyclobrassinin (**28**), rutalexin (**33**), spirobrassinin (**34**), brassicanate A (**43**), and rapalexin A (**53**). Chromatogram **1** = fraction A, positive ion mode; Chromatogram **2** = fraction A negative ion mode; Chromatogram **3** = fraction B, positive ion mode.

The rutalexin peak at t_R = 15.9 min (negative ion mode) indicated two ions at *m/z* 231.0233 and 235.0484 that were consistent with the molecular formulae $C_{11}H_7N_2O_2S$ and $C_{11}H_3{}^2H_4N_2O_2S$, respectively. Based on the peak area of each ion, the percentage of deuterium incorporation was found to be 32% {[47/(99 + 47)] × 100} (**Table 2.2**). The brassicanate A peak at t_R = 17.5 min (negative ion mode) indicated two ions at *m/z* 220.0437 and 224.0688 that were consistent with the molecular formulae $C_{11}H_{10}NO_2S$ and $C_{11}H_6{}^2H_4NO_2S$, respectively. The percentage of deuterium incorporation was calculated based on the peak area of each ion and was found to be 4% {[0.5/(11 + 0.5)] ×

100} (**Table 2.2**). The rapalexin A peak at t_R = 25.7 min (negative ion mode) indicated two ions at *m/z* 203.0284 and 207.0535 that were consistent with the molecular formulae $C_{10}H_7N_2OS$ and $C_{10}H_3{}^2H_4N_2OS$, respectively. Based on the peak area of each ion, the percentage of deuterium incorporation was found to be 12% {[12/(85 + 12)] × 100}. The spirobrassinin peak at t_R = 14.7 min (positive ion mode) indicated two molecular ions at *m/z* 251.0307 and 255.0558 that were consistent with the molecular formulae $C_{11}H_{11}N_2OS_2$ and $C_{11}H_7{}^2H_4N_2OS_2$, respectively. The percentage of deuterium incorporation was calculated based on the peak area of each ion and was found to be 17% {[19/(90 + 19)] × 100}(**Table 2.2**, **Figure 2.2**).

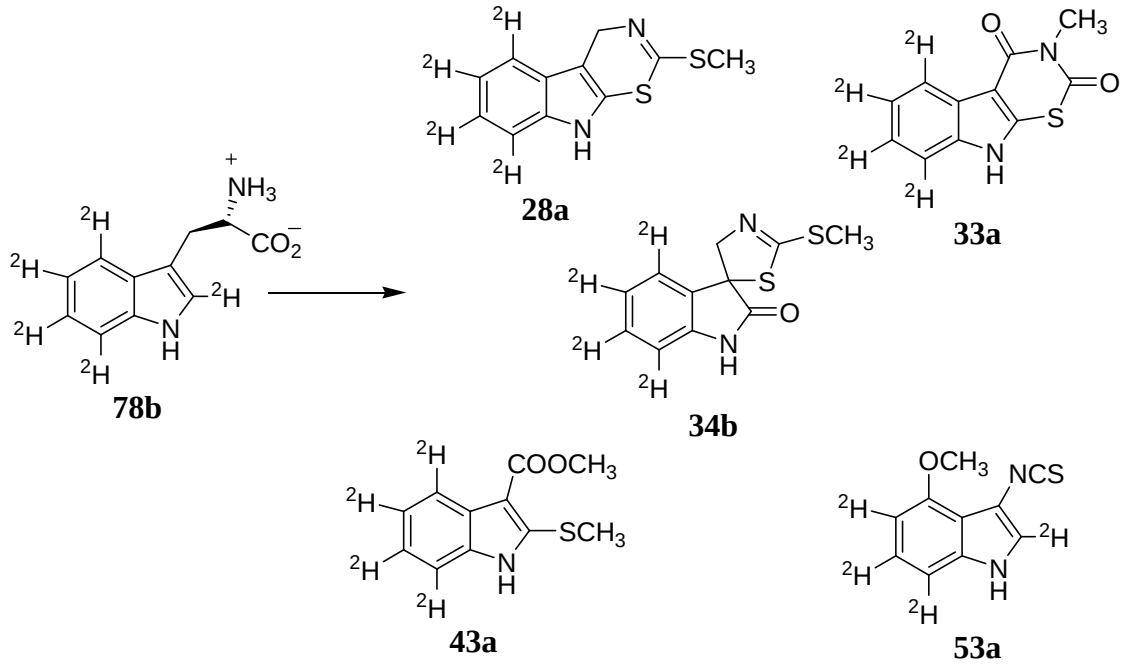

Figure 2.2 Incorporation of *L*-[$^2H_5$]tryptophan (**78b**) into rutabaga phytoalexins: [$^2H_4$]cyclobrassinin (**28a**, 7%), [$^2H_4$]rutalexin (**33a**, 32%), [$^2H_4$]spirobrassinin (**34b**, 17%), [$^2H_4$]brassicanate A (**43a**, 4%), and [$^2H_4$]rapalexin A (**53a**, 12%).

Incorporation of *L*-[2',4',5',6',7'-$^2H_5$]tryptophan (**78b**) into indole glucosinolates was investigated in rutabaga tissues as well. After cutting tissue around the holes from slices incubated with *L*-[2',4',5',6',7'-$^2H_5$]tryptophan, grinding, and extracting, RP-FCC yielded a fraction that contained glucosinolates glucobrassicin (**70**), 4-methoxyglucobrassicin (**156**), and neoglucobrassicin (**199**) (established by HPLC-DAD

and HPLC-MS-ESI) (**Figure 2.3**). Control tissues incubated with non-labeled *L*-tryptophan or with carrier solution were treated similarly.

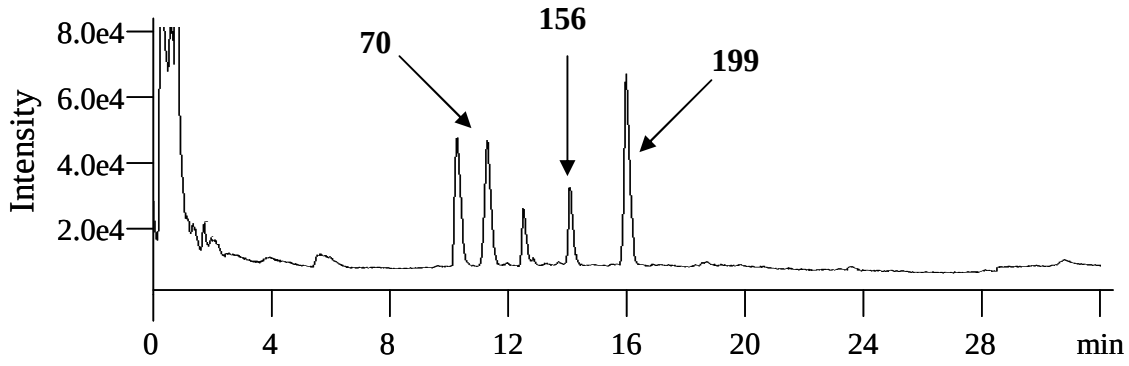

Figure 2.3 HPLC-HRMS-ESI chromatogram of rutabaga glucosinolates: glucobrassicin (**70**), methoxyglucobrassicin (**156**), and neoglucobrassicin (**199**).

HPLC-HRMS-ESI analyses (negative ion mode) of the glucosinolate fraction resulting from feeding of *L*-[2',4',5',6',7'-$^{2}H_5$]tryptophan displayed the glucobrassicin peak at t_R = 12.0 min to contain two ions at *m/z* 447.0537 and 452.0851 that were consistent with the molecular formulae $C_{16}H_{19}N_2O_9S_2$ and $C_{16}H_{14}{}^{2}H_5N_2O_9S_2$, respectively. The ion at *m/z* 452.0851 was not detected in control samples incubated with non-labeled *L*-tryptophan. The percentage of deuterium incorporation was calculated based on the peak area of each ion and was found to be 17 ± 1% (**Table 2.2**). The 4-methoxyglucobrassicin peak at t_R = 14.5 min indicated two ions at *m/z* 477.0643 and 481.0894 that were consistent with molecular formulae $C_{17}H_{21}N_2O_{10}S_2$ and $C_{17}H_{17}{}^{2}H_4N_2O_{10}S_2$, respectively. Based on the peak area of each ion, the percentage of deuterium incorporation was found to be 7 ± 2 %. The neoglucobrassicin peak at t_R = 16.1 min indicated two ions at *m/z* 477.0643 and 482.0956 that were consistent with molecular formulae $C_{17}H_{21}N_2O_{10}S_2$ and $C_{17}H_{16}{}^{2}H_5N_2O_{10}S_2$, respectively. The percentage of deuterium incorporation was calculated from the peak area of each ion and was found to be 12 ± 1 % (**Table 2.2**).

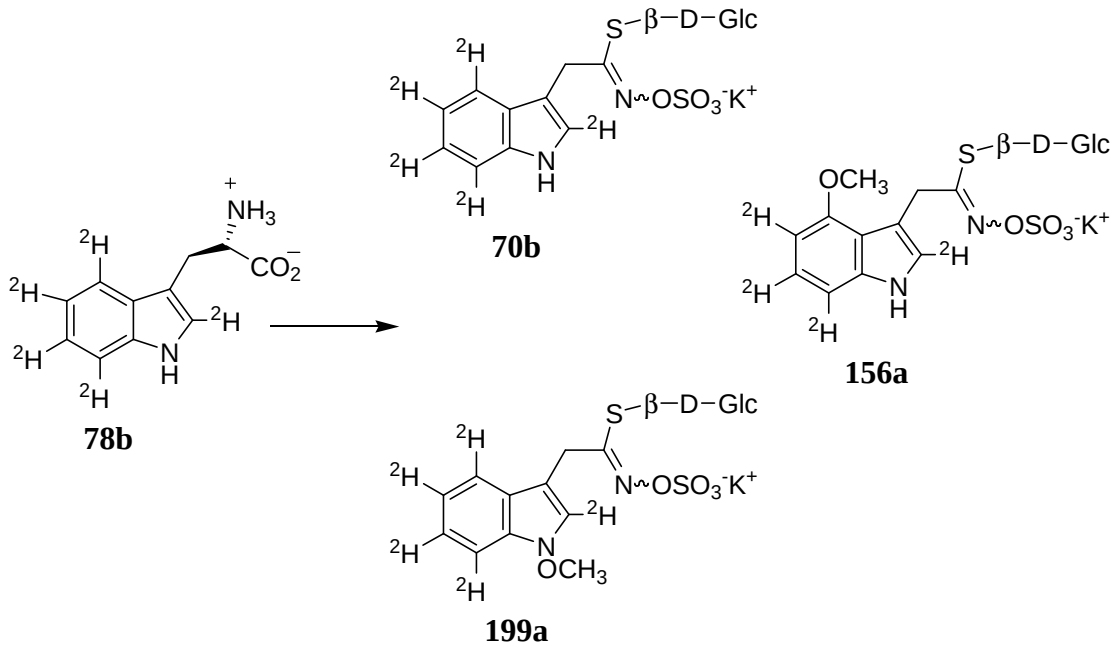

Figure 2.4 Incorporation of *L*-[$^2H_5$]tryptophan (**78b**) into rutabaga glucosinolates: [$^2H_5$]glucobrassicin (**70b**, 17 ± 1%), [$^2H_4$]-4-methoxyglucobrassicin (**156a**, 7 ± 2 %) and [$^2H_5$]neoglucobrassicin (**199a**, 12 ± 1 %).

Table 2.2 Incorporation of *L*-[2',4',5',6',7'-$^2H_5$]tryptophan (**78b**) into rutabaga phytoalexins and glucosinolates

Compound	**% Incorporation**
[4',5',6',7'-$^2H_4$]Cyclobrassinin (**28a**)	[a,c]7
[4',5',6',7'-$^2H_4$]Rutalexin (**33a**)	[a,d]32
[4',5',6',7'-$^2H_4$]Spirobrassinin (**34a**)	[a,c]17
[4',5',6',7'-$^2H_4$]Brassicanate A (**43a**)	[a,d]4
[2',5',6',7'-$^2H_4$]Rapalexin A (**53a**)	[a,d]12
[2',4',5',6',7'-$^2H_5$]Glucobrassicin (**70b**)	[b,d]17 ± 1
[2',5',6',7'-$^2H_4$]4-Methoxyglucobrassicin (**156a**)	[b,d]7 ± 2
[2',4',5',6',7'-$^2H_5$]Neoglucobrassicin (**199a**)	[b,d]12 ± 1

% of ^2H incorporation = $\{[M + n]^{+/-}/([M]^{+/-} + [M + n]^{+/-})\} \times 100$ ($n = 5$).
[a]Incorporation determined from a single feeding experiment.
[b]Incorporation determined from average of two independent experiments ± standard deviation (STD).
[c]Positive ion mode.
[d]Negative ion mode.

The biosynthetic pathways of 1-substituted rutabaga metabolites 1-methoxybrassinin (**18**) and neoglucobrassicin (**199**) were probed with 1-methyl-*L*-tryptophan (**200**), a non-natural compound. Rutabaga root slices were prepared as previously described. After incubation with 1-methyl-*L*-tryptophan (24, 48, 72, and 96 hours), the aqueous phase was collected, was extracted, and was subjected to preliminary clean up to yield fraction A that contained the phytoalexins cyclobrassinin (**28**), rutalexin (**33**), brassicanate A (**43**), rapalexin A (**53**), and fraction B that contained spirobrassinin (**34**) (established by HPLC-DAD and HPLC-MS-ESI). Tissues around the holes were cut, were ground (mortar and pestle), and were extracted. The extracts were subjected to RP-FCC to yield a fraction that contained the glucosinolates glucobrassicin (**70**), 4-methoxyglucobrassicin (**156**), and neoglucobrassicin (**199**) (established by HPLC-DAD and HPLC-MS-ESI). Control slices were incubated with carrier solution and were similarly treated. From HPLC-DAD and HPLC-MS-ESI analyses, no 1-methyl containing phytoalexins or indole glucosinolates were detected under various feeding conditions and incubation periods (**Figure 2.5**). It was also surprising that no 1-methyl-*L*-tryptophan was recovered, neither was any of its metabolic products detected in the extracts.

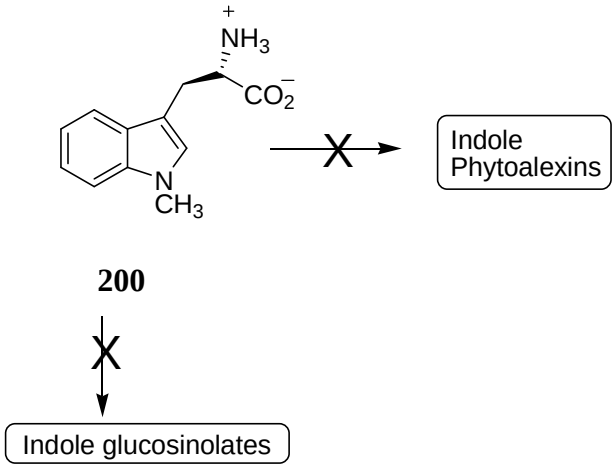

Figure 2.5 Administration of 1-methyl-*L*-tryptophan (**200**) to rutabaga tubers.

Incorporation of [1",1",1"-$^2H_3$]1-methoxyindolyl-3-acetaldoxime (116a)

The biogenesis of neoglucobrassicin (**199**) from 1-methoxyindolyl-3-acetaldoxime (**116**) was investigated. Rutabaga root slices were prepared as previously described and were incubated with [1",1",1"-$^2H_3$]1-methoxyindolyl-3-acetaldoxime (**116a**) for 96 hours; control slices were incubated separately with 1-methoxyindolyl-3-acetaldoxime (**116**) and with carrier solution. Following incubation and extraction, RP-FCC of the extracts yielded a fraction that contained the glucosinolates glucobrassicin (**70**), 4-methoxyglucobrassicin (**156**), and neoglucobrassicin (**199**) (established by HPLC-DAD and HPLC-MS-ESI). HPLC-HRMS-ESI analyses (negative ion mode) of the glucosinolate fraction resulting from feeding of [1",1",1"-$^2H_3$]1-methoxyindolyl-3-acetaldoxime displayed the neoglucobrassicin peak at t_R = 13.8 min containing two ions at *m/z* 477.0643 and 480.0831 that were consistent with molecular formulae $C_{17}H_{21}N_2O_{10}S_2$ and $C_{17}H_{18}{}^2H_3N_2O_{10}S_2$, respectively. The ion at *m/z* 480.0831 was absent in control samples incubated with 1-methoxyindolyl-3-acetaldoxime. Based on the peak area of each ion, the percentage of deuterium incorporation was found to be 6% {[3/(48 + 3)] × 100} (**Figure 2.6**).

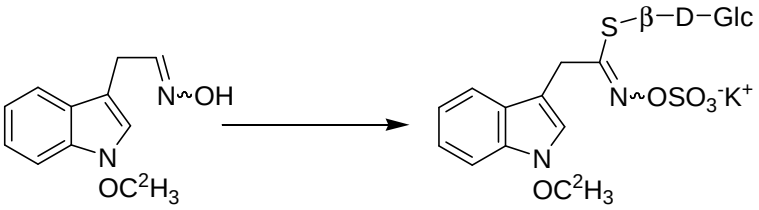

116a **199b**

Figure 2.6 Incorporation of [$^2H_3$]1-methoxyindolyl-3-acetaldoxime (**116b**) into [$^2H_3$]neoglucobrassicin (**199b**, 6%).

Incorporation of 1-methylindolyl-3-acetaldoxime (170)

The biosynthetic pathway(s) of 1-substituted phytoalexins and glucosinolates was further probed with 1-methylindolyl-3-acetaldoxime (**170**). No 1-methyl containing metabolite has been identified from rutabaga or turnip extracts, incorporation of 1-methylindolyl-3-acetaldoxime into phytoalexins or glucosinolates can therefore be

determined by comparing HPLC-DAD chromatograms of fed and control extracts, followed by HPLC-HRMS-ESI analyses to confirm the compound structure. In the present studies, 1-methylindolyl-3-acetaldoxime was administered separately to UV-irradiated rutabaga and turnip root slices. After incubation and extraction, preliminary clean up of the extracts yielded fractions containing phytoalexins and glucosinolates (established by HPLC-DAD and HPLC-MS-ESI); similar experiments were conducted for root slices incubated with carrier solution. Surprisingly, no 1-methyl containing phytoalexin was detected from phytoalexin fractions, but chromatograms of polar fractions indicated a new peak that was absent in those of control fractions. HPLC-HRMS-ESI analyses (negative ion mode) of the new metabolite peak at t_R = 13.5 min indicated an ion at *m/z* 461.0693 that was consistent with molecular formula $C_{17}H_{21}N_2O_9S_2$. The new metabolite structure was deduced to be 1-methylglucobrassicin (**Figure 2.7**). Both rutabaga and turnip root slices metabolized 1-methylindolyl-3-acetaldoxime (**170**) to 1-methylglucobrassicin (**201**).

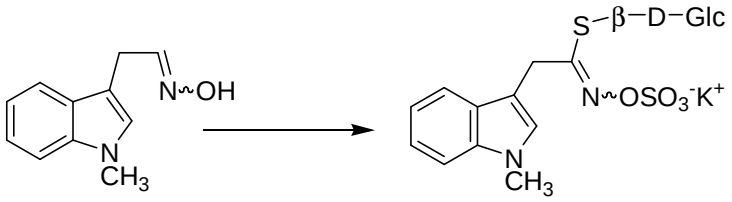

170 **201**

Figure 2.7 Incorporation of 1-methylindolyl-3-acetaldoxime (**170**) into 1-methylglucobrassicin (**201**).

Incorporation of [4',5',6',7'-$^{2}H_4$]indolyl-3-[^{34}S]acetothiohydroxamic acid (174a)

The potential involvement of indolyl-3-acetothiohydroxamic acid in the biosynthetic pathway of indole phytoalexins and glucosinolates was investigated in rutabaga root tubers. Thus, [4',5',6',7'-$^{2}H_4$]indolyl-3-[^{34}S]acetothiohydroxamic acid (**174a**) was administered to UV-irradiated rutabaga root slices followed by 72-hour incubation. Control experiments were conducted similarly by incubating rutabaga root

slices with non-labeled indolyl-3-acetothiohydroxamic acid or with carrier solution. Extraction of the aqueous phase and preliminary clean up of the extracts yielded fraction A that contained the phytoalexins cyclobrassinin (**28**), rutalexin (**33**), brassicanate A (**43**), rapalexin A (**53**), and fraction B that contained spirobrassinin (**34**) (established by HPLC-DAD, HPLC-MS-ESI, and HPLC-HRMS-ESI) (**Figure 2.8**). HPLC-HRMS-ESI analyses (positive ion mode) of the phytoalexin fraction resulting from feeding of [4',5',6',7'-$^{2}H_4$]indolyl-3-[^{34}S]acetothiohydroxamic acid displayed the cyclobrassinin peak at t_R = 30.1 min containing two ions at *m/z* 235.0358 and 241.0567 that were consistent with the molecular formulae $C_{11}H_{11}N_2S_2$ and $C_{11}H_7{}^{2}H_4N_2S^{34}S$, respectively. Based on the peak area of each ion, the percentage of ^{34}S and deuterium incorporation was found to be 5% {[1/(19 + 1)] × 100}. The rutalexin peak at t_R = 15.9 min (negative ion mode) indicated two ions at *m/z* 231.0233 and 235.0484 that were consistent with the molecular formulae $C_{11}H_7N_2O_2S$ and $C_{11}H_3{}^{2}H_4N_2O_2S$, respectively. The percentage of deuterium incorporation was calculated based on the peak areas of each ion and was found to be 11 ± 2 % (**Table 2.3**). The brassicanate A peak at t_R = 17.5 min (negative ion mode) indicated two ions at *m/z* 220.0437 and 224.0688 that were consistent with the molecular formulae $C_{11}H_{10}NO_2S$ and $C_{11}H_6{}^{2}H_4NO_2S$, respectively. Based on the peak area of each ion, the percentage of deuterium incorporation was found to be 3% {[0.3/(10 + 0.3)] × 100} (**Table 2.3**). The rapalexin A peak at t_R = 25.8 min (negative ion mode) indicated four ions at *m/z* 203.0284, 205.0242, 206.0472 and 208.0446 that were consistent with the molecular formulae $C_{10}H_7N_2OS$, $C_{10}H_7N_2O^{34}S$, $C_{10}H_4{}^{2}H_3N_2OS$, and $C_{10}H_4{}^{2}H_3N_2O^{34}S$, respectively. The ion at *m/z* 205.0242 with formula $C_{10}H_7N_2O^{34}S$ suggested incorporation of ^{34}S into rapalexin A (**53d**) which was calculated based on peak area of each ion at *m/z* 203.0284 and 205.0242 and was found to be 57 ± 10 % (**Table 2.3**). The ion at *m/z* 206.0472 consistent with the molecular formula $C_{10}H_4{}^{2}H_3N_2OS$ indicated incorporation of deuterium from indole ring of [4',5',6',7'-$^{2}H_4$]indolyl-3-[^{34}S]acetothiohydroxamic acid into rapalexin A (**53b**). Based on the peak area of each ion at *m/z* 203.0284 and 206.0472 the percentage of deuterium incorporation was found to be 14 ± 9 % (**Table 2.3**). The ion at *m/z* 208.0446 consistent with the molecular formula $C_{10}H_4{}^{2}H_3N_2O^{34}S$ suggested incorporation of ^{34}S and deuterium into rapalexin A (**53c**), the percentage of incorporation was calculated based

on peak area of each ion at *m/z* 203.0284 and 208.0446 and was found to be 4 ± 3 % (**Table 2.3**). The spirobrassinin peak at t_R = 14.6 min (positive ion mode) contained two ions at *m/z* 251.0307 and 257.0516 that were consistent with the molecular formulae $C_{11}H_{11}N_2OS_2$ and $C_{11}H_7{}^2H_4N_2OS^{34}S$, respectively. The percentage of ^{34}S and deuterium incorporation was calculated based on the peak area of each ion and was found to be 8% {[5/(59 + 5)] × 100} (**Table 2.3**).

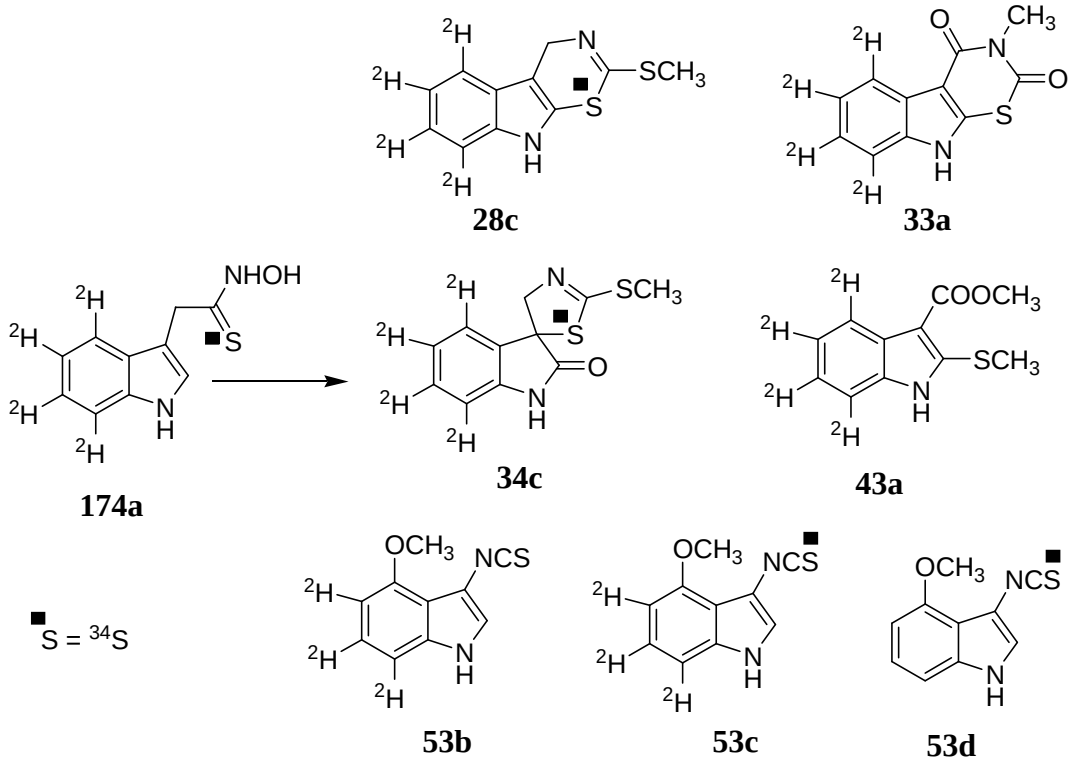

Figure 2.8 Incorporation of [$^2H_4$]indolyl-3-[^{34}S]acetothiohydroxamic acid (**174a**) into rutabaga phytoalexins: ^{34}S-[$^2H_4$]cyclobrassinin (**28c**, 5%), [$^2H_4$]rutalexin (**33a**, 11 ± 2 %), ^{34}S-[$^2H_4$]spirobrassinin (**34c**, 8%), [$^2H_4$]brassicanate A (**43a**, 3%), [$^2H_3$]rapalexin A (**53b**, 14 ± 9 %), ^{34}S-[$^2H_3$]rapalexin A (**53c**, 4 ± 3 %), and [^{34}S]rapalexin A (**53d**, 57 ± 10 %).

The incorporation of [4',5',6',7'-$^2H_4$]indolyl-3-[^{34}S]acetothiohydroxamic acid (**174a**) into rutabaga glucosinolates was investigated in the polar extracts as well. Thus, tissue around the holes was cut and was extracted. Preliminary clean up of the extract yielded a fraction that contained the glucosinolates glucobrassicin (**70**), 4-

methoxyglucobrassicin (**156**), and neoglucobrassicin (**199**) (established by HPLC-DAD and HPLC-MS-ESI). Control slices were treated similarly. HPLC-HRMS-ESI analyses (negative ion mode) of the glucosinolate fraction resulting from feeding [4',5',6',7'-$^{2}H_4$]indolyl-3-[^{34}S]acetothiohydroxamic acid displayed the glucobrassicin peak at t_R = 12.0 min containing two ions at *m/z* 447.0537 and 453.0746 that were consistent with the molecular formulae $C_{16}H_{19}N_2O_9S_2$ and $C_{16}H_{15}{}^{2}H_4N_2O_9S^{34}S$, respectively. These results suggested intact incorporation of [4',5',6',7'-$^{2}H_4$]indolyl-3-[^{34}S]acetothiohydroxamic acid into glucobrassicin (**70c**). The percentage of ^{34}S and deuterium incorporation was calculated based on the peak area of each ion and was found to be 2 ± 1 % (**Figure 2.9**, **Table 2.3**). HPLC-HRMS-ESI analyses of 4-methoxyglucobrassicin peak at t_R = 14.5 min indicated an ion at *m/z* 477.0643 that was consistent with molecular formulae $C_{17}H_{21}N_2O_{10}S_2$, whereas neoglucobrassicin peak at t_R = 16.1 min indicated an ion at *m/z* 477.0643 that was consistent with the molecular formulae $C_{17}H_{21}N_2O_{10}S_2$. The absence of incorporation of [4',5',6',7'-$^{2}H_4$]indolyl-3-[^{34}S]acetothiohydroxamic acid into 4-methoxyglucobrassicin and neoglucobrassicin suggested that indolyl-3-acetothiohydroxamic acid is not a biogenetic precursor in the biosynthetic pathway of these two glucosinolates.

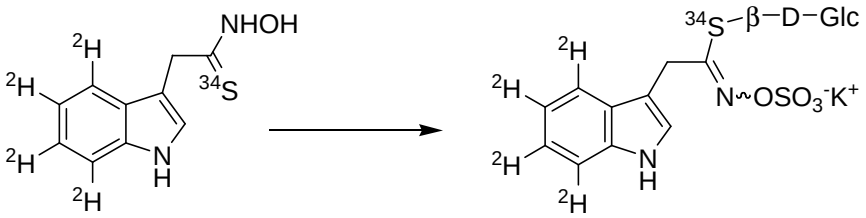

174a **70c**

Figure 2.9 Incorporation of [$^{2}H_4$]indolyl-3-[^{34}S]acetothiohydroxamic acid (**174a**) into ^{34}S-[$^{2}H_4$]glucobrassicin (**70c**, 2 ± 1 %).

Table 2.3 Incorporation of [4',5',6',7'-$^{2}H_4$]indolyl-3-[^{34}S]acetothiohydroxamic acid (**174a**) into rutabaga phytoalexins and glucobrassicin (**70c**)

Compound	% Incorporation
^{34}S-[4',5',6',7'-$^{2}H_4$]Cyclobrassinin (**28c**)	[a,c]5
[4',5',6',7'-$^{2}H_4$]Rutalexin (**33a**)	[b,d]11 ± 2
^{34}S-[4',5',6',7'-$^{2}H_4$]Spirobrassinin (**34c**)	[a,c]8
[4',5',6',7'-$^{2}H_4$]Brassicanate A (**43a**)	[a,d]3
[5',6',7'-$^{2}H_4$]Rapalexin A (**53b**)	[b,d]14 ± 9
^{34}S-[5',6',7'-$^{2}H_4$]Rapalexin A (**53c**)	[b,d]4 ± 3
^{34}S-Rapalexin A (**53d**)	[b,d]57 ± 10
^{34}S-[2',4',5',6',7'-$^{2}H_5$]Glucobrassicin (**70c**)	[b,d]2 ± 1

% of ^{2}H and ^{34}S incorporation = $\{[M + n]^{+/-}/([M]^{+/-} + [M + n]^{+/-})\} \times 100$ ($n = 4$).
[a]Incorporation determined from a single feeding experiment.
[b]Incorporation determined from average of two independent experiments ± standard deviation (STD).
[c]Positive ion mode.
[d]Negative ion mode.

Incorporation of 1-methylindolyl-3-acetothiohydroxamic acid (178)

The incorporation of 1-methylindolyl-3-acetothiohydroxamic acid (**178**) into indole phytoalexins and glucosinolates was investigated. 1-Methylindolyl-3-acetothiohydroxamic acid was separately administered to UV-irradiated rutabaga and turnip slices followed by 48- and 72-hour incubations. The aqueous phase was collected, was extracted, and the resulting extract was subjected to preliminary clean up to yield fraction A that contained the phytoalexins cyclobrassinin (**28**), rutalexin (**33**), brassicanate A (**43**), rapalexin A (**53**), and fraction B that contained spirobrassinin (**34**) (established by HPLC-DAD and HPLC-MS-ESI). Control slices were incubated with carrier solution and were treated similarly. After cutting tissue around the holes, grinding, and extracting, preliminary clean up of the extracts yielded a fraction that contained the glucosinolates glucobrassicin (**70**), 4-methoxyglucobrassicin (**156**), and neoglucobrassicin (**199**) (established by HPLC-DAD and HPLC-MS-ESI). The HPLC-DAD and HPLC-MS-ESI analyses of phytoalexin fractions did not indicate the presence of 1-methyl containing phytoalexins, whereas a new metabolite peak was detected in

glucosinolate extracts. HPLC-HRMS-ESI analyses (negative ion mode) of the new peak at t_R = 13.5 min indicated an ion at *m/z* 461.0693 that was consistent with molecular formula $C_{17}H_{21}N_2O_9S_2$, similar to that obtained from administration of 1-methylindolyl-3-acetaldoxime. The structure of 1-methylglucobrassicin (**201**) was deduced (**Figure 2.10**).

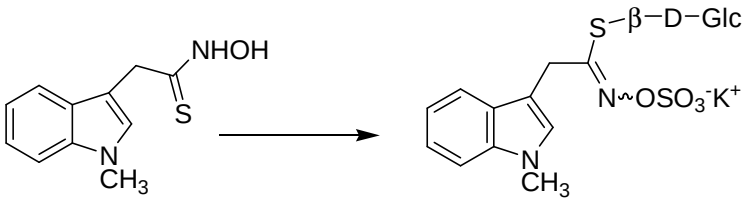

178 **201**

Figure 2.10 Incorporation of 1-methylindolyl-3-acetothiohydroxamic acid (**178**) into 1-methylglucobrassicin (**201**).

Incorporation of [4',5',6',7'-$^2H_4$]indolyl-3-acetonitrile (49a)

[4',5',6',7'-$^2H_4$]Indolyl-3-[^{34}S]acetothiohydroxamic acid (**174a**) decomposes to [4',5',6',7'-$^2H_4$]indolyl-3-acetonitrile (**49a**) under feeding conditions (in carrier solution). Therefore it was important to determine the metabolic products of [4',5',6',7'-$^2H_4$]indolyl-3-acetonitrile and their potential relationship with other rutabaga phytoalexins. A time-course feeding experiment was conducted to determine the metabolism of **49a** in rutabaga tissues (**Figure 2.11**). Firstly, non-isotopically labeled indolyl-3-acetonitrile (**49**) was administered to rutabaga slices that were prepared as previously described. Following incubation for 4, 8, 16, and 24 hours the aqueous phase was collected, was extracted and was subjected to preliminary clean up to yield non-polar fractions. HPLC-DAD analyses of the non-polar fractions after 4-hour incubation indicated two new peaks at t_R = 4.8 and 5.5 min that showed increasing amounts between 4- and 16-hour incubations, then gradual decrease after 16-hour incubation. Between 8- and 16-hour incubation a new metabolite peak with increasing intensity was detected at t_R = 12.3 min. After 24-hour incubation indolyl-3-acetonitrile was completely metabolized, the intensity of the peaks at t_R = 4.8 and 5.5 min decreased significantly whereas that at t_R =

12.3 min increased. The three new peaks were absent in extracts incubated with carrier solution only, suggesting that they were metabolic products of indolyl-3-acetonitrile (**49**). The three metabolites were identified by comparison of their UV spectra and retention times with those of compounds in the HPLC-DAD library. Thus, the metabolites at t_R = 4.8, 5.5, and 12.3 min were identified as indole-3-acetic acid (**202**), indole-3-carboxylic acid (**203**), and methyl indole-3-carboxylate (**121**), respectively. A similar experiment was conducted with [4',5',6',7'-$^2H_4$]indolyl-3-acetonitrile (**49a**). The aqueous phase was extracted after 16-hour incubation to allow for the detection of the three new peaks. No deuterium labeling was detected in any of the phytoalexins cyclobrassinin (**28**), rutalexin (**33**), brassicanate A (**43**), rapalexin A (**53**), and spirobrassinin (**34**) (established HPLC-MS-ESI). The HPLC-HRMS-ESI analyses (negative ion mode) of the three new compounds with peaks at t_R = 4.8, 5.5, and 12.3 min indicated the masses at *m/z* 164.0655, 178.0811, and 178.0811 that were consistent with the molecular formulae $C_9H_2{}^2H_4NO_2$, $C_{10}H_4{}^2H_4NO_2$ and $C_{10}H_4{}^2H_4NO_2$, respectively. The peaks at t_R = 4.8, 5.5, and 12.3 min were consistent with [4',5',6',7'-$^2H_4$]indolyl-3-acetic acid (**202a**), [4,5,6,7-$^2H_4$]indole-3-carboxylic acid (**203a**), and methyl [4,5,6,7-$^2H_4$]indole-3-carboxilate (**121a**), respectively (**Figure 2.11**). HPLC-MS-ESI analyses (negative ion mode) of fractions from tissue extracts did not show other deuterium labeled metabolic products. It was therefore concluded that indolyl-3-acetonitrile in not a precursor of phytoalexins or glucosinolates that are produced in rutabaga tissues.

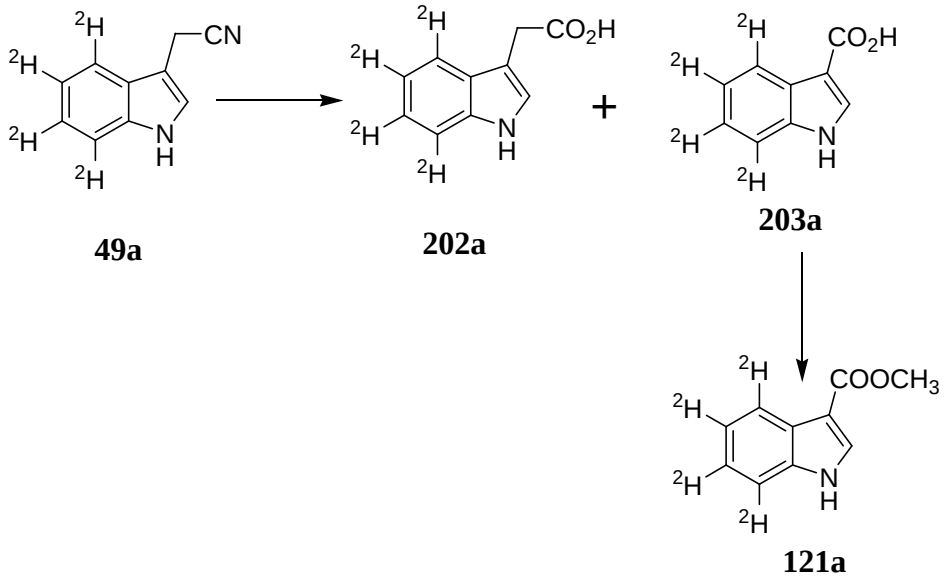

Figure 2.11 Incorporation of [$^2H_4$]indolyl-3-acetonitrile (**49a**) into [$^2H_4$]indolyl-3-acetic acid (**202a**), [$^2H_4$]indole-3-carboxylic acid (**203a**) and methyl [4,5,6,7-$^2H_4$]indole-3-carboxylate (**121a**).

1-(tert-Butoxycarbonyl)indolyl-3-methylisothiocyanate (180) and 1-(tert-butoxycarbonyl)brassinin (181) as potential intermediates

Potential involvement of indolyl-3-methylisothiocyanate (**123**) in the biosynthetic pathway of indole phytoalexins was investigated using 1-(*tert*-butoxycarbonyl)indolyl-3-methyl-isothiocyanate (**180**). Due to instability of indolyl-3-methylisothiocyanate (Hanley et al., 1990; Hanley and Parsley, 1990), the stable 1-(*tert*-butoxycarbonyl)indolyl-3-methyl-isothiocyanate (Kutchy et al., 1997; 1998) was used in the present investigations with 1-Boc group serving as the label. Rutabaga slices were prepared as previously described and were incubated with **180**; control experiments were conducted by incubating slices with carrier solution. After 72-hour incubation the aqueous phase was collected, was extracted and was subjected to preliminary clean up to yield fraction A that contained phytoalexins cyclobrassinin (**28**), rutalexin (**33**), brassicanate A (**43**), rapalexin A (**53**), and fraction B that contained spirobrassinin (**34**) (established by HPLC-DAD and HPLC-MS-ESI). Two new metabolite peaks were detected at t_R = 30.1 and 34.1 min that were absent in chromatogram of control extracts. HPLC-MS-ESI analyses (positive ion mode) of the metabolite with peak at t_R = 34.1 min

contained an ion at *m/z* 337 and fragment ions at *m/z* 230, 174 and 130. The metabolite with peak at t_R = 30.1 min contained an ion at *m/z* 351 and a fragment ion at *m/z* 251. The retention times, UV spectra, and fragmentation patterns of the metabolites at t_R = 30.1 and t_R = 34.1 min were comparable with those of synthetic standards, 1-(*tert*-butoxycarbonyl)spirobrassinin (**196**) and 1-(*tert*-butoxycarbonyl)brassinin (**181**), respectively, (**Figure 2.12**). These results were consistent with the expected involvement of indolyl-3-methylisothiocyanate in the biosynthetic pathway of indole phytoalexins. Additional experiments were conducted by incubating rutabaga root slices with 1-(*tert*-butoxycarbonyl)brassinin (**181**). After 72-hour incubation the aqueous phase was collected, was extracted and was subjected to preliminary clean up to yield a fraction that contained phytoalexins; control experiments were prepared similarly by incubating slices with carrier solution. HPLC-DAD analysis of the phytoalexin fraction displayed a new peak at t_R = 30.1 min that was absent in chromatogram of control extract. The new metabolite was identified as 1-(*tert*-butoxycarbonyl)spirobrassinin (**196**) by comparison of retention time, UV spectra, and fragmentation pattern (established by HPLC-DAD and HPLC-MS-ESI) (**Figure 2.12**).

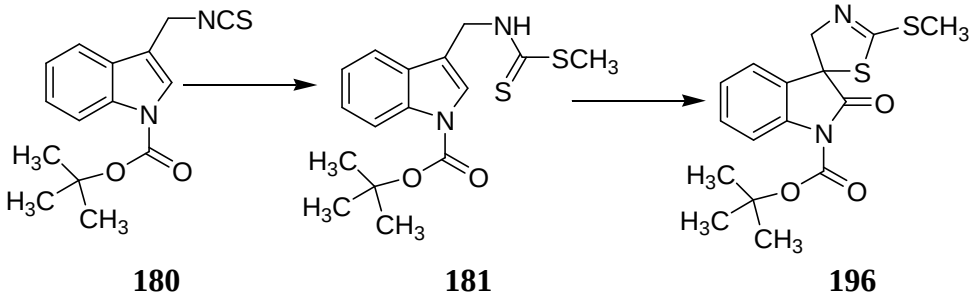

180 **181** **196**

Figure 2.12 Incorporation of 1-(*tert*-butoxycarbonyl)indol-3-ylmethylisothiocyanate (**180**) into 1-(*tert*-butoxycarbonyl)brassinin (**181**) and 1-(*tert*-butoxycarbonyl)spirobrassinin (**196**).

1-Acetylindolyl-3-methylisothiocyanate (183) as a potential intermediate

Boc is a large group that does not occur in natural products whereas the acetyl group is comparatively smaller and occurs in some natural products. 1-Acetylindolyl-3-methylisothiocyanate (**183**) was therefore used to establish the involvement of isothiocyanates in the biosynthetic pathway of indole phytoalexins. Rutabaga and turnip root slices (prepared as previously described) were incubated with **183**; control experiments were conducted similarly by incubating slices with carrier solution. Following 48- and 72-hour incubations, the aqueous phase was extracted and was fractionated to yield fraction A that contained the phytoalexins cyclobrassinin (**28**), rutalexin (**33**), brassicanate A (**43**), rapalexin A (**53**), and fraction B that contained spirobrassinin (**34**) (established by HPLC-DAD and HPLC-MS-ESI). A new peak was detected at t_R = 22.2 min that was absent in the chromatogram of control extracts. HPLC-MS-ESI analyses (positive ion mode) of the phytoalexin fractions indicated ions at *m/z* 172 and 130. The new metabolite was identified as 1-acetylbrassinin (**184**) by comparison of retention time, UV spectra, and fragmentation pattern with those of authentic sample (**Figure 2.13**). The phytoalexin fractions, however, did not yield 1-acetylspirobrassinin (**195**) or any 1-acetyl containing phytoalexins. Incubation of turnip and rutabaga root slices separately with 1-acetylbrassinin (**183**) did not yield any 1-acetly-containing metabolites following 96 hours of incubation.

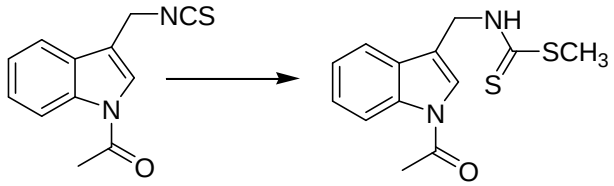

183 **184**

Figure 2.13 Incorporation of 1-acetylindol-3-ylmethylisothiocyanate (**183**) into 1-acetylbrassinin (**184**).

Incorporation of [4',5',6',7'-$^2H_4$]cyclobrassinin (28a)

The biogenetic relationship between cyclobrassinin (**28**) and spirobrassinin (**34**) was investigated in rutabaga and turnip root slices that produce both metabolites. Thus, [4',5',6',7'-$^2H_4$]cyclobrassinin (**28a**) was administered to UV-irradiated rutabaga and turnip slices (prepared as previously described); control experiments were prepared similarly and incubated with cyclobrassinin (**28**) or with carrier solution only. Following incubation for 24, 48, and 72 hours, the aqueous phase was collected, was extracted, and was subjected to preliminary clean up to yield fraction A that contained phytoalexins cyclobrassinin (**28**), rutalexin (**33**), brassicanate A (**43**), rapalexin A (**53**), and fraction B that contained spirobrassinin (**34**) (established by HPLC-DAD and HPLC-MS-ESI). Rutabaga root slices did not produce detectable amounts of spirobrassinin after 24 hours of incubation, but both tissues showed increasing amounts of spirobrassinin from 48- to 72-hour incubations. HPLC-MS-ESI analyses (positive ion mode) of the phytoalexin fractions resulting from feeding [4',5',6',7'-$^2H_4$]cyclobrassinin displayed the spirobrassinin peak at t_R = 13.2 min to contain two ions at *m/z* 251 and 255. The ion at *m/z* 255 was absent in control samples incubated with non-labeled cyclobrassinin. Based on the relative intensity of each molecular ion, deuterium incorporation was found to be 10% {[2/(18 + 2)] × 100} after 24-hour incubation, but 15% {[4/(22 + 4)] × 100} and 6% {[1/(16 + 1)] × 100} after 48- and 72-hour incubations, respectively in turnip root slices (**Figure 2.14**). In rutabaga tissues, deuterium incorporations were 7% {[6/(77 + 6)] × 100} and 4% {[0.9/(24 + 0.9)] × 100} for 48- and 72-hour incubations, respectively (**Table 2.4**). The decrease in incorporations with longer incubation period could result from pool dilution with increasing amount of natural abundant spirobrassinin.

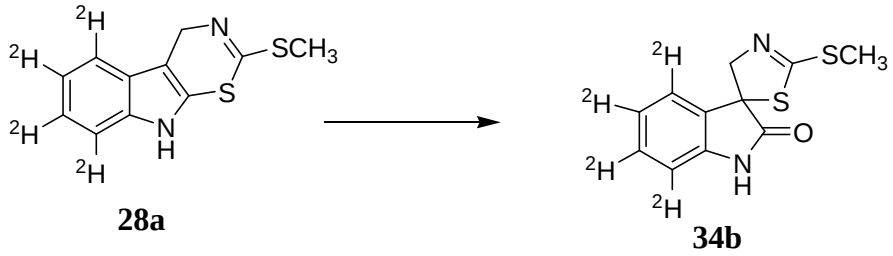

Figure 2.14 Incorporation of [$^2H_4$]cyclobrassinin (**28a**) into [$^2H_4$]spirobrassinin (**34b**).

Table 2.4 Biosynthetic incorporation of [4',5',6',7'-$^2H_4$]cyclobrassinin (**28a**) into [4',5',6',7'-$^2H_4$]spirobrassinin (**34b**) in rutabaga and turnip tissues

	% Deuterium incorporation into spirobrassinin[a,b]	
Incubation (h)	**Rutabaga**	**Turnip**
24	Nd	10
48	7	15
72	4	6

Nd = Not detected.
% of ^2H incorporation = $\{[M + n]^{+/-}/([M]^{+/-} + [M + n]^{+/-})\} \times 100$ ($n = 4$).
[a]Incorporation determined from a single feeding experiment.
[b]Positive ion mode.

Incorporation of [SC$^2H_3$]brassicanal A (39b)

The biogenetic relationship between brassicanal A (**39**) and brassicanate A (**43**) was investigated in rutabaga tissues that produce both metabolites. UV-irradiated root slices (prepared as previously described) were incubated with [SC$^2H_3$]brassicanal A (**39b**). Following 72-hour incubation, the aqueous phase was extracted and was subjected to preliminary clean up to yield fraction A that contained phytoalexins cyclobrassinin (**28**), rutalexin (**33**), brassicanate A (**43**), rapalexin A (**53**), and fraction B that contained spirobrassinin (**34**) (established by HPLC-DAD and HPLC-MS-ESI).; control experiments were prepared similarly and incubated with brassicanal A and with carrier solution. HPLC-MS-ESI analyses (negative ion mode) of the phytoalexin fraction resulting from feeding [SC$^2H_3$]brassicanal A displayed the brassicanate A peak at t_R = 15.2 min to contain two ions at *m/z* 220 and 223. The ion at *m/z* 223 was not detected in

control samples incubated with non-labeled brassicanal A. Based on the relative intensity of the molecular ion the percentage of deuterium incorporation was found to be ≥ 99%, suggesting that brassicanal A could be the last biogenetic intermediate in the biosynthetic pathway of brassicanate A.

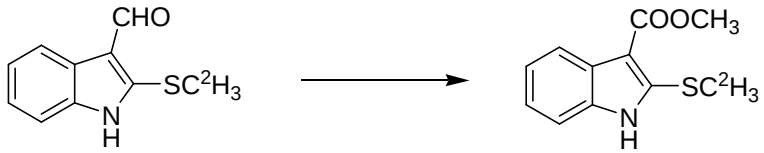

39b **43b**

Figure 2.15 Incorporation of [SC^2H_3]brassicanal A (**39b**) into [SC^2H_3]brassicanate A (**43b** ≥ 99%).

2.2.2.2 Erucastrum gallicum (dog mustard)

Dog mustard is a wild crucifer that was reported to exhibit resistance against the plant pathogen, *S. sclerotiorum* (Lefol et. al, 1997). Biotic (*S. sclerotiorum*) and abiotic [copper(II) chloride] elicitation of dog mustard leaves led to isolation and identification of four phytoalexins: indolyl-3-acetonitrile (**49**), arvelexin (**51**), erucalexin (**38**), and 1-methoxyspirobrassinin (**35**) (Pedras and Ahiahonu 2004; Pedras et al., 2006a). The occurrence of erucalexin and its regioisomer 1-methoxyspirobrassinin in elicited leaves of dog mustard suggested a possible biogenetic relationship between these two metabolites. Toward this end, the biosynthetic pathway of erucalexin and 1-methoxyspirobrassinin, and other dog mustard phytoalexins were investigated.

Time course analyses and feeding experiments

In order to investigate biosynthesis of erucalexin (**38**) and 1-methoxyspirobrassinin (**35**), time course analyses were conducted with detached dog mustard leaves to establish suitable plant age and incubation period for feeding experiments. Plants of different ages, 21, 28 and 35 days were sprayed with a solution of copper(II) chloride (2×10^{-3} M) to induce phytoalexin production. The petiolated leaves were incubated for 24 to 120 hours under continuous light followed by extraction, preliminary clean up and HPLC-

DAD analyses to determine production of phytoalexins; control experiments were prepared similarly from dog mustard leaves sprayed with water. The amounts of erucalexin and 1-methoxyspirobrassinin in leaf extracts were determined by HPLC-DAD using calibration curves (**Table 2.5**). From these analyses, it was established that leaves from 21-day-old plants exhibited a slow uptake of carrier solution, and most of the detached leaves wilted before the end of the experiment period. Plant leaves older than 35 days exhibited faster uptake of carrier solution, but elicitation levels were not as efficient as was observed with 21- and 28-day-old plants. The 28-day-old plants therefore proved more suitable for feeding experiments since their leaf extracts contained higher amounts of erucalexin and 1-methoxyspirobrassinin than the 21-day-old plants, and exhibited efficient uptake of carrier solution. The 28-day-old plant extracts were used to establish a suitable incubation period for feeding experiments. These analyses revealed that the amounts of erucalexin increased from 24-hour incubation to a maximum at 48-hour incubation, after which a decrease was noted from 72- to 120-hour incubations (**Table 2.5**). The amounts of 1-methoxyspirobrassinin were not significantly different between 24- and 48-hour incubations; a significant decrease was noted from 72- to 120-hour incubations. It was also noted that the amounts of erucalexin were consistently higher than those of 1-methoxyspirobrassinin through out the time course analyses. Since maximum production of erucalexin and 1-methoxyspirobrassinin was at 48-hour incubation, this time was used to conduct feeding experiments.

Table 2.5 Production of 1-methoxyspirobrassinin (**35**) and erucalexin (**38**) in 28-day-old detached leaves of dog mustard (Pedras and Okinyo, 2006b)

Phytoalexin	**Incubation time (h)**	**Total amount of phytoalexin (µmole/100 g of fresh tissue ± STD)[a]**
Erucalexin	24	5.9 ± 1.2
	48	**14.9 ± 2.4**
	72	5.8 ± 2.7
	96	5.4 ± 0.1
	120	2.7 ± 1.2
1-Methoxyspirobrassinin	24	3.7 ± 0.2
	48	**3.4 ± 0.5**
	72	1.1 ± 0.6
	96	2.0 ± 0.9
	120	0.7 ± 0.01

[a]Amounts of erucalexin and 1-methoxyspirobrassinin ± standard deviation (STD) were determined from duplicate experiments. In each experiment, three leaves were extracted and subjected to preliminary clean up, followed by HPLC-DAD analysis.

In feeding experiments, 28-day-old dog mustard plants were sprayed with copper(II) chloride (2×10^{-3} M) to the point of run off. After 24-hour incubation the leaves were excised at the petiole and were incubated with perdeuterated compounds (5×10^{-4} M) followed by a second copper(II) chloride spray. Following 48 hours of incubation, the leaves were extracted. The extracts were subjected to preliminary clean up to yield a fraction that contained the phytoalexins 1-methoxyspirobrassinin (**35**), erucalexin (**38**), indolyl-3-acetonitrile (**49**), and arvelexin (**51**) (established by HPLC-DAD and HPLC-MS-ESI). Control experiments were conducted using: (i) doubly-elicited leaves of dog mustard incubated with non-labeled compounds (5×10^{-4} M), (ii) doubly-elicited leaves incubated with carrier solution, (iii) non-elicited leaves incubated with carrier solution.

The percentage of deuterium (^{2}H) incorporation was established according to the equation:

% of ^{2}H incorporation = $[M + n]^+/([M]^+ + [M + n]^+) \times 100$ (n = 3, 4, 7), n is the number of deuterium atoms, and M is the peak area or relative intensity of each molecular ion.

The HPLC-HRMS-ESI data indicated that $[M + n]^+$ was not present in natural abundance samples.

Incorporation of [4',5',6',7'-$^2H_4$]indolyl-3-acetaldoxime (112a)

The origin of indole group in erucalexin and 1-methoxyspirobrassinin was established through administration of [4',5',6',7'-$^2H_4$]indolyl-3-acetaldoxime (**112a**) to doubly elicited detached dog mustard leaves. After 48 hours of incubation the leaves were extracted and extracts subjected to preliminary clean up to yield a fraction that contained the phytoalexins 1-methoxyspirobrassinin (**35**), erucalexin (**38**), indolyl-3-acetonitrile (**49**), and arvelexin (**51**) (established by HPLC-DAD and HPLC-MS-ESI); control experiments were conducted similarly by incubating doubly elicited leaves with non-labeled indolyl-3-acetaldoxime and with carrier solution. HPLC-HRMS-ESI analyses (positive ion mode) of the phytoalexin fraction resulting from feeding [4',5',6',7'-$^2H_4$]indolyl-3-acetaldoxime displayed the erucalexin and 1-methoxyspirobrassinin peaks at t_R = 14.5 and 18.2 min, respectively, to contain two ions at *m/z* 281.0412 and 285.0664 corresponding to the molecular formulae $C_{12}H_{13}N_2O_2S_2$ and $C_{12}H_9{}^2H_4N_2O_2S_2$, respectively. The ion at *m/z* 285.0664 was not detected in control samples incubated with non-labeled indolyl-3-acetaldoxime (**112**). Based on the peak area of each ion, the percentage of deuterium incorporation was found to be 15 ± 3 % for erucalexin and 46 ± 6 % for 1-methoxyspirobrassinin (**Figure 2.16**, **Table 2.6**).

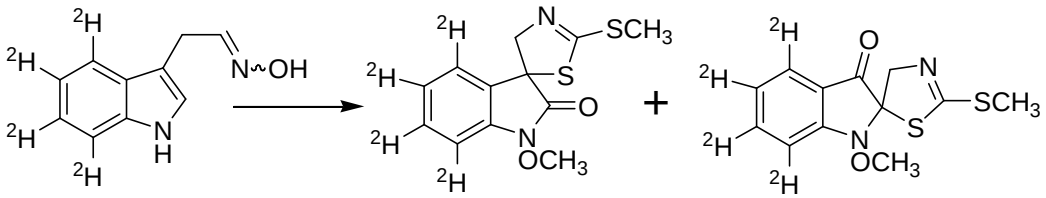

112a **35a** **38a**

Figure 2.16 Incorporation of [$^2H_4$]indolyl-3-acetaldoxime (**112a**) into [$^2H_4$]erucalexin (**38a**, 15 ± 3 %) and [$^2H_4$]1-methoxyspirobrassinin (**35a**, 46 ± 6 %).

Biogenetic relationship between indolyl-3-acetaldoxime (**112**) with other dog mustard phytoalexins, indolyl-3-acetonitrile (**49**) and arvelexin (**51**) was investigated (**Figure 2.17**). These phytoalexins are not detectable by HPLC-MS-ESI and HPLC-HRMS-ESI, but they can be detected by HRMS-EI. In order to carry out this study, dog mustard extracts [(i) incubated with [4',5',6',7'-$^2H_4$]indolyl-3-acetaldoxime (**112a**); (ii) incubated with indolyl-3-acetaldoxime (**112**); (iii) incubated with carrier solution] were subjected to preparative HPLC purification. HRMS-EI analysis of a fraction resulting from feeding [4',5',6',7'-$^2H_4$]indolyl-3-acetaldoxime displayed the indolyl-3-acetonitrile peak to contain two molecular ions at *m/z* 156.0687 and 160.0938 which were consistent with molecular formulae $C_{10}H_8N_2$ and $C_{10}H_4{}^2H_4N_2$, respectively (**Figure 2.17**). The molecular ion at *m/z* 160.0938 was not detected in indolyl-3-acetonitrile fractions from control extract incubated with non-labeled indolyl-3-acetaldoxime. Based on the relative intensity of each molecular ion, the percentage of deuterium incorporation was found to be 89 % {[93/(11 + 93)] × 100}. HRMS-EI analyses of arvelexin (**51**) fraction from feeding [4',5',6',7'-$^2H_4$]indolyl-3-acetaldoxime displayed two molecular ions at *m/z* 186.0793 and 189.0981 that were consistent with molecular formulae $C_{11}H_{10}N_2O$ and $C_{11}H_7{}^2H_3N_2O$, respectively (**Figure 2.17**). The molecular ion at *m/z* 189.0981 was not detected in arvelexin fractions from control extract incubated with non-labeled indolyl-3-acetaldoxime. Percentage of deuterium incorporation was calculated from the relative intensity of each molecular ion and was found to be 41% {[69/(100 + 69)] × 100} (**Figure 2.17**, **Table 2.6**).

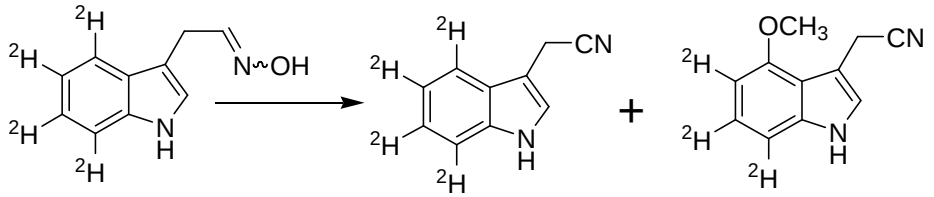

112a **49a** **51a**

Figure 2.17 Incorporation of [$^2H_4$]indolyl-3-acetaldoxime (**112a**) into [$^2H_4$]indolyl-3-acetonitrile (**49a**, 89%) and [$^2H_3$]arvelexin (**51a**, 41%).

Table 2.6 Incorporation of [4',5',6',7'-$^2H_4$]indolyl-3-acetaldoxime (**112a**) into dog mustard phytoalexins

Compound	**% Incorporation**
[4',5',6',7'-$^2H_4$]1-Methoxyspirobrassinin (**35a**)	[a,c]46 ± 6
[4',5',6',7'-$^2H_4$]Erucalexin (**38a**)	[a,c]15 ± 3
[4',5',6',7'-$^2H_4$]Indolyl-3-acetonitrile (**49a**)	[b]89
[4',5',6',7'-$^2H_4$]Arvelexin (**51a**)	[b]41

% of ^2H incorporation = $\{[M + n]^{+/-}/([M]^{+/-} + [M + n]^{+/-})\} \times 100$ ($n = 4$).
[a]Incorporation determined from average of two independent experiments ± standard deviation (STD).
[b]Incorporation determined from a single feeding experiment.
[c]Positive ion mode.

Incorporation of 1-methoxyindolyl-3-acetaldoximes

Biogenetic origin of 1-methoxy group in erucalexin and 1-methoxyspirobrassinin was investigated using perdeuterated 1-methoxyindolyl-3-acetaldoximes: [1",1",1"-$^2H_3$]1-methoxyindolyl-3-acetaldoxime (**116a**), [4',5',6',7'-$^2H_4$]1-methoxyindolyl-3-acetaldoxime (**116b**), and [1",1",1",4',5',6',7'-$^2H_7$]1-methoxyindolyl-3-acetaldoxime (**116c**).

First, doubly elicited dog mustard leaves were incubated with [1",1",1"-$^2H_3$]1-methoxyindolyl-3-acetaldoxime (**116a**) for 48 hours. The leaves were extracted and subjected to preliminary clean up to yield a fraction that contained the phytoalexins 1-methoxyspirobrassinin (**35**), erucalexin (**38**), indolyl-3-acetonitrile (**49**), and arvelexin (**51**) (established by HPLC-DAD and HPLC-MS-ESI); control experiments were prepared similarly by incubating doubly elicited leaves with 1-methoxyindolyl-3-

acetaldoxime (**116**) and with carrier solution. HPLC-HRMS-ESI analyses (positive ion mode) of the phytoalexin fraction from feeding [1",1",1"-$^2H_3$]1-methoxyindolyl-3-acetaldoxime displayed the erucalexin and 1-methoxyspirobrassinin peaks at t_R = 14.5 and 18.2 min, respectively, to contain two ions at *m/z* 281.0412 and 284.061 corresponding to the molecular formulae $C_{12}H_{13}N_2O_2S_2$ and $C_{12}H_{10}{}^2H_3N_2O_2S_2$, respectively (**Figure 2.18**, **Table 2.7**). The ion at *m/z* 284.061 was not detected in control fractions incubated with non-labeled 1-methoxyindolyl-3-acetaldoxime. Deuterium incorporation was calculated based on the peak area of each molecular ion and was found to be 5 ± 3 % for erucalexin and 7 ± 3 % for 1-methoxyspirobrassinin (**Figure 2.18**, **Table 2.7**).

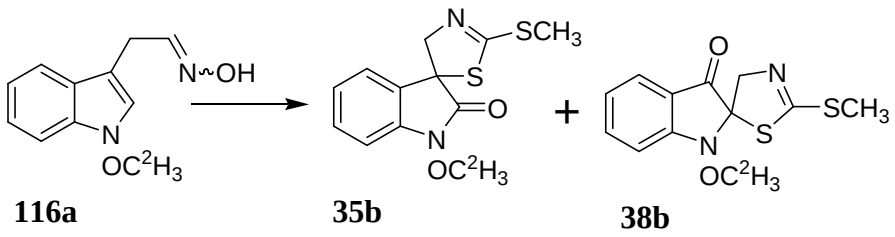

Figure 2.18 Incorporation of [$^2H_3$]1-methoxyindolyl-3-acetaldoxime (**116a**) into 1-methoxyspirobrassinin (**35b**, 7 ± 3 %) and erucalexin (**38b**, 5 ± 3 %).

Next, doubly elicited dog mustard leaves were incubated with [4',5',6',7'-$^2H_4$]1-methoxyindolyl-3-acetaldoxime (**116b**) for 48 hours. The leaves were extracted and subjected to preliminary clean up to yield a fraction that contained the phytoalexins 1-methoxyspirobrassinin (**35**), erucalexin (**38**), indolyl-3-acetonitrile (**49**), and arvelexin (**51**) (established by HPLC-DAD and HPLC-MS-ESI); control experiments were prepared similarly by incubating doubly elicited leaves with 1-methoxyindolyl-3-acetaldoxime (**116**) and with carrier solution. HPLC-HRMS-ESI analyses (positive ion mode) of the phytoalexin fraction from feeding [4',5',6',7'-$^2H_4$]1-methoxyindolyl-3-acetaldoxime displayed the erucalexin and 1-methoxyspirobrassinin peaks at t_R = 14.5 and 18.2 min, respectively, to contain two ions at *m/z* 281.0412 and 285.0664 that were consistent with the molecular formulae $C_{12}H_{13}N_2O_2S_2$ and $C_{12}H_9{}^2H_4N_2O_2S_2$, respectively (**Figure 2.19**). The ion at *m/z* 285.0664 was not detected in control fractions that were

incubated with 1-methoxyindolyl-3-acetaldoxime. Based on the peak area of each ion, deuterium incorporation was found to be 6 ± 4 % for erucalexin and 7 ± 2 % for 1-methoxyspirobrassinin (**Figure 2.19**, **Table 2.7**).

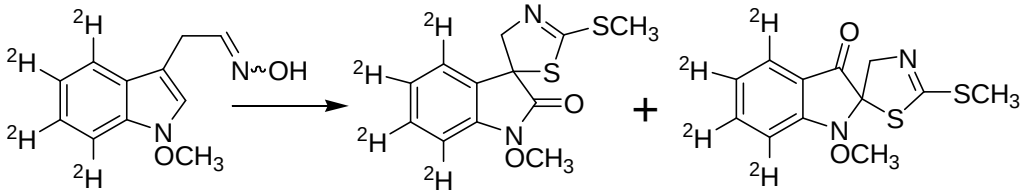

Figure 2.19 Incorporation of [$^2H_4$]1-methoxyindolyl-3-acetaldoxime (**116b**) into [$^2H_4$]1-methoxyspirobrassinin (**35a**, 7 ± 2 %) and [$^2H_4$]erucalexin (**38a**, 6 ± 4 %).

Lastly, [1",1",1",4',5',6',7'-$^2H_7$]1-methoxyindolyl-3-acetaldoxime (**116c**) was administered to doubly elicited dog mustard leaves. Following 48-hour incubation and extraction, preliminary clean up yielded a fraction that contained the phytoalexins 1-methoxyspirobrassinin (**35**), erucalexin (**38**), indolyl-3-acetonitrile (**49**), and arvelexin (**51**) (established by HPLC-DAD and HPLC-MS-ESI); control experiments were prepared similarly by incubating doubly elicited leaves with 1-methoxyindolyl-3-acetaldoxime (**116**) and with carrier solution. HPLC-HRMS-ESI analyses (positive ion mode) of the phytoalexin fraction resulting from feeding [1",1",1",4',5',6',7'-$^2H_7$]1-methoxyindolyl-3-acetaldoxime displayed the erucalexin and 1-methoxyspirobrassinin peaks at t_R = 14.5 and 18.2 min, respectively, to contain two ions at *m/z* 281.0412 and 288.0852 that were consistent with the molecular formulae $C_{12}H_{13}N_2O_2S_2$ and $C_{12}H_6{}^2H_7N_2O_2S_2$, respectively (**Figure 2.20**). The ion at *m/z* 288.0852 was absent in control extracts incubated with non-labeled 1-methoxyindolyl-3-acetaldoxime. The percentage of deuterium incorporation was calculated based on the peak area of each ion and was found to be 3 ± 2 % for erucalexin and 4 ± 3 % for 1-methoxyspirobrassinin (**Figure 2.20**, **Table 2.7**).

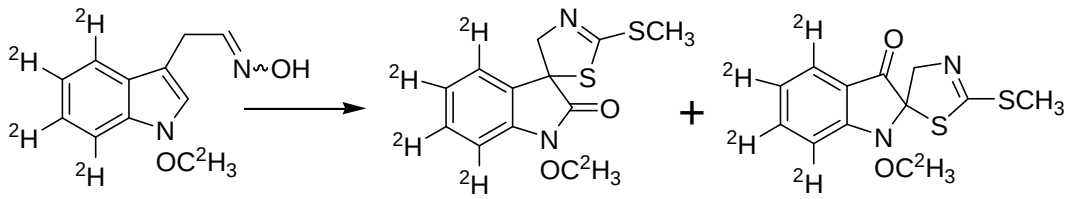

Figure 2.20 Incorporation of [$^2H_7$]1-methoxyindolyl-3-acetaldoxime (**116c**) into [$^2H_7$]1-methoxyspirobrassinin (**35c**, 4 ± 3 %) and [$^2H_7$]erucalexin (**38c**, 3 ± 2 %).

Deuterium labeling of erucalexin and 1-methoxyspirobrassinin indicated only [M + 7]$^+$ suggesting intact incorporation of [$^2H_7$]1-methoxyindolyl-3-acetaldoxime without loss of 1-methoxy group (**Figure 2.20**).

Table 2.7 Incorporation of 1-methoxyindolyl-3-acetaldoximes (**116a**, **116b**, and **116c**) into erucalexin and 1-methoxyspirobrassinin

	% Incorporation	
Precursor	**Erucalexin**	**1-Methoxyspirobrassinin**
[1",1",1"-$^2H_3$]1-methoxyindolyl-3-acetaldoxime (**116a**)	[a,c]5 ± 3	[a,c]7 ± 3
[4',5',6',7'-$^2H_4$]1-methoxyindolyl-3-acetaldoxime (**116b**)	[b,c]6 ± 4	[b,c]7 ± 2
[1",1",1",4',5',6',7'-$^2H_7$]1-methoxyindolyl-3-acetaldoxime (**116c**)	[b,c]3 ± 2	[b,c]4 ± 3

% of ^2H incorporation = {[M + n]$^{+/-}$/([M]$^{+/-}$ + [M + n]$^{+/-}$)} × 100 (n = 3, 4, 7).
[a]Incorporation determined from average of five independent experiments ± standard deviation (STD).
[b]Incorporation determined from average of three independent experiments ± standard deviation (STD).
[c]Positive ion mode.

Incorporation of 1-methoxybrassinins

Biosynthetic pathway of erucalexin and 1-methoxyspirobrassinin was studied with perdeuterated 1-methoxybrassinins; [3,3,3-$^2H_3$]1-methoxybrassinin (**18a**), and [3,3,3,4',5',6',7'-$^2H_7$]1-methoxybrassinin (**18c**) which are advanced precursors in the biosynthetic pathway. Thus, doubly elicited dog mustard leaves were incubated with [3,3,3-$^2H_3$]1-methoxybrassinin (**18a**) for 48 hours followed by extraction. Preliminary clean up of the extract yielded a fraction that contained the phytoalexins 1-methoxyspirobrassinin (**35**), erucalexin (**38**), indolyl-3-acetonitrile (**49**), and arvelexin (**51**) (established by HPLC-DAD and HPLC-MS-ESI); control experiments were prepared similarly by incubating doubly elicited leaves with 1-methoxybrassinin (**18**) and with carrier solution only. HPLC-HRMS-ESI analyses (positive ion mode) of the phytoalexin fraction resulting from feeding [3,3,3-$^2H_3$]1-methoxybrassinin displayed the erucalexin and 1-methoxyspirobrassinin peaks at t_R = 14.5 and 18.2 min, respectively, to contain two ions at *m/z* 281.0412 and 284.0601 which were consistent with molecular formulae $C_{12}H_{13}N_2O_2S_2$ and $C_{12}H_{10}{}^2H_3N_2O_2S_2$, respectively (**Figure 2.21**). The ion at *m/z* 284.0601 was not detected in control fractions incubated with non-labeled 1-methoxybrassinin. Based on the peak area of each molecular ion, deuterium incorporation was found to be 7 ± 3 % for erucalexin and 53 ± 2 % for 1-methoxyspirobrassinin (**Figure 2.21**, **Table 2.8**).

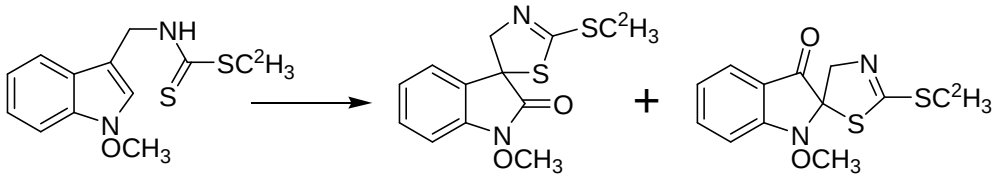

18a **35d** **38d**

Figure 2.21 Incorporation of [$^2H_3$]1-methoxybrassinin (**18a**) into [$^2H_3$]1-methoxyspirobrassinin (**35d**, 53 ± 2 %) and [$^2H_3$]erucalexin (**38d**, 7 ± 3 %) (Pedras and Okinyo, 2006b).

Next, doubly elicited dog mustard leaves were incubated with [3,3,3,4',5',6',7'-$^2H_7$]1-methoxybrassinin (**18c**). After 48 hours the leaves were extracted followed by preliminary clean up to yield a fraction that contained the phytoalexins 1-

methoxyspirobrassinin (**35**), erucalexin (**38**), indolyl-3-acetonitrile (**49**), and arvelexin (**51**) (established by HPLC-DAD and HPLC-MS-ESI); control experiments were prepared similarly by incubating doubly elicited leaves with 1-methoxybrassinin (**18**) and with carrier solution. HPLC-HRMS-ESI analyses (positive ion mode) of the phytoalexin fraction resulting from feeding [3,3,3,4',5',6',7'-$^2H_7$]1-methoxybrassinin displayed the erucalexin and 1-methoxyspirobrassinin peaks at t_R = 14.5 and 18.2 min, respectively, to contain two ions at *m/z* 281.0412 and 288.0852 that were consistent with the molecular formulae $C_{12}H_{13}N_2O_2S_2$ and $C_{12}H_6{}^2H_7N_2O_2S_2$, respectively (**Figure 2.22**). The ion at *m/z* 288.0852 was not detected in control extracts incubated with non-labeled 1-methoxybrassinin. Based on the peak area of each ion, deuterium incorporation was found to be 4 ± 2 % for erucalexin and 64 ± 11 % for 1-methoxyspirobrassinin (**Figure 2.22**, **Table 2.8**).

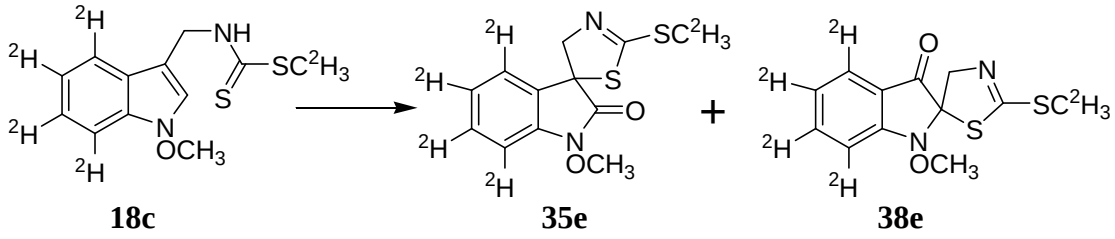

Figure 2.22 Incorporation of [$^2H_7$]1-methoxybrassinin (**18c**) into 1-methoxyspirobrassinin (**35e**, 64 ± 11 %) and erucalexin (**38e**, 4 ± 2 %) (Pedras and Okinyo, 2006b).

HPLC-DAD chromatograms of leaf extracts incubated with 1-methoxybrassinins (**18**, **18a**, **18c**) indicated a new metabolite peak at t_R = 8.9 min that was absent in leaf extracts incubated with carrier solution only. The new metabolite was identified as caulilexin B (**48**) by comparison of retention time and UV spectra with those of an authentic sample. In order to determine deuterium incorporation, fed and control leaf extracts were separated by preparative HPLC to yield caulilexin B at t_R = 8.9 min and 1-methoxybrassitin at 18.1 min in less than 0.1 mg each.

HPLC-HRMS-ESI analysis of caulilexin B (purified from leaf extracts incubated with [3,3,3,4',5',6',7'-$^2H_7$]1-methoxybrassinin) indicated a fragment ion at *m/z* 164.1007 that was consistent with the molecular formula $C_{10}H_6{}^2H_4NO$, suggesting a 1-

methoxyindole-3-methine fragment. The fragmentation pattern is characteristic of 1-methoxy containing phytoalexins such as 1-methoxybrassinin (**18**), 1-methoxybrassitin (**20**), and wasalexins A (**23**) and B (**24**) (Pedras et al., 2006c). HRMS-EI analysis of caulilexin B resulting from extracts fed [3,3,3,4',5',6',7'-$^2H_7$]1-methoxybrassinin displayed an ion at *m/z* 208.1149 that was consistent with the molecular formula $C_{11}H_8{}^2H_4N_2O_2$. These data suggested deuterium incorporation into [4',5',6',7'-$^2H_4$]caulilexin B (**48a**) to be ≥ 99.9% (**Figure 2.23**, **Table 2.9**).

The amount of 1-methoxybrassitin (**20**) increased 5 fold in extracts incubated with 1-methoxybrassinin compared to those incubated with carrier solution only. The HRMS-EI analysis of 1-methoxybrassitin fraction obtained from leaf extracts incubated with [3,3,3,4',5',6',7'-$^2H_7$]1-methoxybrassinin displayed two ions at *m/z* 250.0776 and 257.1215 that were consistent with the molecular formulae $C_{12}H_{14}N_2O_2S$ and $C_{12}H_7{}^2H_7N_2O_2S$, respectively (**Figure 2.23**). Based on the relative intensity of each molecular ion, percentage of deuterium incorporation was found to be 99.6% {[100/(0.4 + 100)] × 100} (**Figure 2.23**, **Table 2.9**), suggesting that 1-methoxybrassinin is immediate precursor of 1-methoxybrassitin.

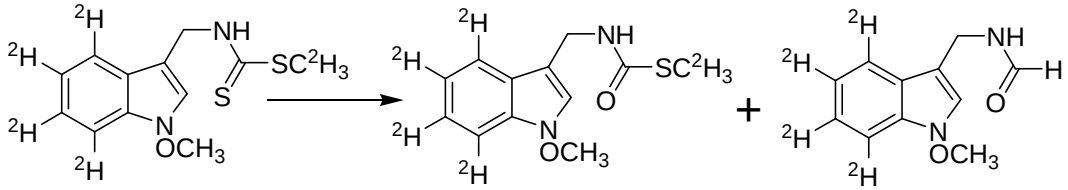

18c **20a** **48a**

Figure 2.23 Incorporation of [$^2H_7$]1-methoxybrassinin (**18c**) into [$^2H_7$]1-methoxybrassitin (**20a**, 99.6%) and [$^2H_4$]caulilexin B (**48a**, ≥ 99.9%).

Table 2.8 Incorporation of 1-methoxybrassinins into erucalexin and 1-methoxyspirobrassinin

	% Incorporation[a,b]	
Precursor	**Erucalexin**	**1-Methoxyspirobrassinin**
[3,3,3-$^2H_3$]1-Methoxybrassinin (**18a**)	7 ± 3	53 ± 2
[3,3,3,4',5',6',7'-$^2H_7$]1-Methoxybrassinin (**18c**)	4 ± 2	64 ± 11

% of ^{2}H incorporation = $\{[M + n]^{+/-}/([M]^{+/-} + [M + n]^{+/-})\} \times 100$ (n = 3, 7).
[a]Incorporation determined from average of three independent experiments ± standard deviation (STD).
[b]Positive ion mode.

Table 2.9 Incorporation of [3,3,3,4',5',6',7'-$^2H_7$]1-methoxybrassinin (**18c**) into 1-methoxybrassitin (**20a**) and caulilexin B (**48a**)

Compound	**% Incorporation[a]**
[1",1",1",4',5',6',7'-$^2H_7$]1-Methoxybrassitin (**20a**)	99.6
[4',5',6',7'-$^2H_4$]Caulilexin B (**48a**)	≥99.9

% of ^{2}H incorporation = $\{[M + n]^{+}/([M]^{+} + [M + n]^{+})\} \times 100$ (n = 4, 7).
[a]Incorporation determined from one set of experiments.

Incorporation of sinalbins B

Sinalbin B (**31**) was detected in stem extracts of white mustard (*Sinapis alba*) elicited with *L. maculans* and was suggested to be a biosynthetic precursor of sinalbin A (**30**). Since sinalbin B contains a 1-methoxy group, its biogenetic relationship with erucalexin was investigated. Thus, doubly elicited dog mustard leaves were incubated with [3,3,3-$^2H_3$]sinalbin B (**31b**) for 48 hours. Following extraction, preliminary clean up yielded a fraction that contained the phytoalexins 1-methoxyspirobrassinin (**35**), erucalexin (**38**), indolyl-3-acetonitrile (**49**), and arvelexin (**51**) (established by HPLC-DAD and HPLC-MS-ESI); control experiments were prepared similarly by incubating doubly elicited leaves with sinalbin B (**31**) and with carrier solution. HPLC-HRMS-ESI analyses (positive ion mode) of the phytoalexin fraction resulting from feeding [3,3,3-$^2H_3$]sinalbin B displayed the erucalexin (**38d**) and 1-methoxyspirobrassinin (**35d**) peaks at t_R = 14.5 and 18.2 min, respectively, to contain two ions at *m/z* 281.0412 and 284.061

that were consistent with molecular formulae $C_{12}H_{13}N_2O_2S_2$ and $C_{12}H_{10}{}^2H_3N_2O_2S_2$, respectively. The ion at *m/z* 284.061 was not detected in control extracts incubated with non-labeled sinalbin B. The percentage of deuterium incorporation was calculated from the peak area of each ion and was found to be 2 ± 0.2 % for erucalexin and 10 ± 1 % for 1-methoxyspirobrassinin (**Figure 2.24**, **Table 2.10**).

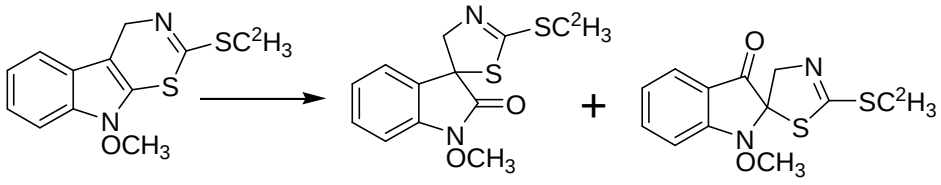

31b **35d** **38d**

Figure 2.24 Incorporation of [$^2H_3$]sinalbin B (**31b**) into [$^2H_3$]1-methoxyspirobrassinin (**35d**, 10 ± 1 %) and [$^2H_3$]erucalexin (**38d**, 2 ± 0.2 %) (Pedras and Okinyo, 2006b).

Next, doubly elicited dog mustard leaves were incubated with [4',5',6',7'-$^2H_4$]sinalbin B (**31a**). After 48 hours, the leaves were extracted followed by preliminary clean up to yield a fraction that contained phytoalexins 1-methoxyspirobrassinin (**35**), erucalexin (**38**), indolyl-3-acetonitrile (**49**), and arvelexin (**51**) (established by HPLC-DAD and HPLC-MS-ESI); control experiments were prepared similarly by incubating doubly elicited leaves with sinalbin B (**31**) and with carrier solution. HPLC-HRMS-ESI analyses (positive ion mode) of the phytoalexin fraction resulting from feeding of [4',5',6',7'-$^2H_4$]sinalbin B displayed the erucalexin and 1-methoxyspirobrassinin peaks at t_R = 14.5 and 18.2 min, respectively, to contain two ions at *m/z* 281.0412 and 285.0664 that were consistent with the molecular formulae $C_{12}H_{13}N_2O_2S_2$ and $C_{12}H_9{}^2H_4N_2O_2S_2$, respectively (**Figure 2.25**). The ion at *m/z* 285.0664 was not detected in control fractions incubated with non-labeled sinalbin B. The percentage of deuterium incorporation was calculated from the peak area of each ion and was found to be 5 ± 0.1 % for erucalexin and 19 ± 7 % for 1-methoxyspirobrassinin (**Figure 2.25**, **Table 2.10**). These results were consistent with those obtained from incorporation of [3,3,3-$^2H_3$]sinalbin B (**31b**).

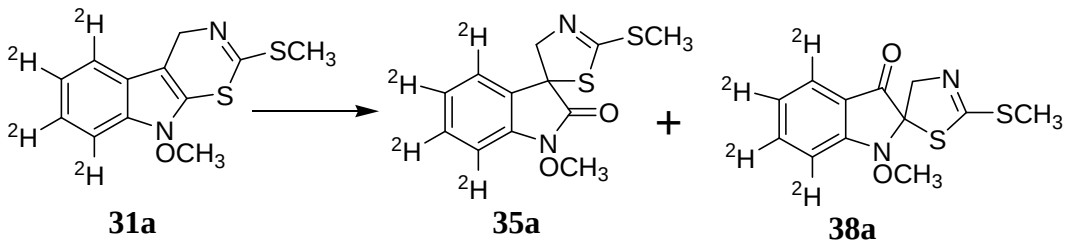

31a **35a** **38a**

Figure 2.25 Incorporation of [$^2H_4$]sinalbin B (**31a**) into [$^2H_4$]1-methoxyspirobrassinin (**35a**, 19 ± 7 %) and [$^2H_4$]erucalexin (**38a**, 5 ± 0.1 %) (Pedras and Okinyo, 2006b).

Table 2.10 Incorporation of sinalbins B (**31a** and **31b**) into erucalexin and 1-methoxyspirobrassinin

	% Incorporation	
Precursor	**Erucalexin**	**1-Methoxyspirobrassinin**
[4',5',6',7'-$^2H_4$]sinalbin B (**31a**)	[a,c]5 ± 0.1	[b,c]19 ± 7
[3,3,3-$^2H_3$]sinalbin B (**31b**)	[a,c]2 ± 0.2	[b,c]10 ± 1

% of ^2H incorporation = $\{[M + n]^{+/-}/([M]^{+/-} + [M + n]^{+/-})\} \times 100$ (n = 3,4).
[a]Incorporation determined from average of two independent experiments ± standard deviation (STD).
[b]Incorporation determined from average of three independent experiments ± standard deviation (STD).
[c]Positive ion mode.

CHAPTER 3

3. Discussion

3.1 Secondary metabolites from *Eruca sativa* (rocket)

Rocket (*Eruca sativa*) was previously reported to exhibit resistance against the phytopathogenic fungus *Alternaria brassicae* (Conn et al., 1988). Considering the role of phytoalexins in plant disease resistance, investigation of phytoalexin production in rocket was carried out. Phytoalexin elicitation followed by analysis of leaf extracts showed arvelexin (**51**) (Pedras et al., 2003a) as the only elicited compound. Bioassay guided isolation using spores of *Cladosporium cucumerinum*, however, led to the isolation of two antifungal metabolites, 4-methylthiobutyl isothiocyanate (**166**) and bis(4-isothiocyanatobutyl)disulfide (**167**). Compounds, **166** and **167** inhibited germination of *C. cucumerinum* spores in TLC biodetection assays. Both metabolites **166** and **167** were previously isolated from rocket and suggested to derive from their respective glucosinolates (Bennett et al., 2002; Cerney et al., 1996). The bis(4-isothiocyanatobutyl)disulfide was proposed to be formed via oxidation of the unstable 4-(mercaptobutyl) isothiocyanate (Cerney et al., 1996), whereas 4-methylthiobutyl isothiocyanate derived from myrosinase hydrolysis of 4-methylthiobutyl glucosinolate (Bennett et al., 2002).

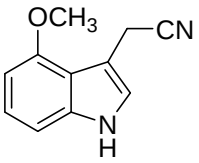

51

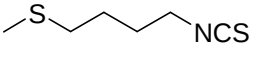

166

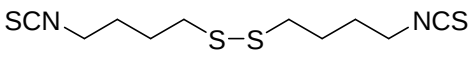

167

Figure 3.1 Antifungal metabolites from rocket (*Eruca sativa*).

In general, crucifers produce a mixture of phytoalexins, whose composition and amounts depend on the type of stress (Pedras et al., 2007b). It was therefore surprising to find that rocket seems to produce only one phytoalexin upon elicitation with copper(II) chloride. Perhaps it would be of interest to analyze tissues infected with different pathogens. In fact, recent results have shown that canola and rapeseed produced phytoalexin mixtures related to the virulence of the pathogen (Pedras et al., 2007e).

3.2 Syntheses of compounds

Preparation of perdeuterated compounds such as [4',5',6',7'-$^2H_4$]indolyl-3-acetaldoxime (**112a**), [4',5',6',7'-$^2H_4$]brassinin (**16a**), [4',5',6',7'-$^2H_4$]cyclobrassinin (**28a**), and [4',5',6',7'-$^2H_4$]sinalbin B (**31a**) required the starting material, [4,5,6,7-$^2H_4$]indole (**105a**), to be at least 99% deuterated. Because the commercially available indoles did not offer this percentage of deuteration at specific sites or were very expensive, a shorter procedure was used to prepare [4,5,6,7-$^2H_4$]indole (**105a**) in two steps and 24% overall yield starting from the readily available NMR solvent [2,3,4,5,6-$^2H_5$]nitrobenzene (**168a**, 99%, $^2H_5$) and 2-chloroacetonitrile (Pedras and Okinyo, 2006a) (**Scheme 3.1**). Indole was previously prepared from 2-nitrophenylacetonitrile which was obtained from toluene in three steps, requiring a chromatographic separation for each step (Van den Berg et al., 1988). Makosza and Winiarski (1984), however, developed a one step reaction in the preparation of 2-nitrophenylacetonitrile and derivatives by employing vicarious nucleophilic substitution of stabilized *R*-chlorocarbanions with nitrobenzene. This method (Makosza and Winiarski, 1984) was therefore adapted to the preparation of [4,5,6,7-$^2H_4$]indole (**105a**) as shown in **Scheme 3.1**. Next [4',5',6',7'-$^2H_4$]indolyl-3-acetonitrile (**49a**) was prepared from [4,5,6,7-$^2H_4$]indolylmagnesium iodide and bromoacetonitrile (Pedras et al., 2003; Pedras and Okinyo, 2006a). Subsequent reduction of [4',5',6',7'-$^2H_4$]indolyl-3-acetonitrile (**49a**) with DIBAH followed by hydrolysis and treatment with $HONH_2 \cdot HCl$ and NaOAc yielded [4',5',6',7'-$^2H_4$]indolyl-3-acetaldoxime (**112a**) (Pedras and Okinyo, 2006) (**Scheme 3.1**). Non-isotopically labeled indolyl-3-acetaldoxime (**112**), and 1-methylindolyl-3-acetaldoxime (**170**) were similarly prepared.

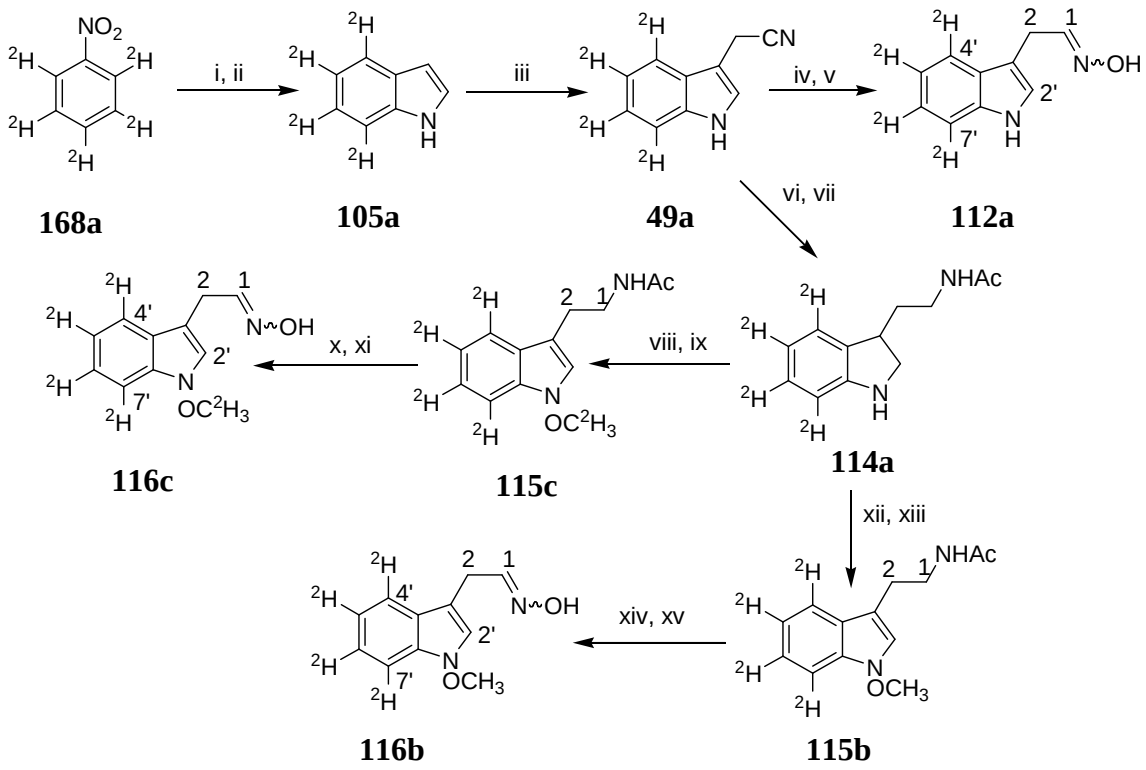

Scheme 3.1 Reagents and conditions: i) $ClCH_2CN$, NaOH, DMSO, 40%; ii) 10% Pd/C, H_2, EtOAc, 61%; iii) Mg, ICH_3, $BrCH_2CN$, Et_2O, 57%; iv) DIBAH; v) $HONH_2 \cdot HCl$, NaOAc, EtOH, 33%; vi) 10% Pd/C, H_2, Ac_2O; vii) $NaBH_3CN$, AcOH; viii) $Na_2WO_4 \cdot 2H_2O$, H_2O_2, CH_3OH; ix) $(C^2H_3O)_2SO_2$, K_2CO_3, CH_3OH; x) NaOH, CH_3OH, reflux; xi) $Na_2WO_4 \cdot 2H_2O$, H_2O_2, CH_3OH, 4% from **49a**; xii) $Na_2WO_4 \cdot 2H_2O$, H_2O_2, CH_3OH; xiii) $(CH_3O)_2SO_2$, K_2CO_3; xiv) NaOH, CH_3OH, reflux; xv) $Na_2WO_4 \cdot 2H_2O$, H_2O_2, CH_3OH, 5% from **49a** (Pedras and Okinyo, 2006a).

Preparation of perdeuterated 1-methoxyindolyl-3-acetaldoximes **116b** and **116c** (**Scheme 3.1**) needed [4',5',6',7'-$^2H_4$]tryptamine as the starting material. Attempts to synthesize [4',5',6',7'-$^2H_4$]tryptamine via hydrogenation of [4',5',6',7'-$^2H_4$]indolyl-3-acetonitrile (**49a**) in ethyl acetate or ethanol were unsuccessful. Hydrogenation of **49a** in acetic anhydride thus provided [4',5',6',7'-$^2H_4$]N_b-acetyltryptamine that was reduced with $NaBH_3CN$ to yield [$^2H_4$]N_b-acetyl-2,3-dihyroindolyl-3-ethylamine (**114a**) (Pedras and Okinyo, 2006a). Oxidation of **114a** with Na_2WO_4/H_2O_2 (Somei and Kawasaki, 1989) and subsequent methylation with $(C^2H_3O)_2SO_2$ or $(CH_3O)_2SO_2$ yielded [1'',1'',1'',4',5',6',7'-$^2H_7$]N_b-acetyl-1-methoxytryptamine (**115c**) and [4',5',6',7'-$^2H_4$]N_b-acetyl-1-methoxytryptamine (**115b**), respectively. The oxidation of the amines proved difficult mostly due to decomposition of the products under the reaction conditions used

(Pedras and Okinyo, 2006a) but were accomplished in 4 – 5% yield (**Scheme 3.1**). Simple and efficient methods of oxidation of aliphatic amines to oximes are however not available. For example, CH_3ReO_3/H_2O_2 catalyzed oxidation of primary alkylamines possessing the α-C-H bond was found to yield mixtures of oximes, nitroso dimers, and azoxy compounds (Yamazaki, 1997).

A number of synthetic strategies have been developed for the preparation of free thiohydroxamic acids as described in the Introduction section (Chimiak et al., 2002; Walter and Schaumann, 1971). The simplest and most efficient preparation involves conversion of primary nitro compounds (alkyl or benzyl) to their respective thiohydroxamic acids using hexamethyldisilathiane (**171**) (Hwu and Tsay, 1990). Indolyl-3-acetothiohydroxamic acid (**174**) or its derivatives were however not reported. In addition, the biosynthetic investigations employing indolyl-3-acetothiohydroxamic acid required labeling of the sulfur and the indolyl ring. Sulfur 34 and deuterium were chosen for labeling experiments since metabolites incorporating them could unambiguously be detected by mass spectrometry (HRMS-ESI). In this work, a simple three step preparation was developed starting from indole-3-carboxaldehyde (**106**) (**Scheme 3.2**). 1-Methylindolyl-3-acetothiohydroxamic acid (**178**) was similarly prepared starting from 1-methylindole-3-carboxaldehyde (**175**). The use of sodium hydride instead of potassium hydride to prepare **174** provided only indolyl-3-acetonitrile (**49**) and indolyl-3-acetaldoxime (**112**) in a 1:1 ratio (**Scheme 3.2**). The ^{13}C NMR data indicated that indolyl-3-acetothiohydroxamic acid (**174**), and not indolyl-3-acetothiohydroximic acid (**204**), is the most likely tautomer present in solution since the C-1 is 189.0 ppm. In general the C-1 of thiohydroximates has lower value (ca 162-172 ppm) (Pedras and Okinyo, 2008).

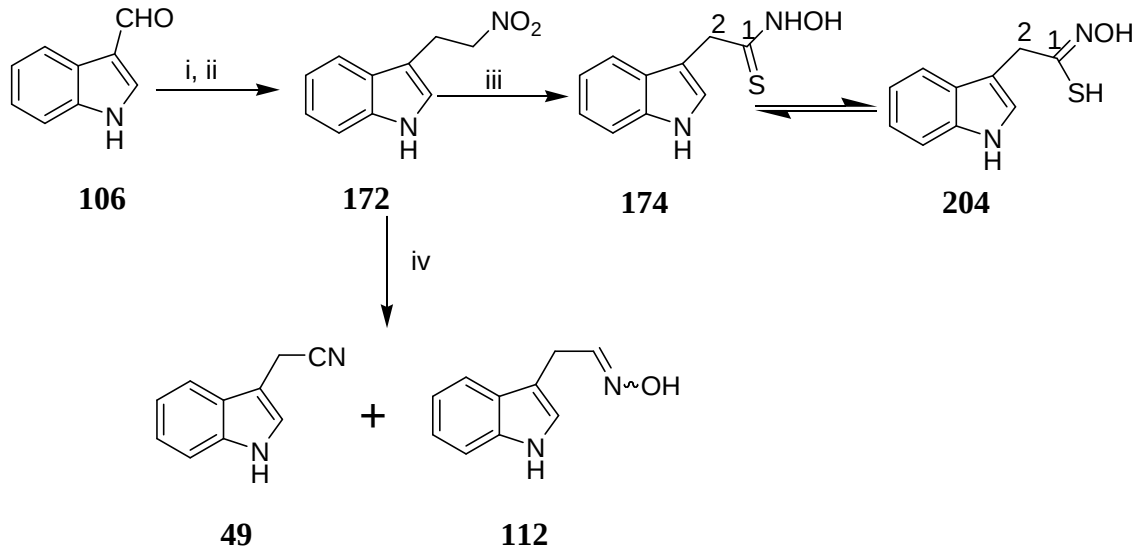

Scheme 3.2 Synthesis of indolyl-3-acetothiohydroxamic acid (**174**). Reagents and conditions: i) CH_3NO_2, NH_4OAc, 128-130 °C, 98%; ii) $NaBH_4$, i-PrOH, SiO_2, $CHCl_3$, 71%; iii) KH, $(Me_3Si)_2S$ (**171**), THF, 74%; . iv) NaH, $(Me_3Si)_2S$, THF (Pedras and Okinyo, 2008).

Once the synthesis of indolyl-3-acetothiohydroxamic acid (**174**) was established (**Scheme 3.2**), the [4',5',6',7'-$^{2}H_4$]indolyl-3-[^{34}S]acetothiohydroxamic acid (**174a**) was synthesized for the first time following steps in **Scheme 3.2** and using [4,5,6,7-$^{2}H_4$]indole-3-carboxaldehyde (**106a**) as the starting material. The ^{34}S-hexamethyldisilathiane (**171a**) was not commercially available, and was therefore prepared (from sulfur 34, sodium, and chlorotrimethylsilane) as described in the Result and Experimental sections. With **171a** in hand, [4',5',6',7'-$^{2}H_4$]indolyl-3-[^{34}S]acetothiohydroxamic acid (**174a**) was prepared following steps in **Scheme 3.2** (Pedras and Okinyo, 2008).

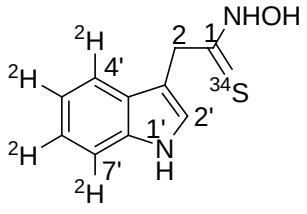

174a

The indolyl-3-methylisothiocyante (**123**) was proposed to be an intermediate in the biosynthetic pathway of brassinin (**16**) (Pedras et al., 2003b; Pedras and Okinyo, 2008). Attempts to synthesize **123** were unsuccessful (Kutchy et al., 1997; 1998) due to its instability (Hanley et al., 1990; Hanley and Parsley, 1990). The synthesis of the stable 1-(*t*-butoxycarbonyl)indolyl-3-methylisothiocyanate (**180**) was reported (Kutchy et al., 1997; 1998). In this thesis, 1-acetylindolyl-3-methylisothiocyanate (**183**) was prepared for the first time (**Scheme 3.3**). The 1-acetylbrassinin (**184**) was obtained from freshly prepared amine **182** following previously established procedures for the preparation of brassinin (**16**) (**Scheme 3.3**, Pedras et al., 2003b) and is described in Result and Experimental sections.

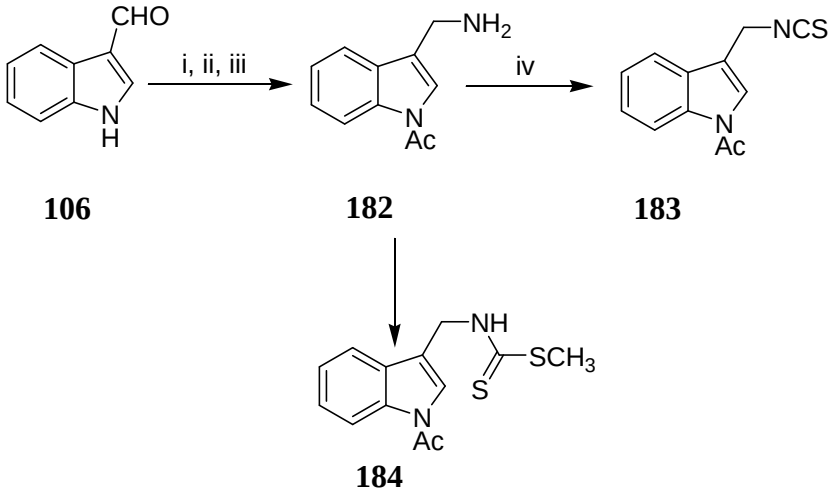

Scheme 3.3 Reagents and conditions: i) Ac_2O, pyridine, 96%; ii) $HONH_2 \cdot HCl$, NaOAc, EtOH, 45-50 ºC, 88%; iii) $NiCl_2 \cdot 6H_2O$, $NaBH_4$, CH_3OH; iv) Cl_2CS, $CaCO_3$, CH_2Cl_2-H_2O, 31% from oxime; v) Et_3N, CS_2, ICH_3, pyridine, 41 % from oxime.

[4',5',6',7'-$^2H_4$]Cyclobrassinin (**28a**) was prepared from [4,5,6,7-$^2H_4$]indole (**105a**) following previously established procedure (Pedras et al., 1998) (**Scheme 3.4**). Perdeuterated 1-methoxybrassinins **18b** and **18c** were obtained from [4,5,6,7-$^2H_4$]indole (**105a**) as shown in **Scheme 3.4** (Pedras and Okinyo, 2006a). [4',5',6',7'-$^2H_4$]Sinalbin B (**31a**) was prepared from [4',5',6',7'-$^2H_4$]1-methoxybrassinin (**18b**) following the established synthesis for sinalbin B (**31**) (Pedras and Zaharia, 2000), whereas [4',5',6',7'-

$^2H_4$]1-methoxyspirobrassinin (**35a**) was prepared from **18b** following the established synthesis for 1-methoxyspirobrassinin (**35**) (**Scheme 3.4**, Pedras et al., 2006a).

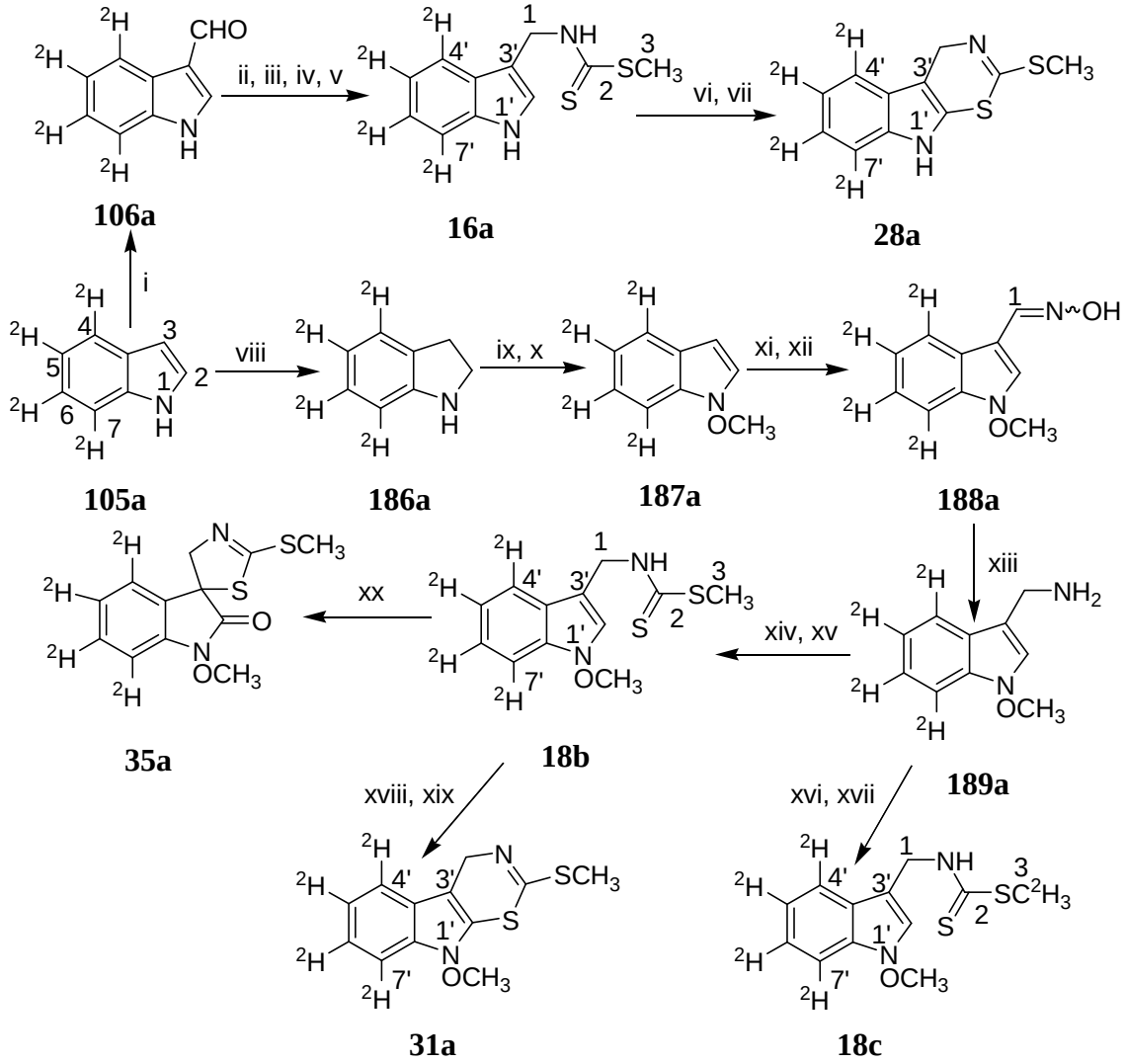

Scheme 3.4 Reagents and conditions: i) $POCl_3$, DMF, 87%; ii) $HONH_2{\cdot}HCl$, Na_2CO_3, EtOH, reflux, 87%; iii) NaOH, Devarda's alloy, CH_3OH; iv) Pyridine, Et_3N, CS_2, 60 min, 0 ºC; v) ICH_3, 50%; vi) pyridine/HBr/Br_2, THF, vii) DBU, 58% (Pedras et al., 1998); viii) $NaBH_3CN$, AcOH, 82%; ix) $Na_2WO_4{\cdot}2H_2O$, H_2O_2; x) $(CH_3O)_2SO_2$, K_2CO_3, CH_3OH, 52%; xi) $POCl_3$, DMF, 93%; xii) $HONH_2{\cdot}HCl$, Na_2CO_3, EtOH, reflux, 99%; xiii) $NaBH_3CN$, $TiCl_3$, NH_4OAc, CH_3OH; xiv) Pyridine, Et_3N, CS_2, 60 min, 0 ºC; xv) ICH_3, 67%; xvi) Pyridine, Et_3N, CS_2, 60 min, 0 ºC; xvii) IC^2H_3, 68% (Pedras and Okinyo, 2006a); xviii) NBS, CH_2Cl_2; xix) Et_3N, 47% (adapted from Pedras and Zaharia, 2000); xx) PCC, CH_2Cl_2, 41% (adapted from Pedras et al., 2006a).

2-Mercaptoindole-3-carboxaldehyde (**135**) was prepared following the established synthetic procedures (Pedras and Okanga, 1999). The **135** was then used to synthesize [SC^2H_3]brassicanal A (**39b**) (**Scheme 3.5**).

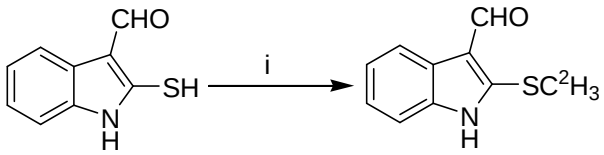

135 **39b**

Scheme 3.5 Synthesis of [SC^2H_3]brassicanal A (**39b**). Reagents and conditions: i) Et_3N, IC^2H_3, Et_2O, 56%.

3.3 Biosyntheses of phytoalexins and glucosinolates

Most phytoalexins (Pedras et al., 2003b; 2007b) and glucosinolates were shown to derive from *L*-tryptophan (**78**) (Josefsson, 1972; Kutáček and Králová, 1972; Mikkelsen et al., 2002; Rausch et al., 1983). A number of new phytoalexins with diverse chemical structures have been recently isolated from crucifers (Pedras et al., 2007b; 2007c). Rutabaga tubers, for example, were shown to produce a variety of previously unknown phytoalexins (Pedras et al., 2004), as well as three indolyl glucosinolates, glucobrassicin (**70**), 4-methoxyglucobrassicin (**156**) and neoglucobrassicin (**199**) (Pedras and Montaut., 2004). Rutabaga tubers therefore, provided a good tissue for biosynthetic studies of phytoalexins and glucosinolates, and to determine the biosynthetic precursors common to these metabolites. To date, dog mustard (*Erucastrum gallicum*) is the only plant known to produce erucalexin (**38**), the first and only phytoalexin known so far to possess a carbon substitution at C-2 of the indolyl group (Pedras et al., 2006a). Deuterium labeling of potential precursors was chosen since small amounts of deuterated metabolites can be detected unambiguously by mass spectrometry (ESI-HRMS or APCI-HRMS or EI). The majority of crucifer phytoalexins can be detected by HPLC-MS-ESI in crude extracts without sample purification (Pedras et al., 2006c). HPLC-HRMS-ESI and EI analyses were therefore carried out to determine the levels of isotope (^2H and ^{34}S) incorporation into various phytoalexins and glucosinolates. In addition, non-isotopically

labeled compounds containing non-natural groups such as methyl, acetyl, and Boc groups were also used in biosynthetic investigations. The resulting metabolites (from feeding non-isotopically labeled compounds) were identified by comparing their UV spectra, retention time and fragmentation patterns from HPLC-MS-ESI analyses with those of authentic standards.

The phytoalexins produced by rutabaga, cyclobrassinin (**28a**), rutalexin (**33a**), spirobrassinin (**34b**), brassicanate A (**43a**), and rapalexin A (**53a**) incorporated *L*-[2',4',5',6',7'-$^{2}H_{5}$]tryptophan (**78b**) in different amounts (established by HPLC-HRMS-ESI). Rutalexin (**33**), previously shown to derive from cyclobrassinin (**28**) in rutabaga root tissues showed the most efficient incorporation of **78b**. Other biosynthetic experiment showed a 99% incorporation of [SC$^{2}H_{3}$]brassicanal A (**39b**) into brassicanate A (**43b**), suggesting that **39** could be the last precursor in the biosynthetic pathway of **43**. Of the three indolyl glucosinolates, glucobrassicin (**70b**) showed the most efficient incorporation of *L*-[2',4',5',6',7'-$^{2}H_{5}$]tryptophan (**78b**), followed by neoglucobrassicin (**199a**), and 4-methoxyglucobrassicin (**156a**). The difference in incorporation may result from additional intermediates (steps involve oxidation and methylation at C-4 and N-1) leading to 4-methoxyglucobrassicin and neoglucobrassicin, respectively.

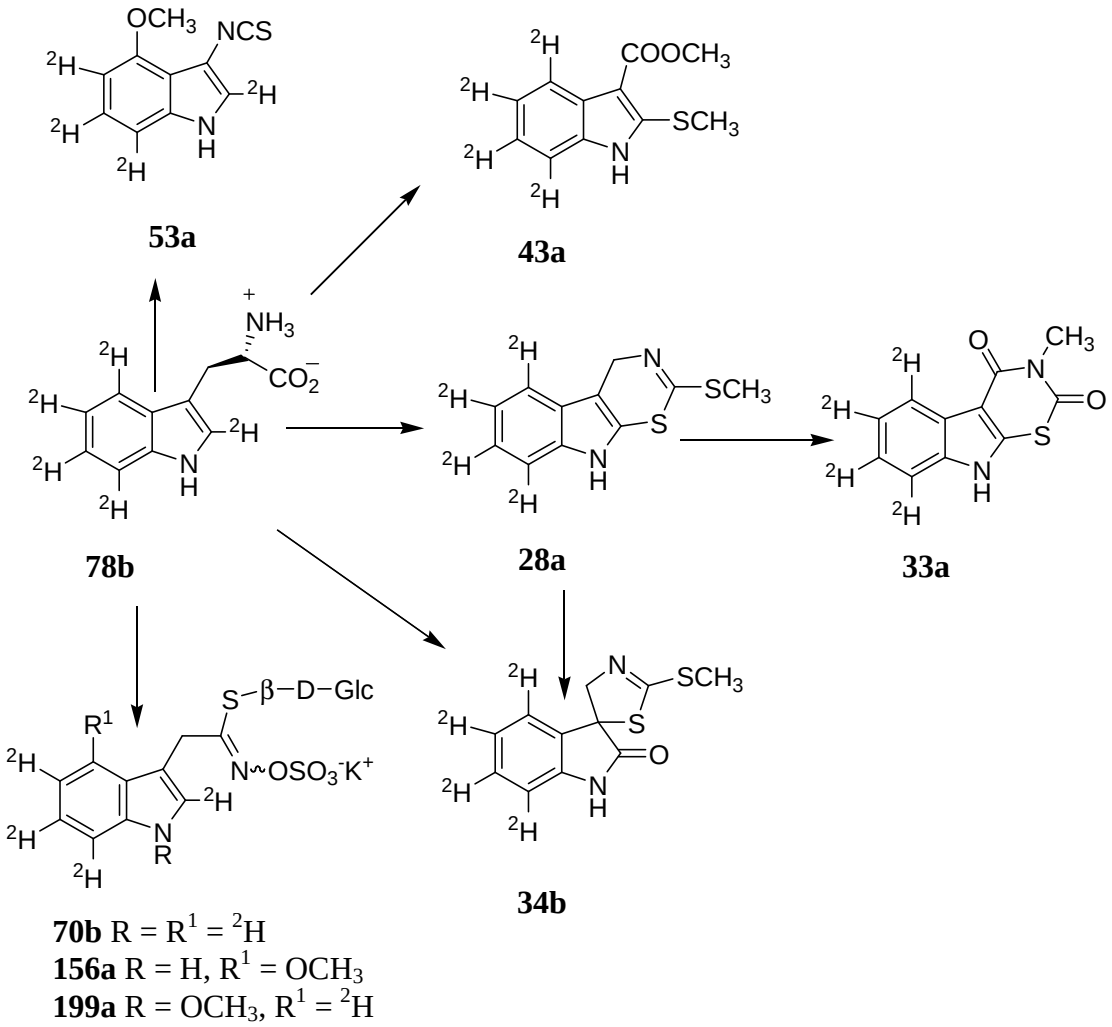

Figure 3.2 Incorporation of *L*-[$^2H_5$]tryptophan (**78b**) into rutabaga phytoalexins and glucosinolates, and cyclobrassinin (**28a**) into spirobrassinin (**34b**).

Previously, absence of incorporation of cyclobrassinin (**28**) into spirobrassinin (**34**) led to a conclusion that **28** is not a biosynthetic precursor of **34** (Monde et al., 1994). On the contrary, the present biosynthetic experiments showed incorporation of cyclobrassinin (**28**) into spirobrassinin (**34**) on incubation with either rutabaga or turnip root slices. Spirobrassinin was not detected in rutabaga after 24 hour incubation, but deuterium incorporation after 48- and 72-hour incubation was 7 and 4%, respectively. In turnip root slices, cyclobrassinin incorporation for 24-, 48- and 72-hour incubation was 10, 15, and 6%, respectively. The incorporation levels in both tissues decreased after 72-hour incubation, perhaps due to dilution with natural abundant spirobrassinin. These results suggested that cyclobrassinin is an intermediate in the biosynthetic pathway of

spirobrassinin, albeit with low incorporation levels compared to brassinin (Pedras et al., 2004). The low incorporation levels of cyclobrassinin may imply that this biosynthetic pathway operates in parallel with direct oxidation of brassinin to spirobrassinin, which is the most favored pathway. Rutabaga and turnip tubers metabolize cyclobrassinin to unidentified products. This metabolism possibly depletes the cyclobrassinin available for the spirobrassinin biosynthesis.

Incubation of rutabaga root slices with 1-methyl-*L*-tryptophan (**200**) under various feeding conditions did not produce detectable amounts of 1-methylated metabolites; neither was **200** recovered from the extracts. Perhaps 1-methyl-*L*-tryptophan (**200**) is metabolized into several polar metabolites.

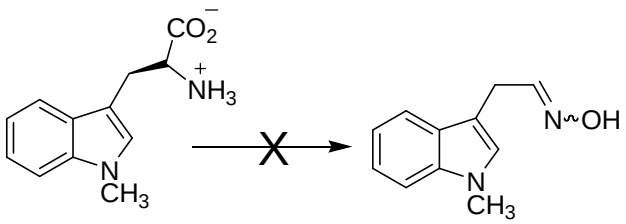

200 **170**

Figure 3.3 Lack of metabolism of 1-methyl-*L*-tryptophan (**200**) into rutabaga phytoalexins and glucosinolates

Although indolyl-3-acetaldoxime (**112**) and 1-methoxyindolyl-3-acetaldoxime (**116**) show incorporation into indolyl phytoalexins and glucosinolates (Pedras et al., 2007b), **112** and **116** have not been detected in any plant tissues, and 1-methoxyindolyl-3-acetaldoxime is not as stable as indolyl-3-acetaldoxime (Pedras and Montaut, 2004). In the biosynthetic experiments using dog mustard (*Erucastrum gallicum*), the incorporation of [4',5',6',7'-$^{2}H_4$]indolyl-3-acetaldoxime (**112a**) into arvelexin (**51a**, **Figure 3.4**) suggested oxidation and methylation at C-4 of **112** to give 4-methoxyindolyl-3-acetaldoxime. These results suggest that possibly 4-methoxy-containing phytoalexins are derived from 4-methoxyindolyl-3-acetaldoxime. The natural occurrence of 4-methoxyindolyl-3-acetaldoxime is not known; it has neither been isolated nor identified from any plant tissue. In this thesis, the biosynthesis of a 4-methoxy-containing phytoalexin from indoyl-3-acetaldoxime is being reported for the

first time. The efficient incorporation of [4',5',6',7'-$^2H_4$]indolyl-3-acetaldoxime (**112a**) into [4',5',6',7'-$^2H_4$]indolyl-3-acetonitrile (**49a**, 89%) suggested that **112** is an immediate precursor in the biosynthetic pathway of **49**.

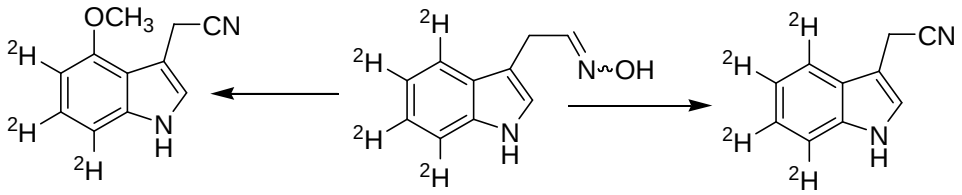

51a **112a** **49a**

Figure 3.4 Incorporation of [$^2H_4$]indolyl-3-acetaldoxime (**112a**) into [$^2H_3$]arvelexin (**51a**) and [$^2H_4$]indolyl-3-acetonitrile (**49a**).

Other biosynthetic experiments using dog mustard showed that the indolyl and 1-methoxy groups of erucalexin (**38**) and 1-methoxyspirobrassinin (**35**) are derived from indolyl-3-acetaldoxime (**112**) and 1-methoxyindolyl-3-acetaldoxime (**116**). The HPLC-HRMS-ESI data indicated incorporation of [4',5',6',7'-$^2H_4$]indolyl-3-acetaldoxime (**112a**) into 1-methoxyspirobrassinin (**35a**, 46 ± 6 %) and erucalexin (**38a**, 15 ± 3 %) (**Figure 3.5**). 1-Methoxyindolyl-3-acetaldoxime (**116**) is a more advanced precursor than indolyl-3-acetaldoxime (**112**) and was therefore expected to exhibit higher incorporation levels since it is closer to erucalexin and 1-methoxyspirobrassinin in the biosynthetic pathway. Contrary to these expectations, [1",1",1"-$^2H_3$]1-methoxyindolyl-3-acetaldoxime (**116a**) incorporation into 1-methoxyspirobrassinin (**35b**) and erucalexin (**38b**) were 7 ± 3 % and 5 ± 3, respectively. Additional experiments employing [4',5',6',7'-$^2H_4$]1-methoxyindolyl-3-acetaldoxime (**116b**) indicated 7 ± 2 and 6 ± 4 % incorporations into 1-methoxyspirobrassinin (**35a**) and erucalexin (**38a**), respectively (**Figure 3.5**). These incorporation levels were still lower that those of [4',5',6',7'-$^2H_4$]indolyl-3-acetaldoxime (**112a**). In order to confirm if the low incorporation of **116** into erucalexin and 1-methoxyspirobrassinin was due to loss of the 1-methoxy groups from **116a** and **116b**, [1",1",1",4',5',6',7'-$^2H_7$]1-methoxyindolyl-3-acetaldoxime (**116c**) was used in the next biosynthetic experiments. It was expected that loss of 1-methoxy group from **116c** would result in metabolites containing four and seven deuterium. HPLC-HRMS-ESI data

however indicated intact incorporation of [1",1",1",4',5',6',7'-$^{2}H_{7}$]1-methoxyindolyl-3-acetaldoxime into 1-methoxyspirobrassinin (**35c**, 4 ± 3 %) and erucalexin (**38c**, 3 ± 2 %) since only $[M + 7]^{+/-}$ peak was detected. These results suggested that the low levels of incorporation of 1-methoxyindolyl-3-acetaldoxime were not due to loss of 1-methoxy group, but likely due to its decomposition since it is not as nearly as stable as indolyl-3-acetaldoxime. Even though low incorporation levels were recorded, 1-methoxyindolyl-3-acetaldoxime appears to be an intermediate in the biosynthetic pathway of both erucalexin and 1-methoxyspirobrassinin. Thus, oxidation and biological methylation of indolyl-3-acetaldoxime gives 1-methoxyindolyl-3-acetaldoxime, which is the biosynthetic precursor of 1-methoxy-containing metabolites (**Figure 3.5**, Pedras et al., 2007b).

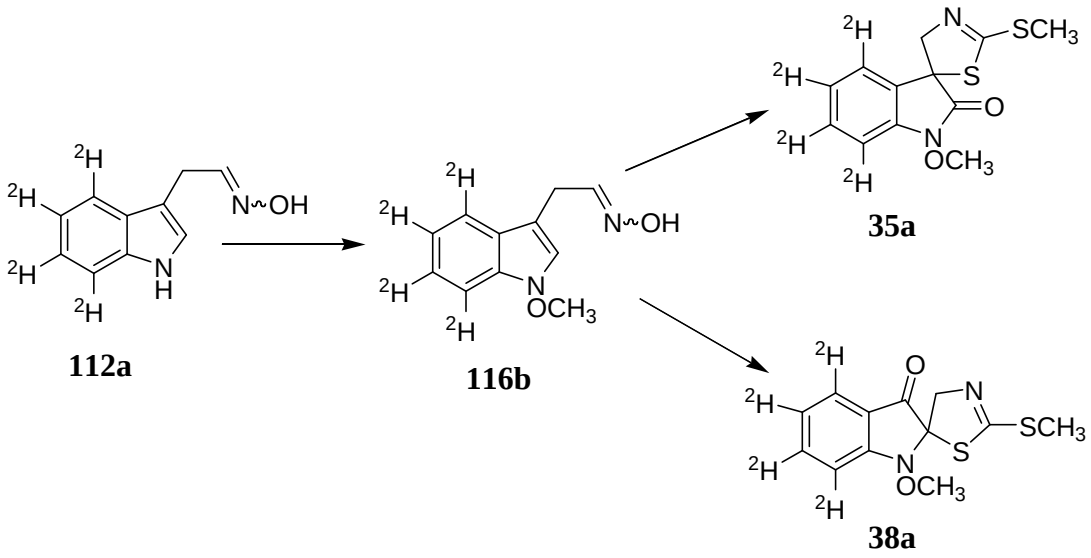

Figure 3.5 Incorporation of [$^{2}H_{4}$]indolyl-3-acetaldoxime (**112a**) and [$^{2}H_{4}$]1-methoxyindolyl-3-acetaldoxime (**116b**) into [$^{2}H_{4}$]1-methoxyspirobrassinin (**35a**) and [$^{2}H_{4}$]erucalexin (**38a**).

In rutabaga and turnip tissues, 1-methylindolyl-3-acetaldoxime (**170**) was not incorporated into phytoalexins, but was metabolized into 1-methylglucobrassicin (**201**, **Figure 3.6**). In other biosynthetic experiments using rutabaga tissues, [1",1",1"-$^{2}H_{3}$]1-methoxyindolyl-3-acetaldoxime (**116a**) was incorporated into neoglucobrassicin (**199b**, **Figure 3.6**).

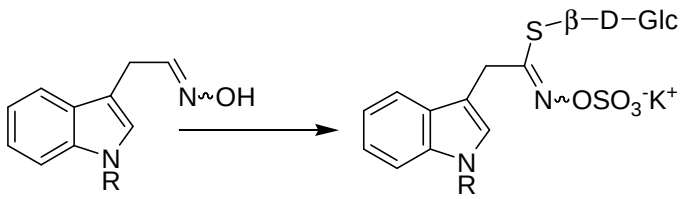

170 R = CH_3 **201** R = CH_3
116 R = OCH_3 **199** R = OCH_3

Figure 3.6 Metabolism of 1-methylindolyl-3-acetaldoxime (**170**) and [$^2H_3$]1-methoxyindolyl-3-acetaldoxime (**116**) in rutabaga root slices.

Indolyl-3-acetothioihydroxamic acid (**174**) is one of the plausible biosynthetic precursors between indolyl-3-acetaldoxime (**112**) and brassinin (**16**). [4',5',6',7'-$^2H_4$]Indolyl-3-[^{34}S]acetothiohydroxamic acid (**174a**) was synthesized for the first time and was incubated with rutabaga root slices. The HPLC-HRMS-ESI data indicated that the phytoalexins cyclobrassinin (**28c**, 5%) and spirobrassinin (**34c**, 8%), as well as the glucosinolate glucobrassicin (**70c**, 2 ± 1 %), incorporated **174a** intact since only [M + 6]$^{+/-}$ peak was detected (**Figure 3.7**). The other phytoalexins rutalexin (**33a**, 11 ± 2 %) and brassicanate A (**43a**, 3%) incorporated only four deuterium from the indolyl group since only the [M + 4]$^{+/-}$ peak was detected (**Figure 3.7**). Since rutalexin (**33**) is biosynthesized from cyclobrassinin (**28**), lack of intact incorporation of **174a** suggested that rutalexin does not derive directly from cyclobrassinin, but through an unidentified intermediate, hence the resulting exchange of sulfur-34. The HPLC-HRMS-ESI analyses of rapalexin A showed incorporation of [M + 2]$^{+/-}$ (**53d**, 57 ± 10 %), [M + 3]$^{+/-}$ (**53b**, 14 ± 9 %), and [M + 5]$^{+/-}$ (**53c**, 4 ± 3 %) ions. The peaks [M + 2]$^{+/-}$, [M + 3]$^{+/-}$, and [M + 5]$^{+/-}$ indicated incorporation of sulfur-34, three deuterium, and sulfur-34 and three deuterium, respectively (**Figure 3.7**). The sulfur-34 incorporated into **53c** and **53d** could possibly be resulting from enzyme-catalyzed exchange of rapalexin A (**53**) S with ^{34}S extruded from decomposed [4',5',6',7'-$^2H_4$]indolyl-3-[^{34}S]acetothiohydroxamic acid. Since rapalexin A consists of 4-methoxyindole that is directly attached to an isothiocyanate, the incorporation of [4',5',6',7'-$^2H_4$]indolyl-3-[^{34}S]acetothiohydroxamic acid (**174a**) into **53b** and **53c** (**Figure 3.7**) suggested a degradation of the

acetothiohydroxamic side chain of **174a** to possibly yield [4',5',6',7'-$^{2}H_4$]indole. Oxidation and methylation at C-4 gives 4-methoxyindole, the plausible biosynthetic precursor of rapalexin A (**53b** and **53c**, **Figure 3.7**). In the case of glucosinolates, the intact incorporation of [4',5',6',7'-$^{2}H_4$]indolyl-3-[^{34}S]acetothiohydroxamic acid (**174a**) into glucobrassicin (**70c**, 2 ± 1%), and its lack of incorporation into 4-methoxyglucobrassicin (**156**) and neoglucobrassicin (**199**) suggested that **174** is not a biosynthetic precursor of **156** and **199**. Overall, these results suggested that the N-1 and C-4 methoxy groups are introduced before formation of indolyl-3-acetothiohydroxamic acid. Previous biosynthetic studies showed 1-methoxyindolyl-3-acetaldoxime (**116**) to be the first 1-methoxy-containing intermediate between indolyl-3-acetaldoxime (**112**) and 1-methoxybrassinin (**18**). In the present biosynthetic studies, indolyl-3-acetaldoxime (**112**) was incorporated into arvelexin (**51**) whereas 1-methoxyindolyl-3-acetaldoxime (**116**) was incorporated into neoglucobrassicin (**199**). These results showed that oxidation and methylation (N-1 and C-4) occurred at the indolyl-3-acetaldoxime stage, and that 1-methoxyindolyl-3-acetaldoxime and 4-methoxyindolyl-3-acetaldoxime are the first methoxy-containing intermediates in the biosynthesis of 1- or 4-methoxy-containing phytoalexins and glucosinolate.

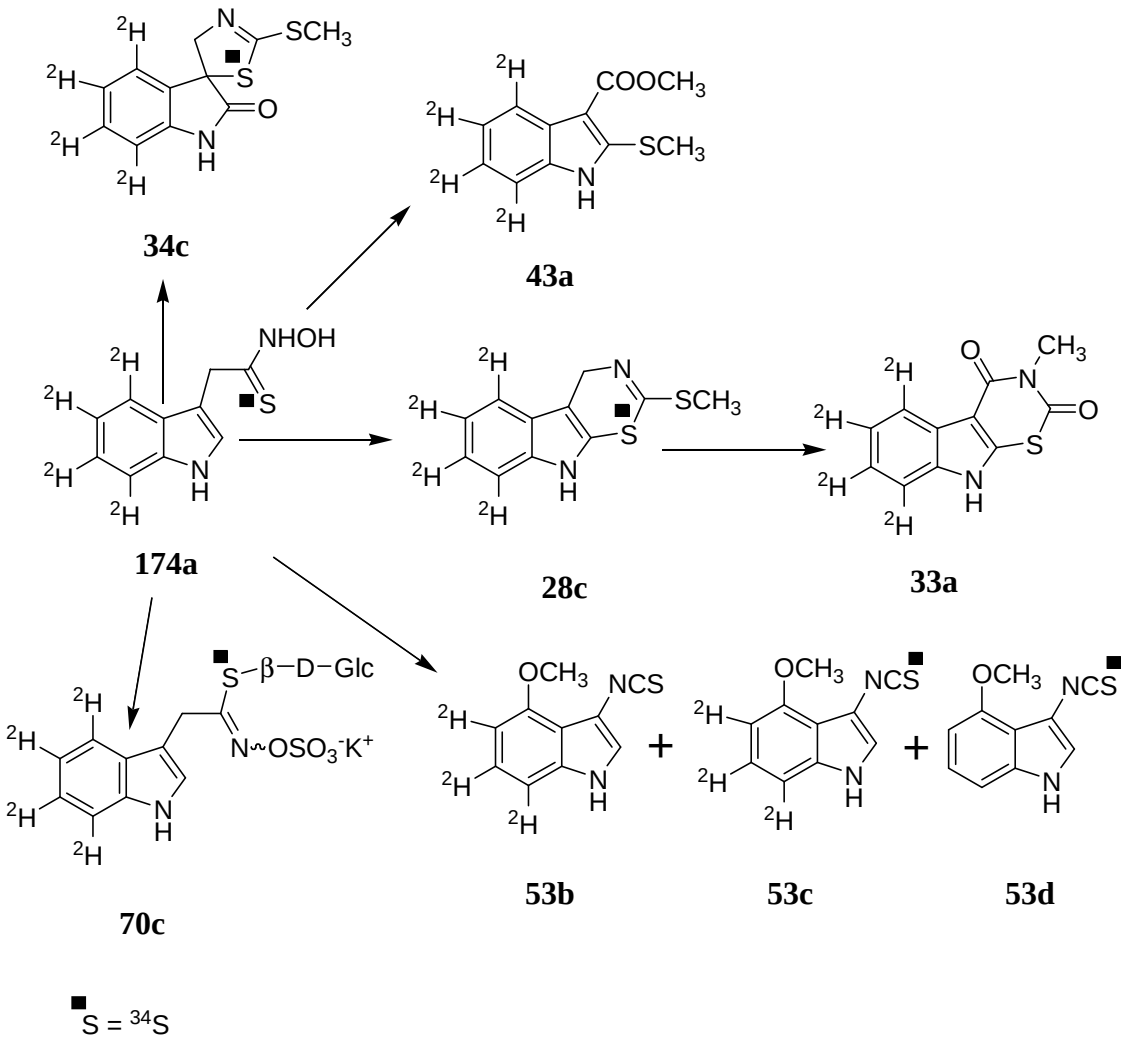

Figure 3.7 Incorporation of [$^{2}H_4$]indolyl-3-[^{34}S]acetothiohydroxamic acid (**174a**) into rutabaga phytoalexins and into glucobrassicin (**70c**).

The metabolism of 1-methylindolyl-3-acetothiohydroxamic acid (**178**) into 1-methylglucobrassicin (**201**, **Figure 3.8**) in rutabaga root slices indicated that 1-methoxy containing metabolites such as neoglucobrassicin (**199**) must then be deriving from 1-methoxyindolyl-3-acetothiohydroxamic acid. The metabolism of 1-methylindolyl-3-acetaldoxime (**170**) (**Figure 3.6**) and 1-methylindolyl-3-acetothiohydroxamic acid (**178**) (**Figure 3.12**) into 1-methylglucobrassicin (**201**) and not into phytoalexins produced by turnip and rutabaga tissues suggested that the post-aldoxime enzymes in the biosynthetic pathway of indolyl glucosinolates are not substrate-specific compared to those in the biosynthetic pathway of phytoalexins. As described in the Introduction section, many

post-aldoxime enzymes in the biosynthetic pathway of glucosinolates recognize the functional groups but not the side chain (aliphatic, aromatic, indolyl) (Grubb and Abel, 2006; Halkier and Gershenzon, 2006), hence the results obtained with **170** (**Figure 3.6**) and **178** (**Figure 3.8**).

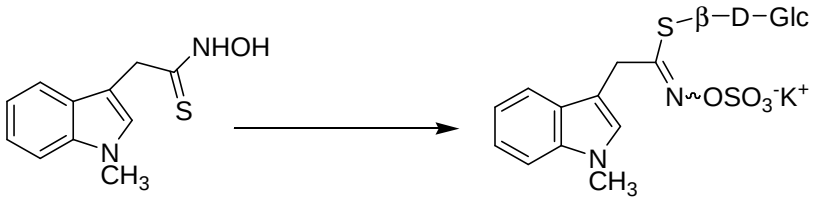

178 **201**

Figure 3.8 Metabolism of 1-methylindolyl-3-acetothiohydroxamic acid (**178**) in rutabaga and turnip root slices.

On standing in the carrier solution, indolyl-3-acetothiohydroxamic acid (**174**) decomposes to indolyl-3-acetonitrile (**49**) with extrusion of sulfur. Since phytoalexins such as rutalexin (**33**) and brassicanate A (**43**) did not incorporate ^{34}S from **174a**, the biogenetic relationship between indolyl-3-acetonitrile with rutabaga phytoalexins was investigated. Incubation of rutabaga root slices with [4',5',6',7'-$^{2}H_4$]indolyl-3-acetonitrile (**49a**) yielded as metabolic products, [4,5,6,7-$^{2}H_4$]indolyl-3-acetic acid (**202a**), [4,5,6,7-$^{2}H_4$]indole-3-carboxylic acid (**203a**), and [4',5',6',7'-$^{2}H_4$]methyl indole-3-carboxylate (**121a**) (**Figure 3.9**). Since the phytoalexins or indole glucosinolates did not show deuterium incorporation from [4',5',6',7'-$^{2}H_4$]indolyl-3-acetonitrile, the previous detected deuterium incorporations were therefore from [4',5',6',7'-$^{2}H_4$]indolyl-3-[^{34}S]acetothiohydroxamic acid (**174a**) or a derivative.

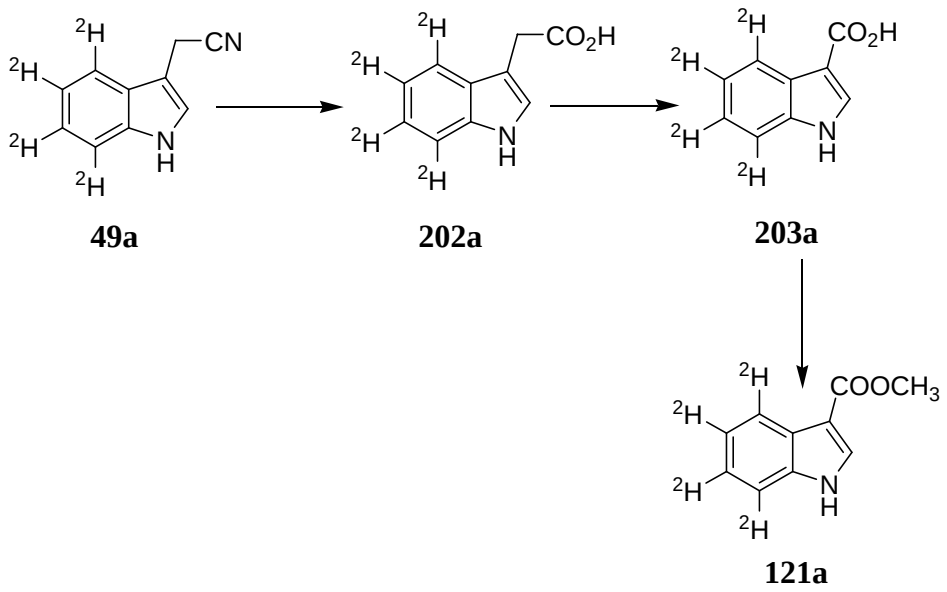

Figure 3.9 Metabolism of [$^2H_4$]indolyl-3-acetonitrile (**49a**) in rutabaga root slices.

The metabolism of 1-(*tert*-butoxycarbonyl)indolyl-3-methylisothiocyanate (**180**) (by rutabaga root slices) to 1-(*tert*-butoxycarbonyl)brassinin (**181**) and 1-(*tert*-butoxycarbonyl)spirobrassinin (**196**), and additional experiments showing metabolism of 1-(*tert*-butoxycarbonyl)brassinin (**181**) to 1-(*tert*-butoxycarbonyl)spirobrassinin (**196**) were consistent with the proposed biosynthetic pathway of indole phytoalexins (Pedras et al., 2003b) (**Figure 3.10**). Similar to **180**, 1-acetylindolyl-3-methylisothiocyanate (**183**) was metabolized to 1-acetylbrassinin (**184**), and not into 1-acetylspirobrassinin (**195**) (**Figure 3.10**). Incubation of either rutabaga or turnip root slices with 1-acetylbrassinin (**184**) for 96 hours did not yield detectable amount of 1-acetylspirobrassinin (**195**) or any 1-acetyl-contanining phytoalexin. Perhaps 1-acetylspirobrassinin (**195**) is readily hydrolyzed in the plant tissue unlike 1-(*tert*-butoxycarbonyl)spirobrassinin (**196**).

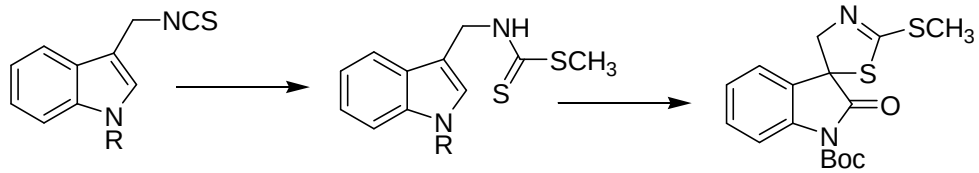

180 R = Boc
183 R = Acetyl

181 R = Boc
184 R = Acetyl

196

Figure 3.10 Metabolism of 1-(*tert*-butoxycarbonyl)indolyl-3-methylisothiocyanate (**181**) and 1-acetylindolyl-3-methylisothiocyanate (**183**) in rutabaga and turnip root tissues.

The biosynthetic pathways of 1-methoxyspirobrassinin (**35**) and erucalexin (**38**) were studied using deuterium labeled 1-methoxybrassinin (**18**) and sinalbin B (**31**) (**Figure 3.11**). The HPLC-HRMS-ESI data indicated incorporation of [3,3,3-$^2H_3$]1-methoxybrassinin (**18a**) into 1-methoxyspirobrassinin (**35d**, 53 ± 2 %) and erucalexin (**38d**, 7 ± 3 %) in detached dog mustard leaves (Pedras et al., 2007b; Pedras and Okinyo, 2006b). Incorporation of [3,3,3-$^2H_3$]1-methoxybrassinin (**18a**) into erucalexin suggested a possible C-3 to C-2 side chain migration in 1-methoxybrassinin to yield 1-methoxyisobrassinin that undergoes spirocyclization to give erucalexin. Additional experiments employing [3,3,3,4',5',6',7'-$^2H_7$]1-methoxybrassinin (**18c**) indicated intact incorporation into 1-methoxyspirobrassinin (**35e**, 64 ± 11 %) and erucalexin (**38e**, 4 ± 2 %) since only $[M + 7]^{+/-}$ peaks were detected from HPLC-HRMS-ESI analyses. These observations supported the proposed side chain migration in the biosynthesis of erucalexin, and also showed that the rearrangement is intramolecular. The occurrence of intramolecular rearrangement was further demonstrated by incorporation of [3,3,3-$^2H_3$]sinalbin B (**31b**) into both 1-methoxyspirobrassinin (**35d**, 10 ± 1 %) and erucalexin (**38d**, 2 ± 0.2 %). Additional biosynthetic experiments with [4',5',6',7'-$^2H_4$]sinalbin B (**31a**) indicated incorporation of four deuterium into both 1-methoxyspirobrassinin (**35a**, 19 ± 7 %) and erucalexin (**38a**, 5 ± 0.1 %) (Pedras et al., 2007b; Pedras and Okinyo, 2006b). Sinalbin B derives from 1-methoxybrassinin and is therefore a closer precursor to erucalexin and 1-methoxyspirobrassinin in the biosynthetic pathway. The incorporation levels of sinalbin B into erucalexin were however closer to those obtained from 1-methoxybrassinin, but much lower in 1-methoxyspirobrassinin. An efficient

incorporation of sinalbin B was expected since it is an advanced precursor in the biosynthetic pathway. The low levels of incorporation of sinalbin B into 1-methoxyspirobrassinin (compared to 1-methoxybrassinin) possibly indicates that sinalbin B is not a direct precursor, but serves as additional pathway to 1-methoxyspirobrassinin, or perhaps sinalbin B is not efficiently taken up by the plant tissues. In chemical stability studies, sinalbin B (**31**) was shown to decompose to undetermined products (Pedras and Zaharia, 2000). In the present biosynthetic studies, the instability of **31** in the precursor solution may have contributed to the low incorporation levels observed in erucalexin (**38**) and 1-methoxyspirobrassinin (**35**).

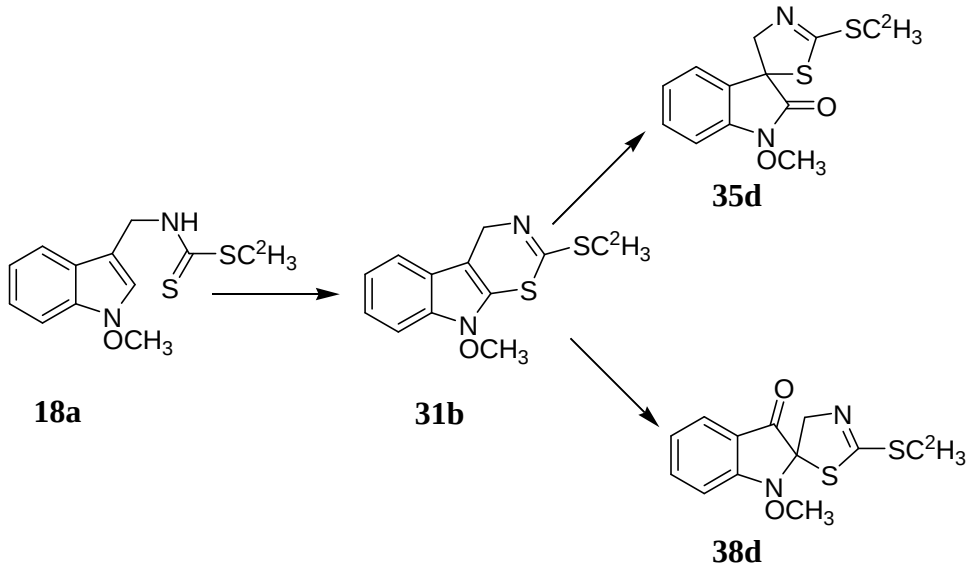

Figure 3.11 Incorporation of [$^2H_3$]1-methoxybrassinin (**18a**) and [$^2H_3$]sinalbin B (**31b**) into 1-methoxyspirobrassinin (**35d**) and erucalexin (**38d**).

Erucalexin yields undetermined products upon standing at room temperature (in CH_3CN) due to its instability. In general, the incorporation levels of most of the precursors administered were higher in 1-methoxyspirobrassinin than in erucalexin. The observed difference could in part be attributed to different rates of transportation of these precursors to different compartments where these metabolites are biosynthesized. On the other hand, biosynthesis of erucalexin involves a molecular rearrangement with concomitant spirocyclization, whereas that of 1-methoxyspirobrassinin goes through a

one step oxidative spirocyclization. Possibly the additional step(s) in the biosynthetic pathway(s) of erucalexin may be contributing to pool dilution with the natural abundance. More so, production of erucalexin is about 4-5 times that of 1-methoxyspirobrassinin, this further suggests pool dilution in the biosynthetic pathway of erucalexin with a resultant low level of incorporation.

[3,3,3,4',5',6',7'-$^{2}H_{7}$]1-Methoxybrassinin (**18c**) was efficiently incorporated into [3,3,3,4',5',6',7'-$^{2}H_{7}$]1-methoxybrassitin (**20a**, 99.6%) suggesting that **18** could be the immediate precursor (**Figure 3.12**). Caulilexin B (**48**) was detected in extracts of dog mustard leaves incubated with 1-methoxybrassinin. The EI data indicated deuterium composition of [4',5',6',7'-$^{2}H_{4}$]caulilexin B (**48a**) to be ≥ 99.9% suggesting that the indolyl ring was solely derived from [3,3,3,4',5',6',7'-$^{2}H_{7}$]1-methoxybrassinin (**18c**, **Figure 3.12**). It, however, remains to be established whether caulilexin B (**48**) is directly derived from 1-methoxybrassinin (**18**), or through 1-methoxybrassitin (**20**). Although caulilexin B was not detected in extracts not fed 1-methoxybrassinin, it appears that the enzyme(s) involved in its biosynthesis are expressed in the presence of this precursor.

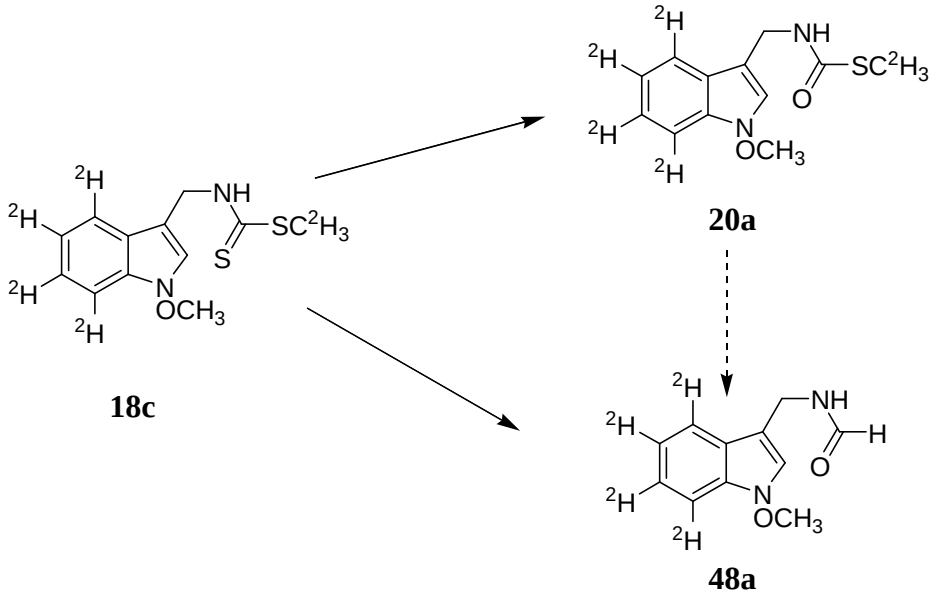

Figure 3.12 Incorporation of [$^{2}H_{7}$]1-methoxybrassinin (**18c**) into [$^{2}H_{7}$]1-methoxybrassitin (**20a**) and [$^{2}H_{4}$]caulilexin B (**48a**). Dashed arrow shows proposed biosynthetic pathway.

3.4 Conclusion

The incorporation of *L*-[2',4',5',6',7'-$^{2}H_5$]tryptophan (**78b**) into the phytoalexins cyclobrassinin (**28a**), rutalexin (**33a**), spirobrassinin (**34b**), brassicanate A (**43a**), and rapalexin A (**53a**), as well as glucosinolates, glucobrassicin (**70b**), 4-methoxyglucobrassicin (**156a**) and neoglucobrassicin (**199a**) show that the indolyl moiety of these metabolites derives from *L*-tryptophan (**78**) (Pedras et al., 2007b).

The incorporation of [4',5',6',7'-$^{2}H_4$]indolyl-3-acetaldoxime (**112a**) and perdeuterated 1-methoxyindolyl-3-acetaldoximes into 1-methoxyspirobrassin (**35**) and erucalexin (**38**) was consistent with previous studies (Pedras et al., 2004). These observations suggested oxidation and methylation of indolyl-3-acetaldoxime to gives 1-methoxyindolyl-3-acetaldoximes in the biosynthesis of 1-methoxybrassinin (Pedras et al., 2004), the advanced precursor of 1-methoxy-containing phytoalexins such as 1-methoxyspirobrassin (**35**) and erucalexin (**38**) (Pedras and Okinyo, 2006b). 1-Methoxyindolyl-3-acetaldoxime (**116**) is a biosynthetic precursor of 1-methoxy-containing phytoalexins (Pedras et al., 2007b) as well as indolyl glucosinolate neoglucobrassicin (**199**). The metabolism of 1-methylindolyl-3-acetaldoxime (**170**) and 1-methylindolyl-3-acetothiohydroxamic acid (**178**) into 1-methylglucobrassicin (**201**) and not into indolyl phytoalexins suggested that the enzymes in the biosynthetic pathway of indolyl glucosinolates are specific to the functional groups, but not the indolyl side chain, unlike enzymes in the biosynthetic pathway of phytoalexins. Incorporation of [4',5',6',7'-$^{2}H_4$]indolyl-3-acetaldoxime (**112a**) into arvelexin (**51**) indicated oxidation and methylation of C-4 of indolyl-3-acetaldoxime, and that 4-methoxy-containing phytoalexins and 4-methoxyglucobrassicin could be derived from 4-methoxyindolyl-3-acetaldoxime. Indolyl-3-acetaldoxime (**112**) is a biogenetic precursor of indolyl-3-acetonitrile (**49**), but **49** is not a precursor of phytoalexins produced by rutabaga.

The intact incorporation of [4',5',6',7'-$^{2}H_4$]indolyl-3-[^{34}S]acetothiohydroxamic acid (**174a**) into phytoalexins cyclobrassinin (**28c**) and spirobrassinin (**34c**), and glucosinolate glucobrassicin (**70c**) suggested that **174a** could be the last common intermediate between brassinin and glucobrassicin (Pedras and Okinyo, 2008). Lack of incorporation of **174a** into 4-methoxyglucobrassicin (**156**) and neoglucobrassicin (**199**) indicated that oxidation and methylation occurs before the formation of indolyl-3-acetothiohydroxamic acid.

The metabolism of 1-(*tert*-butoxycarbonyl)indolyl-3-methylisothiocyanate (**180**) by rutabaga root slices into 1-(*tert*-butoxycarbonyl)brassinin (**181**) and 1-(*tert*-butoxycarbonyl)spirobrassinin (**196**) was consistent with the previously proposed biosynthetic pathway (Pedras et al., 2003b). The metabolism of 1-acetylindolyl-3-methylisothiocyanate (**183**) into 1-acetylbrassinin (**184**) in both rutabaga and turnip root slices supported the previous results from metabolism of **180**.

The incorporation of cyclobrassinin (**28a**) into spirobrassinin (**34b**) was shown in rutabaga and turnip root slices. Although the levels of incorporation were much lower than those of brassinin (**16**) (Monde et al., 1994; Pedras et al., 2004), this pathway appears to contribute to the biosynthesis of spirobrassinin contrary to earlier reports (Monde et al., 1994). In addition, similar to the biogenetic relationship of NH-containing phytoalexins (cyclobrassinin and spirobrassinin), sinalbin B (**31**) incorporation into 1-methoxyspirobrassinin (**35**) was much lower than that of 1-methoxybrassinin (**18**) (Pedras and Okinyo, 2006b). Intact incorporation of [3,3,3,4',5',6',7'-$^{2}H_{7}$]1-methoxybrassinin (**18c**) into erucalexin (**38e**) suggested an intramolecular rearrangement. Caulilexin B (**48**) appeared to be derived from 1-methoxybrassinin (**18**), although its biosynthesis from 1-methoxybrassitin (**20**) is a likely pathway.

A map of the biosynthetic pathways studied in this thesis is shown in **Figure 3.13**. *L*-tryptophan (**78**) is transformed to indolyl-3-acetaldoxime (**112**). Dehydration of **112** gives indolyl-3-acetonitrile (**49**), whereas oxidation and methylation at C-4 followed by dehydration gives arvelexin (**51**). Oxidation of indolyl-3-acetaldoxime (**112**), conjugation with cysteine, followed by *C-S* lyase catalyzed hydrolysis of the *C-S* bond yields indolyl-3-acetothiohydroxamic acid (**174**) (Halkier and Gershenzon, 2006; Pedras and Okinyo, 2008), possibly the last common intermediate between brassinin (**16**) and glucobrassicin (**70**) (Pedras and Okinyo, 2008). Lossen-type rearrangement of **174** would give indolyl-3-methylisothiocyanate (**123**) that is thiomethylated to yield brassinin (**16**) (Pedras and Okinyo, 2008), the precursor of many other NH-containing indolyl phytoalexins (Pedras et al., 2007b). In the present biosynthetic studies, indolyl-3-acetothiohydroxamic acid (**174**) was incorporated into the phytoalexins cyclobrassinin (**28**), spirobrassinin (**34**), rutalexin (**33**) and brassicanate A (**43**) (Pedras and Okinyo,

2008), all previously shown to derive from brassinin (**16**) (Pedras et al., 2004), as well as the new phytoalexin rapalexin A (**53**).

The 1-methoxy-containing phytoalexins **20**, **31**, **35**, **38**, and **48** are derived from 1-methoxybrassinin (**18**), their biosynthesis from 1-methoxyindolyl-3-acetaldoxime (**116**) possibly follows a similar pathway as that of NH-containing phytoalexins. 1-Methoxyspirobrassinin (**35**) and erucalexin (**38**) were also shown to be biosynthesized from sinalbin B (**31**) (Pedras and Okinyo, 2006b).

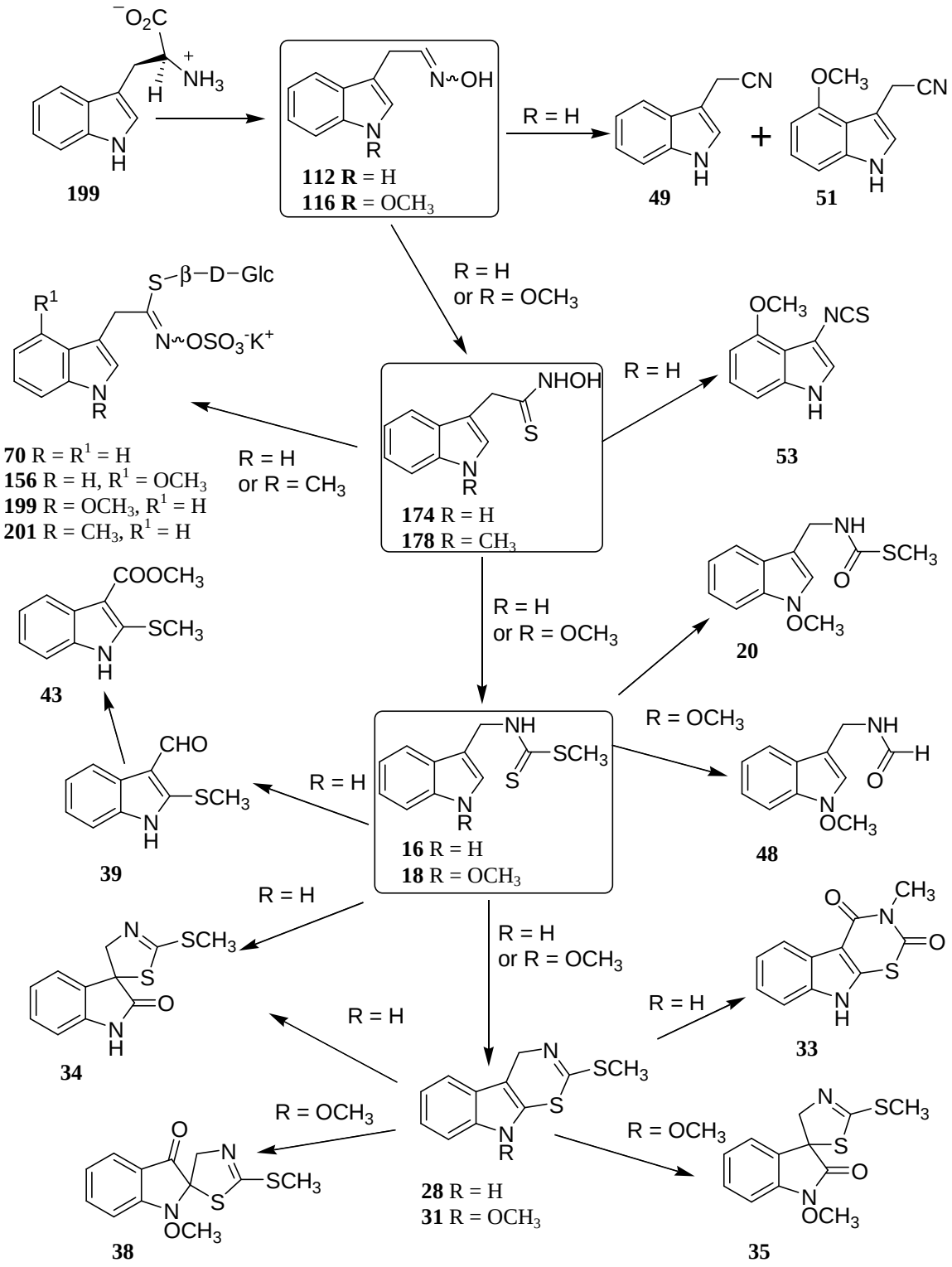

Figure 3.13 Map of biosynthetic pathway of crucifer phytoalexins and glucosinolates **70**, **156**, **199**, and **201**.

CHAPTER 4

4. Experimental

4.1 General

All chemicals were purchased from Sigma-Aldrich Canada Ltd., Oakville, ON, except for isotope-labeled compounds that were purchased from Cambridge Isotope Laboratories Inc., Andover, MA, and C/D/N Isotopes Inc., Pointe-Claire, Quebec. All solvents were HPLC grade and were used as such, except chloroform and dichloromethane that were redistilled. The solvents used in the syntheses were dried and freshly distilled before use. The following drying agents were used: DMF over molecular sieves, Et_2O and THF over Na/benzophenone, and CH_2Cl_2 over CaH_2.

Analytical TLC was performed on precoated silica gel TLC plates (Merck, Kieselgel 60 F_{254}, 5 × 2 cm × 0.2 mm layer thickness) aluminum sheets. The compounds were eluted with suitable solvent systems, then visualized under UV light (254/366 nm), and by dipping the plates in a 5% (w/v) aqueous phosphomolybdic acid solution containing 1% (w/v) cerium(IV) sulfate and 4% (v/v) H_2SO_4, followed by heating at 200 ^oC.

PTLC was performed on precoated silica gel, (Merck, Kieselgel 60 F_{254}, 20 × 20 cm × 0.25 mm thickness). The compounds were eluted with suitable solvent systems (v/v), then visualized under UV light (254/366 nm).

FCC was performed on silica gel, Merck grade 60, mesh size 230-400, 60 Å or on J. T. Baker reversed phase C-18 silica gel, 40 µm, 275 Å.

HPLC analysis was carried out with an Agilent 1100 series or Hewlett Packard HPLC systems equipped with quaternary pump, autosampler and diode array detector (wavelength range 190-600 nm), degasser and a Hypersil octadecylsilane (ODS) column

(5 µm particle size silica, 200 × 4.6 mm I.D.), equipped with an in-line filter. The mobile phase consisted; Method A: linear gradient of water-acetonitrile (75:25 to 25:75 in 35 min, to 0:100 in 5 min) and a flow rate of 1 mL/min; Method B: linear gradient of water-acetonitrile (100:0 to 50:50 in 25 min, to 100:0 in 5 min) and a flow rate of 1 mL/min. Samples were dissolved in acetonitrile for Method A, and in methanol-water (50:50) for Method B.

HPLC-MS-ESI analysis was carried out with an Agilent 1100 series HPLC system equipped with an autosampler, binary pump, degasser, and a diode array detector connected directly to a mass detector (Agilent G2440A MSD-Trap-XCT ion trap mass spectrometer) with an ESI source. Chromatographic separation was carried out at room temperature using an Eclipse XSB C-18 column (5 µm particle size silica, 150 × 4.6 mm I.D.). The mobile phase consisted of a linear gradient of; Method A: 0.2% formic acid in water and 0.2% formic acid in acetonitrile (75:25 to 25:75 in 35 min, to 0:100 in 5 min) and a flow rate of 1 mL/min; Method B: 0.2% formic acid in water and 0.2% formic acid in acetonitrile (90:10 to 50:50 in 25 min, to 90:10 in 5 min) and a flow rate of 1 mL/min. Data acquisition was carried out in positive and negative polarity modes in a single LC run. Data processing was carried out by Agilent Chemstation Software. Samples were dissolved in acetonitrile for Method A, and in methanol-water (50:50) for Method B.

HPLC-HRMS-ESI was performed on an Agilent HPLC 1100 series directly connected to QSTAR XL Systems Mass Spectrometer (Hybrid Quadrupole-TOF LC/MS/MS) with turbo spray ESI source. Chromatographic separation was carried out at room temperature using a Hypersil ODS C-18 column (5 µm particle size silica, 200 × 2.1 mm I.D.) or a Hypersil ODS C-18 column (5 µm particle size silica, 100 × 2.1 mm I.D.). The mobile phase consisted of a linear gradient of; Method A: 0.1% formic acid in water and 0.1% formic acid in acetonitrile (75:25 to 25:75 in 35 min, to 0:100 in 5 min) and a flow rate of 0.25 mL/min; Method B: 0.1% formic acid in water and 0.1% formic acid in acetonitrile (97:3 to 50:50 in 25 min, to 97:3 in 10 min) and a flow rate of 0.25 mL/min. Data acquisition was carried out in either positive or negative polarity mode per LC run. Data processing was carried out by Analyst QS Software. Samples were dissolved in acetonitrile for Method A and in methanol-water (50:50) for Method B.

GC analysis was performed on a Varian CP-3800 GC equipped with a split (30:1) capillary autosampler, 30 m × 0.25 mm (I.D.) VF-5ms (front) and VF-17ms (back) (0.25 µm film thickness) capillary columns and FID. The carrier gas was helium at a flow rate of 1 mL/min. The temperature program comprised of an initial temperature of 80 ºC (2 min) to 300 ºC at 10 ºC/min and a hold at this temperature for 5 min.

GC-MS analysis was performed on a Fisons GC 8000 series model 8060 equipped with a split (30:1) capillary injector directly connected to a VG 70 SE Mass Spectrometer. The MS was operated in the EI mode at 70 eV and a trap current of 100 µA. The source temperature was held at 200 ºC and the multiplier voltage at 250 V. The mass range was set at 25 – 350. The GC-MS column used was DB-5ms, 30 m × 0.20 mm (I.D.) and 0.25 µm film thickness. The carrier gas was helium at a flow rate of 1 mL/min. The temperature program involved initial temperature of 40 ºC (5 min) to 200 ºC at 10 ºC/min and a hold at this temperature for 15 min.

NMR spectra were recorded on 500 MHZ Bruker Avance spectrometer. For ^{1}H NMR (500 MHz), the chemical shifts (δ) values are reported in parts per million (ppm) relative to the internal standard TMS. The δ values are referenced to $CHCl_3$ in C^2HCl_3 at 7.27 ppm or referenced to CH^2H_2CN in C^2H_3CN at 1.94 ppm. Multiplicities are indicated by the following symbols: s = singlet, d = doublet, dd = doublet of doublets, m = multiplet and br = broad. For ^{13}C NMR (125.8 MHz) the δ values are referenced to C^2HCl_3 (77.23 ppm) or C^2H_3CN (118.69 ppm).

MS [high resolution (HR), electron ionization (EI)] were obtained on a VG 70 SE mass spectrometer employing a solids probe.

Seeds of rocket (*E. sativa*) were purchased from a commercial seed company. Dog mustard (*E. gallicum*) seeds were obtained from Plant Gene Resources, Agriculture and Agric-Food Canada Research Station, Saskatoon, Sk. The seeds were sown in commercial potting soil mixture, and plants were grown in a growth chamber under controlled environmental conditions (22ºC/18ºC, with 16/8 day/night cycle) for 2-5 weeks. Rutabaga and turnip roots were purchased from Sobeys, Preston Avenue, Saskatoon, Sk.

4.2 Analysis of antifungal secondary metabolites from rocket

4.2.1 Time-course analysis

Time course analysis was carried out to determine the production of antifungal metabolites by rocket. Three-week old plants were sprayed with $CuCl_2$ (2×10^{-3} M) solution to the point of run-off. Leaves were excised at 24-hour intervals up to 168 hours (each experiment was carried out in triplicate). Fresh leaf weights were measured and the leaves were frozen in liquid nitrogen, were crushed with a glass rod, and then extracted in EtOAc (30 mL) overnight. The EtOAc extract was filtered off and the solvent was removed under reduced pressure. Non-elicited leaves (control experiment) were similarly treated. The HPLC-UV profiles of extracts from both elicited and control leaves were recorded. Antifungal compounds were visualized by carrying out TLC biodetection with *Cladosporium cucumerinum*.

4.2.2 TLC biodetection

A solution of double strength potato dextrose broth (PDB) was prepared by autoclaving a suspension of PDB (4.8 g) in H_2O (100 mL), and spores of *C. cucumerinum* were added to make a concentration of 1×10^6 spores/mL. Bioassays were conducted following previously established method (Pedras and Sorensen, 1998). Samples were spotted on 2 × 20 cm TLC plate strips (aluminum backing), which were developed using solvent system, EtOAc-hexane (60:40). The developed plates were air dried (60 min), were sprayed with the spore suspension prepared above, and were incubated under high humidity in the dark for 36 h. Control plates were similarly prepared but without spotting leaf extracts. From these experiments, the antifungal areas appeared white (due to inhibition of spore germination) against a dark gray background due to fungal growth. The white spots were not observed in control plates.

4.2.3 Isolation of secondary metabolites from rocket

In order to isolate the antifungal compounds, a large scale experiment was carried out. Elicited rocket leaves from 40 pots (358 g of fresh leaf weight) were divided into three Erlenmeyer flasks, then frozen in liquid nitrogen, crushed with a glass rod, and extracted with hexane (250 mL per flask) overnight. The hexane extract was filtered off and the remaining residue was sequentially extracted with EtOAc and CH_3OH (250 mL per flask), respectively. From TLC biodetection experiments, all the three extracts had similar inhibition spots and were thus combined for purification purposes. The combined crude extracts were purified by FCC (hexane-EtOAc, 80:20 – 0:100, then CH_2Cl_2-CH_3OH, 95:5 v/v). The resulting fractions were analyzed by HPLC-DAD and TLC biodetection. A fraction showing a peak at t_R = 34.7 min on HPLC chromatogram exhibited inhibition of spore germination on TLC plate and was further purified by FCC (hexane-EtOAc, 100:0 - 80:20; then CH_2Cl_2-CH_3OH, 100:0 to 99:1, v/v) to yield bis(4-isothiocyanatobutyl)disulfide (56.9 mg, **167**).

The next fraction that exhibited antifungal activity showed a peak at a t_R = 22.5 min on HPLC-DAD analysis. This fraction was further purified by a combination of FCC (hexane-EtOAc, 100:0 to 90:10, v/v) and PTLC (hexane-EtOAc, 80:20, v/v multiple development) to yield 4-methylthiobutyl isothiocyanate (4.9 mg, **166**).

4.2.4 Chemical characterization of metabolites from rocket

4.2.4.1 4-Methylthiobutyl isothiocyanate (166)

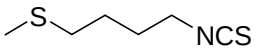

166

Colorless oil.

HPLC-DAD Method A, t_R = 22.5 min.

^{1}H NMR (C^2HCl_3) δ 3.58 (dd, *J* = 6, 6 Hz, 2H), 2.56 (dd, *J* = 7, 7 Hz, 2H), 1.87 (s, 3H), 1.85 (m, 2H), 1.76 (m, 2H).

^{13}C NMR (C^2HCl_3) δ 131.0, 45.1, 33.7, 29.2, 26.2, 15.8.

HR-EIMS *m/z* measured: 161.0331 (161.0333 calcd. for $C_6H_{11}NS_2$).

EIMS *m/z* (% relative abundance); 161 $[M]^+$ (100), 146 (52).

4.2.4.2 Bis(4-isothiocyanatobutyl)disulfide (167)

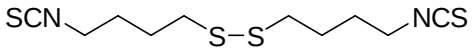

167

Yellowish oil.

HPLC-DAD Method A, t_R = 34.7 min.

^{1}H NMR (C^2HCl_3) δ 3.59 (dd, *J* = 6, 6 Hz, 2H), 2.74 (dd, *J* = 6.5, 6.5 Hz, 2H), 1.85 (m, 4H).

^{13}C NMR (C^2HCl_3) δ 130.9, 45.1, 38.3, 29.0, 26.4.

HR-EIMS *m/z* measured: 292.0196 (292.0196 calcd. for $C_{10}H_{16}N_2S_4$).

EIMS *m/z* (% relative abundance); 292 $[M]^+$ (10), 114 (100), 87 (14), 71 (69), 55 (52).

4.3 Syntheses of compounds

4.3.1 [4',5',6',7'-$^2H_4$]Indolyl-3-acetaldoxime (112a)

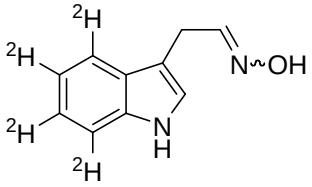

112a

A solution of DIBAH (850 μL, 1.28 mmol) in toluene was added drop wise to a solution of [4',5',6',7'-$^2H_4$]indolyl-3-acetonitrile (**49a**, 100 mg, 0.63 mmol) in dry toluene (8 mL) cooled to -78 °C under an atmosphere of argon. The reaction mixture was allowed to stir at -78 °C for 10 min, was diluted with ice-cold HCl (10 mL, 2 M) and immediately extracted in EtOAc (20 mL × 3) (Miyashita et al., 1997). The combined

organic extract was washed with H_2O (10 mL × 2), was dried over Na_2SO_4, and was concentrated under reduced pressure to yield crude [4',5',6',7'-$^2H_4$]indolyl-3-acetaldehyde, which was used for the next step without purification. A solution of $HONH_2$·HCl (111 mg, 1.60 mmol) and CH_3COONa (131 mg, 1.60 mmol) in H_2O (1 mL) was added to a cooled solution (1 °C) of crude [4',5',6',7'-$^2H_4$]indolyl-3-acetaldehyde in EtOH (8.5 mL). The reaction mixture was allowed to stir at 1 °C for 10 min, and then at r.t. for 15 min. The reaction mixture was concentrated, the residue was taken in H_2O (15 mL), was extracted with EtOAc (15 mL × 4), the combined organic extract was dried over Na_2SO_4 and was concentrated under reduced pressure. Separation by FCC (CH_2Cl_2-CH_3OH, 97:3, v/v) yielded [4',5',6',7'-$^2H_4$]indolyl-3-acetaldoxime (**112a**, 36.8 mg, 33% yield from **49a**). Integration of ^{1}H NMR signals indicated the presence of *syn* and *anti* isomers (1.1:0.9) (Pedras and Okinyo, 2006a).

HPLC-DAD Method A, two peaks at t_R = 11.8 and 12.9 min.
Major isomer: ^{1}H NMR (500 MHz C^{2}H$_3$CN) δ 9.17 (br s, NH), 8.37 (s, OH), 7.49 (dd, *J* = 6, 6 Hz, 1H), 7.12 (d, *J* = 2 Hz, 1H), 3.60 (d, *J* = 6 Hz, 2H).
Minor isomer: ^{1}H NMR (500 MHz C^{2}H$_3$CN) δ 9.17 (br s, NH), 8.85 (s, OH), 7.15 (d, *J* = 1 Hz, 1H), 6.83 (dd, *J* = 5, 5 Hz, 1H), 3.78 (d, *J* = 5 Hz, 2H).
HR-EIMS *m/z* measured 178.1044 (178.1044 calcd for $C_{10}H_6{}^2H_4N_2O$).
EIMS *m/z* (relative abundance) 178 $[M]^+$ (76), 134 (100).

4.3.2 Indolyl-3-acetaldoxime (112)

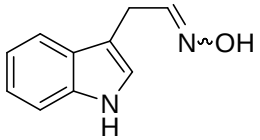

112

A solution of DIBAH (850 μL, 1.28 mmol) in toluene was added drop wise to a solution of indolyl-3-acetonitrile (**49**, 100 mg, 0.64 mmol) in dry toluene (8 mL) cooled to -78 °C under an atmosphere of argon. The reaction mixture was allowed to stir at -78

°C for 10 min, was diluted with ice-cold HCl (10 mL, 2 M) and immediately extracted in EtOAc (20 mL × 3) (Miyashita et al., 1997). The combined organic extract was washed with H_2O (10 mL × 2), was dried over Na_2SO_4, and was concentrated under reduced pressure to yield crude indolyl-3-acetaldehyde. The crude indolyl-3-acetaldehyde was treated as reported above for [4',5',6',7'-$^2H_4$]indolyl-3-acetaldehyde to yield indolyl-3-acetaldoxime (**112**, 35.7 mg, 32% yield from **49**, Pedras and Okinyo, 2006a).

HPLC-DAD Method A, two peaks at t_R = 11.8 and 12.9 min.
Major isomer: ^{1}H NMR (500 MHz C^{2}H$_3$CN) δ 9.16 (br s, NH), 8.85 (s, OH), 7.57 (d, *J* = 8 Hz, 1H), 7.43 (d, *J* = 8 Hz, 1H), 7.17 (dd, *J* = 8 Hz, 1H), 7.15 (s, 1H), 7.08 (dd, *J* = 7.5, 7.5 Hz, 1H), 6.84 (dd, *J* = 5.5 Hz, 1H), 3.78 (d, *J* = 5.5 Hz, 2H).
Minor isomer: ^{1}H NMR (500 MHz C^{2}H$_3$CN) δ 9.16 (br s, NH), 8.37 (s, OH), 7.57 (d, *J* = 8 Hz, 1H), 7.50 (dd, *J* = 6 Hz, 1H), 7.43 (d, *J* = 8 Hz, 1H), 7.17 (dd, *J* = 8, 8 Hz, 1H), 7.12 (s, 1H), 7.08 (dd, *J* = 7.5, 7.5 Hz, 1H), 3.61 (d, *J* = 6 Hz, 2H).
HR-EIMS *m/z* measured 174.0793 (174.0793 calcd for $C_{10}H_{10}N_2O$).
EIMS *m/z* (relative abundance) 174 $[M]^+$ (57), 157 (20), 130 (100), 117 (14), 103 (12).

4.3.3 [4',5',6',7'-$^2H_4$]1-Methoxyindolyl-3-acetaldoxime (116b)

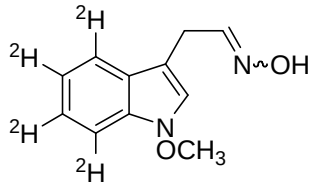

116b

Ten percent Pd/C (80 mg) was added to a solution of [4',5',6',7'-$^2H_4$]indolyl-3-acetonitrile (**49a**, 80 mg, 0.50 mmol) in Ac_2O (4 mL), and the mixture was stirred at r.t. under H_2 atmosphere (balloon pressure). After 14 h the catalyst was filtered off, the filtrate was concentrated under reduced pressure, the residue was dissolved in CH_2Cl_2 (15 mL), was washed with a 10% solution of $NaHCO_3$ (8 mL), H_2O (8 mL × 2), and was

dried over Na_2SO_4. After removal of the solvent under reduced pressure, crude [4',5',6',7'-$^2H_4$]N_b-acetyltryptamine was obtained (87.9 mg, 85%) in sufficient purity to use directly in the next step. To a solution of [4',5',6',7'-$^2H_4$]N_b-acetyltryptamine (100 mg, 0.495 mmol) in glacial acetic acid (2 mL) at r.t., $NaBH_3CN$ (47 mg, 0.74 mmol) was added in portions. The reaction mixture was allowed to stir for 3 h at room temperature, was diluted with H_2O (5 mL), was basified with NaOH, and was extracted with Et_2O (15 mL × 3). The combined organic extract was dried over Na_2SO_4 and concentrated under reduced pressure to yield crude [4',5',6',7'-$^2H_4$]N_b-acetyl-2,3-dihydrotryptamine (**114a**, 117 mg, 99%), which was used in the next step without purification. A solution of $Na_2WO_4 \cdot 2H_2O$ (17.2 mg, 0.0943 mmol) in H_2O (199 μL) was added to a solution of [4',5',6',7'-$^2H_4$]N_b-acetyl-2,3-dihydrotryptamine (112.8 mg, 0.542 mmol) in CH_3OH (2.2 mL) cooled to -20 ºC under stirring, followed by drop wise addition of a solution of H_2O_2 (520 μL, 5.42 mmol) in CH_3OH (540 μL). After being stirred at r.t. for 10 min, K_2CO_3 (601 mg, 4.44 mmol) and $(CH_3O)_2SO_2$ (78 μL, 0.87 mmol) were added under vigorous stirring at r.t. (Somei and Kawasaki, 1989). After 60 min, the reaction mixture was diluted with H_2O (12 mL), was extracted with Et_2O (20 mL × 3), the combined organic extract was dried over Na_2SO_4 and was concentrated under reduced pressure to yield crude [4',5',6',7'-$^2H_4$]N_b-acetyl-1-methoxytryptamine (**115b**, 79.4 mg, 62%). A solution of the crude [4',5',6',7'-$^2H_4$]N_b-acetyl-1-methoxytryptamine (79.4 mg) in 15% methanolic solution of NaOH (20 mL) was allowed to reflux for 24 h. After removing the solvent under reduced pressure, the residue was taken in H_2O, was extracted with CH_2Cl_2-CH_3OH (95:5, v/v), was dried over Na_2SO_4 and was concentrated under reduced pressure to yield crude [4',5',6',7'-$^2H_4$]1-methoxytryptamine (41 mg, 63%). An aqueous solution of $Na_2WO_4 \cdot 2H_2O$ (1.4 mg, 0.0042 mmol) in H_2O (60 μL) was added to the solution of [4',5',6',7'-$^2H_4$]1-methoxytryptamine (41 mg, 0.21 mmol) in CH_3OH (400 μL), the mixture was cooled to -15 ºC and H_2O_2 (48 μL, 0.5 mmol) was added under stirring (Burckard et al., 1965). After being stirred for 60 min at r.t., the mixture was diluted with H_2O (5 mL), was basified with 20% NaOH, was extracted with CH_2Cl_2 (20 mL × 3), the combined organic extract was dried over Na_2SO_4 and the solvent was removed under reduced pressure to afford a crude residue (24.3 mg). The crude residue was separated by preparative TLC (CH_2Cl_2-CH_3OH, 95:5, v/v) to yield [4',5',6',7'-$^2H_4$]1-

methoxyindolyl-3-acetaldoxime (**116b**, 4.8 mg, 5% yield over 5 steps). Integration of ^{1}H NMR signals indicated the presence of *syn* and *anti* isomers (1.1:0.9) (Pedras and Okinyo, 2006a).

HPLC-DAD Method A, two peaks at t_R = 14.5 and 15.4 min.
Major isomer: ^{1}H NMR (500 MHz $C^{2}HCl_3$) δ 7.60 (dd, *J* = 6, 6 Hz, 1H), 7.15 (s, 1H), 4.08 (s, 3H), 3.64 (d, *J* = 6 Hz, 2H).
Minor isomer: ^{1}H NMR (500 MHz $C^{2}HCl_3$) δ 7.17 (s, 1H), 6.93 (dd, *J* = 5, 5 Hz, 1H), 4.09 (s, 3H), 3.83 (d, *J* = 5 Hz, 2H).
HR-EIMS *m/z* measured 208.1142 (208.1149 calcd for $C_{11}H_8{}^{2}H_4N_2O_2$).
EIMS *m/z* (relative abundance) 208 $[M]^+$ (100), 190 (25), 164 (45), 159 (54), 132 (70).

4.3.4 [1",1",1",4',5',6',7'-$^{2}H_7$]1-Methoxyindolyl-3-acetaldoxime (116c)

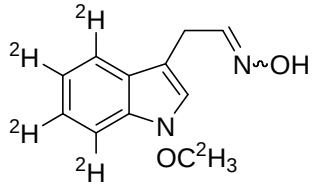

116c

A solution of $Na_2WO_4{\cdot}2H_2O$ (32.3 mg, 0.098 mmol) in H_2O (206 μL) was added to a solution of [4',5',6',7'-$^{2}H_4$]*N*$_b$-acetyl-2,3-dihydrotryptamine (**114a**, 117 mg, 0.563 mmol) in CH_3OH (2.3 mL) under stirring. The mixture was cooled to -20 ºC and a solution of H_2O_2 (541 μL, 5.63 mmol) in CH_3OH (562 μL) was added drop wise. After being stirred for 10 min at r.t., K_2CO_3 (623 mg, 4.50 mmol) and $(C^{2}H_3O)_2SO_2$ (85 μL, 0.90 mmol) were added to the reaction mixture under vigorous stirring (Somei and Kawasaki, 1989). After being stirred for 60 min at r.t., the reaction mixture was diluted with H_2O (12 mL), was extracted with Et_2O (20 mL × 3), the combined organic extract was dried over Na_2SO_4 and was concentrated under reduced pressure to yield crude [1",1",1",4',5',6',7'-$^{2}H_7$]*N*$_b$-acetyl-1-methoxytryptamine (**115c**, 84.8 mg, 63%). The crude [1",1",1",4',5',6',7'-$^{2}H_7$]*N*$_b$-acetyl-1-methoxytryptamine (84.8 mg) was treated as reported

above for [4',5',6',7'-$^2H_4$]N_b-acetyl-1-methoxytryptamine (**116b**) to yield [1",1",1",4',5',6',7'-$^2H_7$]1-methoxyindolyl-3-acetaldoxime (**116c**, 4.2 mg, 4% yield over 5 steps). Integration of ^{1}H NMR signals indicated the presence of *syn* and *anti* isomers (1.1:0.9) (Pedras and Okinyo, 2006a).

HPLC-DAD Method A, two peaks at t_R = 14.5 and 15.4 min.
Major isomer: ^{1}H NMR (500 MHz C^2HCl_3) δ 7.60 (dd, *J* = 6, 6 Hz, 1H), 7.15 (s, 1H), 3.64 (d, *J* = 6 Hz, 2H).
Minor isomer: ^{1}H NMR (500 MHz C^2HCl_3): δ 7.17 (s, 1H), 6.93 (dd, *J* = 5, 5 Hz, 1H), 3.83 (d, *J* = 5 Hz, 2H).
HR-EIMS *m/z* measured 211.1335 (211.1338 calcd for $C_{11}H_5{}^2H_7N_2O_2$).
EIMS *m/z* (relative abundance) 211 $[M]^+$ (100), 193 (29), 167 (48), 159 (51), 132 (61).

4.3.5 [1",1",1"-$^2H_3$]1-Methoxyindolyl-3-acetaldoxime (116a)

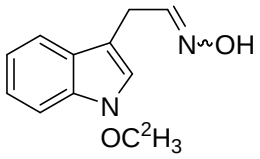

116a

Py (0.5 mL) was added to a solution of tryptamine (1 g) in Ac_2O (1.5 mL) under stirring. After 60 min the reaction mixture was dissolved in CH_2Cl_2 (10 mL), was washed with a 10% solution of $NaHCO_3$ (8 mL), H_2O (8 mL × 2), and was dried over Na_2SO_4. The solvent was removed under reduced pressure to yield crude N_b-acetyltryptamine (quant.) which was used in the next step without purification. To a solution of N_b-acetyltryptamine (500 mg, 2.48 mmol) in glacial acetic acid (8 mL) was added $NaBH_3CN$ (232 mg, 3.72 mmol) in portions. After 3 h at room temperature, the reaction mixture was diluted with H_2O (5 mL), was basified with 20% NaOH, and was extracted with Et_2O (30 mL × 3). The combined organic extract was dried over Na_2SO_4, was concentrated under reduced pressure, and the resulting residue was subjected to FCC (CH_2Cl_2-CH_3OH, 98:2 and 97:3, v/v) to yield N_b-acetyl-2,3-dihydrotryptamine

(**114**) (398 mg, 79%). A solution of $Na_2WO_4 \cdot 2H_2O$ (56.4 mg, 0.171 mmol) in H_2O (390 μL) was added to a stirred solution of *N*b-acetyl-2,3-dihydrotryptamine (200 mg, 0.980 mmol) in CH_3OH (3.9 mL) cooled to -20 ºC, followed by drop wise addition of a solution of H_2O_2 (875 μL, 9.10 mmol) in CH_3OH (980 μL). After being stirred at r.t. for 10 min, K_2CO_3 (18 g, 7.84 mmol) and $(C^2H_3O)_2SO_2$ (135 μL, 1.57 mmol) were added under vigorous stirring at r.t. (Somei and Kawasaki, 1989). After 60 min the reaction mixture was diluted with H_2O (20 mL), was extracted with Et_2O (30 mL × 3), the combined organic extract was dried over Na_2SO_4 and was concentrated under reduced pressure. The residue was subjected to FCC (CH_2Cl_2-CH_3OH, 98:2 v/v) to yield [1",1",1"-$^2H_3$]*N*b-acetyl-1-methoxytryptamine (140.5 mg, 61%). A solution of [1",1",1"-$^2H_3$]*N*b-acetyl-1-methoxytryptamine (140.5 mg) in 15% methanolic solution of NaOH (28 mL) was allowed to reflux for 24 h. After removing the solvent under reduced pressure, the residue was dissolved in water (20 mL), was extracted with CH_2Cl_2-CH_3OH (95:5, v/v, 40 mL × 3), was dried over Na_2SO_4 and was concentrated under reduced pressure to yield crude [1",1",1"-$^2H_3$]1-methoxytryptamine (**115a**, 101.6 mg, 88%). An aqueous solution of $Na_2WO_4 \cdot 2H_2O$ (2.24 mg, 0.00680 mmol) in H_2O (95 μL) was added to the solution of [1",1",1"-$^2H_3$]1-methoxytryptamine (66 mg, 0.34 mmol) in CH_3OH (630 μL). The mixture was cooled to -15 ºC and H_2O_2 (79 μL, 0.82 mmol) was added under stirring (Burckard et al., 1965). After being stirred for 60 min at r.t., the mixture was diluted with H_2O (8 mL), was basified with 20 % NaOH, was extracted with CH_2Cl_2 (20 mL × 3), the combined organic extract was dried over Na_2SO_4 and the solvent was removed under reduced pressure. The residue was subjected to FCC (CH_2Cl_2-CH_3OH, 100:0, 98:2 and 90:10 v/v), followed by PTLC (CH_2Cl_2-CH_3OH, 98:2 v/v) to yield [1",1",1"-$^2H_3$]1-methoxyindolyl-3-acetaldoxime (**116a**, 28.1 mg, 40% yield, Pedras and Montaut, 2004).

HPLC-DAD Method A, two peaks at t_R = 14.5 and 15.4 min.

^{1}H NMR (500 MHz C^2HCl_3) δ 7.58-7.61 (m, 2H), 7.43-7.46 (m, 2H), 7.26-7.30 (m, 2H), 7.18 (s, 1H), 7.13-7.17 (m, 2H), 6.95 (dd, *J* = 5, 5 Hz, 1H), 3.84 (d, *J* = 5 Hz, 2H), 3.65 (d, *J* = 6 Hz, 2H).

HR-EIMS *m/z* measured 207.1082 (207.1087 calcd for $C_{11}H_9{}^2H_3N_2O_2$).

EIMS *m/z* (relative abundance) 207 $[M]^+$ (100), 163 (36), 129 (40), 102 (17).

4.3.6 1-Methoxyindolyl-3-acetaldoxime (116)

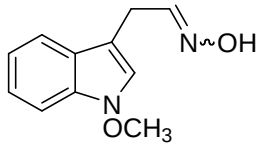

116

A solution of $Na_2WO_4 \cdot 2H_2O$ (56.4 mg, 0.171 mmol) in H_2O (390 μL) was added to a stirred solution of N_b-acetyl-2,3-dihydrotryptamine (**114**, 200 mg, 0.980 mmol) in CH_3OH (3.9 mL) cooled to -20 ºC. The mixture was treated with drop wise addition of a solution of H_2O_2 (875 μL, 9.10 mmol) in CH_3OH (980 μL). After being stirred at r.t. for 10 min, K_2CO_3 (18 g, 7.84 mmol) and $(CH_3O)_2SO_2$ (145 μL, 1.60 mmol) were added under vigorous stirring at r.t. (Somei and Kawasaki, 1989). After 60 min the reaction mixture was diluted with H_2O (20 ml), was extracted with Et_2O (30 mL × 3), the combined organic extract was dried over Na_2SO_4 and was concentrated under reduced pressure. The residue was subjected to FCC (CH_2Cl_2-CH_3OH, 98:2 v/v) to yield N_b-acetyl-1-methoxytryptamine (152.6 mg, 67%). The N_b-acetyl-1-methoxytryptamine (100 mg) was treated as reported above for [1",1",1"-$^2H_3$]N_b-acetyl-1-methoxytryptamine (**116a**) to yield 1-methoxyindolyl-3-acetaldoxime (**116**, 23.7, mg, 27% yield, Pedras and Montaut, 2004).

HPLC-DAD Method A, two peaks at t_R = 14.5 and 15.4 min.

^1H NMR (500 MHz C^2HCl_3) δ 7.59-7.63 (m, 2H), 7.44-7.46 (m, 2H), 7.27-7.31 (m, 2H), 7.17 (s, 1H), 7.15-7.16 (m, 2H), 6.95 (dd, *J* = 5.5, 5.5 Hz, 1H), 4.09 (s, 3H), 4.08 (s, 3H), 3.85 (d, *J* = 5 Hz, 2H), 3.66 (d, *J* = 6 Hz, 2H).

HR-EIMS *m/z* measured 204.0885 (204.0899 calcd for $C_{11}H_{12}N_2O_2$).

EIMS *m/z* (relative abundance) 204 $[M]^+$ (8), 173 (71), 160 (100), 145 (49), 129 (55), 117 (37), 102 (33).

4.3.7 1-Methylindolyl-3-acetonitrile (169)

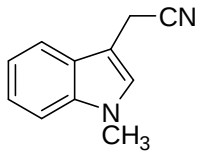

169

NaH (66.8 mg, 1.67 mmol) and ICH_3 (104 µL, 1.67 mmol) were added to cooled solution (0 °C) of indolyl-3-acetonitrile (**49**, 130 mg, 0.833 mmol) in dry THF (10 mL) under stirring. After 105 min, the reaction mixture was diluted with ice-cold H_2O (20 mL) and was extracted with CH_2Cl_2 (30 mL × 3). The combined organic extract was dried over Na_2SO_4, was concentrated under reduced pressure and the residue obtained was subjected to FCC (CH_2Cl_2-hexane, 70:30, then 80:20, v/v) to yield 1-methylindolyl-3-acetonitrile (**169**, 135.9 mg, 96% yield).

HPLC-DAD Method A, t_R = 17.7 min.
^{1}H NMR (500 MHz C^2HCl_3) δ 7.60 (d, *J* = 8 Hz, 1H), 7.36 (d, *J* = 8 Hz, 1H), 7.31 (dd, *J* = 7.5, 7.5 Hz, 1H), 7.20 (dd, *J* = 7.5, 7.5 Hz, 1H), 7.11 (s, 1H), 3.85 (s, 2H), 3.80 (s, 3H).
HR-EIMS *m/z* measured 170.0843 (170.0844 calcd for $C_{11}H_{10}N_2$).
EIMS *m/z* (relative abundance) 170 $[M]^+$ (100), 144 (60), 128 (13), 115 (12).

4.3.8 1-Methylindolyl-3-acetaldoxime (170)

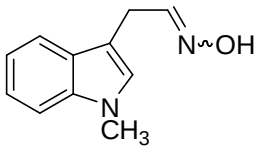

170

A solution of DIBAH (790 µL, 1.18 mmol) in toluene was added drop wise to a solution of 1-methylindolyl-3-acetonitrile (**169**, 100 mg, 0.588 mmol) in dry toluene (6.5 mL) cooled to -78 °C under argon atmosphere. The reaction mixture was allowed to stir

at -78 °C for 10 min, was diluted with ice-cold HCl (10 mL, 2 M) and immediately extracted with EtOAc (30 mL × 2). The combined organic extract was washed with H_2O (10 mL × 2), was dried over Na_2SO_4 (Pedras and Okinyo 2006a), and was concentrated under reduced pressure to yield 1-methylindolyl-3-acetaldehyde which was used for the next step without purification. A solution of $HONH_2$·HCl (104.3 mg, 1.50 mmol) and CH_3COONa (123.1 mg, 1.50 mmol) in H_2O (1 mL) was added to a cooled solution (0 °C) of indolyl-3-acetaldehyde in EtOH (8.5 mL) under stirring. The reaction mixture was treated as reported above for indolyl-3-acetaldoxime (**112**). Separation by FCC (CH_2Cl_2-CH_3OH, 98:2, v/v) yielded 1-methylindolyl-3-acetaldoxime (**170**, 73.3 mg, 66% yield).

HPLC-DAD Method A, two peaks at t_R = 12 and 11.3 min.
^{1}H NMR (500 MHz C^{2}H$_3$CN) δ 8.84 (s, OH), 7.56 (d, *J* = 8 Hz, 1H), 7.37 (d, *J* = 8 Hz, 1H), 7.22 (dd, *J* = 7.5, 7.5 Hz, 1H), 7.09 (dd, *J* = 7.5, 7.5 Hz, 1H), 7.06 (s, 1H), 6.84 (dd, *J* = 5.5, 5.5 Hz, 1H), 3.77 (d, *J* = 7.5 Hz, 2H), 3.76 (s, 3H).
HR-EIMS *m/z* measured 188.0955 (188.0950 calcd for $C_{11}H_{12}N_2O$).
EIMS *m/z* (relative abundance) 188 $[M]^+$ (56), 171 (22), 144 (100), 131 (14).

4.3.9 ^{34}S-Hexamethyldisilathiane (171a) and hexamethyldisilathiane (171)

$(CH_3)_3Si^{34}SSi(CH_3)_3$ **171a**

$(CH_3)_3SiSSi(CH_3)_3$ **171**

Hexamethyldisilathiane (**171**) was synthesized in 69% yield (based on S) by a modification of reported procedure (So and Boudjouk, 1989; 1992). The optimized synthetic conditions were employed in preparation of ^{34}S-hexamethyldisilathiane (**171a**). Finely cut pieces of Na (270.5 mg, 11.8 mmol) were added to a dry two-necked 50 mL round-bottomed flask charged with sulfur-34 (200 mg, 5.88 mmol) and naphthalene (70.9 mg, 0.553 mmol) in dry THF (6 mL). The reaction mixture was sonicated for about 2 h during which sodium and sulfur dissolves. The color of the reaction mixture changes

from yellow to orange to brown to light yellow to green to light green. The reaction mixture was then refluxed for 2 h, was cooled in ice-bath followed by drop wise addition of chlorotrimethylsilane (2.2 mL, 17.64 mmol) and the reaction mixture turns purple. The reaction mixture was stirred in ice-bath for further 10 min, then at r.t. for 3 h. A short-path distillation apparatus was used to distil off THF and excess chlorotrimethylsilane at atmospheric pressure. ^{34}S-Hexamethyldisilathiane (**171a**) was then distilled off under vacuum (b.p. 68-71 ºC at 510 torr) and was obtained as a colorless vile smelling liquid in 60% yield based on ^{34}S (633.5 mg). The ^{34}S-hexamethyldisilathiane was analyzed by GC and GC-MS-EI.

GC t_R = 5.15 min.
GC-MS-EI *m/z* (relative abundance) 180 $[M]^+$ (50), 165 (100).

4.3.10 [4',5',6',7'-$^2H_4$]Indolyl-3-[^{34}S]acetothiohydroxamic acid (174a)

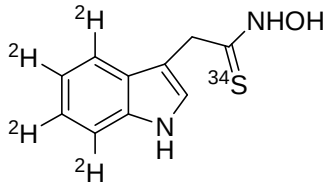

174a

Freshly distilled $POCl_3$ (260 µL, 2.84 mmol) was added drop wise to a solution of [4,5,6,7-$^2H_4$]indole (**105a**, 313 mg, 2.58 mmol) in DMF (2 mL) and the reaction mixture was stirred at r.t. After 50 min, a solution of aqueous NH_3 (10 mL, 28%) was added and the reaction mixture was extracted with EtOAc (60 mL × 3), the combined organic extract was washed with ice-cold H_2O (30 mL × 2), was dried over Na_2SO_4 and was concentrated under reduced pressure to yield [4,5,6,7-$^2H_4$]indole-3-carboxaldehyde (**106a**, 332.9 mg, 87%, Pedras et al., 1998). NH_4OAc (96.4 mg, 1.25 mmol) was added to a suspension of [4,5,6,7-$^2H_4$]indole-3-carboxaldehyde (332.9 mg, 2.23 mmol) in CH_3NO_2 (966 µL, 17.84 mmol). The resulting mixture was refluxed at 128 - 130 °C for

2 h (Canoira et al., 1989). The reaction mixture was then diluted with H_2O (20 mL), was extracted with CH_2Cl_2 (35 mL × 3), and the combined organic extract was washed with H_2O (40 mL), then brine (40 mL), was dried over Na_2SO_4 and was concentrated under reduced pressure to yield [4',5',6',7'-$^2H_4$]3-(2-nitrovinyl)indole (**172a**) in 99% (422 mg). To a mixture of [4',5',6',7'-$^2H_4$]3-(2-nitrovinyl)indole (422 mg, 2.20 mmol) and silica gel (4.40 g) in isopropanol (6.4 mL) and $CHCl_3$ (35 mL) $NaBH_4$ (341 mg, 92 mmol) was added in portions of ca 85 mg over 15 min (Sinhababu and Borchardt, 1983). The reaction mixture was stirred for further 60 min, during which the intense yellow color of the reaction mixture disappeared. The excess $NaBH_4$ was then destroyed with 2 M HCl, the reaction mixture was filtered off and the silica gel was rinsed with CH_2Cl_2 (20 mL × 3). The combined organic extract was washed with H_2O (40 mL), was dried over Na_2SO_4 and was concentrated under reduced pressure. The reaction mixture was subjected to FCC (CH_2Cl_2) to yield [4',5',6',7'-$^2H_4$]3-(2-nitroethyl)indole (**173a**, 178 mg, 42%) as a brown solid. KH (331 mg, 2.47 mmol) in a dry 50 mL round-bottomed flask was rinsed with n-hexanes under atmosphere of argon to give a white powder. The flask was kept in ice-bath and a solution of [4',5',6',7'-$^2H_4$]3-(2-nitroethyl)indole (60 mg, 0.309 mmol) in dry THF (4 mL) was added drop wise. After stirring for 30 min with cooling in ice-bath, the reaction mixture was allowed to warm up to r.t. and stirred for an additional 60 min. The reaction flask was wrapped with aluminum foil and ^{34}S-hexamethyldisilathiane (**171a**, 310 µL, 1.43 mmol) was added drop wise (Hwu and Tsay, 1990). After 60 min, the reaction mixture was cooled in an ice-bath, was diluted with ice-cold H_2O (5 mL), was neutralized with 5% H_2SO_4 (2 mL), was extracted with CH_2Cl_2 (30 mL × 2), the combined organic extract was dried over Na_2SO_4, and the solvent was removed under reduced pressure. The residue was subjected to FCC (CH_2Cl_2-EtOAc, 100:0, then 60:40, v/v) to yield [4',5',6',7'-$^2H_4$]indolyl-3-[^{34}S]acetothiohydroxamic acid (**174a**, 49.8 mg, 76% yield) as brownish crystals (Pedras and Okinyo, 2008).

HPLC-HRMS-ESI Method A, t_R = 13.1 min.

^{1}H NMR (500 MHz C^{2}HCl$_3$) δ 8.26 (br s, 1H), 7.20 (s, 1H), 4.27 (s, 2H).

HPLC-HRMS-ESI *m/z* measured 213.0797 (213.0795 calcd for $C_{10}H_7{}^2H_4N_2O^{34}S$).

HPLC-MS-ESI *m/z* (relative abundance) 213 $[M + H]^+$ (100), 195 (15), 180 (13), 134 (18).

FTIR ν_{max} (KBr)/cm^{-1}; 3410, 3307, 3056, 2904, 1552, 1455, 1419, 1353, 1339, 1227, 1131, 1062, 971, 744.

4.3.11 [4',5',6',7'-$^2H_4$]Indolyl-3-acetothiohydroxamic acid (174b)

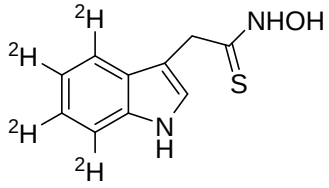

174b

KH (331 mg, 2.47 mmol) in a dry 50 mL round-bottomed flask was rinsed with n-hexanes under an atmosphere of argon to give a white powder. The reaction flask was kept in an ice-bath and a solution of [4',5',6',7'-$^2H_4$]3-(2-nitroethyl)indole (60 mg, 0.309 mmol) in dry THF (4 mL) was added drop wise. After stirring for 30 min with cooling in an ice-bath, the reaction mixture was allowed to warm up to r.t. and stirred for an additional 60 min. The reaction flask was wrapped with aluminum foil and hexamethyldisilathiane (**171**, 258 µL, 1.24 mmol) was added drop wise (Hwu and Tsay, 1990). The reaction mixture was then treated as reported above for [4',5',6',7'-$^2H_4$]indolyl-3-[^{34}S]acetothiohydroxamic acid (**174a**) to yield [4',5',6',7'-$^2H_4$]indolyl-3-acetothiohydroxamic acid (**174b**, 50.5 mg, 78% yield) as brownish crystals (Pedras and Okinyo, 2008).

HPLC-HRMS-ESI Method A, t_R = 13.1 min.

^{1}H NMR (500 MHz C^2HCl_3) δ 8.26 (br s, 1H), 7.20 (s, 1H), 4.26 (s, 2H).

HPLC-HRMS-ESI *m/z* measured 211.0830 (211.0837 calcd for $C_{10}H_7{}^2H_4N_2OS$).

HPLC-MS-ESI *m/z* (relative abundance) 211 $[M + H]^+$ (100), 193 (16), 178 (14), 134 (17).

4.3.12 Indolyl-3-acetothiohydroxamic acid (174)

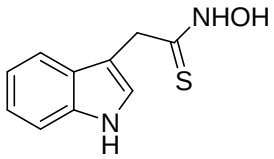

174

NH_4OAc (148.8 mg, 1.93 mmol) was added to a suspension of indolyl-3-carboxaldehyde (**106**, 500 mg, 3.44 mmol) in CH_3NO_2 (1.5 mL, 27.5 mmol). The resulting mixture was refluxed at 128 - 130 °C for 2 h. The reaction mixture was then diluted with H_2O (40 mL), was extracted with CH_2Cl_2 (60 mL × 3), and the combined organic extract was washed with H_2O (60 mL), then brine (60 mL), was dried over Na_2SO_4 and was concentration under reduced pressure to yield 3-(2'-nitrovinyl)indole (**172**, 642 mg, 98%) (Canoira et al., 1989). To a mixture of 3-(2'-nitrovinyl)indole (400 mg, 2.13 mmol) and silica gel (4.26 g) in isopropanol (6.3 mL) and $CHCl_3$ (34 mL) $NaBH_4$ (330 mg, 8.73 mmol) was added in portions of ca 83 mg over 15 min (Sinhababu and Borchardt, 1983). The reaction mixture was then treated as reported above for [4',5',6',7'-$^2H_4$]-3-(2-nitrovinyl)indole (**172a**) to yield 3-(2'-nitroethyl)indole (**173**, 204.7 mg, 51%) as a brown solid. KH (338 mg, 2.53 mmol) was rinsed with n-hexanes under atmosphere of argon to give a white powder. The reaction flask was kept in an ice-bath and a solution of 3-(2'-nitroethyl)indole (60 mg, 0.316 mmol) in dry THF (4 mL) was added drop wise. After stirring for 30 min with cooling in an ice-bath, the reaction mixture was allowed to warm up to r.t. and stirred for an additional 60 min. The reaction flask was wrapped with aluminum foil and hexamethyldisilathiane (**171**, 306 µL, 1.48 mmol) was added drop wise (Hwu and Tsay, 1990). The reaction mixture was then treated as reported above for [4',5',6',7'-$^2H_4$]indolyl-3-[^{34}S]acetothiohydroxamic acid (**174a**) to yield indolyl-3-acetothiohydroxamic acid (**174**, 48.1 mg, 74% yield) (Pedras and Okinyo, 2008).

HPLC-HRMS-ESI Method A, t_R = 13.1 min.

^{1}H NMR (500 MHz $C^{2}HCl_3$) δ 8.26 (br s, 1H), 7.54 (d, *J* = 8 Hz, 1H), 7.44 (d, *J* = 8 Hz, 1H), 7.28 (dd, *J* = 7.5, 7.5 Hz, 1H), 7.17-7.24 (m, 2H), 4.26 (s, 2H).

^{13}C NMR (125.8 MHz $C^{2}HCl_3$) δ 189.0, 136.7, 126.9, 124.5, 123.5, 121.0, 119.0, 111.9, 107.2, 36.9.

HPLC-HRMS-ESI *m/z* measured 207.0579 (207.0586 calcd for $C_{10}H_{11}N_2OS$).

HPLC-MS-ESI *m/z* (relative abundance) 207 $[M + H]^+$ (100), 189 (22), 174 (39), 130 (35).

4.3.13 1-Methylindolyl-3-acetothiohyrodroxamic acid (178)

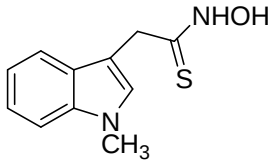

178

NaH (110 mg, 2.76 mmol) and ICH_3 (172 µL, 2.76 mmol) were added to a cooled solution (0 °C) of indole-3-carboxaldehyde (**106**, 200 mg, 1.38 mmol) in dry THF (20 mL) with stirring under argon atmosphere. After 45 min of stirring at 0 °C, the reaction mixture was poured into ice-cold H_2O (40 mL), was extracted with EtOAc (60 mL × 3), the combined organic extract was washed with brine, was dried over Na_2SO_4, and was concentrated under reduced pressure. The crude mixture was subjected to FCC (CH_2Cl_2-CH_3OH, 100:0-98:2, v/v) to yield 1-methylindole-3-carboxaldehyde (**175**, 215 mg, 98%). NH_4OAc (54.4 mg, 0.706 mmol) was added to a suspension of 1-methylindole-3-carboxaldehyde (200 mg, 1.26 mmol) in CH_3NO_2 (547 µL, 10.1 mmol) and the resulting mixture was refluxed at 128 - 130 °C for 2 h (Canoira et al., 1989). The reaction mixture was then diluted with H_2O (20 mL), was extracted with Cl_2Cl_2 (30 mL × 3), and the combined organic extract was washed with H_2O (20 mL), then brine (20 mL), was dried over Na_2SO_4 and was concentrated under reduced pressure to yield 1-methyl-3-(2'-nitrovinyl)indole (**176**, 249 mg, 98%,). To a mixture of 1-methyl-3-(2'-nitrovinyl)indole (249 mg, 1.23 mmol) and silica gel (2.46 g) in isopropanol (3.7 mL) and $CHCl_3$ (20 mL), $NaBH_4$ (191 mg, 54 mmol) was added in portions of ca 48 mg over 15 min (Sinhababu

and Borchardt, 1983). The reaction mixture was then treated as reported above for [4',5',6',7'-$^{2}H_4$]-3-(2-nitrovinyl)indole (**172a**). Separation of the crude mixture by FCC (CH_2Cl_2-hexane, 80:20, v/v) yielded 1-methyl-3-(2'-nitroethyl)indole (**177**, 158.1 mg, 63%). KH (262 mg, 1.96 mmol) was rinsed with n-hexanes under an atmosphere of argon to give a white powder. The reaction flask was kept in an ice-bath and a solution of 1-methyl-3-(2'-nitroethyl)indole, (100 mg, 0.490 mmol) in dry THF (5.5 mL) was added drop wise. After stirring for 30 min with cooling in an ice-bath, the reaction mixture was allowed to warm up to r.t. and stirred for an additional 60 min. The reaction flask was wrapped with aluminum foil and hexamethyldisilathiane (207 µL, 0.980 mmol) was added drop wise (Hwu and Tsay, 1990). The reaction mixture was then treated as reported above for [4',5',6',7'-$^{2}H_4$]indolyl-3-[^{34}S]acetothiohydroxamic acid (**174a**). The resulting crude mixture was separated by FCC (CH_2Cl_2-EtOAc, 100:0, then 80:20, v/v) to yield 1-methylindolyl-3-acetothiohydroxamic acid (**178**, 71.8 mg, 67% yield) as brownish oil which solidified on cooling to 5 °C.

HPLC-HRMS-ESI Method A, t_R = 17.2 min.

^{1}H NMR (500 MHz $C^{2}HCl_3$) δ 7.53 (d, *J* = 8 Hz, 1H), 7.42 (d, *J* = 8 Hz, 1H), 7.30 (dd, *J* = 7.5, 7.5 Hz, 1H), 7.18-7.25 (m, 2H), 4.25 (s, 2H), 3.82 (s, 3H).

HPLC-HRMS-ESI *m/z* measured 221.0830 (221.0837 calcd for $C_{11}H_{13}N_2OS$).

HPLC-MS-ESI *m/z* (relative abundance) 221 $[M + H]^+$ (92), 203 (7), 189 (11), 165 (7), 144 (100).

4.3.14 1-(*tert*-Butoxycarbonyl)indol-3-ylmethylisothiocyanate (180)

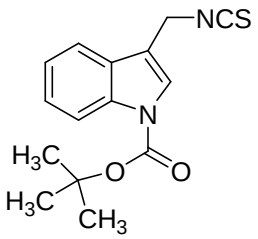

180

A solution of Boc_2O (364.5 mg, 1.67 mmol) in THF (2 mL) was added to a stirred solution of indole-3-carboxaldehyde (**106**, 200 mg, 1.38 mmol) in THF (6 mL). The reaction mixture was cooled to 5 °C and DMAP was added. After 20 min, the reaction mixture was concentrated under reduced pressure and the resulting residue was subjected to FCC (hexane-EtOAc, 60:40, v/v) to yield 1-(*tert*-butoxycarbonyl)indole-3-carboxaldehyde (345.8 mg, quant.). A solution of $HONH_2 \cdot HCl$ (133 mg, 1.92 mmol) and Na_2CO_3 (93.6 mg, 0.883) in H_2O (360 μL) was added to a stirred solution of 1-(*tert*-butoxycarbonyl)indole-3-carboxaldehyde (300 mg, 1.22 mmol) in EtOH (2.3 mL). The resulting mixture was heated for 5 min at 50 °C. the reaction mixture was then concentrated under reduced pressure and the residue was taken in H_2O (6 mL), and was extracted with Et_2O (10 mL × 3). The combined organic extract was dried over Na_2SO_4 and was concentrated under reduced pressure to yield crude 1-(*tert*-butoxycarbonyl)indolyl-3-carboxaldehyde oxime (330 mg, quant.) which was used without purification. A solution of 1-(*tert*-butoxycarbonyl)indolyl-3-carboxaldehyde oxime (120 mg, 0.462 mmol) in CH_3OH (4.6 mL) was added to a solution of $NiCl_2 \cdot 6H_2O$ (109.8 mg, 0.462) in CH_3OH (7 mL). $NaBH_4$ (112.7 mg, 2.98 mmol) was added in one portion and the reaction mixture was stirred for 5 min. The black precipitate that formed was filtered off and the filtrate was concentrated to about a third of the original volume. The remaining mixture was poured into H_2O (23 mL) containing aqueous NH_3 (700 μL, 28%), and was extracted with EtOAc (15 mL × 3). The combined organic extract was dried over Na_2SO_4 and was concentrated to yield 1-(*tert*-butoxycarbonyl)indol-3-ylmethanamine (**179**, 106.5 mg, 94%) which was used for the next step without purification. A solution of 1-(*tert*-butoxycarbonyl)indolyl-3-methanamine (106.5 mg, 0.433 mmol) in CH_2Cl_2 (1.4 mL) was added drop wise (ca 6 min) to a vigorously stirred mixture of Cl_2CS (33 μL, 0.43 mmol) and $CaCO_3$ (55.6 mg, 0.550 mmol) in CH_2Cl_2/H_2O (1.4/2.8 mL). After 5 min, the two layers were separated and the aqueous solution was extracted with CH_2Cl_2 (10 mL × 3). The combined organic extract was filtered over charcoal, the solvent was removed under reduced pressure and the residue was subjected to FCC (benzene) to yield 1-(*tert*-butoxycarbonyl)indolyl-3-methyl isothiocyanate (**180**, 74 mg, 56% yield, Kutschy et al., 1997; 1998).

HPLC-DAD Method A, t_R = 37.6 min.

^{1}H NMR (500 MHz C^2HCl_3) δ 8.18 (d, *J* = 6.5 Hz, 1H), 7.65 (s, 1H), 7.59 (d, *J* = 8 Hz, 1H), 7.40 (dd, *J* = 7.5, 7.5 Hz, 1H), 7.33 (dd, *J* = 7.5, 7.5 Hz, 1H), 4.83 (s, 2H), 1.71 (s, 9H).

HR-EIMS *m/z* measured 288.0937 (288.0933 calcd for $C_{15}H_{16}N_2O_2S$).

EIMS *m/z* (relative abundance) 288 $[M]^+$ (10), 232 (22), 205 (9), 174 (21), 130 (64), 57 (100).

4.3.15 1-Acetylindol-3-ylmethylisothiocyanate (183)

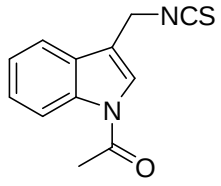

183

Pyridine (4 mL) was added to a stirred suspension of indole-3-carboxaldehyde (**106**, 200 mg, 1.38 mmol) in Ac_2O (4 mL). After 90 min, the reaction mixture was diluted with toluene and concentrated to yield 1-acetylindole-3-carboxaldehyde (253 mg, 98%) which was used in the next step without purification. A solution of $HONH_2{\cdot}HCl$ (74.4 mg, 17 mmol) and CH_3COONa (87.8 mg, 17 mmol) in H_2O (2.5 mL) was added to a solution of 1-acetylindole-3-carboxaldehyde (200 mg, 17 mmol) in EtOH (17 mL), the resulting mixture was heated for 10 min (47 - 50 °C) with stirring. The reaction mixture was concentrated under reduced pressure, the residue was taken in H_2O (10 mL), was extracted with Et_2O (30 mL × 3), the combined organic extract was dried over Na_2SO_4, and was concentrated to yield 1-acetylindole-3-carboxaldehyde oxime (182.1 mg, 84%). A solution of $NiCl_2{\cdot}H_2O$ (141 mg, 0.594 mmol) in CH_3OH (6 mL) was added to a solution of 1-acetylindole-3-carboxaldehyde oxime (120 mg, 0.594 mmol) in CH_3OH (9 mL). The reaction mixture was cooled to 0 °C and $NaBH_4$ (144.1 mg, 6.45 mmol) was added in one portion (Kutschy et al., 1997; 1998). After stirring for 10 min, the black precipitate that formed was filtered off and the filtrate was concentrated to about a third of the original volume. The remaining mixture was poured into H_2O (20 mL) containing

aqueous NH_3 (1 mL, 28%), and was extracted with EtOAc (30 mL × 2). The combined organic extract was dried over Na_2SO_4, was concentrated, and the crude mixture was subjected to FCC (CH_2Cl_2-CH_3OH-NH_4OH 28%, 92:8:1, v/v) to yield 1-acetylindol-3-ylmethanamine (**182**, 78 mg). A solution of **182** in CH_2Cl_2 (1.5 mL) was added drop wise (ca 8 min) to a vigorously stirred mixture of Cl_2CS (31 μL, 0.41 mmol) and $CaCO_3$ (53 mg, 0.52 mmol) in CH_2Cl_2-H_2O (1.5:3 mL, Kutschy et al., 1997; 1998). After being stirred for 5 min the two layers were separated and the aqueous solution was extracted with CH_2Cl_2 (10 mL × 3). The combined organic extract was filtered over charcoal, the solvent was removed under reduced pressure and the residue was purified by FCC (CH_2Cl_2) to yield 1-acetylindolyl-3-methyl isothiocyanate (**183**, 42 mg, 31% yield from 1-acetylindole-3-carboxaldehyde oxime).

HPLC-DAD Method A, t_R = 24.9 min.
^{1}H NMR (500 MHz C^2HCl_3) δ 8.46 (d, *J* = 8 Hz, 1H), 7.55 (s, 1H), 7.56 (d, *J* = 8 Hz, 1H), 7.47 (dd, *J* = 8, 8 Hz, 1H), 7.36 (dd, *J* = 7.5, 7.5 Hz, 1H), 4.85 (s, 2H), 2.66 (s, 3H).
^{13}C NMR (125.8 MHz C^2HCl_3): δ 168.6, 136.4, 134.7, 128.5, 126.4, 124.4, 123.6, 118.9, 117.2, 116.6, 41.1, 24.2.
HR-EIMS *m/z* measured 230.0520 (230.0514 calcd for $C_{12}H_{10}N_2OS$).
EIMS *m/z* (relative abundance) 230 $[M]^+$ (18), 172 (32), 130 (100), 102 (7).

4.3.16 [4',5',6',7'-$^2H_4$]Brassinin (16a)

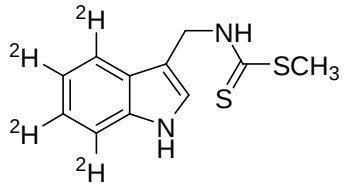

16a

A solution of $HONH_2$·HCl (102.6 mg, 1.48 mmol) and Na_2CO_3 (78.2 mg, 0.738 mmol) in H_2O (1.5 mL) was added to a solution of [4,5,6,7-$^2H_4$]indole-3-carboxaldehyde (110 mg, 0.738 mmol) in EtOH (3 mL). The resulting mixture was refluxed (68 - 70 ºC)

for 45 min. EtOH was evaporated and the residue was washed with ice-cold H_2O (3 mL) to yield [4',5',6',7'-$^2H_4$]indolyl-3-carboxaldehyde oxime (**185a**, 105.5 mg, 87%). A solution of NaOH (24 mL, 1 M) was added to a solution of [4',5',6',7'-$^2H_4$]indolyl-3-carboxaldehyde oxime (95 mg, 0.638) in CH_3OH (4.7 mL) and the resulting solution was cooled in an ice-bath. Devarda's alloy (3 g) was added to the cooled mixture with stirring at r.t. After 50 min the reaction mixture was diluted with H_2O (20 mL), and was filtered under vacuum. The reaction mixture was concentrated under reduced pressure, and the remaining mixture was extracted with Et_2O (60 mL × 3). The combined organic extract was dried over Na_2SO_4 and was concentrated under reduced pressure to yield [4',5',6',7'-$^2H_4$]indolyl-3-methanamine (**117a**, 61.3 mg, 71%) which was used in the next step without purification. Et_3N (57 μL, 0.41 mmol) and CS_2 (24 μL, 0.42 mmol) were added to a cooled solution (0 ºC) of [4',5',6',7'-$^2H_4$]indolyl-3-methylamine (61.3 mg, 0.41 mmol) in pyridine (580 μL). After stirring for 60 min at 0 ºC, ICH_3 (26 μL, 0.41 mmol) was added and the reaction mixture was kept at 5 ºC for 90 min. The reaction mixture was then diluted with H_2O (4 mL), was extracted with Et_2O (15 mL × 3), the combined organic extract was dried over Na_2SO_4 and concentrated under reduced pressure. The crude product was separated by FCC (hexane-CH_2Cl_2, 60:40 to 80:20, v/v) to yield [4',5',6',7'-$^2H_4$]brassinin (**16a**, 69.6 mg, 50% yield from **185a**, Pedras et al., 1998).

HPLC-DAD Method A, t_R = 20.1 min.

^{1}H NMR (500 MHz C^2H_3CN) δ 9.25 (br s, 1H), 8.25 (br s, 1H), 7.31 (s, 1H), 5.04 (d, *J* = 5 Hz, 2H), 2.55 (s, 3H).

HR-EIMS *m/z* measured 240.0694 (240.0693 calcd for $C_{11}H_8{}^2H_4N_2S_2$); EIMS *m/z* (relative abundance) 240 $[M]^+$ (36), 166 (12), 134 (100), 106 (13).

4.3.17 Brassinin (16)

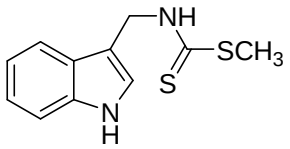

16

A solution of $HONH_2 \cdot HCl$ (190 mg, 2.74 mmol) and Na_2CO_3 (161 mg, 1.52 mmol) in H_2O (2.7 mL) was added to a solution of indole-3-carboxaldehyde (**106**, 200 mg, 1.38 mmol) in EtOH (6 mL). The resulting mixture was refluxed (68 - 70 ºC) for 45 min. EtOH was evaporated and the residue was filtered off and washed with ice-cold H_2O (10 mL) to yield indole-3-carboxaldehyde oxime (**185**, 213 mg, 96%). A solution of NaOH (10 mL, 1 M) was added to a solution of indole-3-carboxaldehyde oxime (40 mg, 0.25 mmol) in CH_3OH (2 mL) and the resulting solution was cooled in an ice-bath. Devarda's alloy (1.2 g) was added to the cooled mixture with stirring at r.t. After 50 min the reaction mixture was diluted with H_2O (10 mL), and was filtered under vacuum. The reaction mixture was then concentrated under reduced pressure, the remaining aqueous mixture was extracted with Et_2O (30 mL × 3). The combined organic extract was dried over Na_2SO_4 and was concentrated under reduced pressure to yield indolyl-3-methanamine (**117**, 31 mg, 85%) which was treated as reported above for [4',5',6',7'-$^2H_4$]brassinin (**16a**) to yield brassinin (**16**, 31.1 mg, 53% yield from **117**, Pedras et al., 1998).

HPLC-DAD Method A, t_R = 20.1 min.

^{1}H NMR (500 MHz C^{2}H$_3$CN) δ 9.26 (br s, 1H), 8.25 (br s, 1H), 7.63 (d, *J* = 8 Hz, 1H), 7.42 (d, *J* = 8 Hz, 1H), 7.30 (s, 1H), 7.16 (dd, *J* = 8, 8 Hz, 1H), 7.08 (dd, *J* = 8, 8 Hz, 1H), 5.03 (d, *J* = 5 Hz, 2H), 2.55 (s, 3H).

HR-EIMS *m/z* measured 236.0438 (236.0442 calcd for $C_{11}H_{12}N_2S_2$).

EIMS *m/z* (relative abundance) 236 $[M]^+$ (27), 162 (8), 130 (100), 102 (11).

4.3.18 [3,3,3-$^2H_3$]1-Methoxybrassinin (18a)

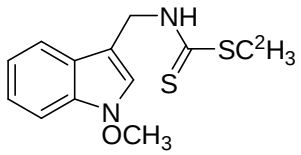

18a

A solution of $Na_2WO_4 \cdot 2H_2O$ (98.3 mg, 0.298 mmol) in H_2O (600 μL) was added to a stirred solution of indoline (**186**, 199 mg, 1.70 mmol) in CH_3OH (5 mL) and the suspension was then cooled to -20 °C. A solution of H_2O_2 (1.4 mL, 15 mmol) in CH_3OH (1.7 mL) was added drop wise to the cooled suspension over 10 min, the reaction mixture was stirred at r.t. for 10 min, after which solid K_2CO_3 (1.88 g, 13.6 mmol) and $(CH_3O)_2SO_2$ (245 μL, 2.72 mmol) were added under vigorous stirring (Somei and Kawasaki, 1989). After being stirred for 10 min, the reaction mixture was diluted with H_2O (20 mL), was extracted with Et_2O (30 mL × 3), the combined organic extract was dried over Na_2SO_4 and was concentrated under reduced pressure. The crude material was separated by FCC (hexane-CH_2Cl_2, 70:30, v/v) to yield 1-methoxyindole (**187**, 112 mg, 45%). Freshly distilled $POCl_3$ (69 μL, 0.75 mmol) was added to a solution of 1-methoxyindole (100 mg, 0.68 mmol) in DMF (600 μL) and the reaction mixture was stirred at r.t. After 40 min, a solution of aqueous NH_3 (4 mL, 28 %) was added to the reaction mixture followed by extraction with Et_2O (10 mL × 3). The combined organic extract was dried over Na_2SO_4 and was concentrated under reduced pressure to yield 1-methoxyindole-3-carboxaldehyde (113 mg, 96 %). A solution of $HONH_2 \cdot HCl$ (91 mg, 1.2 mmol) and Na_2CO_3 (61.5 mg, 0.580 mmol) in H_2O (870 μL) was added to a solution of 1-methoxyindole-3-carboxaldehyde (114.7 mg, 0.655 mmol) in EtOH (3 mL). The resulting reaction mixture was refluxed (83 - 85 ºC) for 60 min, was diluted with H_2O (3 mL) and was extracted with Et_2O (20 mL × 3). The combined organic extract was washed with brine (10 mL × 2), was dried over Na_2SO_4 and was concentrated under reduced pressure to yield 1-methoxyindole-3-carboxaldehyde oxime (**188**, 131.4 mg, 99 %). $NaBH_3CN$ (182 mg, 2.88 mmol) and NH_4OAc (245.5 mg, 3.18 mmol) were added to a solution of 1-methoxyindole-3-carboxaldehyde oxime (55 mg, 0.29 mmol) in

CH_3OH (695 μL) cooled to 0 ºC and the resulting mixture was treated with $TiCl_3$ in 2 M HCl (892 μL, 2.04 mmol) neutralized with NaOH (Pedras and Zaharia, 2000). After being stirred for 15 min at 0 ºC the reaction mixture was diluted with H_2O (2.4 mL), was basified with 5 M NaOH (mL) and was extracted with CH_2Cl_2 (15 mL × 3). The combined organic extract was dried over Na_2SO_4 and was concentrated under reduced pressure to yield crude 1-methoxyindolyl-3-methanamine (**189**, 43 mg) which was used in the next step without purification (Pedras and Zaharia, 2000). Et_3N (38 μL, 0.27 mmol) and CS_2 (15 μL, 0.25 mmol) were added to a solution of the amine **189** (43 mg, 0.24 mmol) in pyridine (115 μL) cooled to 0 ºC. After being stirred for 60 min at 0 ºC, IC^2H_3 (15 μL, 0.24 mmol) was added and the reaction mixture was kept at 5 ºC for 90 min. The reaction mixture was diluted with H_2O (2 mL), was extracted with Et_2O (10 mL × 2), the combined organic extract was dried over Na_2SO_4 and was concentrated under reduced pressure. The reaction mixture was separated by FCC (hexane-CH_2Cl_2, 60:40 to 50:50, v/v) to yield [3,3,3-$^2H_3$]1-methoxybrassinin (**18a**, 41 mg, 53% yield from oxime **188**, Pedras and Okinyo, 2006a).

HPLC-DAD Method A, t_R = 25.3 min.

^1H NMR (500 MHz C^2HCl_3) δ 7.62 (d, *J* = 8 Hz, 1H), 7.47 (d, *J* = 8 Hz, 1H), 7.35 (s, 1H), 7.32 (dd, *J* = 7, 7 Hz, 1H), 7.18 (dd, *J* = 7.5, 7.5 Hz, 1H), 7.02 (br s, 1H), 5.04 (d, *J* = 4 Hz, 2H), 4.12 (s, 3H).

HR-EIMS *m/z* measured 269.0732 (269.0736 calcd for $C_{12}H_{11}{}^2H_3N_2OS_2$).

EIMS *m/z* (relative abundance) 269 $[M]^+$ (7), 238 (100), 187 (14), 160 (81), 145 (19), 129 (37).

4.3.19 [4',5',6',7'-$^2H_4$]1-Methoxybrassinin (18b)

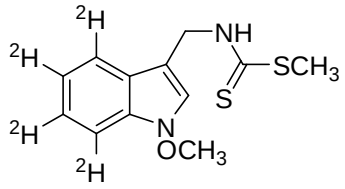

18b

$NaBH_3CN$ (195 mg, 1.68 mmol) was added to a stirred solution of [4,5,6,7-$^2H_4$]indole (**105a**, 135 mg, 1.12 mmol) in glacial acetic acid (2 mL) under an argon atmosphere. The reaction mixture was stirred at r.t. for 60 min, was diluted with H_2O (4 mL), was basified with NaOH (mL), was extracted with Et_2O (30 mL × 3), the combined organic extract was dried over Na_2SO_4 and was concentrated under reduced pressure. The crude material was separated by FCC (CH_2Cl_2) to yield [4,5,6,7-$^2H_4$]indoline (**186a**, 113.2 mg, 82%). A solution of $Na_2WO_4 \cdot 2H_2O$ (53 mg, 0.16 mmol) in H_2O (0.35 mL) was added to the stirred solution of [4,5,6,7-$^2H_4$]indoline (113.2 mg, 0.920 mmol) in CH_3OH (3 mL) and the suspension was cooled to -20 °C. A solution of H_2O_2 (766 µL, 7.96 mmol) in CH_3OH (1 mL) was added drop wise to the cooled suspension. The reaction mixture was stirred at r.t. for 10 min, after which solid K_2CO_3 (12 g, 7.36 mmol) and $(CH_3O)_2SO_2$ (133 µL, 1.47 mmol) were added under vigorous stirring (Somei and Kawasaki, 1989). After being stirred for 10 min, the reaction mixture was diluted with H_2O (20 mL), was extracted with Et_2O (30 mL × 3), the combined organic extract was dried over Na_2SO_4 and was concentrated under reduced pressure. The crude material was separated by FCC (hexane-CH_2Cl_2, 70:30, v/v) to yield [4,5,6,7-$^2H_4$]1-methoxyindole (**187a**, 73 mg, 52%). Freshly distilled $POCl_3$ (69 µL, 0.75 mmol) was added to a solution of [4,5,6,7-$^2H_4$]1-methoxyindole (102 mg, 0.68 mmol) in DMF (600 µL) and the reaction mixture was stirred at r.t. After 40 min, a solution of aqueous NH_3 (4 mL, 28%) was added to the reaction mixture, the reaction mixture was extracted with Et_2O (10 mL × 3), the combined organic extract was dried over Na_2SO_4 and was concentrated under reduced pressure to yield [4,5,6,7-$^2H_4$]1-methoxyindole-3-carboxaldehyde (113 mg, 93%). A solution of $HONH_2 \cdot HCl$ (80.6 mg, 1.16 mmol) and

Na_2CO_3 (61.5 mg, 0.580 mmol) in H_2O (810 μL) was added to a solution of [4,5,6,7-$^2H_4$]1-methoxyindole-3-carboxaldehyde (103 mg, 0.580 mmol) in EtOH (2.7 mL). The resulting mixture was refluxed (85 ºC) for 60 min, was diluted with H_2O (3 mL) and was extracted with Et_2O (20 mL × 3). The combined organic extract was washed with brine (10 mL × 2), was dried over Na_2SO_4 and was concentrated under reduced pressure to yield [4',5',6',7'-$^2H_4$]1-methoxyindolyl-3-carboxaldehyde oxime (**188a**, 122.1 mg, 99 %). $NaBH_3CN$ (163 mg, 2.58 mmol) and NH_4OAc (219 mg, 2.84 mmol) were added to a solution of **188a** (50 mg, 0.26 mmol) in CH_3OH (640 μL) cooled to 0 ºC and the resulting mixture was treated with $TiCl_3$ in 2 M HCl (795 μL, 24 mmol) neutralized with NaOH (Pedras and Zaharia, 2000). After being stirred for 15 min at 0 ºC, the reaction mixture was diluted with H_2O (2.2 mL), was basified with NaOH (5 M) and was extracted with CH_2Cl_2 (15 mL × 3). The combined organic extract was dried over Na_2SO_4 and was concentrated under reduced pressure to yield crude [4',5',6',7'-$^2H_4$]1-methoxyindolyl-3-methanamine (**189a**, 40.33 mg) which was used in the next step without purification. Et_3N (34 μL, 0.25 mmol) and CS_2 (13 μL, 0.22 mmol) were added to a cooled solution (0 ºC) of [4',5',6',7'-$^2H_4$]1-methoxyindolyl-3-methanamine (40.3 mg, 0.224 mmol) in pyridine (105 μL). After being stirred for 60 min at 0 ºC, ICH_3 (14 μL, 0.22 mmol) was added to the reaction mixture which was kept at 5 ºC for 90 min. The reaction mixture was diluted with H_2O (2 mL), was extracted with Et_2O (10 mL × 2), the combined organic extract was dried over Na_2SO_4 and was concentrated under reduced pressure. The resulting crude reaction mixture was separated by FCC (hexane-CH_2Cl_2, 60:40 to 50:50, v/v) to yield [4',5',6',7'-$^2H_3$]1-methoxybrassinin (**18b**, 46.5 mg, 67% yield from **188a**, Pedras and Okinyo, 2006a).

HPLC-DAD Method A, t_R = 25.3 min.

^{1}H NMR (500 MHz C^2HCl_3) δ 7.35 (s, 1H), 7.04 (br s, NH), 5.04 (d, *J* = 4.5 Hz, 2H), 4.12 (s, 3H), 2.67 (s, 3H).

HR-EIMS *m/z* measured 270.0794 (270.0795 calcd for $C_{12}H_{10}{}^2H_4N_2OS_2$).

EIMS *m/z* (relative abundance) 270 $[M]^+$ (6), 239 (64), 222 (15), 191 (8), 164 (100), 149 (15), 133 (43).

4.3.20 [3,3,3,4',5',6',7'-$^2H_7$]1-Methoxybrassinin (18c)

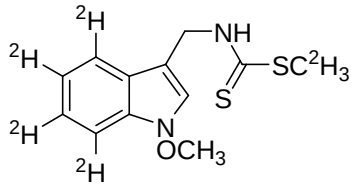

18c

Et_3N (37 μL, 0.27 mmol) and CS_2 (15 μL, 0.24 mmol) were added to a cooled solution (0 ºC) of freshly prepared amine **189a** (44 mg, 0.24 mmol) in pyridine (118 μL). After being stirred for 60 min at 0 ºC, IC^2H_3 (16 μL, 0.24 mmol) was added and the reaction mixture was treated as reported above for [4',5',6',7'-$^2H_3$]1-methoxybrassinin (**18b**) to yield [3,3,3,4',5',6',7'-$^2H_7$]1-methoxybrassinin (**18c**, 52.7 mg, 68% yield from oxime **188a**, Pedras and Okinyo, 2006a).

HPLC-DAD Method A, t_R = 25.3 min.

^1H NMR (500 MHz C^2HCl_3) δ 7.32 (br s, 1H), 7.04 (br s, NH), 5.02 (br s, 2H), 4.11 (s, 3H).

HR-EIMS *m/z* measured 273.0984 (273.0987 calcd for $C_{12}H_7{}^2H_7N_2OS_2$).

EIMS *m/z* (relative abundance) 273 $[M]^+$ (7), 242 (100), 191 (12), 164 (85), 149 (19), 133 (40).

4.3.21 1-Methoxybrassinin (18)

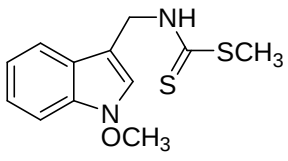

18

Et_3N (37 μL, 0.27 mmol) and CS_2 (14 μL, 0.24 mmol) were added to a solution of freshly prepared amine **189** (42.1 mg, 0.238 mmol) in pyridine (112 μL) cooled to 0 ºC.

After being stirred for 60 min at 0 ºC, ICH_3 (15 μL, 0.238 mmol) was added and the reaction mixture was treated as reported above for [4',5',6',7'-$^2H_3$]1-methoxybrassinin (**18b**) to yield 1-methoxybrassinin (**18**, 44.6 mg, 57% yield from oxime **188**, Pedras and Okinyo, 2006a).

HPLC-DAD Method A, t_R = 25.3 min.

^{1}H NMR (500 MHz C^2HCl_3) δ 7.62 (d, *J* = 8 Hz, 1H), 7.47 (d, *J* = 8 Hz, 1H), 7.35 (s, 1H), 7.32 (dd, *J* = 8, 8 Hz, 1H), 7.19 (dd, *J* = 8, 8 Hz, 1H), 7.03 (br s, 1H), 5.04 (d, *J* = 4 Hz, 2H), 4.12 (s, 3H), 2.67 (s, 3H).

HR-EIMS *m/z* measured 266.0556 (266.0548 calcd for $C_{12}H_{14}N_2OS_2$).

EIMS *m/z* (relative abundance) 266 $[M]^+$ (5), 235 (89), 187 (14), 160 (100), 145 (29), 129 (61).

4.3.22 1-Methylbrassinin (192)

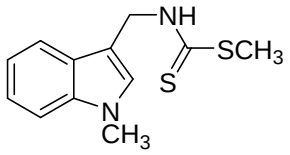

192

A solution of $HONH_2 \cdot HCl$ (87.6 mg, 1.26 mmol) and Na_2CO_3 (66.7 mg, 0.629) in H_2O (826 μL) was added to a stirred solution of 1-methylindole-3-carboxaldehyde (**175**, 100 mg, 0.629 mmol) in EtOH (3 mL). The resulting mixture was refluxed (80 – 83 °C) for 30 min. The solvent was evaporated and the residue was taken in H_2O (20 mL), and was extracted with Et_2O (20 mL × 3). The combined organic extract was dried over Na_2SO_4 and the reaction mixture was concentrated under reduces pressure to yield crude 1-methylindole-3-carboxaldehyde oxime (**190**, 101.9 mg, 93 %). A solution of NaOH (18 mL, 1 M) was added to a solution of **190** (80 mg, 0.46 mmol) in CH_3OH (4 mL) and the resulting mixture was cooled in an ice-bath. Devarda's alloy (2.13 g) was added to the cooled mixture with stirring at r.t. After 90 min the reaction mixture was diluted with H_2O (20 mL), and was filtered under vacuum. The reaction mixture was concentrated under reduced pressure, and the remaining aqueous mixture was extracted with Et_2O

(120 mL × 3). The combined organic extract was dried over Na_2SO_4 and was concentrated under reduced pressure to yield crude 1-methylindolyl-3-methanamine (**191**, 64 mg, 90 %) which was used in the next step without purification. Et_3N (61 μL, 0.44 mmol) and CS_2 (24 μL, 0.40 mmol) were added to a cooled solution (0 ºC) of the amine **191** (64 mg, 0.40 mmol) in pyridine (190 μL). After being stirred for 60 min at 0 ºC, ICH_3 (25 μL, 0.40 mmol) was added and the reaction mixture was treated as reported above for [4',5',6',7'-$^2H_3$]1-methoxybrassinin (**18b**) to yield 1-methylbrassinin (**192**, 60.2 mg, 52% yield from oxime **190**).

HPLC-DAD Method A, t_R = 24.4 min.
^{1}H NMR (500 MHz C^{2}HCl$_3$) δ 7.63 (d, *J* = 8 Hz, 1H), 7.36 (d, *J* = 8 Hz, 1H), 7.30 (dd, *J* = 8, 8 Hz, 1H), 7.18 (dd, *J* = 8, 8 Hz, 1H), 7.10 (s, 1H), 5.05 (d, *J* = 3.5 Hz, 2H), 3.80 (s, 3H), 2.66 (s, 3H).
HR-EIMS *m/z* measured 250.0603 (250.0598 calcd for $C_{12}H_{14}N_2S_2$).
EIMS *m/z* (relative abundance) 250 $[M]^+$ (25), 144 (100), 176 (11).

4.3.23 1-(*tert*-Butoxycarbonyl)brassinin (181)

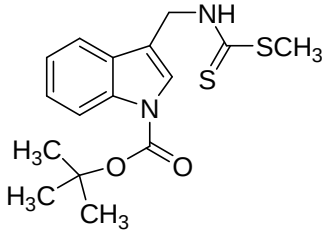

181

Et_3N (62 μL, 0.45 mmol) and CS_2 (24 μL, 0.41 mmol) were added to a cooled solution of freshly prepared amine **179** (100 mg, 0.407 mmol) in pyridine (600 μL) at 0 ºC. After stirring for 60 min at 0 ºC, ICH_3 (26 μL, 0.41 mmol) was added and the reaction mixture was kept at 5 ºC. After 90 min the reaction mixture was diluted with H_2O (5 mL), was extracted with Et_2O (20 mL × 3), the combined organic extract was dried over Na_2SO_4 and was concentrated. The crude product was purified by FCC

(hexane-EtOAc, 70:30, v/v) to yield 1-(*tert*-butoxycarbonyl)brassinin (**181**, 112 mg, 72% yield from 1-(*tert*-butoxycarbonyl)indolyl-3-carboxaldehyde oxime, Kutschy et al., 1997; 1998).

HPLC-DAD Method A, t_R = 34.1 min.

^{1}H NMR (500 MHz C^2HCl_3) δ 7.68 (d, *J* = 8 Hz, 1H), 7.56 (d, *J* = 8 Hz, 1H), 7.31 (dd, *J* = 8, 8 Hz, 1H), 7.25 (dd, *J* = 8, 8 Hz, 1H), 6.90 (s, 1H), 5.06 (d, *J* = 3.5 Hz, 2H), 2.66 (s, 3H), 1.74 (s, 9H).

HR-EIMS *m/z* measured 336.0967 (336.0966 calcd for $C_{16}H_{20}N_2O_2S_2$).

EIMS *m/z* (relative abundance) 336 $[M]^+$ (5), 288 (10), 232 (22), 174 (22), 130 (64), 57 (100).

4.3.24 1-Acetylbrassinin (184)

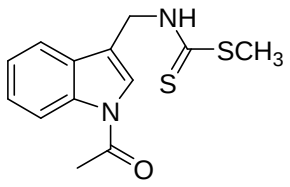

184

Et_3N (49 μL, 0.35 mmol) and CS_2 (21 μL, 0.35 mmol) were added to a solution of freshly prepared amine **182** (33 mg, 0.18 mmol) in CH_2Cl_2 (2 mL) at r.t. After stirring for 90 min, ICH_3 (13 μL, 0.21 mmol) was added with stirring for further 20 min. The reaction mixture was concentrated, and the crude product was subjected to FCC (CH_2Cl_2) to yield 1-acetylbrassinin (**184**, 28.4 mg, 41% yield from 1-acetylindole-3-carboxaldehyde oxime).

HPLC-DAD Method A, t_R = 22.2 min.

^{1}H NMR (500 MHz C^2HCl_3) δ 7.65 (d, *J* = 8 Hz, 1H), 7.53 (d, *J* = 8 Hz, 1H), 7.28 (dd, *J* = 8, 8 Hz, 1H), 7.22 (dd, *J* = 8, 8 Hz, 1H), 7.01 (s, 1H), 5.07 (d, *J* = 3.5 Hz, 2H), 2.66 (s, 3H), 2.64 (s, 3H).

HR-EIMS *m/z* measured 278.0550 (278.0548 calcd for $C_{13}H_{14}N_2OS_2$).

EIMS *m/z* (relative abundance) 278 $[M]^+$ (9), 230 (16), 172 (29), 130 (100), 102 (7).

4.3.25 [4',5',6',7'-$^2H_4$]Indolyl-3-acetonitrile (49a)

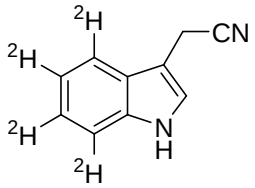

49a

ICH_3 (400 μL, 2.80 mmol) was added to Mg (turnings, 80 mg, 3.3 mmol) in dry Et_2O (5 mL) with stirring under argon atmosphere. After the Mg was consumed, excess ICH_3 was distilled off and fresh dry Et_2O (4 mL) was added. A solution of [4,5,6,7-$^2H_4$]indole (**105a**, 100 mg, 0.830 mmol) in dry Et_2O (700 μL) was added drop wise and the mixture was allowed to stir for 15 min at r.t., followed by drop wise addition of bromoacetonitrile (160 μL, 2.70 mmol, Pedras et al., 2003a). After being stirred for 20 min, the reaction mixture was concentrated under reduced pressure and the residue was taken in H_2O (40 mL). The resulting mixture was neutralized with HCl (2 mL, 1 M) and was extracted with CH_2Cl_2 (30 mL × 3). The combined organic extract was dried over Na_2SO_4 and was concentrated to dryness under reduced pressure. Separation by FCC (hexane-CH_2Cl_2, 50:50 to 20:80) yielded [4',5',6',7'-$^2H_4$]indolyl-3-acetonitrile (**49a**, 75.7 mg, 57% yield, Pedras and Okinyo, 2006a).

HPLC-DAD Method A, t_R = 12.9 min.

^1H NMR (500 MHz C^2HCl_3) δ 8.23 (br s, NH), 7.24 (s, 1H), 3.86 (s, 2H).

HR-EIMS *m/z* measured 160.0940 (160.0939 calcd for $C_{10}H_4{}^2H_4N_2$).

EIMS *m/z* (relative abundance) 160 $[M]^+$ (62), 159 (100), 134 (32).

4.3.26 [4,5,6,7-$^2H_4$]Indole (105a)

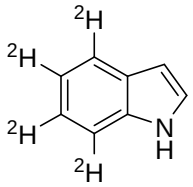

28

A solution of [2,3,4,5,6,-$^2H_5$]nitrobenzene (**168a**, 4.2 mL, 39 mmol) and chloroacetonitrile (250 μL, 3.94 mmol) in DMSO (3.9 mL) was added drop wise over 30 min to a thoroughly stirred suspension of NaOH (1.60 g, 39.4 mmol) in DMSO (3.9 mL) at 20 ºC (Makosza and Winiarski, 1984). After 60 min, the reaction mixture was poured into ice-cold HCl (25 mL, 1 M), was diluted with H_2O (10 mL), and was extracted with $CHCl_3$ (50 mL × 3). The combined organic extract was washed with H_2O (70 mL), was dried over Na_2SO_4 and was concentrated under reduced pressure. Separation by FCC (hexane-CH_2Cl_2, 100:0 to 25:75) yielded a mixture of [3,4,5,6,-$^2H_4$]2-nitrophenylacetonitrile and [2,3,5,6,-$^2H_4$]4-nitrophenylacetonitrile (in a 10:1 ratio, 40% yield). Next, 10% Pd/C (220 mg) was added to the solution of [3,4,5,6,-$^2H_4$]2- and [2,3,5,6,-$^2H_4$]4-nitrophenylacetonitrile (200 mg) in freshly distilled EtOAc (20 mL) and the resulting reaction mixture was stirred under H_2 atmosphere (balloon pressure) at r.t. After 40 h, the catalyst was filtered off, and the filtrate was concentrated under reduced pressure. The residue was taken in CH_2Cl_2 (15 mL), was washed with HCl (10 mL × 2, 1 M), was dried over Na_2SO_4 and was concentrated under reduced pressure to yield [3,4,5,6,-$^2H_4$]indole (**105a**, 97.7 mg, 61% yield, Pedras and Okinyo, 2006a).

HPLC-DAD Method A, t_R = 15.1 min.

^{1}H NMR (500 MHz C^{2}HCl$_3$) δ 8.12 (br s, NH), 7.23 (br s, 1H), 6.61 (br s, 1H).

HR-EIMS *m/z* measured 121.0827 (121.0830 calcd for $C_8H_3{}^2H_4N$).

EIMS *m/z* (relative abundance) 121 $[M]^+$ (100), 94 (22), 71 (11), 69 (12), 57 (17).

4.3.27 [4',5',6',7'-$^2H_4$]Cyclobrassinin (28a)

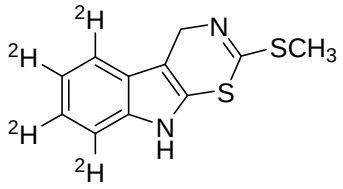

28a

Pyridinium bromide perbromide (41 mg, 0.13 mmol) was added to a stirred solution of [4',5',6',7'-$^2H_4$]brassinin (**16a**, 30 mg, 0.13 mmol) in dry THF (4 mL). After 40 min, DBU (59 μL, 0.40 mmol) was added and reaction mixture was stirred for further 60 min. The reaction mixture was concentrated under reduced pressure and was subjected to FCC (CH_2Cl_2-hexane, 80:20 to 100:0, v/v) to yield [4',5',6',7'-$^2H_4$]cyclobrassinin (**28a**, 17.4 mg, 58% yield, Pedras et al., 1998).

HPLC-DAD Method A, t_R = 25.7 min.
^{1}H NMR (500 MHz C^2HCl_3) δ 7.92 (br s, 1H), 5.10 (s, 2H), 2.57 (s, 3H).
HR-EIMS *m/z* measured 238.0537 (238.0536 calcd for $C_{11}H_6{}^2H_4N_2S_2$).
EIMS *m/z* (relative abundance) 238 $[M]^+$ (11), 165 (100), 121 (60).

4.3.28 Cyclobrassinin (28)

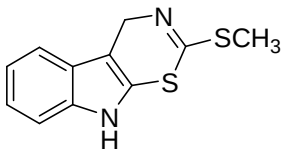

28

Pyridinium bromide perbromide (27.8 mg, 0.087 mmol) was added to a stirred solution of brassinin (**16**, 20 mg, 0.085 mmol) in dry THF (2.5 mL). After stirring for 40 min, DBU (40 μL, 0.27 mmol) was added and the reaction mixture was treated as

reported above for [4',5',6',7'-$^2H_4$]cyclobrassinin (**28a**) to yield cyclobrassinin (**28**, 8.7 mg, 44%, yield, Pedras et al., 1998).

HPLC-DAD Method A, t_R = 25.7 min.

^{1}H NMR (500 MHz C^2HCl_3) δ 7.92 (br s, 1H), 7.49 (d, *J* = 7.5 Hz, 1H), 7.33 (d, *J* = 8 Hz, 1H), 7.14-7.20 (m, 2H), 5.10 (s, 2H), 2.57 (s, 3H).

HR-EIMS *m/z* measured 234.0274 (234.0285 calcd for $C_{11}H_{10}N_2S_2$).

EIMS *m/z* (relative abundance) 234 $[M]^+$ (13), 161 (100), 117 (43).

4.3.29 1-Methylcyclobrassinin (193*)*

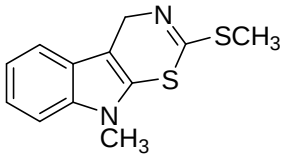

193

NaH (5.1 mg, 0.13 mmol) and ICH_3 (8 μL, 0.13 mmol) were added to a stirred solution of cyclobrassinin (**28**, 15 mg, 064 mmol) in dry THF (2 mL) at 0 ºC. After being stirred for 1 h at 0 ºC, the reaction mixture was treated with ice-cold H_2O (10 mL), was extracted with CH_2Cl_2 (15 mL × 3), the combined organic extract was dried over Na_2SO_4 and was concentrated. The residue obtained was subjected to FCC (CH_2Cl_2-hexane, 60:40 and 100:0, v/v) to yield 1-methylcyclobrassinin (**193**, 13 mg, 82% yield, Kutschy et al., 1998).

HPLC-DAD Method A, t_R = 32.5 min.

^{1}H NMR (500 MHz C^2HCl_3) δ 7.50 (d, *J* = 8 Hz, 1H), 7.31 (d, *J* = 8 Hz, 1H), 7.21 (dd, *J* = 8 Hz, 1H), 7.14 (dd, *J* = 7.5, 7.5 Hz, 1H), 5.10 (s, 2H), 3.66 (s, 3H), 2.59 (s, 3H).

HR-EIMS *m/z* measured 248.0440 (248.0442 calcd for $C_{12}H_{12}N_2S_2$).

EIMS *m/z* (relative abundance) 248 $[M]^+$ (14), 175 (100), 130 (15).

4.3.30 [4',5',6',7'-$^2H_4$]Sinalbin B (31a)

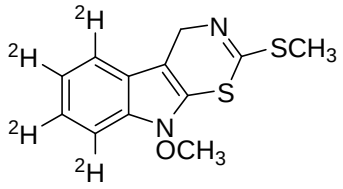

31a

N-Bromosuccinimide (13.2 mg, 0.074 mmol) was added to a solution of [4',5',6',7'-$^2H_4$]1-methoxybrassinin (**18b**, 20 mg, 0.074 mmol) in dry CH_2Cl_2 (1 mL). After being stirred for 10 min at r.t., Et_3N (21 μL, 0.15 mmol) was added and the reaction mixture was stirred for further 5 min (Pedras and Zaharia, 2000). Silica gel was immediately added to the reaction mixture which was concentrated to dryness at r.t. and was subjected to FCC (hexane-EtO_2, 90:10, v/v) to yield [4',5',6',7'-$^2H_4$]sinalbin B (**31a**, 9.3 mg, 47% yield).

HPLC-DAD Method A, t_R = 33.9 min.
^{1}H NMR (500 MHz C^2H_3CN) δ 5.10 (s, 2H), 4.02 (s, 3H), 2.61 (s, 3H).
HR-EIMS *m/z* measured 268.0648 (268.0642 calcd for $C_{12}H_8{}^2H_4N_2OS_2$).
EIMS *m/z* (relative abundance) 268 $[M]^+$ (19), 236 (46), 195 (68), 165 (100), 121 (58).

4.3.31 [3,3,3-$^2H_3$]Sinalbin B (31b)

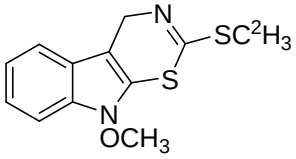

31b

N-Bromosuccinimide (13.2 mg, 0.074 mmol) was added to a solution of [3,3,3-$^2H_3$]1-methoxybrassinin (**18a**, 20 mg, 0.074 mmol) in dry CH_2Cl_2 (1 mL). After being stirred for 10 min at r.t., Et_3N (21 μL, 0.15 mmol) was added and the reaction mixture

was stirred for further 5 min (Pedras and Zaharia, 2000). The reaction mixture was then treated as described above for [4',5',6',7'-$^2H_4$]sinalbin B (**31a**) to yield [3,3,3-$^2H_3$]sinalbin B (**31b**, 10 mg, 51 % yield).

HPLC-DAD Method A, t_R = 33.9 min.
^{1}H NMR (500 MHz C^{2}H$_3$CN) δ 7.53 (d, *J* = 8 Hz, 1H), 7.49 (d, *J* = 8 Hz, 1H), 7.27 (dd, *J* = 8, 8 Hz, 1H), 7.18 (dd, *J* = 8, 8 Hz, 1H), 5.11 (s, 2H), 4.03 (s, 3H).
HR-EIMS *m/z* measured 267.0578 (267.0579 calcd for $C_{12}H_9{}^2H_3N_2OS_2$).
EIMS *m/z* (relative abundance) 267 $[M]^+$ (21), 235 (33), 191 (69), 161 (100), 117 (54).

4.3.32 Sinalbin B (31)

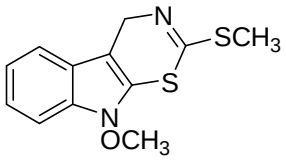

31

N-Bromosuccinimide (13.3 mg, 075 mmol) was added to a solution of 1-methoxybrassinin (**18**, 20 mg, 075 mmol) in dry CH_2Cl_2 (1 mL). After 10 min of stirring at r.t., Et_3N (21 μL, 0.15 mmol) was added and the reaction mixture was stirred for further 5 min (Pedras and Zaharia, 2000), and was treated as reported above for [4',5',6',7'-$^2H_4$]sinalbin B (**31a**) to yield sinalbin B (**31**, 8.3 mg, 42% yield).

HPLC-DAD Method A, t_R = 33.9 min.
^{1}H NMR (500 MHz C^{2}H$_3$CN) δ 7.52 (d, *J* = 8 Hz, 1H), 7.48 (d, *J* = 8 Hz, 1H), 7.26 (dd, *J* = 8, 8 Hz, 1H), 7.18 (dd, *J* = 7.5, 7.5 Hz, 1H), 5.10 (s, 2H), 4.06 (s, 3H), 2.60 (s, 3H).
HR-EIMS *m/z* measured 264.0387 (264.0391 calcd for $C_{12}H_{12}N_2OS_2$).
EIMS *m/z* (relative abundance) 264 $[M]^+$ (22), 232 (100), 191 (69), 161 (90), 117 (71).

4.3.33 [4',5',6',7'-$^2H_4$]1-Methoxyspirobrassinin (35a)

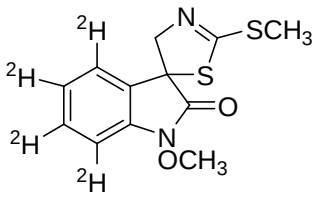

35a

PCC (111.7 mg, 0.518 mmol) was added in one portion to a stirred solution of [4',5',6',7'-$^2H_4$]1-methoxybrassinin (**18b**, 20 mg, 0.074 mmol) in CH_2Cl_2 (1 mL). After being stirred for 60 min at r.t. (Pedras et al., 2006a), the reaction mixture was diluted with CH_2Cl_2, silica gel was added and the mixture was concentration to dryness, and was subjected to FCC (hexane-EtOAc, 80:20, v/v) to yield [4',5',6',7'-$^2H_4$]1-methoxyspirobrassinin (**35a**, 8.6 mg, 41% yield).

HPLC-DAD Method A, t_R = 18.2 min.

^{1}H NMR (500 MHz C$^2H_3$CN) δ 4.60 (d, *J* = 15.5 Hz, 1H), 4.46 (d, *J* = 15.5 Hz, 1H), 3.99 (s, 3H), 2.62 (s, 3H).

HR-EIMS *m/z* measured 284.0588 (284.0591 calcd for $C_{12}H_8{}^2H_4N_2O_2S_2$).

EIMS *m/z* (relative abundance) 284 $[M]^+$ (78), 253 (11), 225 (28), 180 (46), 152 (100), 120 (17).

4.3.34 1-Methoxyspirobrassinin (35)

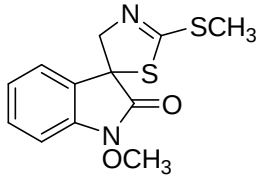

35

PCC (113.2 mg, 0.525 mmol) was added in one portion to a stirred solution of 1-methoxybrassinin (**18**, 20 mg, 0.075 mmol) in CH_2Cl_2 (1 mL). After being stirred for 60 min at r.t., the reaction mixture was treated as reported above for [4',5',6',7'-$^2H_4$]1-methoxyspirobrassinin (**35a**) to yield 1-methoxyspirobrassinin (**35**, 8.7 mg, 41% yield, Pedras et al., 2006a).

HPLC-DAD Method A, t_R = 18.2 min.

^{1}H NMR (500 MHz C^{2}H$_3$CN) δ 7.39-7.43 (m, 2H), 7.17 (d, *J* = 7.5 Hz, 1H), 7.06 (d, *J* = 7.5 Hz, 1H), 4.60 (d, *J* = 15.5 Hz, 1H), 4.46 (d, *J* = 15.5 Hz, 1H), 3.99 (s, 3H), 2.62 (s, 3H).

HR-EIMS *m/z* measured 280.0343 (280.0340 calcd for $C_{12}H_{12}N_2O_2S_2$).

EIMS *m/z* (relative abundance) 280 $[M]^+$ (73), 249 (11), 221 (28), 176 (45), 148 (100), 116 (16).

4.3.35 1-Methylspirobrassinin (194)

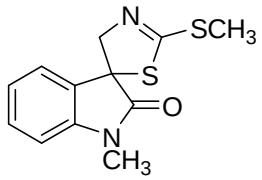

194

NaH (4.8 mg, 0.12 mmol) and ICH_3 (7.5 μL, 0.12 mmol) were added to a cooled solution (0 ºC) of spirobrassinin (**34**, 15 mg, 0.06 mmol) in dry THF (2 mL) under stirring. After stirring for 60 min at 0 ºC, ice-cold H_2O (10 mL) was added. The resulting mixture was extracted with EtOAc (15 mL × 3), the combined organic extract was dried over Na_2SO_4 and was concentrated under reduced pressure. The crude extract was subjected to FCC (CH_2Cl_2-CH_3OH, 99:1 and 98:2, v/v) to yield 1-methylspirobrassinin (**194**, 14.4 mg, 91% yield, Pedras and Hossain, 2006).

HPLC-DAD Method A, t_R = 16.9 min.

^{1}H NMR (500 MHz C^{2}HCl$_3$) δ 7.38 (d, *J* = 7.5 Hz, 1H), 7.34 (dd, *J* = 8, 8 Hz, 1H), 7.12 (dd, *J* = 7.5, 7.5 Hz, 1H), 6.85 (d, *J* = 8 Hz, 1H), 4.63 (d, *J* = 15 Hz, 1H), 4.53 (d, *J* = 15 Hz, 1H), 3.25 (s, 3H), 2.67 (s, 3H).

HR-EIMS *m/z* measured 264.0397 (264.0391 calcd for $C_{12}H_{12}N_2OS_2$).

EIMS *m/z* (relative abundance) 264 $[M]^+$ (71), 217 (67), 191 (100), 159 (35), 130 (38).

4.3.36 1-Acetylspirobrassinin (195)

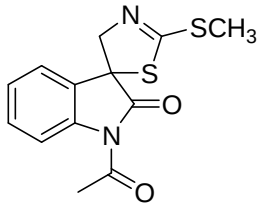

195

Pyridine (500 μL) was added to a stirred solution of spirobrassinin (**34**, 5 mg) in Ac_2O (500 μL). After being stirred for 60 min, the reaction mixture was diluted with toluene and was concentrated under reduced pressure to yield 1-acetylspirobrassinin (**195**, 4.8 mg, 80% yield).

HPLC-DAD Method A, t_R = 16.9 min.

^{1}H NMR (500 MHz C^{2}HCl$_3$) δ 7.39 (d, *J* = 7.5 Hz, 1H), 7.36 (dd, *J* = 8, 8 Hz, 1H), 7.14 (dd, *J* = 7.5, 7.5 Hz, 1H), 6.88 (d, *J* = 8 Hz, 1H), 4.62 (d, *J* = 15 Hz, 1H), 4.48 (d, *J* = 15 Hz, 1H), 2.66 (s, 3H), 2.64 (s, 3H).

HR-EIMS *m/z* measured 292.0339 (292.0340 calcd for $C_{13}H_{12}N_2O_2S_2$).

EIMS *m/z* (relative abundance) 292 $[M]^+$ (100), 250 (70), 203 (26), 177 (100), 145 (38), 117 (34).

4.3.37 1-(*tert*-Butoxycarbonyl)spirobrassinin (196)

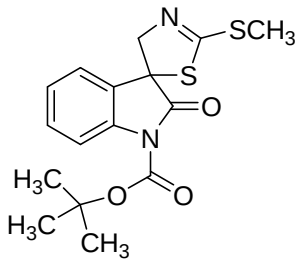

196

A solution of Boc_2O (21 mg, 0.096 mmol) in THF (200 µL) was added to a stirred solution of spirobrassinin (**DO-075**, 20 mg, 0.08 mmol) in THF (600 µL). The reaction mixture was cooled to 5 ºC and DMAP (0.21 mg, 0.0017 mmol) was added. After being stirred for 40 min, the reaction mixture was concentrated under reduced pressure and was subjected to FCC (hexane-EtOAc, 50:50, v/v) to yield 1-(*tert*-butoxycarbonyl)spirobrassinin (**196**, 31.4 mg, quant.).

HPLC-DAD Method A, t_R = 30.1 min.

^{1}H NMR (500 MHz C^2HCl_3) δ 7.40 (d, *J* = 7.5 Hz, 1H), 7.37 (dd, *J* = 8, 8 Hz, 1H), 7.16 (dd, *J* = 7.5, 7.5 Hz, 1H), 6.80 (d, *J* = 8 Hz, 1H), 4.64 (d, *J* = 15 Hz, 1H), 4.55 (d, *J* = 15 Hz, 1H), 2.65 (s, 3H), 1.75 (s, 9H).

HR-EIMS *m/z* measured 350.0767 (350.0759 calcd for $C_{16}H_{18}N_2O_3S_2$).

EIMS *m/z* (relative abundance) 350 $[M]^+$ (7), 250 (61), 203 (15), 177 (31), 149 (19), 116 (11), 57 (100).

4.3.38 [SC^2H_3]Brassicanal A (39b)

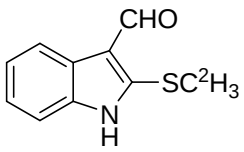

39b

$NaHCO_3$ (504 mg, 6 mmol) and P_4S_{10} (800 mg, 1.80 mmol) were added to a solution of oxindole (**197**, 400 mg, 3 mmol) in dry THF (8 mL). The reaction mixture was stirred at r.t. for 2.5 h and then filtered, the filtrate was concentrated to remove THF. Ice-cold H_2O was added to the residue and the flask kept in an ice-bath. The precipitate that formed was filtered off to yield indoline-2-thione (**198**, 322.4 mg, 72%). NaH (373 mg, 15.8 mmol) was added to a stirred solution of indoline-2-thione (200 mg, 1.34 mmol) in HCOOEt (3.8 mL, 47.4 mmol). After 5 min, the reaction mixture was diluted with H_2O (10 mL), was acidified with HCl (2.5 M), and the precipitate that formed was filtered off to yield 2-mercaptoindole-3-carboxaldehyde (113 mg). The remaining aqueous solution was extracted with EtOAc (100 mL × 3), the combined organic extract was dried over Na_2SO_4 and was concentrated to yield 2-mercaptoindole-3-carboxaldehyde (**135**, 100 mg). The total yield of 2-mercaptoindole-3-carboxaldehyde obtained was 213 mg (90%, Pedras and Okanga, 1999). Et_3N (35 μL, 0.25 mmol) and IC^2H_3 (32 μL, 0.51) were added to a solution of 2-mercaptoindole-3-carboxaldehyde (30 mg, 0.17 mmol) in dry Et_2O (2 mL). The reaction mixture was allowed to stir for 20 min and the precipitate that formed was filtered off and rinsed with Et_2O (5 mL × 3). The filtrate was washed with H_2O (10 mL), was dried over Na_2SO_4 and was concentrated. The crude reaction mixture was subjected to FCC (CH_2Cl_2-CH_3OH, 98:2, v/v) to yield [SC^2H_3]brassicanal A (**39b**, 18.3 mg, 56% yield).

HPLC-DAD Method A, = 11.3 min.

^{1}H NMR (500 MHz C^2H_3CN) δ 10.14 (s, 1H), 8.05 (d, *J* = 8.5 Hz, 1H), 7.45 (d, *J* = 8.5 Hz, 1H), 7.22-7.24 (m, 2H).

HR-EIMS *m/z* measured 194.0591 (194.0593 calcd for $C_{10}H_6{}^2H_3NOS$).

EIMS *m/z* (relative abundance) 194 $[M]^+$ (100), 176 (25), 160 (63), 148 (22), 121 (11).

4.3.39 Brassicanal A (39)

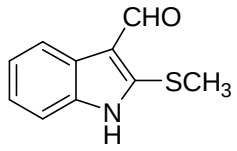

39

Et_3N (47 μL, 0.34 mmol) and ICH_3 (42 μL, 0.68) were added to a solution of 2-mercaptoindole-3-carboxaldehyde (40 mg, 0.27 mmol) in dry Et_2O (2 mL). The reaction mixture was allowed to stir for 20 min and was treated as described above for [SC^2H_3]brassicanal A (**39b**) to yield brassicanal A (**39**, 24 mg, 56% yield, Pedras and Okanga, 1999).

HPLC-DAD Method A, = 11.3 min.

^{1}H NMR (500 MHz C^2H_3CN) δ 10.14 (s, 1H), 8.05 (d, *J* = 8.5 Hz, 1H), 7.45 (d, *J* = 8.5 Hz, 1H), 7.22-7.24 (m, 2H), 2.64 (s, 3H).

HR-EIMS *m/z* measured 191.0409 (191.0405 calcd for $C_{10}H_9NOS$).

EIMS *m/z* (relative abundance) 191 $[M]^+$ (100), 176 (27), 158 (89), 148 (26), 130 (15).

4.4 Administration of precursors to rutabaga and turnip

4.4.1 Extraction of phytoalexins

Rutabaga (*B. napus* L. ssp. *rapifera*) and turnip (*B. rapa*) roots tubers were cut horizontally in 10-15 mm thick discs and cylindrical holes (16 mm in diameter) were made on one surface of the discs with a cork-borer (Pedras et al., 2004). The discs were kept in tightly sealed plastic boxes and incubated at 20 °C in darkness. After 24 h, the discs were UV-irradiated on the surface with holes for 20 min, and were incubated for further 24 h. Precursors (5×10^{-4} M) dissolved in H_2O-CH_3OH-Tween 80 (95/5/0.05 v/v) or H_2O- CH_3OH-Tween 80-DMSO (95/5/0.05/0.1 v/v for cyclobrassinin, **28**) were

pipetted into each hole (500 µL per hole) and the discs were further incubated at 20 °C in darkness. Following adsorption of precursor solution, the holes were filled with water. The aqueous solution in the holes was withdrawn with a pipette after appropriate incubation period (24, 48, 72 or 96 h) and was extracted with EtOAc (30 mL × 2). The combined organic extract was dried over Na_2SO_4 and solvent was removed under reduced pressure. The residue obtained was dissolved in CH_3CN (400 µL) and was analyzed by HPLC-DAD. The residue was then subjected to preliminary clean up by micro-FCC in a Pasteur pipette column packed with silica gel to 35 mm, eluting with 20 mL of CH_2Cl_2 and then 20 mL of CH_2Cl_2-EtOAc (40:60, v/v) to yield two fractions. The phytoalexin containing fractions obtained were analyzed by HPLC-DAD, HPLC-MS-ESI, and HPLC-HRMS-ESI. Control experiments were similarly prepared by incubating rutabaga and turnip root tubers with non-labeled precursors or with carrier solution only.

4.4.2 Extraction of glucosinolates

Tissue around the holes was cut, was soaked in CH_3OH, was ground (pestle and mortar) and was extracted with an aqueous CH_3OH solution. Extraction was carried out overnight on a shaker at 170 rpm, after which the tissue was filtered off and the filtrate was concentrated under reduced pressure. The residue obtained was subjected to RP-FCC (H_2O-CH_3CN, 100:0; 90:10, 80:20, v/v) to yield 3 fractions containing a mixture of indole glucosinolates. The fractions were dissolved in H_2O-CH_3OH (50:50) and were analyzed by HPLC-DAD, HPLC-MS-ESI, and HRMS-ESI.

4.5 Administration of precursors to *E. gallicum* (dog mustard)

4.5.1 Time course experiments

In order to carry out feeding experiments with dog mustard, the maximum production period of erucalexin (**38**) and 1-methoxyspirobrassinin (**35**) was determined using detached leaves. Dog mustard plants were grown in growth chambers with a 16-h photoperiod (22ºC/18ºC) at ambient humidity. The 28-day old plants were sprayed with $CuCl_2$ (2×10^{-3} M) solution in the growth chambers. After 24-h incubation, the leaves

were excised at the base of petiole and immediately immersed into distilled H_2O (1 mL) in a vial. The petiolated leaves were sprayed with $CuCl_2$ (2×10^{-3} M) solution followed by incubation at r.t. under continuous light. After 24-h incubation, leaves were frozen in liquid nitrogen, ground with a glass rod and were extracted in EtOAc (30 mL) overnight. The extract was filtered and was concentrated under reduced pressure. The residue obtained was subjected to preliminary clean up through a micro-FCC column employing a Pasteur pipette column packed with silica gel to 35 mm and eluting with 20 mL of CH_2Cl_2 and then 20 mL of CH_2Cl_2-EtOAc (25:75, v/v). The leaves were similarly extracted after 48-, 72-, 96- and 120-h incubation periods, each experiment was performed in duplicate. The fractions obtained were analyzed by HPLC-DAD and the amounts of erucalexin and 1-methoxyspirobrassinin present was determined from calibration curves prepared from pure erucalexin and 1-methoxyspirobrassinin. From these experiments, the maximum production of erucalexin was detected after 48-h incubation and this incubation period was adapted for feeding experiments. To prove that the observed metabolites were phytoalexins, similar experiments were carried out with leaves sprayed with water. HPLC-DAD analysis did not indicate the presence of erucalexin, 1-methoxyspirobrassinin or any elicited metabolites in these extracts.

4.5.2 Administration of precursors

Plants were grown and elicited as discussed for the time course analyses. The petiolated leaves from elicited 28-day-old plants were placed in vials containing 1 mL of precursor (5×10^{-4} M) dissolved in H_2O-CH_3OH-Tween 80 (95/5/0.05 v/v). Following uptake of precursor solution, the vials were filled with H_2O and were incubated for 48 h under continuous light. The leaves were extracted as described for time course analyses, and the phytoalexin containing fractions were analyzed by HPLC-DAD, HPLC-MS-ESI and HPLC-HRMS-ESI.

CHAPTER 5 : References

Agerbirk, N., Olsen, C. E., Soerensen, H., 1998. Initial and final products, nitriles, and ascorbigens produced in myrosinase-catalyzed hydrolysis of indole glucosinolates. J. Agric. Food. Chem. 46, 1563-1571.

Agrawal, A. A., Conner, J. K., Johnson, M. T. J., Wallsgrove, R., 2002. Ecological genetics of an induced plant defense against herbivores: additive genetic variance and cost of phynotypic plasticity. Evolution 56, 2206-2213.

Agrawal, A. A., Kurashige, N. S., 2003. A role for iosthiocyanates in plant resistance against the specialist herbivore *Pieris papae*. J. Chem. Ecol. 29, 1403-1415.

Alford, É. R., Perry, L. G., Qin, B., Vivanco, J. M., Paschke, M. W., 2007. A putative allelopathic agent of Russian knapweed occurs in invaded soils. Soil Biol. Biochem. 39, 1812-1815.

Anaya, A. L., Mata, R., Sims J. J., González-Coloma, A., Cruz-Ortega, R., Guadano, A., Hernández-Bautista, B. E., Midland, S. L., Rios, G., Gómez-Pompa, A., 2003. Allelochemical potential of *Callicarpa acuminate*. J. Chem. Ecol. 29, 2761-2776.

Bailey, J. A., Mansfield, J. W. Eds., in Phytoalexins. Blackie and Son, Glasgow, U.K., 1992, pp 1-16.

Bais, H. P., Walker, T. S., Kennan, A. J., Stermitz, F. R., Vivanco, J. M., 2003. Structure-dependent phytotoxicity of catechins and other flavonoids: flavonoid conversions by cell-free protein extracts of *Centaurea maculosa* (Spotted Knapweed) roots. J. Agric. Food Chem. 51, 897-901.

Bais, H. P., Walker, T. S., Stermitz, F. R., Hufbauer, R. A., Vivanco, J. M., 2002. Enantiomeric-dependent phytotoxicity and antimicrobial activity of (±)catechins. A rhizosecreted racemic mixture from spotted knapweed. Plant Physiol. 128, 1173-1179.

Bak, S., Feyereisen, R., 2001. The involvement of two P450 enzymes, CYP83B1 and CYP83A1, auxin homeostasis and glucosinolate biosynthesis. Plant Physiol. 127, 108-118.

Bak, S., Tax, F. E., Feldmann, K. A., Galbraith, D. W., Feyereisen, R., 2001. CYP83B1, a cytochrome P450 at the metabolic branch point in auxin and indole glucosinolate biosynthesis in Arabidopsis. Plant Cell 13, 101-111.

Baker, A. M., Molotsane, R., Müller, C., Shaffner, U., Städler, E., 2006. Chemosensory and behavioral responses of the turnip sawfly, Athalia rosae, to glucosinolates and isothiocyanates. Chemoecology 16, 209-218.

Bednarek, P., Schneider, B., Svatos, A., Oldham N. J., Hahlbrook, K., 2005. Structural complexity, differential response to infection, and tissue specificity of indolic and phenylpropanoid secondary metabolism in Arabidopsis roots. Plant Physiol. 138, 1058-1070.

Bennett, R. N., Mellon, F. A., Botting N. P., Eagles, J., Rosa, E. A. S., Williamson, G., 2002. Identification of the major glucosinolates (4-mecaptobutyl glucosinolate) in the leaves of *Eruca sativa* L. (salad rocket). Phytochemistry 61, 25-30.

Bones, A, M., Rossiter, J. T., 2006. The enzymatic and chemically induced decomposition of glucosinolates. Phytochemistry 1053-1067.

Brader, G., Tas, É, Palva, E. T., 2001. Jasmonate-dependent induction of indole glucosinolates in Arabidopsis by culture filtrates of the nonspecific pathogen *Erwinia carotovora*. Plant Physiol. 126, 849-860.

Browne, L. M., Conn, K. L., Ayer, W. A., Tewari, J. P., 1991. The camalexins: new phytoalexins produced in leaves of *Camelina sativa* (Cruciferae). Tetrahedron 47, 3909-3914.

Brydan, G. A., Ryan, D. E., 1966. Thiobenzoylphenylhydroxylamine: Potential analytical reagent. Anal. Chim. Acta 35, 190-194.

Burckard, P., Fleury, J-P., Weiss, F. 1965. Contribution à l'étude de l'oxydation des amines par l'eau oxygénée en présence de pertungstate alcalin. Bull. Soc. Chim. Fr. 10, 2730-2733.

Canoira, L., Rodriguez, J. G., Subirats, J. B., Escario, J-A., Jimenez, I., Martinez-Fernandez, A. R., 1989. Synthesis, structure and anti-fungal activity of 3-(2'-nitrovinyl)indoles. J. Med. Chem. 24, 39-42.

Cataldi, T. R. I., Rubino, A., Lelario, F., Bufo, S. A., 2007. Naturally occurring glucosinolates in plant extracts of rocket salad (*Eruca sativa* L.) identified by liquid chromatography coupled with negative ion electrospray ionization and quadrupole ion-trap mass spectrometry. Rapid. Commun. Mass Spectrom. 21, 2374-2388.

Cerney, M. S., Taube, E., Battaglia R. J., 1996. Identification of bis(4-isothiocyanatobutyl)disulfide and its precursor from rocket salad (*Eruca sativa*). Agric. Food Chem. 44, 3835-3839.

Chen, S., Glawischnig, E., Jørgensen, K., Naur, P., Jørgensen, B., Olsen, C-E., Hansen, C. H., Rasmussen, H., Pickett, J. A., Halkier, B. A., 2003. CYP79F1 and CYP79F2 have distinct functions in the biosynthesis of aliphatic glucosinolates in Arabidopsis. Plant J. 33, 923-937.

Chimiak, A., Przychodzen, W., Rachon, J., 2002. The thiohydroximate system. Heteroat. Chem. 13, 169-194.

Conn, K. L., Tewar, J. P., Dahiya, J. S., 1988 Resistance to *Alternaria brassicae* and phytoalexin elicitation in rapeseed and other crucifers Plant Sci. 56, 21-25.

Dahyia, J. S., Rimmer, S. R., 1988. Phytoalexin accumulation in tissues of *Brassica napus* inoculated with *Leptosphaeria maculans*. Phytochemistry 27, 3105-3107.

Dawson, G. W., Hick, A. J., Bennett, R. N., Donald, A., Pickett, J. A., Wallsgrove, R. M., 1993. Synthesis of glucosinolate precursors and investigations into the biosynthesis of phenylalkyl- and methythioalkylglucosinolates. J. Biol. Chem. 268, 27154-27159.

Daxenbichler, M. E., Spencer, G. F., Carlson, D. G., Rose, G. B., Brinker, A. M., Powell, R. G., 1991. Glucosinolate composition of seeds from 297species of wild plants. Phytochemistry 30, 2623-2638.

Dayan, F. E., Romagni, J. G., Duke, S O., 2000. Investigating the mode of action of natural phytotoxins. J. Chem. Ecol. 26, 2079-2094.

Dewick, P. M., 1984. The biosynthesis of cyanogenic glycosides and glucosinolates. Nat. Prod. Rep. 1, 546-549.

Dewick, P. M., 1998. The biosynthesis of shikimate metabolites. Nat. Prod. Rep. 15, 17-58.

Dixon, R. A., 2005. Engineering of plant natural product pathways. Curr. Opin. Plant Biol. 8, 329-336.

Dixon, R. A., Harrison, M. J., Lamb, C. J., 1994. Early events in the activation of plant defense responses. Annu. Rev. Phytopathol. 32, 479-501.

Doughty, K. J., Porter, A. J. R., Morton, A. M., Kiddle, G., Bock, C. H., Wallsgrove, R., 1991. Variation in the glucosinolate content of oilseed rape (*Brassica napus* L.) leaves II. Response to infection by *Alternaria brassicae* (Berk.) Sacc. Ann. Appl. Biol. 118, 469-477.

Du, L., Lykkesfeldt, J., Olsen, E. C., Halkier, B. A., 1995. Involvement of cytochrome P450 in oxime production in glucosinolate biosynthesis as demonstrated by an *in vitro* microsomal enzyme system isolated from jasmonic acid-induced seedlings of *Sinapis alba* L. Proc. Natl. Acad. Scie. USA 92, 12505-12509.

Fahey, J. W., Zalcmann, A. T., Talalay, P., 2001. The chemical diversity and distribution of glucosinolates and isothiocyanates among plants. Phytochemistry 56, 5-51.

Falk, K. L., Vogel, C., Textor, S., Bartram, S., Hick, A., Pickett, J. A., Gershenzon, J., 2004. Glucosinolate biosynthesis: demonstration and characterization of the condensing enzyme of the chain elongation cycle in *Eruca sativa*. Phytochemistry 65, 1073-1084.

Gabrys, B., Tjallingii, W. F., 2002. The role of sinigrin in host plant recognition by aphids during initial plant penetration. Entomol. Exp. Appl. 104, 89-93.

Gardiner, J. B., Morra, M. J., Eberlein, C. V., Brown, P. D., Borek, V., 1999. Allelochemicals released in soil following incorporation of rapeseed (Brassica napus) green manures. J. Agric. Food Chem. 47, 3837-3842.

Giamoustaris, A., Mithen, R., 1995. The effect of modifying the glucosinolate content of leaves of oilseed rape (Brassica napus ssp oleifera) on its interaction with specialist and generalist pests. Ann. Appl. Biol. 126, 347-363.

Glaswischnig, E., Hansen, B. G., Olsen, C. E., Halkier, B. A., 2004. Camalexin is synthesized from indole-3-acetaldoxime, a key branching point between primary and secondary metabolism in *Arabidopsis*. Proc. Natl. Acad. Sci. USA 101, 8245-8250.

Glending, T. M., Poulton, J. E., 1988. Glucosinolate biosynthesis. Plant Physiol. 86, 319-321.

Glending, T. M., Poulton, J. E., 1990. Partial purification and characterization of a 3'-phosphoadenosine-5'-phosphosulfate; desulfoglucosinolate sulfotransferase from cress (*Lepidium sativum*). Plant Physiol. 94, 811-818.

Goetz, J. K., Schraudolf, H., 1983. Two natural indole glucosinolates from Brassicaceae. Phytochemistry 22, 905-907.

Graser, G., Oldham, N. J., Brown, P. D., Temp, U., Gershenzon, J., 2001. The biosynthesis of benzoic acid glucosinolate esters in *Arabidopsis thaliana*. Phytochemistry 57, 23-32.

Graser, G., Schneider, B., Oldham, N. J., Gershenzon, J., 2000. The methionine chain elongation pathway in the biosynthesis of glucosinolates in *Ercuca sativa* (Brassicaceae). Arch. Biochem. Biophys. 378, 411-419.

Grubb, C. D., Abel, S., 2006. Glucosinolate metabolism and its control. Trends Plant Sci. 11, 89-100.

Grubb, C. D., Zipp, B. J., Ludwig-Müller, J., Masuno, M. N., Molinski, T. F., Abel, S., 2004. Arabidopsis glucosyltransferase UGT74B1 functions in glucosinolate biosynthesis and auxin homeostasis. Plant J. 40, 893-908.

Gugel, R. K., Séguin-Swartz, G., Petrie, A., 1990. Pathogenicity of 3 isolates *Leptosphaeria maculans* on *Brassica* species and other crucifers. Can. J. Plant Pathol. 12, 75-82.

Hachinohe, M., Matsumoto, H., 2005. Involvement of reactive oxygen species generated from melanin synthesis pathway in phytotoxicity of L-DOPA. J. Chem. Ecol. 31, 237-245.

Hachinohe, M., Sunohara, Y., Matsumoto, H., 2004. Absorption, translocation and metabolism of L-DOPA in barnyardgrass and lettuce: their involvement in species-selective phytotoxic action. Plant Growth Regul. 43, 237-243.

Halkier, B. A., Gershenzon, J., 2006. Biology and biochemistry of glucosinolates. Ann. Rev. Plant Biol. 57, 303-333.

Halkier, B. A., Møller, B. L., 1991. Involvement of cytochrome P-450 in the biosynthesis of dhurin in Sorghum bicolor (L.) Moench. Plant Physiol. 96, 10-17.

Hammerschmidt, R., 1999. Phytoalexins: what have we learned after 60 years? Annu. Rev. Phytopathol. 37, 285-306.

Hanley, B. A., Parsley, K. R., 1990. Identification of 1-methoxyindolyl-3-methyl isothiocyanate as an indole glucosinolate breakdown product. Phytochemistry 29, 769-771.

Hanley, B. A., Parsley, K. R., Lewis, J. A., Fenwick, G. R., 1990. Chemistry of indole glucosinolates: intermediacy of indol-3-ylmethyl isothiocyanate in the enzymatic hydrolysis of indole glucosinolates. J. Chem. Soc. Perkin Trans. 1, 2273-2276.

Hansen, B. G., Halkier, B. A., 2005. New insight into the biosynthesis and regulation of indole compounds in *Arabidopsis thaliana*. Planta 221, 603-606.

Hansen, C. H., Du, L., Naur, P., Olsen, C. E., Axelsen, K. B., Hick, A. J., Pickett, J. A., Halkier, B. A., 2001b. CYP83B1 is the oxime-metabolizing enzyme in the glucosinolate pathway of *Arabidopsis*. J. Biol. Chem. 276, 24790-24796.

Hansen, C. H., Wittstock, U., Olsen, C. E., Hick, A. J., Pickett, J. A., Halkier, B. A., 2001a. Cytochrome P450 CYP79F1 from *Arabidopsis* catalyzes the conversion of dihomomethionine and trihomomethionine to the corresponding aldoximes in the biosynthesis of aliphatic glucosinolates. J. Biol. Chem. 276, 11078-11085.

Harvey, J. A., Nouhuys, S. V., Biere, A., 2005. Effects of quantitative variation in allelochemicals in *Plantago lanceolata* on development of a generalist and a specialist herbivore and their endoparasitoids. J. Chem. Ecol. 31, 287-302.

Hemm, M. R., Ruegger, M. O., Chapple, C., 2003. The Arabidopsis *ref2* mutant is defective in gene encoding CYP83A1 and shows both phenylpropanoid and glucosinolate phenotypes. Plant Cell 15, 179-194.

Hull, A. K., Vij, R., Celenza, J. L., 2000. *Arabidopsis* cytochrome P450s that catalyze the first step of tryptophan-dependent indole-3-acetic acid biosynthesis. Proc. Natl. Acad. Scie. USA 97, 2379-2384.

Hwu, J. R., Lin, C-F., Tsay, S-C., 2005. Hexamethyldisilathiane in novel chemical transformations: concept of "counterattack reagents". Phosphorus, Sulfur, and Silicon 180, 1389-1393.

Hwu, J. R., Tsay, S-C., 1990. Counterattack reagents: thiosilanes in the conversion of nitro compounds to thiohydroxamic acids and thiohydroximates. Tetrahedron 46, 7413-7428.

Jain, J. C., GrootWassink, J. W. D., Kolenovsky, A. D., Underhill, E. W., 1990. Purification and properties of 3'-phosphoadenosine-5'-phosphosulphate: desulfoglucosinolate sulphotransferase from *Brassica juncea* cell cultures. Phytochemistry 29, 1425-1428.

Jain, J. C., Michayluk, M. R., GrootWassink, J. W. D., Underhill, E. W., 1989. Distributions of enzymes catalyzing glucosylation and sulfation steps of glucosinolate biosynthesis in *Brassica juncea* seedlings and cultured cells. Plant Sci. 64, 25-29.

Jensen, K. A., Pedersen, C., 1961. Studies of thio acids and their derivatives. II. Carboxymethyl dithioesters. Acta Chem. Scand. 15, 1087-1096.

Jiang, R-W., Hon, P-M., Xu, Y-T., Chan, Y-M., Xu, H-X., Shaw, P-C., But, P. P-H., 2006. Isolation and chemotaxonomic significance of tuberostemospironine-type alkaloids from Stemona tuberose. Phytochemistry, 67, 52-57.

Jimenez, L. D., Ayer, W. A., Tewari, J. P., 1997. Phytoalexins produced in the leaves of *Capsella bursa-pastoris* (shepherd's purse). Phytoprotection 78, 99-103.

Josefsson, E., 1972. Conversion of indole-3-acetaldehyde oxime to 3-indolylmethyl-glucosinolate in *Sinapis alba*. Physiol. Plant. 27, 236-239.

Kato-Noguchi, H., 2004. Allelopathic substance in rice root exudates: rediscovery of momilactone B as an allelochemical. J. Plant Physiol. 161, 271-276.

Kato-Noguchi, H., Ino, T., 2002. Rice seedlings release allopathic substances. Biol. Plant. 46, 157-159.

Kato-Noguchi, H., Ino, T., 2004. Release level of momilactone B from rice plants. Plant Prod. Sci. 7, 189-190.

Kato-Noguchi, H., Ino, T., Ichii, M., 2003. Changes in release levels of momilactone B into the environment from rice throughout its life cycle. Func. Plant Biol. 30, 995-997.

Kato-Noguchi, H., Ino, T., Sata, N., Yamamura, S., 2002. Isolation and identification of a potent allelopathic substance in rice root exudates. Physiol. Plant. 115, 401-405.

Kim, S-J., Ishii, G., 2006. Glucosinolate profiles in the seeds, leaves and roots of rocket salad (*Eruca sativa* Mill.) and anti-oxidative activities of intact plant powder and purified 4-methoxyglucobrassicin. Soil Sci. Plant Nutr. 52, 394-400.

Klein, M., Reichelt, M., Gershenzon, J., Papenbrock, J., 2006. The three desulfoglucosinolate sulfotransferase proteins in *Arabidopsis* have different substrate specificities and are differentially expressed. FEBS J. 273, 122-136.

Koch, B., Nielsen, V. S., Halkier, B. A., Olsen, C. E., Møller, B. L., 1992. The biosynthesis of cyanogenic glucosides in seedlings of cassava (*Manihot esculenta* Crantz). Arch. Biochem. Biophys. 292, 141-150

Kong, C. H., Li, H. B., Hu, F., Xu, X. H., Wang, P., 2006. Allelochemicals released by rice roots and residues in soil. Plant Soil 288, 47-56.

Kryomann, J., Textor, S., Tokuhisa, J. G., Falk, K. L., Bartram, S., Gershenzon, J., Mitchell-Olds, T., 2001. A gene controlling variation n *Arabidopsis* glucosinolate composition is part of the methionine chain elongation pathway. Plant Physiol. 127, 1077-1088.

Kuć, J., 1995. Phytoalexins, stress metabolism, and disease resistance in plants. Annu. Rev. Phytopathol. 33, 275-297.

Kutáček, M., Králová, M., 1972. Biosynthesis of the glucobrassicin aglycone from ^{14}C and ^{15}N labelled *L*-tryptophan precursors. Biol. Plant. 14, 279-285.

Kutáček, M., Procházka, Ž., Vereš, K., 1962. Biogenesis of glucobrassicin, the *in vitro* precursor of ascorbigen. Nature 194, 393-394.

Kutschy, P., Achbergerová, I., Dzurilla, M., Takasugi, M., 1997. Synthesis of indole phytoalexins brassinin and cyclobrassinin *via* [1-(*tert*-Butoxycarbonyl)indol-3-yl]methyl isothiocyanate as the key biomimetic intermediate. Synlett 289-290.

Kutschy, P., Dzurilla, M., Takasugi, M., Achbergerová, I., Homzová, R., Rácová, M., 1998. New syntheses of indole phytoalexins and related compounds. Tetrahedron 54, 3549-3566.

Lane, A. L., Kubanek, J., 2006. Structure-activity relationship of chemical defenses from the freshwater plant Micranthemum umbrosum. Phytochemistry 67, 1224-1231.

Latxague, L., Gardrat, C., Coustille, J. L., Viaud, M. C., Rollin, P., 1991. Identification of enzymatic degradation products from synthesized glucobrassicin by gas chromatography-mass spectromentry. J. Chromatogr. 586, 166-170.

Lefol, C., Séguin-Swartz, G., Morrall, R. A. A., 1997. Resistance to *Sclerotinia sclerotiorum* in a weed related to canola. Can. J. Plant Pathol. 19, 113 (Abstr.).

Li, Q., Eigenbrode, S. D., Stringam, G. R., Thiagarajah, M. R., 2000. Feeding and growth of *Plutella xylostella* and *Spodotpera eridania* on *Brassica juncea* with varying glucosinolate concentrations and myrosinase activity. J. Chem. Ecol. 26, 2401-2419.

Li, Y., Kiddle, G. A., Bennett, R. N., Wallsgrove, R. M., 1999. Local and systematic changes in glucosinolates in Chinese and European cultivars of oilseed rape (*Brassica napus*) after inoculation with *Sclerotinia sclerotiorum* (stem rot). Annu. Appl. Biol. 134, 45-58.

Makosza, M., Winiarski, J., 1984. Vicarious nucleophilic substitution of hydrogen in nitroarenes with α-substituted nitriles and esters. Direct α-cyanoalkylation and α-carbalkoxyalkylation of nitroarenes. J. Org. Chem. 49, 1494-1499.

Manici, L. M., Lazzeri, L., Baruzzi, G., Leoni, O., Galletti, S., Palmieri, S., 2000. Suppressive activity of some glucosinolate enzyme degradation products on *Phythium irregulare* and *Rhizoctonia solani* in sterile soil. Pest Manage. Sci. 56, 921-926.

Manici, L. M., Lazzeri, L., Palmieri, S., 1997. In vitro fungitoxic activity of some glucosinolates and their enzyme-derived products toward plant pathogenic fungi. J. Agric. Food Chem. 45, 2768-2773.

Mann, J., 1994. Chemical aspects of biosynthesis. Oxford University Press, Oxford, UK, pp. 2-4.

Mari, M., Leoni, O., Iori, R., Cembali, T., 2002. Antifungal vapour-phase activity of allyl isothiocyanate against *Penicillium expansum* on pears. Plant Pathol. 51, 231-236.

Marvel, C. S., Radzitzky, P., Brader, J. J., 1955. An improved preparation of dithioesters and some reactions and spectral properties of these compounds. J. Am. Chem. Soc. 77, 5997-6000.

Mayton, H. S., Olivier, C., Vaughn, S. F., Loria, R., 1996. Correlation of fungicidal activity of *Brassica* species with allyl isthiocyanate production in macerated leaf tissues. Phytopathology 86, 267-271.

Mewis, I., Appel, H. M., Hom, A., Raina, R., Schultz, J. C., 2005. Major signaling pathways modulate Arabidopsis glucosinolate accumulation and response to both phloem-feeding and chewing insects. Plant Physiol. 138, 1149-1162.

Mewis, I. Z., Ulrich, C., Schnitzler, W. H., 2002. The role of glucosinoaltes and their hydrolysis products in oviposition and host-plant finding by cabbage webworm, *Hellula undalis*. Entomol. Exp. Appl. 105, 129-139.

Mikkelsen, M. D., Hansen, C. H., Wittstock, U., Halkier, B. A., 2000. Cytochrome P450 CYP79B2 from *Arabidopsis* catalyses the conversion of tryptophan to indole-3-acetaldoxime, a precursor of indole glucosinolates and indole-3-acetic acid. J. Biol. Chem. 275, 33712-33717.

Mikkelsen, M. D., Naur, P., Halkier, B. A., 2004. Arabidopsis mutants in the *C-S* lyase of glucosinolate biosynthesis establish a critical role for indole-3-acetaldoxime in auxin homeostasis. Plant J. 37, 770-777.

Mikkelsen, M. D., Petersen, B. L., Olsen, C. E., Halkier, B. A., 2002. Biosynthesis and metabolic engineering of glucosinolates. Amino acids 22, 279-295.

Mithen, R. F., Lewis, B. G., Fenwick, G. R., 1986. In vitro activity of glucosinolates and their products against *Leptosphaeria maculans*. Trans. Br. Mycol. Soc. 87, 433-440.

Mithen, R. F., Lewis, B. G., Heaney, R. K., Fenwick, G. R., 1987. Glucosinolates of wild and cultivated *Brassica* species. Phytochemistry 26, 1969-1973.

Mithen, R. F., Magrath, R., 1992. Glucosinolates and resistance to *Leptosphaeria maculans* in wild and cultivated Brassica species. Plant Breed. 108, 60-68.

Mitsuo, M., Undherhill, E. W., 1971. Purification and properties of a UDP glucose: thiohydroximate glucosyltransferase from higher plants. Phytochemistry 10, 2279-2286.

Miyashita, K., Kondoh, K., Tsuchiya, K., Miyabe, H., Imanishi, T., 1997. Synthesis of several 3-substituted 2-trifluoromethylindoles *via* Mannich reaction of 2-trifluoromethylindoles. Chem.Pharm. Bull. 45, 932-935.

Mizukami, S., Nagata, K., 1966. Thiohydroxamic acids and their metal chelates. I. Synthesis of thiohydroxamic acids and O-methyl-thiohydroxamic acids. Chem. Pharm. Bull. 14, 1249-1255.

Monde, K., Katsui, N., Shirata, A., Takasugi, M., 1990a. Brassicanal A and B, novel sulfur-containing phytoalexins from the Chinese cabbage *Brassica campestris* L. ssp. *pekinensis*. Chem Lett. 209-210.

Monde, K., Sasaki, K., Shirata, A., Takasugi, M., 1990b. 4-Methoxybrassinin, a sulphur-containing phytoalexin from *Brassica oleracea*. Phytochemistry 29, 1499-1500.

Monde, K., Sasaki, K., Shirata, A., Takasugi, M., 1991a. Brassicanal C and two dioxindoles from cabbage. Phytochemistry 30, 2915-2917.

Monde, K., Sasaki, K., Shirata, A., Takasugi, M., 1991b. Methoxybrassenins A and B, sulphur-containing stress metabolites from *Brassica oleracea* var. *capitata*. Phytochemistry 30, 3921-3922.

Monde, K., Takasugi, M., Ohnishi, T., 1994a. Biosynthesis of cruciferous phytoalexins. J. Am. Chem. Soc. 116, 6650-6657.

Monde, K., Takasugi, M., Shirata, K., 1995b. Three sulfur-containing stress metabolites from Japanese radish. Phytochemistry 39, 581-586.

Monde, K., Takasugi, M., Takasugi, M., Kobayashi, K., Somei, M., 1994b. Dehydro-4-methoxycyclobrassinin, a sulfur containing phytoalexin isolated from turnip *Brassica campestris* L. ssp. *rapa*. Heterocycles 38, 263-267.

Monde, K., Tamura, K., Takasugi, M., 1995a. No involvement of methoxybrassinin in the biosynthesis of cyclobrassinin. Phytochemistry 39, 587-589.

Monde, K., Tanaka, A., Takasugi, M., 1996. Trapping experiment with aniline for a biosynthetic intermediate of sulfur-containing cruciferous phytoalexins. J. Org. Chem. 61, 9053-9054.

Nafisi, M., Goregaoker, S., Botanga, C. J., Glawischnig, E., Olsen, C. E., Halkier, B. A., Glazebrook, J., 2007. *Arabidopsis* cytochrome P450 monooxygenase 71A13 catalyzes the conversion of indole-3-acetaldoxime in camalexin synthesis. Plant Cell 19, 2039-2052.

Naur, P., Hansen, C. H., Bak, S., Hansen, B. G., Jensen, N. B., Nielsen, H. L., Halkier, B. A., 2003b. CYP79B1 from *Sinapis alba* converts tryptophan to indole-3-acetaldoxime. Arch. Biochem. Biophys. 409, 235-241.

Naur, P., Petersen, B. L., Mikkelsen, M. D., Bak, S., Rasmussen, H., Olsen, C. E., Halkier, B. A., 2003a. CYP83A1 and CYP83B1, two nonredundant cytochrome P450 enzymes metabolizing oximes in the biosynthesis of glucosinolates in Arabidopsis. Plant Physiol. 133, 63-72.

Nishihara, E., Parvez, M. M., Araya, H., Fujii, Y., 2004. Germination growth response of different plant species to the allelochemical L-3,4-dihydroxyphenylalanine (L-DOPA). Plant Growth Regul. 42, 181-189.

Nishihara, E., Parvez, M. M., Araya, H., Kawashima, S., Fujii, Y., 2005. L-3,4-Dihydroxyphenylalanine (L-DOPA), an allelochemical exuded from velvetbean (*Mucuna pruriens*) roots. Plant Growth Regul. 45, 113-120.

Olivier, C., Vaughn, S. F., Mizubuti, S. G., Loria, R., 1999. Variation in allyl isothiocyanate production within *Brassica* species and correlation with fungicidal activity. J. Chem. Ecol. 25, 2687-2701.

Osbourne, A. E., 1996. Preformed antimicrobial compounds and plant defense against fungal attack. Plant Cell 8, 1821-1831.

Pedras, M. S. C., Adio, A. M., 2007. Phytoalexins and phytoanticipins from the wild crucifers *Thellungiella halophila* and *Arabidopsis thaliana*: rapalexin A and wasalexins and camalexin. Phytochemistry, in press.

Pedras, M. S. C., Adio, A. M., Suchy, M., Okinyo D. P. O., Zheng, Q-A., Jha, M., Sarwar, M. G., 2006c. Detection, characterization and identification of crucifer phytoalexins using high-performance liquid chromatography with diode array detection and electrospray ionization mass spectrometry. J. Chromatogr. A 1133, 172-183.

Pedras, M. S. C., Ahiahonu, P. W. K., 2004. Phytotoxin production and phytoalexin elicitation by the phytopathogenic fungus *Sclerotinia sclerotiorum*. J. Chem. Ecol. 30, 2163-2179.

Pedras, M. S. C., Chumala, P. B., Suchy, M., 2003a. Phytoalexins from *Thlaspi arvense*, a wild crucifer resistant to virulent *Leptosphaeria maculans*: structure, synthesis and antifungal activity. Phytochemistry 64, 949-956.

Pedras, M. S. C., Hossain, M., 2006. Metabolism of crucifer phytoalexins in *Sclerotinia sclerotiorum*: detoxification of strongly antifungal compournds involves glucosylation. Org. Biomol. Chem. 4, 2581-2590.

Pedras, M. S. C., Jha, M., Ahiahonu, P. W. K., 2003b. The synthesis and biosynthesis of phytoalexins produced by cruciferous plants. Curr. Org. Chem. 7, 1635-1647.

Pedras, M. S. C., Jha, M., Minic, Z., Okeola, O. G., 2007f. Isosteric probes provide structural requirements essential for detoxification of the phytoalexin brassinin by the fungal pathogen *Leptosphaeria maculans*. Bioorg. Med. Chem. 15, 6054-6061.

Pedras, M. S. C., Loukaci, A., Okanga, F. I., 1998. The cruciferous phytoalexins brassinin and cyclobrassinin are intermediates in the biosynthesis of brassilexin. Bioorg. Med. Chem. Lett. 8, 3037-3038.

Pedras, M. S. C., Montaut, S., 2004. The biosynthesis of crucifer phytoalexins: unprecedented incorporation of a 1-methoxyindolyl precursor. Chem. Commun., 452-453.

Pedras, M. S. C., Montaut, S., Suchy, M., 2004. Phytoalexins from the crucifer rutabaga: structures, syntheses, biosyntheses, and antifungal activity. J. Org. Chem. 69, 4471-4476.

Pedras, M. S. C., Montaut, S., Xu, Y., Khan, A. Q., Loukaci, A., 2001. Assembling the biosynthetic puzzle of crucifer metabolites: indole-3-acetaldoxime is incorporated efficiently into phytoalexins but glucobrassicin is not. Chem. Commun. 1572-1573.

Pedras, M. S. C., Montaut, S., Zaharia, I. L., Gai, Y., Ward, D. E., 2003c. Transformation of host-selective toxin destruxin B by wild crucifers: probing a detoxification pathway. Phytochemistry 64, 957-963.

Pedras, M. S. C., Nycholat, C. M., Montaut, S., Xu, Y., Khan, A. Q., 2002. Chemical defenses of crucifers: elicitation and metabolism of phytoalexins and indole-3-acetonitrile in brown mustard and turnip. Phytochemistry 59, 611-625.

Pedras, M. S. C., Okanga, F. I., 1999. Strategies of cruciferous pathogenic fungi: detoxification of the phytoalexin cyclobrassinin by mimicry. J. Agric. Food Chem. 47, 1196-1202.

Pedras, M. S. C., Okanga, F. I., Zaharia, I. L., Khan, A. Q., 2000. Phytoalexins from crucifers: synthesis, biosynthesis, and biotransformation. Phytochemistry 53, 161-176.

Pedras, M. S. C., Okinyo D. P. O., 2006a. Syntheses of perdeuterated indoles and derivatives as probes for the biosyntheses of crucifer phytoalexins. J. Label. Compd. Radiopharm. 49, 33-45.

Pedras, M. S. C., Okinyo D. P. O., 2006b. *En route* to erucalexin: a unique rearrangement in the crucifer phytoalexin biosynthetic pathway. Chem. Commun. 1848-1850.

Pedras, M. S. C., Okinyo D. P. O., 2008. Remarkable incorporation of the first sulphur containing indole derivative: another piece in the puzzle of crucifer phytoalexins. Org. Biomol. Chem. 6, 51-54.

Pedras, M. S. C., Sarwar, M. G., Suchy, M., Adio, A. M., 2006b. The phytoalexins from cauliflower, caulilexins A, B and C: Isolation, structure, syntheses and antifungal activity. Phytochemistry 67, 1503-1509.

Pedras, M. S. C., Smith, K. C., 1997. Sinalexin, a phytoalexin from white mustard elicited by destruxin B and Alternaria brassicae. Phytochemistry 46, 833-837.

Pedras, M. S. C., Sorensen, J. L., 1998. Phytoalexin accumulation and antifungal compounds from the crucifer wasabi. Phytochemistry 49, 1959-1965.

Pedras, M. S. C., Sorensen, J. L., Okanga, F. I., Zaharia, I. L., 1999. Wasalexins A and B, new phytoalexins from wasabi: isolation, synthesis, and antifungal activity. Bioorg. Med. Chem. Lett. 9, 3015-3020.

Pedras, M. S. C., Suchy, M., Ahiahonu, P. W. K., 2006a. Unprecedented chemical structure and biomimetic synthesis of erucalexin, phytoalexin from the wild crucifer *Erucastrum gallicum*. Org. Biomol. Chem. 4, 691-701.

Pedras, M. S. C., Zaharia, I. L., 2000. Sinalbin A and B, phytoalexins from *Sinapis alba*: elicitation, isolation and synthesis. Phytochemistry 55, 213-216.

Pedras, M. S. C., Zaharia, I. L., 2001. Unprecedented Vilsmeier formylation: expedient syntheses of the cruciferous phytoalexins sinalexin and brassilexin and discovery of a new heteroatomic ring system. Org. Lett. 3, 1213-1216.

Pedras, M. S. C., Zheng, Q-A., Gadagi, R. S., 2007a. The first naturally occurring aromatic isothiocyanates, rapalexins A and B, are cruciferous phytoalexins. Chem. Commun. 1848-1850.

Pedras, M. S. C., Zheng, Q-A., Gadagi, R. S., Rimmer, S. R. 2007e. Phytoalexins and polar metabolites from the oilseeds canola and rapeseed: differential metabolic responses to the biotroph Albugo candida and to abiotic stress. Phytochemistry, in press.

Pedras, M. S. C., Zheng, Q-A., Sarma-Mamillapalle, V. K., 2007b. The Phytoalexins from Brassicacea: Structure, biological activity, synthesis and biosynthesis. Nat. Prod. Commun. 2, 319-330.

Pedras, M. S. C., Zheng, Q-A., Sarwar, G. M., 2007c. Efficient synthesis of brussalexin A, remarkable phytoalexins from Brussels sprouts. Org. Biomol. Chem. 5, 1167-1169.

Perry, L. G., Thelen, G. C., Ridenour, W. M., Weir, T. L., Callaway, R. M., Paschke, M. W., Vivanco, J. M., 2005. Dual role for an allelochemical: (±)catechin from *Centaurea maculosa* root exudates regulates conspecific seedling establishment. J. Ecol. 93, 1126-1135.

Piotrowski, M., Schemenewitz, A., Lopukhina, A., Müller, A., Janowitz, T., Weiler, E. M., Oecking, C., 2004. Desulfoglucosinolate sulfotransferases from *Arabidopsis thaliana* catalyze the final step in the biosynthesis of the glucosinolate core structure. J. Biol. Chem. 279, 50717-50725.

Przychodzen, W., 2006. Lawesson's reagent for direct thionation of hydroxamic acids: substituents effect on LR reactivity. Heteroat. Chem. 17, 676-684.

Przychodzen, W., Doszczak, L., Rachon, J., 2005. Substituent effects on 15N NMR chemical shifts in selected N-alkylthiohydroxamic acids. A comparative study. Magn. Reson. Chem. 43, 27-30.

Ramadas, S. R., Srinivasan, P. S., Ramachandran, J., Sastry, V. V. S. K., 1983. Methods of synthesis of dithiocarboxylic acids and esters. Synthesis 605-722.

Rask, L., Andreasson, E., Ekbom, B., Eriksson, S., Pontoppidan, B., Meijer, J., 2000. Myrosinase:gene family evolution and herbivore defense in Brassicaceae. Plant Mol. Biol. 42, 93-113.

Rausch, T., Butcher, D. N., Hilgenberg, W., 1983. Indole-3-methylglucosinolate biosynthesis and metabolism in clubroot diseased plants. Physiol. Plant 58, 93-100.

Reed, D. W., Davin, L., Jain, J. C., Deluca, V., Nelson, L., Underhill, E. W., 1993. Purification and properties of UDP-Glucose: Thiohydroximate Glucosyltransferase from *Brassica napus* L. seedlings. Arch. Biochem. Biophys. 305, 526-532.

Reintanz, B., Lehnen, M., Reichelt, M., Gershenzon, J., Kowalczyk, M., Sandberg, G., Godde, M., Uhl, R., Palme, K., 2001. *bus*, a Bushy Arabidopsis CYP79F1 knockout mutant with abolished synthesis of short-chain aliphatic glucosinolates. Plant Cell 13, 351-367.

Renwick, J. A. A., 2002. The chemical world of crucivores: lures, treats and traps. Entomol. Exp. Appl. 104, 35-42.

Roessingh, P., Städler, E., Fenwick, G. R., Lewis, J. A., Nielsen, J. K., Hurter, J., Ramp, T., 1992. Oviposition and tarsal chemoreceptors of the cabbage root fly are stimulated by glucosinolates and host plant extracts. Entomol. Exp. Appl. 65, 267-282.

Saito, I., Sugiyama, H., Yamamoto, A., Muramatsu, S., Matsuura, T., 1984. Photochemical hydrogen-deuterium exchange reaction of tryptophan. The role in nonradiative decay of singlet tryptophan. J. Am. Chem. Soc. 106, 4286-4287.

Sarwar, M., Kirkegaard, J. A., Wong P. T. W., Desmarchelier, J. M., 1998. Biofumigation potential of Brassicas – III. In vitro toxicity of isothiocyanates to soil-borne fungal pathogens. Plant Soil 201, 103-112.

Schuhegger, R., Nafisi, M., Mansourova, M., Petersen, B. L., Olsen, C. E., Svatoš, A., Halkier, B. A., Glawischnig, E., 2006. CYP71B15 (PAD3) catalyzes the final step in camalexin biosynthesis. Plant Physiol. 141, 1248-1254.

Schuster, J., Knill, T., Reichelt, M., Gershenzon, J., Binder, S., 2006. BRANCHED-CHAIN AMINOTRANSFERASE4 is part of the chain elongation pathway in the biosynthesis of methionine-derived glucosinolates in *Arabidopsis*. Plant Cell 18, 2664-2679.

Shao, H., Peng, S., Wei, X., Zhang, D., Zhang, C., 2005. Potential allelochemicals from invasive weed Mikania micrantha H. B. K. J. Chem. Ecol. 31, 1657-1667.

Shizuka, H., Serizawa, M., Shimo, T., Saito, I., Matsuura, T., 1988. Fluoresence-quenching of tryptophan. Remarkable efficient internal proton-induced quenching and charge-transfer quenching. J. Am. Chem. Soc. 110, 1930-1934.

Shraudolf, H., 1966. Der stoffwechsel von indolederivaten in Sinapis alba L. synthese und umsetzung vol L-tryptophan in etiolierten hyptokotylsementen nach applikation von indole-2-^{14}C. Phytochemistry 5, 83-90.

Simmonds, M. S. J., Blaney, W. M., Mithen, R., Birch, A. N. E., Lewis, J., 1994. Behavioural and chemosensory responses of the turnip root fly (*Delia floralis*) to glucosinolates. Entomol. Exp. Appl. 71, 41-57.

Sinhababu, A. K., Borchardt, R. T., 1983. Silica gel-assisted reduction of nitrostyrenes to 2-aryl-1-nitroalkanes with sodium borohydride. Tetrahedron Letters 24, 227-230.

Smith, B. J., Kirkegaard, J. A., 2002. *In vitro* inhibition of soil microorganisms by 2-phenylethyl isothiocyanate. Plant Pathol. 51, 585-593.

So, J-H., Boudjouk, P., 1989. Convenient synthesis of hexamethyldisilathiane and tetramethyldisilathiane. Synthesis 4, 306-307.

So, J-H., Boudjouk, P., 1992. Hexamethyldisilathiane. Inorg. Synth. 29, 30-32.

Soares, A. R., Ferrarese, M. L. L., Siqueira, R. C., Böhm, F. N, K, Z, M., Ferrarese-Filho, O., 2007. L-DOPA increases lignification associated with *Glycine max* root growth-inhibition. J. Chem. Ecol. 33, 265-275.

Somei, M., Kawasaki, T., 1989. A new and simple synthesis of 1-hydroxyindole derivatives. Heterocycles 29, 1251-1254.

Stermitz, F. R., Bais, H. P., Foderaro, T. A., Vivanco, J. M., 2003. 7,8-Benzoflavone: a phytotoxin from root exudates of invasive Russian Knapweed. Phytochemistry 64, 493-497.

Takasugi, M., Katsui, N., Shirata, A., 1986. Isolation of three novel sulphur-containing phytoalexins from the Chinese cabbage *Brassica campestris* L. ssp. *pekinensis*. J. Chem. Soc., Chem. Comm. 1077-1078.

Takasugi, M., Monde, K., Katsui, N., Shirata, A., 1988. Novel sulphur-containing phytoalexins from the Chinese cabbage *Brassica campestris* L. ssp. *pekinensis* (Cruciferae). Bull. Chem. Soc. Japan 61, 285-289.

Tan, A-M., He, H-P., Zhang, M., Wang, Z-T., Hao, X-J., 2007. Two new sesquiterpenes from *Ligularia lankongensis*. Helv. Chim. Acta 90, 101-104.

Textor, S., Bartram, S., Kryomann, J., Falk, K. L., Hick, A., Pickett, J. A., Gershenzon, J., 2004. Biosynthesis of methionine-derived glucosinolates in *Arabidopsis thaliana*: recombinant expression and characterization of methylthioalkylmalate synthase, the condensing enzyme of the chain-elongation cycle. Planta 218, 1026-1035.

Textor, S., Kraker, J-W., Hause, B., Gershenzon, J., Tokuhisa, J. G., 2007. MAM3 catalyzes formation of all aliphatic glucosinolate chain lengths in Arabidopsis. Plant Physiol. 144, 60-71.

Tierens, K. F. M., Thomma, B. P. H., Brouwer, M., Schmidt, J., Kistner, K., Porzel, A., Mauch-Mani, B., Cammue, B. P. A., Broekaert, W. F., 2001. Study of the role of antimicrobial glucosinolate-derived isothiocyanates in resistance of Arabidopsis to microbial pathogens. Plant Physiol. 125, 1688-1699.

Tomczyk, M., 2006. Secondary metabolites from *Potentilla argentea*. Biochem. Syst. Ecol. 34, 770-773.

Traw, M.B., 2002. Is induction response negatively correlated with constitutive resistance in black mustard? Evolution 56, 2196-2205.

Tsuji, J., Zook, M., Somerville, S., Last, R., Hammerschmidt, R., 1993. Evidence that tryptophan is not a direct a direct biosynthetic intermediate of camalexin in Arabidopsis thaliana. Physiol. Mol. Plant Pathol. 3, 221-229.

Van den Berg, E. M. M., Baldew, A. U., De Goede, A. T. J. W., Raap, J., Lugtenburg, J., 1988. Synthesis of three isotopomers of *L*-tryptophan via a combination of organic synthesis and biotechnology. Recl. Trav. Chim. Pays-Bas 107, 73-81.

Van Dam, N. M., Raaijmakers, C. E., van der Putten, W. H., 2005. Root herbivory reduces growth and survival of the shoot feeding specialist *Pieris rapae* on *Brassica nigra*. Entomol. Exp. Appl. 115, 161-170.

VanEtten, H. D., Mansfield, J. W., Bailey, J. A., Farmer, E. E., 1994. Two classes of plant antibiotics: phytoalexins versus phytoanticipins. Plant Cell 6, 1191-1192.

Vermeulen, M., Zwanenburg, B., Chittenden, G. J. F., Verhagen, H., 2003. Synthesis of isothiocyanate-derived mercapturic acids. Eur. J. Med. Chem. 38, 729-737.

Walter, W., Schaumann, E., 1971. The chemistry of thiohydroxamic acids. Synthesis 111-130.

Weir, T. L., Park, S-W., Vivanco J. M., 2004. Biochemical and physiological mechanisms mediated by allelochemicals. Curr. Opin. Plant Biol. 7, 472-479.

Wittstock, U., Halkier, B. A., 2000. Cytochrome P450 CYP79A2 from *Arabidopsis thaliana* L. catalyzes the conversion of L-phenylalanine to phenylacetaldoxime in the biosynthesis of benzylglucosinolate. J. Biol. Chem. 275, 14659-14666.

Xu, Y., Zhan, J., Wijeratne, E. M. K., Burns, A. M., Gunatilaka, A. A. L., Molnar, I., 2007. Cytotoxic and antihaptotactic beauvericin analogues from precursor-directed biosynthesis with the insect pathogen *Beauveria bassiana* ATCC 7159. J. Nat. Prod. 70, 1467-1471.

Xue, P-F., Luo, G., Zeng, W., Zhao, Y-Y., Liang, H., 2005. Secondary metabolites from *Potentilla multifida* L. (Rosaceae). Biochem. Syst. Ecol. 33, 725-728.

Yamazaki, S. 1997. Methyltrioxorhenium-catalyzed oxidation of secondary and primary amines with hydrogen peroxide. Bull. Chem. Soc. Jpn. 70, 877-883.

Zook, K., 1998. Biosynthesis of camalexin from tryptophan pathway intermediates in cell-suspension cultures of Arabidopsis. Plant Physiol. 118, 1389-1393.

Zook, K., Hammerschmidt, R., 1997. Origin of the thiazole ring of camalexin, a phytoalexin from *Arabidopsis thaliana*. Plant Physiol. 113, 463-468.

Appendix

A.1 Quantification of [4',5',6',7'-$^{2}H_4$]1-methoxyspirobassinin (35a) using LC-MS-ESI and LC-HRMS-ESI

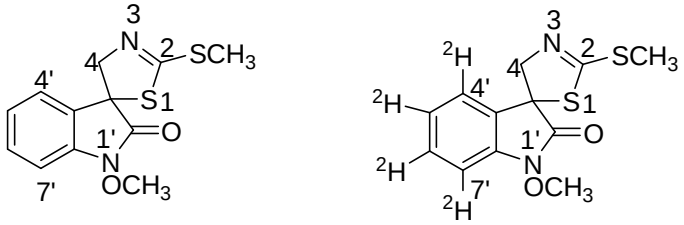

35 **35a**

Figure A.1 1-Methoxyspirobrassinin (**35**) and [4',5',6',7'-$^{2}H_4$]1-methoxyspirobrassinin (**35a**).

In this work, incorporation of isotopically (^{2}H, ^{34}S) labeled precursors into secondary metabolites (phytoalexins and indolyl glucosinolates) were established by LC-MS-ESI [Ion Trap (IT)], LC-HRMS-ESI [quadrupole-time of flight (Q-ToF)], and HRMS-EI [double focusing magnetic sector (DFMS)] analyses. The reproducibility and accuracy of the LC-MS-ESI (IT) and LC-HRMS-ESI (Q-ToF) methods of anlyses were compared using standard mixtures (**Tables A.1** and **A.2**) of 1-methoxyspirobrassinin (**35**) and [4',5',6',7'-$^{2}H_4$]1-methoxyspirobrassinin (**35a**). The standard mixtures were prepared to allow comparison of incorporation levels between 1 and 50%. Additional analytical methods, ^{1}H-NMR and HRMS-EI (DFMS), were used to analyze the standard mixtures and the results obtained were compared with those of LC-MS-ESI (IT) and LC-HRMS-ESI (Q-ToF) analyses (**Tables A.1** and **A.2**).

The percentage amounts of [4',5',6',7'-$^{2}H_4$]1-methoxyspirobrassinin (**35a**) present in the mixtures (**Tables A.1** and **A.2**) were determined by the methods:

1) LC-MS-ESI, LC-HRMS-ESI, and HRMS-EI analyses

(Eq.1) % of **35a** = $\{[M + n]^{+/-}/([M]^{+/-} + [M + n]^{+/-})\} \times 100$ ($n = 4$)

n is the number of deuterium atoms, and M is the peak area or relative intensity of the molecular ion peak in the mixtures containing **35** and **35a**.

2) ^{1}H NMR analyses

(**Eq.2**) % of **35a** = $\{([H\text{-}4a/b] - [H\text{-}7'])/[H\text{-}4a/b]\} \times 100$

[H-7'] is the integration of proton peak due to H-7', and [H-4] is the integration of the proton peak due to 2H-4a/b (δ_H 4.60 or 4.46) in the mixtures containing **35** and **35a**.

The proton peak due to H-7' (δ_H 7.06) is well separated and simple, this peak was integrated and calibtrated as 1, and was used as a standard to intergrate the peaks due to 2H-4a/b (δ_H 4.60 and 4.46) (**Figures A.1** and **A.2**). The integration values of proton peaks due to H-4a (δ_H 4.60) and H-4b (4.46) (**Figure A.2**) were therefore used to calculate the percentage amounts of [4',5',6',7'-$^{2}H_4$]1-methoxyspirobrassinin (**35a**) in the mixtures according to equation **Eq.2** and are summarized in **Table A.1**.

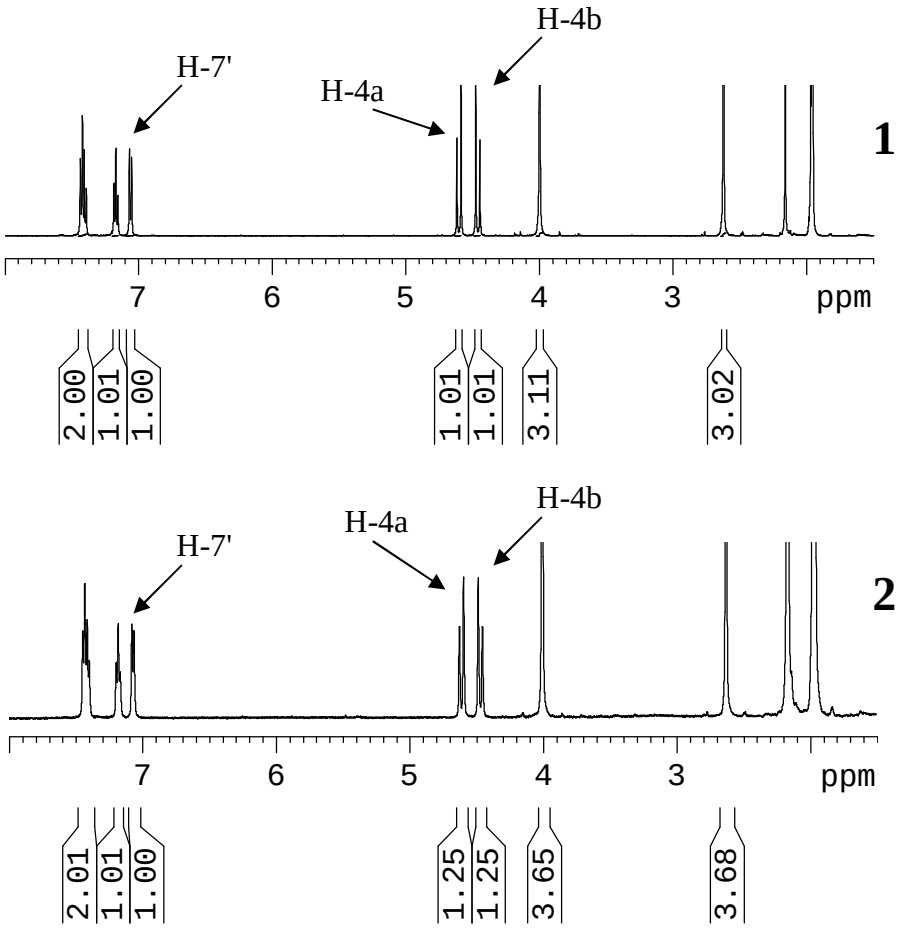

Figure A.2 ^{1}H NMR spectra of 1-methoxyspirobrassinin (**35**) and [4',5',6',7'-$^{2}H_4$]1-methoxyspirobrassinin (**35a**). Spectrum **1** = 1-methoxyspirobrassinin; Spectrum **2** = mixture of 1-methoxyspirobrassinin (**35**) and [4',5',6',7'-$^{2}H_4$]1-methoxyspirobrassinin (**35a**).

A.1.1 Deuterated component is 10 - 50% of the mixture (Standard mixtures A)

Stock solutions of 1-methoxyspirobrassinin (**35**) and [4',5',6',7'-$^{2}H_4$]1-methoxyspirobrassinin (**35a**) were prepared at concentrations of 1.76×10^{-3} M. From each stock solution of **35** and **35a**, 500.0 µL were withdrawn, combined, and were evaporated to dryness. The resulting mixture (**A-1**) was taken in $C^{2}H_3CN$ (500.0 µL) and was analyzed by ^{1}H-NMR. From mixture **A-1**, 100.0 µL were withdrawn and analyzed by HPLC-MS-ESI (IT), HPLC-HRMS-ESI (Q-ToF), and HRMS-EI (DFMS) (**Table**

A.1). To the remaining mixture **A-1** was added 500.0 µL from stock solution of 1-methoxyspirobrassinin (**35**). The resulting mixture, **A-2**, was evaporated to dryness and similarly analyzed as **A-1** above. Following ^{1}H-NMR analysis, 100.0 µL of **A-2** were withdrawn and the remaining portion was treated as **A-1** above to prepare mixtures **A-3** and **A-4** respectively (**Table A.1**). Stock solutions of 1-methoxyspirobrassinin (**35**) and [4',5',6',7'-$^{2}H_4$]1-methoxyspirobrassinin (**35a**) were similarly analyzed by ^{1}H-NMR, HPLC-MS-ESI, HPLC-HRMS-ESI, and HRMS-EI.

Table A.1 Quantification of the amounts of [4',5',6',7'-$^{2}H_4$]1-methoxyspirobrassinin (**35a**) present in a mixture with 1-methoxyspirobrassinin (**35**) using LC-MS-ESI.

Mixture	**LC-MS-ESI[a,c,e] (IT)**		**LC-HRMS-ESI[a,d,e] (Q-ToF)**	**HRMS-EI[a,d] (DFMS)**	**^{1}H-NMR[b,d]**
	Av (%)	**STD**			
A-1	50.0	0.57	50.0	50.0	50.0
A-2	34.0	1.07	33.0	36.0	37.0
A-3	18.0	0.84	17.0	21.0	25.0
A-4	12.0	0.45	10.0	16.0	20.0

[a]The percentage amounts of [$^{2}H_4$]1-methoxyspirobrassinin (**35a**) in the mixtures **A-1** to **A-4** calculated according to equation **Eq.1**.
[b]The percentages amounts of [$^{2}H_4$]1-methoxyspirobrassinin (**35a**) in the mixtures **A-1** to **A-4** calculated according to equation **Eq.2**.
[c]% of **35a** calculated from average of three independent determinations ± standard deviation (STD).
[d]% of **35a** calculated from one determination.
[e]Positive ion mode.

As shown in **Table A.1**, LC-MS-ESI (IT) analyses were conducted in triplicate measurements. There were no significant differences in the percentage amounts calculated for LC-MS-ESI (IT) and LC-HRMS-ESI (Q-ToF) analyses (**Table A.1**). The percentages obtained from HRMS-EI (DFMS) analyses were slightly higher than those obtained from LC-MS-ESI and LC-HRMS-ESI, but showed similar trend (**Table A.1**). Although percentages from ^{1}H-NMR analyses were slightly higher than those obtained by LC-MS-ESI, LC-HRMS-ESI, and HRMS-EI, these analyses have shown that either

or both LC-MS-ESI (IT) and LC-HRMS-ESI (Q-ToF) can be used to determine levels of incorporation in the study of biosynthetic pathway(s) of crucifer phytoalexins.

A.1.2 Deuterated component is less than 10% of the mixture (Standard mixtures B)

The accuracy of the of LC-MS-ESI (IT) method in the determination of secondary metabolites incorporating less than 10% of the precursor was established with standard mixtures of [4',5',6',7'-$^{2}H_4$]1-methoxyspirobrassinin (**35a**) and 1-methoxyspirobrassinin (**35**). Thus, stock solutions of **35a** and **35** were prepared at concentrations of 2.85×10^{-4} M. Stock solution of 1-methoxyspirobrassinin (90.0 µL) was added to that of [4',5',6',7'-$^{2}H_4$]1-methoxyspirobrassinin (10.0 µL), followed by addition of CH_3CN (400.0 µL) to the resulting solution to give mixture **B-1**. The prepared mixture **B-1** was analyzed by LC-MS-ESI (IT) and HRMS-EI (DFMS) in triplicate measurements (**Table A.2**). The remaining mixtures, **B-2** to **B-5** were similarly prepared by mixing stock solutions of 1-methoxyspirobrassinin (92.0, 94.0, 96.0 and 98.0 µL) with that of [4',5',6',7'-$^{2}H_4$]1-methoxyspirobrassinin (8.0, 6.0, 4.0, and 2.0 µL), respectively, that were treated as **B-1** above, followed by LC-MS-ESI and HRMS-EI analyses. The percentage amounts of [4',5',6',7'-$^{2}H_4$]1-methoxyspirobrassinin in the mixtures were calculated (similar to standard mixtures **A**) and are summarized in **Table A.2**.

Table A.2 Quantification of the amounts of [4',5',6',7'-$^2H_4$]1-methoxyspirobrassinin (**35a**) present in a mixture with 1-methoxyspirobrassinin (**35**).

Mixture	LC-MS-ESI[a,b,c] (IT)		HRMS-EI[a,b] (DFMS)	
	Av. (%)	STD	Av. (%)	STD
B-1	8.0	0.4	11.0	0.1
B-2	6.0	0.3	9.0	0.2
B-3	5.0	0.3	7.0	0.0
B-4	3.0	0.2	5.0	0.2
B-5	2.0	0.1	2.0	0.1

[a]The percentage amounts of [$^2H_4$]1-methoxyspirobrassinin (**35a**) in the mixtures **B-1** to **B-5** calculated according to equation **Eq.1**.
[b]% of **35a** calculated from average of three independent determinations ± standard deviation (STD).
[c]Positive ion mode.

As shown in **Table A.2**, the percentage amounts of [4',5',6',7'-$^2H_4$]1-methoxyspirobrassinin (**35a**) in the mixtures from LC-MS-ESI (IT) analyses were slightly lower than those obtained from HRMS-EI (DFMS) analyses. The percentage amounts of up to 2% of [4',5',6',7'-$^2H_4$]1-methoxyspirobrassinin in the mixtures were detected with good reproducibility.

A.1.3 Conclusion

These analyses (**Tables A.1** and **A.2**) show that both LC-MS-ESI (IT) and LC-HRMS-ESI (Q-ToF) methods can be used to accurately establish the incorporation of various precursors into different secondary metabolites even at low incorporations. The data obtained from these quantification studies suggest that the two methods, LC-MS-ESI (IT) and LC-HRMS-ESI (Q-ToF), provide sufficient information for accurate determination of levels of incorporation.

The HRMS-EI (DFMS) analysis is also accurate and reproducible (**Tables A.2**). Howeve, unlike LC-MS-ESI (IT) and LC-HRMS-ESI (Q-ToF) that analyzes mixtures of secondary metabolites, HRMS-EI requires sample separation. Secondary metabolites are normarly obtained in very small quantities, thus limiting the applicability of HRMS-EI in their analysis.